University of Nairobi

School of Engineering

SPATIAL MODELING OF BIODIVERSITY AND CARBON STORAGE ALONG THE INHABITED SLOPES OF MOUNT KILIMANJARO (TANZANIA) AND TAITA HILLS (KENYA)

BY

DICKENS ONYANGO ODENY

NO: F80/85601/2012

PhD thesis submitted for the Degree of Doctor of Philosophy in Geographic Information Systems, in the Department of Geospatial and Space Technology of the University of Nairobi

July, 2020

Declaration

I, **DICKENS ONYANGO ODENY**, hereby declare that this thesis is my original work. To the best of my knowledge, the work presented here has not been presented as a thesis in any other university.

DICKENS ONYANGO ODENY	.....	13/07/2020
Name of student	Signature	Date

This thesis has been submitted for examination with our approval as university supervisors.

Prof. Faith Karanja	.....	15/7/2020
Name of Supervisor	Signature	Date

Prof. Robert Marchant		.....17/07/2020…
Name of Supervisor	Signature	Date

Prof. Petri Pellika		…24/07/2020……..
Name of Supervisor	Signature	Date

Dedication

Throughout this period of study I have received immense support from my family, friends and well-wishers. Prayers from my family kept me optimistic about finishing this study and encouragement from friends and well-wishers made me stay focused. Every journey has its beginning and a memoir, and mine is no different. I thank God and express my deepest gratitude to all these people who have been around me and keeping me encouraged to the successful end of this journey. I particularly wish to point out the following who have been icons in my life: my mother Abigael Atieno who has continuously and relentless offered prayers for her children, me being one of them; my late grandmother Margaret Obiero who spiritedly fought for my education; and my uncle Paul Pascal Ouma who made great sacrifices at the formative stages of my education and shaped my future.

This thesis is, therefore, dedicated to my late grandmother Margret Obiero Ogola (Dana Nyagumba) who has been a gift from heaven and for whom I thank God.

Acknowledgement

The financial support for the PhD study was provided by the Ministry for Foreign Affairs of Finland through Climate Change Impacts on ecosystem Services and Food Security in Eastern Africa (CHIESA - ICIPE) project, which covered both tuition and fieldwork. CHIESA through the University of York (United Kingdom) also provided student stipend for the entire period of my study. Field exposure on working with the Hemisperical camera and SunScan device was provided by Prof. Petri Pellikka of the University of Helsinki. These instruments were provided by Prof. Rob Marchant of the University of York for sampling during the entire period of fieldwork. Wilson Mchomvu and his son (Owden) greatly assisted in the fielwork in Kilimanjaro (Tanzania), while in Taita Hills (Kenya), I was assisted by Darius Kimuzi of Taita Hills Research Station of University of Helsinki who was also helpful in the identification of plants.

Prof. Rob played an important role in ensuring that I got good training by the right experts. Nicholas Deere of the York Institute for Tropical Ecosystems (KITE) guided me on processing of hemispherical images with CanEye programme and thresholding in Matlab. Dr. Philip Platts of the University of York provided technical guidance on statistical analysis in R, spatial modelling and species distribution modelling technique when I was at UoY.

The Department of Geospatial and Space Technology (University of Nairobi) and the National Museums of Kenya provided in kind support and a conduicive environment for working.

Fieldwork and writing of this thesis was supervised by Prof. Faith Karanja of the Department of Geospatial and Space Technology (University of Nairobi), Prof. Rob Marchant (University of York) and Prof. Petri Pellikka (University of Helsinki).

I am indeed grateful and highly indepted to all the individuals and institutions mentioned above.

ABSTRACT

The inhabited montane areas in Mount Kilimanjaro and Taita Hills are threatened by expansion and intensification of agriculture. Due to poor cropland management and destruction of remnant indigeneous forests on the slopes, soil conditions and micro-climate are deteriorating. This has ultimately compromised resilience of the plant species and carbon sequestration in the areas. The resilience will further be risked by climate change in the region which shows montane areas will be more vulnerable. Thus, the study aimed at determining model relationships of vegetation structures and carbon storage to environmental variables on the inhabited slopes of montane areas. One hectare plot was used for sampling Woody Plant Species (WPS), tree biometries (diameter>10 cm) along transects. Biodiversity indices, richness and diversity indices were used to determine distribution of WPS in different sites and types of cropland. Allometric model was used for estimating the above-ground carbon storage (AGCS) from tree biometries. Ground based Remote Sensing, hemispherical photography and SunScan canopy analyzer for measuring LAI in VALERI plots. Univariate and test statistics was performed on WPS, AGCS, LAI between site and types of cropland. Generalized Linear Model (GLM) was used for predicting response variable from spatial predictors physical, edaphic variables, vegetation index (EVI) and population density in R programme. GLM prediction models were used for spatial upscaling of response variables using maths algebra tool in ArcGIS 10.2. Impact of climate change on distributions of selected WPS *Albizia gummifera* (Albizia), *Mangifera indica* (Mango) and *Persea americana* (Avocado) was analysed under RCP 4.5 and 8.5 projections for peak periods of 2055 and 2085 with a machine-learning technique. Woody Plant Species Richness significantly differ between sites (t=3.06, p=0.002) and types of cropland with only 32% of the species shared between the two sites. The spatial distribution of WPSR is significantly explained by multivariate model with predictors SOC + I(Elev.^{2}) in Kilimanjaro (R^2=0.78 , p=0.00 , AIC=67.42) and predictors I(Elev.^{2}) + Slope + Population Density in Taita Hills (R^2=0.97 , p=0.00 , AIC=36.91). Spatial model for AGCS in Kilimanjaro is better explained by multivariate predictor SOC + CEC + pH + BD) (R^2=0.94, p=0.00, AIC=91.33) and in Taita Hills model predictor Elev. + Slope + Population Density) shows a better spatial model distribution (R^2=0.79, p=0.01, AIC=71.11). LAI spatial distribution in Kilimanjaro is strong and significantly varies mostly with elevation but no significant distribution is observed in Taita Hills with all variables. Projection of species distribution under baseline climate condition shows Taita Hills has significantly higher proportion of suitable areas for Albizia, Mango and Avocado than in Kilimanjaro (F=153.17, p=0.01). Avocado will experience upshift in minimum elevation range in Kilimanjaro under all RCPs except RCP 8.5, 2085 which will decrease in proportion of suitable area and fragmentation under RCP4.5 (2055) and RCP8.5 (2055). Mango will experience downshift, which will increase proportion of suitable areas in Kilimanjaro under RCP 8.5, 2085 with fragmentation of the areas occurring under RCP4.5 (2055 & 2085) and RCP8.5 (2055). Downshift in Albizia and Mango will occur which will increase proportion of suitable areas in Taita Hills under RCP 8.5, 2085. The distributions of biodiversity in montane areas are explained by multivariate predictors, which however differ on sites. Climate change projections will cause varied response of some species shifting upslope and other downslope with habitat fragmentation occurring in the montane areas. Effective monitoring of the inhabited montane areas should use WPSR, AGCS and LAI developed models for sustainable conservation of biodiversity and improved carbon sequestration. While, mitigation measures for climate change should have different choices of plant species for downslope and upslope in order contribute high AGC sequestration and sustainable livelihood on the slopes.

Key words: Environmental Variables, Woody Plant Species, Agro-forestry, Cropped Land, Carbon Storage, Climate Change, Leaf Area Index

Table of Content

List of Figures

List of Tables

Abbreviations and Acronyms

AFRICLIM	Africa Climate
AGCS	Above-Ground Carbon Storage
AIC	Akaike Information Criterion
ANNs	Artificial Neural Networks
ANOVA	Analysis of Variance
AUC	Area Under Curve
BF3	Beam Fraction Sensor Type 3
BD	Bulk Density
Ct/ha	Carbon Tonne per Hectare
CCA	Canonical Correlation Analysis
CEC	Cation Exchange Capacity
CHIESA	Climate Change Impacts on ecosystem Services and Food Security in Eastern Africa
CO_2	Carbon Dioxide
DBH	Diameter at Breast Height
EABH	Eastern Afromontane Biodiversity Hotspot
EAM	Eastern Arc Mountains
ETM	Enhanced Thematic Mapper
EVI	Enhanced Vegetation Index
GBIF	Global Biodiversity Information Facility
GLC	Global Land Cover
GCM	Generalized Circulation Model
GLM	Generalized Linear Model
GPS	Global Positioning System
IPCC	Intergovernmental Panel on Climate Change
KCarbMod	Mount Kilimanjaro Carbon Storage Model
KINAPA	Kilimanjaro National Park
KITE	York Institute for Tropical Ecosystems
KRichMod	Mount Kilimanjaro Species Richness Model
LAI	Leaf Area Index
LAI_{EFF}	Effective Leaf Area Index
LAI_{Hemi}	Leaf Area Index derived from Hemispherical Camera

$LAI_{SunScan}$	Leaf Area Index derived from SunScan Device
LAI_{TRUE}	True Leaf Area Index
LED	Light Emitting Diode
LM	Linear Model
LSM	Least square Method
LSR	Least Square Regression
MAP	Mean Annual Precipitation
MAT	Mean Annual Temperature
Maxent	Maximum Entropy
SE	Standard Error
Mg C ha^{-1}	Mega Carbon per Hectare
MHz	Mega Hertz
mmy^{-1}	Millimeter Per Year
MODIS	Moderate Resolution Imaging Spectroradiometer
Mount	Mountain
NASA	National Aeronautics and Space Administration
NDVI	Normalized Difference Vegetation Index
NIR	Near Infra-Red
PAR	Photosynthetically Active Radiation
PDA	Personal Digital Assistance
PgC	Picogram of Carbon
pH	Potential of Hydrogen ion concentration
Pop.	Population
PopDen	Population Density
PROTA	Plant Resources of Tropical Africa
QGIS	Quantum Geographical Information System
RCP	Representative Concentration Pathway
REN	Relative Equivalent Noise
RSE	Residual Standard Error
ROC	Receiver Operating Curve
SD	Standard Deviation
SDM	Species Distribution Modeling
SOC	Soil Organic Carbon

SVIs	Spectral Vegetation Indices
SWIR	Short Wave Infrared
t C ha^{-1}	Trillion Carbon per Hectare
TCarbMod1	Taita Hills Carbon Storage Model
TRAC	Tracing radiation and Architecture of Canopies
TRichMod	Taita Hills Species Richness Model
VALERI	VALidation of European Remote sensing Instruments
VEN	Vegetation Equivalent Noise
W/m^2	Watts per square Meter
WPS	Woody Plant Species
WPSR	Woody Plant Species Richness
WSG	Wood Specific Gravity

CHAPTER 1: INTRODUCTION

1.1. Research Background

Eastern Africa hosts the coastal forests and the Eastern Afromontane Biodiversity Hotspot (EABH), which are two of the 34 global biodiversity hotspots known worldwide for hosting significant endemic plant and animal species. The EABH is comprised of Eastern Arc Mountains (EAM) that runs from the Taita Hills of the southern Kenya to the Makambako Gap in southern Udzungwa Mountains and Mount Kilimanjaro of Tanzania. The EAM and Mount Kilimanjaro contain similar plant taxa, which suggests that the areas were spatially connected in the past or possibly by long-distance dispersal.

Similar to the tropical mountain, the climate variables in the Eastern Arc Mountains also vary with elevation (Hall et al., 2009; McCain, 2005; Rickart, 2001). Decrease in species diversity along elevation with a mid-elevation hump is a common pattern seen in the tropical mountains (Rahbek, 1995; Heaney, 2001). The Eastern Arc mountain blocks are isolated, humid and are separated by drylands. Due to this, the forests have high levels of species richness and endemism in all biological groups, with many species endemic to just one or a few mountain ranges (Lovett, 1990; Hall et al., 2009). Montane areas of Taita Hills and Kilimanjaro draw clear differences from the period of their geologic formations and structure that contribute to the characteristics of biodiversity and soils therein. While Taita Hills are formed by the ancient crystalline rocks, Kilimanjaro is formed more by recent volcanic activities (Lovett and Wasser, 2008). Due to this difference and substantiated difference on the mountains periods of exposure to a relatively stable climate, Taita Hills among other eastern arc mountain houses quite a significant number of endemic species. The montane areas, however, are very close to each other by distance and have similar climate characteristics.

One of the most significant impacts of forest fragmentation is on carbon storage of forest fragments. Generally, all transitions in land cover whether wetlands, trees outside forest, agroforests, and plantations affect carbon storage. Deforestation in the tropics contributes about one fifth of the total anthropogenic CO_2 emissions to the atmosphere. Forest carbon is retained and increased where loging is reduced (Pinard and Cropper 2000). The decline of carbon in relation to logging of timber depends on the volume of timber extracted, damages to the remaining stand, and the response of vegetation to opening. The accumulation of carbon in biomass in forest is also reduced by an increase in fire frequency (Pinard and Cropper 2000). The rate of recovery are site specific and depend on productivity of site, composition of species, alteration in necromass stores, long-term effect of non-

detrimental tree damage, the duration of elevated mortality rates following logging, and impacts of soil damage on vegetation recovery.

The amount of carbon stored in a logged or silviculturally managed forest is influenced by factors and processes that are both internal to the system (e.g. species composition, growth rates, decay rate) and external (e.g. rotation times, logging damage, timber volume extracted) (Pinard and Cropper 2000). Pinard and Cropper (2000) simulated model of carbon storage over a 1000 year span in the unlogged forest. Their study demonstrates carbon storage dynamics over long period of time through: above-ground biomass (necromass) across 500 years following logging; canopy layers (by *dbh* class) and pioneer trees, and; carbon storage in soil, coarse woody debris stores, small woody litter and fine litter. Carbon storage fluctuated between 200 and 265 Mg C ha^{-1}. mean carbon storage over a 60 year simulation was 220 Mg C ha^{-1} (SD = 11); above-ground biomass ranged from 130 to 220 Mg C ha^{-1} and showed a mean value of 166 Mg C ha^{-1} (SD = 19.5) over a 60 year simulation, and 170 Mg C ha^{-1} (SD=23) over a 500 year simulation.

Three types of cropland are classified based on how the land is managed; these include rice fields, the cropped land and agro-forestry systems (IPCC, 2006). The latter has vegetation structure (current or potentially) falling below the thresholds used for the IPCC Forest Land category (Hairiah et al., 2011). Agro-forestry leads to a more and sustainable production system and benefits to farmers, than many treeless alternatives (Sanchez, 1995; Leakey, 1996). Cropland coverage varies in East Africa from an estimation of 1.8% (Friedl et al., 2002), to 12.5% (Raman-Kutty and Foley) and 22.7% GLC 2000 (JRL, 2005) in the late 20^{th} century (Doherty, 2010). Over 50% of the area around Mount Kilimanjaro (sub-montane) is under cropland (Pfeifer et al., 2012); while, cropland in Taita Hills expands at the expense of shrublands and thickets (Pellikka et al., 2013). Cropland expansion is attributed to population growth (Balmore et al., 2001) which has increased food demand. The conversion of natural vegetation types into cropland adversely affect production of natural systems (Landmann and Dubovyk, 2014) including storage of carbon in the system. Carbon fluxes on woodland and forest areas converted to different types cropland considerably varies. For instance, about 10 Mg C ha^{-1} and 40 – 180 Mg C ha^{-1} above-ground carbon is lost when woodland and forest areas are converted into agro-forestry, respectively. While, 25 Mg C ha^{-1} and 80 to 400 Mg C ha^{-1} above-ground carbon and soil organic carbon is lost when woodland and forest areas converted into cropped land which is under continuous cropping (Hairiah, et al., 2011). Information of carbon storage in the region is based on large scale assessments. In tropical Africa, carbon storage in cropland is estimated at 5.30 Mg C ha^{-1}; however, cropland with preserved natural trees is estimated at 91.50 Mg C ha^{-1}(Baccini et al., 2008). However, estimated range of median range of carbon in East

Africa cropland ranges from 1.60 to 4.80 Mg C ha^{-1} (Pfeifer et al., 2013). Thus, the potential differential interplays of climate with the above-ground carbon and soil carbon in cropped land and agro-forestry is eminent in the slopes of Taita Hills and Mount Kilimanjaro. A synergy from other soil factors may substantially contribute to the visible or imperceptible interactions. These interactions may be locally based depending on how the croplands have been managed over long period of time. Management of carbon sequestration on cropland will meet the demand for carbon balance in the above ground and conservation of biodiversity (Hairiah, et al., 2011).

LAI plays important role in influencing microclimate within- and the below-canopy microclimate, intercepting canopy water, extinguishing solar radiation, and the exchange of water and carbon gas (Bréda 2003). Any change in canopy LAI is accompanied by modifications in stand productivity (Bréda 2003). Estimation of LAI can be conducted using direct and indirect approaches. The indirect LAI determination are normally chosen over direct approaches because they are generally faster, amenable to automation, and thus allow for a larger spatial sample to be acquired (Pfeifer et al. 2012; Gonsamo 2009). LAI can be estimated indirectly using ground based optical instruments and remote sensing techniques. The latter uses theoretical light extinction models which relies on measurements of light transmission, gap fraction, and canopy reflectances (see Gonsamo 2009). Ground based optical measurements of LAI can be undertaken by measuring of; diffuse light transmission or record canopy gaps within hemispherical view (e.g., LAI-2000 and hemispherical photography); the direct solar irradiance (sunflecks) (e.g., DEMON, quantum sensors, and TRAC), and; vertical distribution of canopy elements (optical point-quadrant method). Estimation of LAI from remotely sensed data uses empirical models which consist of mathematical combinations of two or more spectral bands of optical sensor data to generate Spectral Vegetation Indices (SVIs) (Pfeifer et al. 2012). SVIs maximizes sensitivity to characteristics of vegetation while minimizes soil background reflectance, topographic, directional, and atmospheric effects which are confounding factors (Gonsamo, 2009). SVIs correlate with LAI and biomass productivity (Sjöström et al., 2011). Normalized Difference Vegetation Index (NDVI) is the commonly used SVI. Some statistical approaches such as the Least Square Regression (LSR) analysis can be used to retrieve LAI based on relationship with SVI and produced regional scale LAI map (Gonsamo 2009).

Climate change is likely to affect fire incidences in woodlands by altering their intensity, frequency, extent, and seasonality in tropical Africa. Individual species are likely to shift in ranges in African woodland due to climate change. Increased emissions of CO_2 is related to temperature increase, which affects species, populations, and ecosystems through climate change (Lovejoy, 2010). The geographical distribution of some species and timing of their life cycles is changing (Root et al.

2003). Species occuring at high altitudes are vulnerable due to limitation of expansion in upslope ranges (Lovejoy, 2010). Crop plant diversity along altitudes are uniquely different due to variation in water availability, temperature and soil factors along the elevation gradients. Thus, crop distributions are now threatened by the impacts of climate change and changes in land use. East Africa has experienced variation in climate, witnessing a variation of rainfall distribution and quantity over space and through time (Marchant et al., 2007). The East Africa montane forests have continuously received orographic rainfall, or occult precipitation (Marchant et al., 2007; Hemp, 2006; Servant et al., 1993; Maley and Elenga, 1993), which makes them unique in biodiversity over the adjacent lowland areas. Croplands in the mountain areas receive relatively high amount of rainfall but varying between 800 to 1400 mmy^{-1} in Taita Hills (Himberg, 2011), and to 1800 mmy^{-1} in Kilimanjaro (Misana, et al., 2012). Due to high population densities in these areas, they support small-scale farming typically consisting of mixed crops and tree crops while monocropping systems are predominant in the lowland areas which receive considerably lower amount of rainfall.

The distribution and survival species in the 21st century will adversely be affected by climate change though at present, land use is conspicuously the main cause of habitat loss and species extinction (Dawson et al., 2011). Climate change will make agriculture vulnerable to climate change due water balance requirement. Subsistence farmers will be adversely affected since they are not resilient to climate change (Verchot et. al., 2006). Due to this, agro-forestry is gaining popularity for enhancing resilience of agricultural landscape to climate change by enhancing carbon sequestration, improving food production, and increasing crop productivity (Verchot et al., 2006; Schroeder 1994).

Despite importances attributed to agro-forestry system, knowledge on its potential interactions with climate is not well developed. This include absence of reliable prediction models of impact of climate to agro-forestry systems (Luedeling et al. 2013) while monocultured crops can reasonably be projected with process-based crop models. Predictive models used for evaluating organisms can be used in understanding agricultural systems. Under this assumption, Species Distribution Modeling (SDM), impacts of climate change on agroforestry can be projected (Luedeling et al., 2013). This approach however, encounters challenge of lack of data by most Natural History Museums and Herbarium collections. As a result, sample size (training samples) is often small to a hundred or less (Philips et al., 2004) which affects accuracy when modelling (Phillips 2006). Lastly, resolution of environmental data are coarse and does not synchronizes with climate variables at local scale where climatic condition sharply changes with steep gradient (Platts et al., 2014; Luedeling et al., 2013).

1.2. Problem statement

Biodiversity and carbon storage in the Eastern Arc Mountains are potentially threatened by the expansion of agricultural activities and exploitation of forest resources (Pellikka et al., 2009). The inhabited and cultivated areas were once under forest or woodland that however has gradually been lost by expansion of agricultural activities. Poor cropland management on the lower montane areas compromises the resilience of the woody plant species and the ability of the areas to sequester more carbon in the above-ground. The eminent destruction has adversely affected the micro-climate which has adversely affected growth of crops and potential regeneration of woody plant species in the area. Thus, vegetation zonation along the montane areas are adversely disrupted and fragmented in the inhabited slopes of montane areas. The montane areas are currently experiencing change in climatic condition due to the global warming (Platt et al., 2008). There will be a potential upshift of species in high altitudes due to vulnerability to climate change (Lovejoy, 2010). The adaptation capacity of plant species (trees and crops) to extreme climatic conditions, parasite infestations and prevalence of diseases will be reduced. In East Africa, the mean annual temperatures will increase by 1.8˚C to 4.3˚C by 2080 (Hove et al., 2011) and precipitation will increase but varied in some regions. Climate change will cause a superimposed effect on biodiversity in Taita Hills and Mount Kilimanjaro.

Most of the studies in the montane areas mostly focus issues in forest habitats with less attention on the inhabited areas of the mountains. Another observation made in most studies is that they are based on regional scale which provides more general issues in the region than local based solution.

1.3. Objectives of the study

1.3.1. Main Objectives

This study was aimed at assessing the influence of dynamics of physical environmental factors and climate change in the montane areas on the distribution of the woody plant species and their structures (carbon storage and leaf area index) in Taita Hills (Kenya) and Mount Kilimanjaro (Tanzania).

1.3.2. Specific Objectives

The specific objectives, therefore, were to:

1. determine correlations of environmental variables along the elevation gradient of Taita Hills and Mount Kilimanjaro
2. assess the distribution and diversity of the woody plant species along the elevation gradient of Taita Hills and Mount Kilimanjaro

3. analyze the distribution of carbon storage in Taita Hills and Mount Kilimanjaro
4. assess impacts of climate change on selected species in Taita Hills and Mount Kilimanjaro
5. determine the Leaf Area Index in Taita Hills and Mount Kilimanjaro

1.4. Research Questions

1. Is there intercorrelation of environmental variables in types of cropland and along the elevation gradient of inhabited montane areas?
2. How does the woody plant species distributed in types of cropland and by variations of environmental variables in montane areas?
3. What is the distribution of the above-ground carbon storage in types of cropland and how are they affected by variations of environmental variables in montane areas?
4. Does the distribution of LAI affected by the type of cropland and variations of environmental variables in montane areas?
5. What is the potential impact of the projected climate change scenario on suitable areas and minimum elevation range for woody plant species?

1.5. Study justification

The geologic origin and period of formation of Taita Hills and Mount Kilimanjaro provide clear difference on the two montane areas. Taita Hills consist of the ancient crystalline mountains, while Kilimanjaro consist more of the recent volcanic mountain (Lovett and Wasser, 2008). This influence the kind of species making Taita Hills unique with its endemic species. Hence, the structure of the woody species contributing to the carbon storage and LAI in the montane areas needs to be determined.

The montane areas are very fertile, having high amount of rainfall distribution that has promoted high population growth on the slopes. While his is true, the slopes of the montane areas are under agricultural practices that affect species richness, carbon storage and LAI distribution along the elevation gradient. Effect of cropland on vegetation structure on the slopes requires an understanding that could be useful in the development of conservation strategies.

Taita-Taveta and Kilimanjaro ecosystems are among the Eastern Afromontane Biodiversity Hotspot (EABH) that are potentially affected by climate and agricultural activities. Forests in Taita have been reduced to just a few remnant patches (Pellika et al., 2009) due to human activities. While, in Mount Kilimanjaro, downward shifting of cloud forests in the past three decades is attributed to climate-induced fires (Hemp, 2009).

It is therefore, envisaged that the extent and speed of climate change will severely affect distribution ranges of endemic plant species, habitat and water provision to low lying areas. Thus, the adaptive capacity of trees, crops and local community might be challenged. Attention should, therefore, be paid to addressing these threats through integration of biological research and spatial modeling that will provide direction for biodiversity conservation.

1.6. Significance of the Research

The study aim at improving knowledge on understanding how variation of physical factors and cropland management along the elevation affects the vegetation structures of woody plant species, carbon storage and LAI. Derived knowledge would be vital for application on biodiversity conservation and agricultural development in the area.

Interaction model for the physical factors and vegetation structures would be important in identification of appropriate interventions along the elevation gradients and on the type of cropland in Taita Hills and Mount Kilimanjaro. In addition, interaction model will, therefore, enable prediction of responses to climate and land use changes at a species level in order to strengthen conservation initiatives in these areas.

It is envisaged that the outcome of this research will be very important for policy formulations and decision makers in agricultural and biodiversity conservation. These will include the Ministry of Agriculture, agriculture based NGOs and farmers. The use of the information generated by this study will provide an opportunity for mitigating impact of climate change not only in Taita Hills and Mount Kilimanjaro but mainstreamed across the country.

1.7. Scope of Work

This study mainly focuses on the distribution of response variables (biodiversity and carbon storage) on the elevation gradients of inhabited slopes of Taita Hills and Mount Kilimanjaro. Predictor variables were mainly the physical variables (elevation and slope), edaphic variables (pH, CEC, BD and SOC) and climate variables (MAT and MAP). The physical variables are the main determinant of climate conditions in the montane areas which ultimately influences the distribution of woody plant species and carbon storage. Edaphic variables selected on the basis of their direct influence vegetation have on them hence they can portray the condition of vegetation in the environment. Only few variables of climate and soil were selected because of high intercorrelation which would produce similar relationships with the response variables. Biodiversity aspects are restricted to the Woody Plant Species Diversity and Richness, whereby trees with diameter at breast height of 10 cm are

considered in the analysis. Leaf Area Index measurements from SunScan and Hemispherical photos are used in this study together with the Enhanced Vegetation Index. Carbon storage assessed here is the above-ground Carbon Storage of measured derived from biomass generated from tree biometric measurements of diameter at breast height and height of the tree.

1.8. Organization of the Report

This report has five chapters with sub-sections. Chapter one is an introduction of the study which covers research background, problem statement, objective of the study, research questions, justification and significance of the study. The second chapter consists of literature review on montane biodiversity, carbon storage, species distribution modelling, and climate change and leaf area index. The third chapter presents materials and methods used in carrying out the research in the field and analysis. Chapter four presents results and discussion on the research objectives. Discussion of results is combined in one sub-chapter at the end of chapter four. Chapter five has conclusions and recommendations for the study.

CHAPTER 2: LITERATURE REVIEW

2.1 Montane Biodiversity

Globally, the mountain regions constitute an estimated 20-24% of the surface area and these are scattered throughout the latitudes. The distribution of montane biodiversity patterns in the mountain regions is determined by the extensive highland areas. The mountain regions consist of biodiversity hotspot that has high levels of species richness and endemism (Cronin et. al., 2015; Oates et. al., 2004). Some of the hotspots are the West African Forests Biodiversity Hotspot and Eastern Afromontane Biodiversity Hotspot. The former consists of the Biafran Forest and Highlands (BFH) that is divided ino three ecoregions; Highlands of Cameroon, the montane forests of Mount Cameroon-Bioko and Cross-Sanaga-Bioko (Cronin et. al., 2015; Olson et. al., 2001). In Biafran Forests and Highlands, biodiversity is not evenly distributed however, the patterns of endemism relates with the elevational gradient having the concentration of species increasing towards the highland areas (Barthlott et al., 1996; Oates et al., 2004; Cronin et al., 2015). The biogeography and geology of the mountains has an influence on the distribution of the montane biodiversity. Montane areas with similar geologic evolution and biogeographic history tend to have similar biodiversity patterns and endemism in Bioko, Mount Cameroon and mainland Africa are more similar to those of the outer islands of the Gulf of Guinea (Jones et al., 1994).

The Eastern Afromontane Biodiversity Hotspot consists of several merged “ecoregions” ranging between latitudes 22°N and 22°S (Burgess et al., 2004a), and 34 biodiversity hotspots (BirdLife International, 2012). The Climate of this region is mainly driven by the Inter-Tropical Convergence Zone and the El Nino Southern Oscillation (BirdLife International, 2012). The Afromontane climate has relatively stabilized over the recent period due to the effect of the Indian Ocean. In the recent past however, variation in climate variables have been observed; for instance in the East Africa, climate variability has been documented with the variation of rainfall distribution and quantity over space and time (Marchant et al., 2007). Unlike other forests, the montane forests have continuously received orographic rainfall, occult precipitation, which depend on the presence of vegetation, or strip moisture from the air (Marchant et al., 2007; Hemp, 2006; Servant et al., 1993; Maley and Elenga, 1993).

Topography plays important role by influencing the climate across a landscape; for instance, highland areas influences rainfall by forcing moisture laden air to rise, cool and condense, acting as water tower to the surrounding lowlands (Marchant et al., 2007; Gasse,2002). The topographic phenomenon on climate is also observed on its influence on the distribution of vegetation

(Stephenson, 1989). In particular, elevation is pointed out to be a strong determinant of the distribution of the tree species in the montane areas (Hemp, 2006; Vazques and Givnish, 1998; Gentry, 1995; Woldu et al., 1989, Hamilton et al., 1989). Alves et al., (2010) cites account by Grubb (1977) on how vegetation zonation can be compressed within short elevation gradients influencing the appearance of montane cloud forests in lower elevations. Edaphic discontinuity and changes in microclimate can be observed over short gradients than longer elevation gradient distance, (Alves et al., 2010; Ashton, 2003; Takyu et al., 2003; Daws et al., 2002).

2.2. Carbon Storage

An assessment of the distribution of carbon storage in the earth's biosphere indicates that about 19% of the carbon occurs in plants and 81 % are located in soil (IPCC, 2007). Within the biosphere, 31% occurs in the biomasses and 69 % are in the soil in forests in the tropical, temperate and boreal areas. An estimation of 50% of carbon occurs in the tropical forests, while the other 50% is in the soil. One-third of the tropical forest and 25% of the tropical forest carbon stock occurs in Africa (Marshall et. al., 2012; Saatchi et al., 2011). The mountain regions form unique ecosystems that play important role in carbon storage in biosphere and carbon sequestration, particularly in arid and semi-arid areas (IPCC, 2007; Moser et. al., 2005; Vare et. al 2003; Spehn and Korner, 2005). Forests are estimated to sequester the largest fraction of carbon stock at 1,640 PgC of terrestrial ecosystem (IPCC, 2007; Sabine et. al., 2004). Thus, they are vital pools of carbon which continuously exchange CO_2 with the atmosphere (Oyebo, 2011). These pools, however, are vulnerable to landuse and climate change (IPCC 2007). Reforestation of degraded forest and development in agro-forestry would contribute to stabilizing the atmospheric CO_2 (Unruh et. al., 1993), and mitigation of climate change (IPCC, 2007). Different vegetation types are highly influenced by climate variation over landscape. Increase of the distribution of woody plant species from the semi-arid to humid conditions in Southern Africa is observed by Brien (1993). In the recent past, the assessment of climatology layers with historical MODIS-derived estimates of woody vegetation fractional cover explain changes of the woody vegetation cover in Africa (Good and Caylor, 2011). In a local scale, variation in climate and soil has been shown to cause site differences in the tree life history within a community (Muller-Landau, 2004). Under such circumstance, the mean Wood Specific Gravity (WSG) differs from close distance sites among species and communities (Muller-Landau, 2004). WSG is highly correlated with the density of carbon per unit volume and thus is of direct importance for estimating ecosystem carbon storage and fluxes (Muller-Landau, 2004; Brown, 1997, Fearnside, 1997, Nelson et al., 1999). Large

scale estimation of biomass, and carbon storage, requires a combination of ground-based and remote sensing methods (Marshall et. al., 2012).

In this study, the focus is on carbon storage at two sites in the Eastern Afromontane Biodiversity Hotspots, along transects with mosaics of various land-use. Since remotely-sensed spectral reflectance measurements are potentially useful in predicting biomass (Gemmell, 1995; Shugart et al., 2000; Phr and Donoghue, 2000; Baccini et al., 2008), relationship of MODIS-EVI was used to upscale plot carbon to a wider connected landscape of transect buffer. This is then used to explore interaction of carbon storage with the climatological layers along the elevation gradient under concomitant influences of soil and population, within and between sites.

2.3. Climate Change

Changes in CO_2 level in the atmosphere influences changes in the physical environment related to temperature increase, which has culminated in climate change. Populations, species and ecosystems respond to these changes (Lovejoy, 2010). The geographical distribution and timing of life cycles of some species is changing (Root, et. al. 2003). Species in high altitudes are vulnerable to climate change because upslope movement in search of suitable conditions is limited (Lovejoy, 2010). Crop plant diversity along altitudes uniquely varies due to difference in water availability, temperature and soil factors. It is currently evident that ecosystem services offered by the habitats are now threatened by climate change and anthropogenic land use changes. It has been estimated that about 12% of the endemic species will become extinct by 2100 as a result of climate change, and further loss will be caused by land use changes, mainly deforestation.

Studies of species migration of the Holocene period, when climatic warming was at a lower rate than is projected by the Generalized Circulation Models show that: (1) species shifted their geographical ranges, generally northwards; (2) responses of species were individualistic - the rates and direction of migration differed among taxa and species assemblages did not remain the same an (3) Species responded in an equilibrium manner and, at the continental scale of evaluation, competition and dispersal mechanisms did not seem to play a large role in the responses of species (Iverson and Prasad 1998). Currently, greenhouse warming is on the rise and the landscape fragmentation might affect competition, dispersal ability, and non-equilibrium

Important driving factors in vegetation modeling are climatic, edaphic, and topographic variables. In presence of environmental variables, geographical distribution of vegetation can be predicted. According to Iverson and Prasad (1998), modeling of vegetation pattern at local scale depends largely on local variations of topography and geomorphology (see Iverson and Prasad 1998). At

regional scales, overall vegetation patterns have been assumed to depend more on general climatic patterns.

Representative Concentration Pathways (RCPs) are set of scenario containing emission, concentration and landuse trajectories. There are four trajectories that describe four possible future climate scenarios depending on how much greenhouse gases are emitted; these include RCP8.5, RCP6, RCP4.5 and RCP2.6. These trajectories were adopted by IPCCC in 2014 for future climate simulations and research. The RCP8.5 is unique by an increasing emission of greenhouse gas over time, a representative of scenarios that lead to high concentration levels of greenhouse gas (Riahi, et al., 2007). RCP6 is a scenario where total radiative forcing stabilized shortly after 2100 without overshoot, by the application of variety of technologies and strategies for reducing emissions of greenhouse gas (Fujino, et al., 2006; Hijioka, et al., 2008). The RCP4.5 is a scenario where the total radiative forcing stabilize shortly after 2100, without overshooting target level of the long-run radiative forcing (Clarke, et al., 2007; Smith and Wigley, 2006; Wise, et al., 2009). The RCP2.6 is a representative of scenarios that lead to a very low concentration levels of the greenhouse gas. It is a "peak-and-decline" scenario. Its radiative forcing level first reaches a value of around 3.1 W/m2 by mid-century, and returns to 2.6 W/m^2 by 2100.

2.4. Species Distribution Modeling

2.4.1. Species distribution models

There are varieties of modeling techniques that can be used for developing species distribution model. These models commonly utilize associations between environmental variables and known species occurrence records to identify environmental condition within which population can be maintained (Pearson, 2007). The spatial distribution suitable for the species can then be estimated across a study region. Environmental conditions are characterized for suitable species and then, identification of suitable environment in space is done.

Environmental conditions suitable for species may be characterized using either mechanistic or correlative approach. Mechanistic models aim to incorporate physiologically limiting mechanisms in species tolerance to environmental conditions. The models require detailed understanding of the physiological response of species to environmental factors and therefore difficult to develop for all but for most well understood species (Pearson, 2007). Correlative models aim to estimate the environmental conditions that are suitable for a species by associating known species occurrence records with suites of environmental variables that can reasonably be expected to affect the species

physiology and probability of persistence. The central premise of this approach is that the observed distribution of a species provides useful information pertaining to the environmental requirements of that species.

The widely used species distribution models are correlative and they involve two types of model input data namely: 1) known species' occurrence records and 2) a suite of environmental variables. 'Raw' environmental variables, such as daily precipitation records collected from weather stations are often processed to generate model inputs. The species occurrence records and environmental variables are entered into an algorithm that aims to identify environmental conditions that are associated with species occurrence. In most cases, algorithm that can integrate more than two environmental variables is preferred since species are likely to respond to multiple factors. Also, algorithms that can incorporate interactions among variables are also preferred (Elith et al. 2006). Species distribution models that have been used mostly are the statistical (e.g. generalized linear models and generalized additive models). Other approaches are based on machine-learning techniques; maximum entropy [MAXENT] and artificial neural networks [ANNs]) (Pearson, 2007). One key factor the model algorithm requires is species data type. ANNs algorithm requiresd data on observed species absence and operates by contrasting sites where species has been detected with sites where the species has been recorded as absence. Reliable absence data is often not available; hence other algorithms that do not require obsence are handy. Maxent algorithm is therefore important in this case because it uses 'presence only' data with a background environmental data for entire study area. In addition, maxent can utilize both continuous and categorical variables to produce a continuous output predictions.

2.4.2. Maximum Entropy (Maxent)

Species distribution modeling using Maxent is based on machine learning technique. Maxent refers to an implementation of the maximum entropy method. According to Pearson (2007) the method uses 'background' environmental data for the entire study area. It focuses on how environment where the species is known to occur relates to the environment across the study area (the 'background'). The approach taken in this study is to approximate unknown probability distribution π over a finite set X, (which was the pixels in the study area) as explained by Phillips et al. (2006). The distribution π assigns a non-negative probability $\pi(x)$ to each x, and these probabilities sum to 1. The approximation of π is also a probability distribution, which is denoted as $\hat{\pi}$. The entropy of $\hat{\pi}$ is defined as:

$$H\left(\hat{\pi}\right) = \sum_{x \in X} \hat{\pi}(x) \ln \hat{\pi}(x) \tag{2.1}$$

Where *ln* is the natural logarithm. The entropy is non-negative and is at most the natural log of the number of elements in *X*. entropy is described as "a measure of how much 'choice' is involved in the selection of event" (Phillips, 2006). Thus, a distribution with higher entropy involves more choices (i.e., it is less constrained). The maximum entropy principle can therefore, be interpreted as saying that no unfound constraints should be placed on $\hat{\pi}$, or alternatively. In the recent past, maximum entropy principle has been of interest to the machine learning community, with major contribution being the development of efficient algorithms for finding the Maxent distribution. The constraints of the unknown probability distribution π is formalized by assuming that we have a set of known real-valued functions $f_1, \ldots, f_n$ on X, known as "features" (which for this case are the environmental variables or functions thereof). It is assumed that the information known about π is characterized by expectations (averages) of the features under π. Each feature f_j assigns a real value f_j(x) to each point x in X. The expectation of the feature f_j under π is defined as $\sum_{x \in X} \pi(x) f_j(x)$ and denoted by $\pi[f_j]$, which in general for any probability distribution ρ and function f, the notation $p[f]$ is used to denote the expectation of f and p. feature expectations $\pi[f_j]$ was approximated using a set of sample points $x_1, \ldots, x_m$ drawn independently from X (with replacement) according to the probability distribution π (Phillips et. al., 2006). The empirical average of f_j is $\frac{1}{m}\sum_{i=1}^{m} f_j(x_i)$, which can be written as $\tilde{\pi}[f_j]$ where $\tilde{\pi}$ is the uniform distribution on the sample points and used as an estimate of $\pi[f_j]$. Based on the maximum entropy principle, the probability distribution $\hat{\pi}$ of maximum entropy was sought subject to the constant that each feature f_j has the same mean under $\hat{\pi}$ as observed empirically, i.e.

$$\hat{\pi}[f_j] = \tilde{\pi}[f_j] \text{ for each feature } f_j \tag{2.2}$$

Mathematical theory of convex duality can be used to show that this characterization uniquely determines $\hat{\pi}$, and that $\hat{\pi}$ has an alternative characterization, which can only be described as follows, considering all probability distributions of the form;

$$q_\lambda(x) = \frac{e^{\lambda . f(x)}}{Z_\lambda} \tag{2.3}$$

Where λ is a vector of n real-valued coefficients or feature weights, *f* denotes the vector of all *n* features, and Z_λ is a normalizing constant that ensures that q_λ sums to 1 (Gibbs distributions). Convex duality shows that the Maxent probability distribution $\hat{\pi}$ is exactly equal to the Gibbs probability distribution q_λ that maximizes the likelihood (i.e. probability) of the sum *m* sample points. It also minimizes the negative log likelihood of the sample points

$$\tilde{\pi}[-\ln(q_\lambda)] \tag{2.4}$$

Which can also be written as $\ln Z_\lambda - \frac{1}{m}\sum_{i=1}^{m} \lambda.f(x_i)$ and termed as the "log loss". The empirical feature means will typically not be equal to the true means but will only approximate them. The means under $\hat{\pi}$ was restricted to be close to their empirical values by relaxing the constraint in $\hat{\pi}[f_j] = \tilde{\pi}[f_j]$ (see 2004; Phillips et al., 2006) by replacing it with $\left|\hat{\pi}[f_j] - \tilde{\pi}[f_j]\right| \le \beta_j$, for each feature f_j for some constant β_j. This also changes the dual characterization, resulting in a form of ℓ_1-regularization: the Maxent distribution is now shown to be the Gibbs distribution that minimizes

$$\tilde{\pi}[-\ln(q_\lambda)] + \beta_j|\lambda_j| \tag{2.5}$$

Where the first term is the *log loss*, while the second term penalizes the use of large values for the weights λ_j (the environmental variable). Regularization forces Maxent to focus on the most important features, and ℓ_1-regularization tend to produce models with few non-zero λ_j values (Williams, 1995; Phillips et al., 2006). Such models are less likely to overfit, because they have fewer parameters.

2.5. Leaf Area Index

LAI has been defined in different ways, as captured by Gonsamo (2009), based on various leaf shape and area. However, the purpose for which LAI is derived normally determines its definitions. These include analysis of vegetation growth, physiological activity, light attenuation, which are studied on the basis of common measurements of LAI. Gonsamo (2009) provides an overview of the most common measures of LAI as adopted in this review; 'total LAI', 'One sided LAI', horizontally projected LAI, and hemi-surface LAI. The definition of 'total LAI' was used in earlier studies of needle areas for coniferous and currently rarely used (Gonsamo 2009). Common values for LAI uses definitions of 'one-sided' and 'horizontally projected' LAI. LAI definition of 'One sided' lacks the

meaning for non-flat, highly clumped, or rolled leaves. The most widely accepted definition of LAI is the 'hemi-surface LAI', defined as the one half the total leaf surface area per unit ground surface area projected on the horizontal datum (Gonsamo 2009; Pfeifer et al. 2012). LAI can as well be defined as;

$$LAI = L / A \tag{2.6}$$

Where L is the leaf area of a canopy per unit surface area A on ground. In case of non-flat leaves, LAI can be defined as half the total intercepting area per unit surface area on the ground. The relationship between projected area and total or half surface area of leaves are shape specific. For instance, a disk and a sphere with the same diameter have the same maximum projected area, but the sphere intercepts twice as much as light as the disk with random angular distribution when averaged for all radiation incidence angles. It therefore implies that half the surface area of a sphere is twice the area of half the surface area of a disk (Gonsamo, 2009).

LAI drives both the within- and the below-canopy microclimate, determines and controls canopy water interception, radiation extinction, water and carbon gas exchange and is, therefore, a key component of biogeochemical cycles in ecosystems (Bréda, 2003). It has wider application in models since it is a major deriving factor in soil- vegetation-atmosphere, biogeochemical cycles and agro-meteorology models (Gonsamo, 2009). Any change in canopy LAI (by frost, storm, defoliation, drought, management practice) is accompanied by modifications in stand productivity (Bréda, 2003). Estimation of LAI can be conducted by using direct and indirect approaches. Current study focuses on the latter.

2.5.1. Indirect LAI determination

Here leaf area is determined by inferences from observations of another variable. They are generally faster, amenable to automation, and thus allow for a lager spatial sample to be acquired. Indirect methods of estimating LAI in situ can be divided in two categories: (1) indirect contact LAI measurements and; (2) indirect non-contact measurements. There are ground-based measurements that usually integrate over one single stand only while air-and space-borne measurements are applied for determining LAI on landscape or forest level (Gonsamo, 2009).

2.5.2. Allometric technique

The technique relies on relationships between leaf area and dimensions of the woody plant element carrying the green leaf biomass i.e. tree height, crown base height, stem diameter etc. Allometric relations between leaf area determined via destructive sampling and the basal area of the

physiologically active sapwood area have been proposed. Such sapwood-to-leaf-area conversions are based on the pipe model theory that stems and branches are considered an assemblage of pipes supporting a given amount of foliage. The highest correlation coefficient were found between sapwood area and leaf area (Jonchkeere, 2004) very high correlation coefficients between stem basal area and leaf area, and between Diameter-at-Breast-Height (DBH) and leaf area (Jonchkeere, 2004) of trees in the same stand. The use of sapwood area or DBH to predict LAI may result in considerable LAI overestimation. Physiologically, the amount of foliage supported by sapwood decreases as tree approach maximum height, likely because of hydraulic limitations to water transport in all trees that lead to cavitations of vessels (Gower, et al., 1999). The relationship between leaf area and sapwood area is governed by sapwood permeability as indicated by the linear relation between leaf area and the product of sapwood area and sapwood permeability. Sapwood area, sapwood permeability, and the product of these two variables decreased with depth through the crown of the trees. According to Gower, et al., (1999) the method is more appropriate than optical gap fraction-based measurements, for stands with high leaf area, because these optical measurements saturate at LAI values of about 5. Allometric equations are restricted because of their site-specificity, as sapwood area/leaf area relationships have been shown to be stand-specific and dependent on season, site fertility – e.g. nutrition and soil water availability -, local climate, and canopy structure – e.g. age, stand density, tree size and forest management (Jonchkeere, 2004).

2.5.3. Optical Remote Sensing of Leaf Area Index

Indirect approaches have enabled efficient estimation of LAI efficient for canopy structure over large areas (Pfeifer, et al., 2012; Gonsamo, 2009). Indirect methods derives LAI from measurements of the transmission of radiation through canopy which make use of the radiative transfer theory (Jonckheere et al., 2006; Breda, 2003). The methods are non-destructive that applies statistical and probability approach to foliar element pattern in the canopy (Bréda 2003). Remote sensing methods and ground based optical instruments are used for estimating LAI indirectly by measuring light transmission, gap fraction, and canopy reflectances using theoretical light extinction models (Gonsamo 2009). Ground based optical measurements of LAI uses related light extinction models to describe canopy structural variables. Thus, three types of ground based optical measure can be used; measuring diffuse light transmission (canopy gaps) within hemispherical view (e.g., hemispherical photography and LAI-2000); measuring the vertical distribution of canopy elements (optical point-quadrant method), and; measuring the direct solar irradiance (sunflecks) at a known solar angles along a transect (e.g., DEMON, quantum sensors, and TRAC), and (c)

2.5.4. Empirical models for estimating LAI

Empirical models for LAI can be estimated from remotely sensed data which typically relies on Spectral Vegetation Indices (SVIs) consisting of mathematical combinations of two or more spectral bands of optical sensor data (Pfeifer et al., 2012). SVIs correlate with LAI and productivity (Sjöström et al., 2011). Empirical model rely on physically based relationships between LAI and canopy spectral reflectance. Spectral reflectance and transmittance of leaves in the near infrared region is high and absorptance is low. Early studies indicated leaf reflectance measurements of visible and near infrared energy strongly correlates between the Red and Near Infrared transmittance ratio and LAI measured on ground (Gonsamo 2009). The most commonly used SVI is the Normalized Difference Vegetation Index (NDVI). SVIs maximize sensitivity to the characteristics of vegetation but minimizes reflectance from soil, directional, atmospheric, and topographic effects which are apparently confounding factors (Gonsamo, 2009). The shortwave infrared (SWIR) reflectance in SVIs can be used to minimize the influences of background soil or land cover variation during empirical LAI modeling. Remotely sensed spectral bands can be related with the amount of photosynthetic biomass (through algebraic combinations) and all bare soil form a line in spectral space.

Least Square Regression (LSR) analysis, which combines linear, exponential and polynomial regressions can be used for empirical retrieval of LAI based on LAI-SVI relationship. Thus, large scale regional LAI map can be produced using LSR techniques (Gonsamo 2009). However, LSR normally has limitation in application; it assumes that the structural data model for deriving unbiased estimates errors are spatially independent and there is no measurement errors in the independent (SVI) variable. However, LSR can be a biased predictor when there is error in measurement arising from functional than structural data model. In the presence of measurement errors, modified least square and Thiel-Sen regression analysis has been demonstrated by Fernandes and Leblanc (2005) (Gonsamo, 2009) to approximate analysis of its prediction confidence intervals. LSR limitations has, however, been circumvented by constructing an integrated, Canonical Correlation Analysis (CCA), index to represent multiple predictor variables in a simple linear context (Gonsamo 2009). CCA proved to be powerful tool for empirical retrieval of LAI (Heiskanen, 2006; Lee et al., 2004). LAI-SVI empirical relationship and can be established by fitting measured LAI values to the corresponding SVI using LSR, generic form expressed as:

$$LAI = f(SVI) \tag{2.7}$$

Advantage of the SVI based empirical approach over physically based reflectance or canopy models, is its simplicity and ease of computation. However, it is associated with two major difficulties: (a) SVI normally approaches a saturation level asymptotically when LAI exceeds a certain value, depending on the type of SVI and; there is no unique relationships between LAI and SVI of a choice, but rather a family of relationships, each a function of chlorophyll content and/or other canopy characteristics, soil background effects and external conditions. Thus, there is no universal SVI-LAI equation applicable to diverse vegetation type; it is, therefore, difficult to use the empirical LAI modeling with large remote sensing images. Based on these limitations and considering the theoretical formulation of SVI-LAI relationships, SVI predicting power and stability can be assessed based on:

$$SVI = f(LAI) \tag{2.8}$$

This equation is used to localize SVI-LAI solutions. Sensitivity analysis of SVI to LAI has been carried out by various studies. These include the relative equivalent noise (REN) and vegetation equivalent noise (VEN) to represent noise in SVI (Gonsama, 2009).

2.6. Sustainable Development Goals

The 2030 Agenda for Sustainable Development has 17 Goals that were adopted by Member States of the United Nations in the year 2015 (United Nations, 2017). Relevant to this study is SDGs 13 and 15 which are interrelated. SDG 15 focuses on protection and restoration of biodiversity which helps in mitigating climate change through providing landscape resilience to the impacts. Currently, climate change is partially driven by land use changes which destroy landscape potential to sequester carbon. In turn, climate change affects species distribution especially in montane areas where species range shifts upslope or downslope. The alteration of climate pattern in the region will adversely affect growth of agricultural crops and distribution natural plants on the landscape. Thus, long term carbon sequestration and system resilience is precarious. Mitigating climate change and its impacts requires anchorage of strategies on the Paris Agreement on climate change. Most nations, the Government of Kenya included, have followed up by preparing the Nationally Determined Contributions (NDCs) (United Nations, 2017). The NDCs outlines development approaches and actions aimed at lowering greenhouse gas emissions and building climate resilience. This study plays important role in contributing information on carbon sequestration in montane areas and potential impact of climate change on agroforestry and carbon sequestration. Reducing GreenHouse Gases is part of NDC commitment by the Government of Kenya pursued by relevant authorities.

2.7. Statistical Analysis

Research samples can be analyzed by different types of statistics. One of the simplest statistical analyses that are important to subject sample data is a common descriptive statistics. The descriptive statistic analysis provides simple summaries about sample and observations made during research. Analysis of distribution of a single variable in statitstics is referred to as univariate analysis while analysis of more than one variable is bivariate or multivariate analysis (Johnson and Wicherin, 2007; Ruohonen, 2011). The range analysis is an aspect of descriptive statistics that describes the minimum and the maximum values distribution of sample data; while frequency describe how many times certain values or feature appears in a set of sample data. The central tendency of sample data is described by mean, median and mode. The mean measures the average of sum of values in a sample data and the median measures the distribution of data value in the middle of a set of sampe data. Visual inspections of data provide a quick check on normal distribution of univariate sample data. These include the frequency distribution (histogram), boxplot, P-P plot (probability-probability plot), and Q-Q plot (quantile-quantile plot) (Johnson and Wicherin, 2007). Commonly used for inspecting normally distributed data for single variables is boxplot; this is because it shows more information than other visual inspections. Beyond the descriptive statistics, inferential statistics are used when conclusion needs to be drawn about sample data. Some of inferential statistical test for distributions of data are Fisher's F test which is used for comparing variance of two independent data samples. Independent T-Test - Tests for the difference between the same variable from different populations. Student's t test is used in small-sample work for comparing two parameter estimates (McCrawley, 2007). While, the Fisher's F, in analysis of variance (ANOVA) is used for comparing two variances (Ruohonen, 2011). Student t test and ANOVA tests variables that are in continuous scale and approximate normally distributed. Mean is the representative measure for normally distributed continuous variable and statistical methods used to compare between the means are called parametric methods. For non-normal continuous variable, median is representative measure, and in this situation, comparison between the groups is performed using non-parametric methods. Most parametric test has an alternative nonparametric test.

Quantitative measures of dependence include correlation analysis; Pearson's R is used when both variables are continuous or Spearman's rho if one or both are not continuous variables. Pearson's R correlation tests for the strength of the association between two continuous variables. Simple regression can also be used to measure dependence, which tests how change in the predictor variable predicts the level of change in the outcome variable. Multiple linear regression is performed to test how changes in the combination of two or more predictor variables predict the level of change in the

outcome variable (Johnson and Wicherin, 2007). Many of the basic statistical methods such as regression and Student's t test assume that variance is constant, but in many applications this assumption is untenable. GLM comes in handy since it is used when variance is not constant, and/or when the errors are not normally distributed (McCrawley, 2007).

2.8. Summary

This section addresses issues on the distribution of biodiversity, carbon storage and Leaf Area Index and species distribution modeling under the climate change specifically in East Africa. Most of the studies have been focused on the forest areas not taking consideration of the inhabited part of the mountain slopes to be important areas for species conservation. The carbon storage on the inhabited parts of the mountain slopes cannot be neglected as these areas potentially form conservation hotspot due to challenges it present to biodiversity conservation. Very important but less conspicuous in most studies are role of croplands on biodiversity (especially species richness) and carbon storage. Despite most studies concentrating on the influence of physical factors, cropland matrix are also important to look at since they potentially affect biodiversity and carbon storage.

Most of researches on mountain biodiversity always focus on one mountain. Consideration of the potential effect of evolution on the mountain on bioversity has not been made. For instance, comparative studies on mountain areas that evolved differently like Taita Hills and Mount Kilimanjaro (Eastern Arc Mountain) are scanty in libraries. The evolution of these mountains affects their soils and underlying geology hence, the plant species and even agricultural activities.

This study was based in Taita Hills and Mount Kilimanjaro up to the highest elevation with croplands. Focus on the two mountains was to provide any local or site based difference intrinsic to the mountain areas.

CHAPTER 3: STUDY MATERIALS AND METHODS

3.1 Study Area

3.1.1. Kenya - Taita Hills

The location of Taita Hills occur within Taita-Taveta County, previously mentioned in other literature as Taita-Taveta District (Himberg, 2011). The county occurs between 2^0 46′ South and 4^0 10 South and longitudes 30^0 14′ east and 37^0 36′ east. It is bordered by Tana River, Kitui and Makueni Counties to the north, Kwale and Kilifi counties to the east, Kajiado County to the northwest and the Republic of Tanzania to the south and southwest (Fig. 3.1).

Taita Hills are a series of the eastern arc mountains located in south-eastern Kenya. The hills are unique in their geomorphologic setup amidst the low plain lands of Tsavo. The area is divided into three major Agro-Ecological Zones; upper zone, lower zone and volcanic foothills. The lower zone comprises of Tsavo plains that range from 400 to 600 m above sea level (Himberg, 2006). The Taita Hills transend the volcanic foothills from 700 to 2208 m above sea level (Pellika, 2009). However, an illustrative mountainous part of Taita Hills, that forms the upper zone, is vivid from 1,200 m above sea level (Himberg, 2006). The highest peak in Taita Hills is Vuria at 2208 m followed by Yale at 2115m. The central mountain massive area is called Dabida; others include Mbololo, Sagala and Kasigau. The area of study is marked by a transect that runs from lowland in Mwatate area at elevation 840m asl through to high areas in Vuria (2200m a.s.l.). The volcanic foothills in Taveta Division has potential for underground water and springs emanating from Taita Hills; while the lower plain has precious gemstones that are mined.

The area experiences two rainy seasons per year. The long rains fall on the hills from March to May and the short rains from October to December. Up in the hills the average rainfall is 1,500mm or more per year while surrounding plains have a maximum of 500 mm per year.

The southeastern slopes of Taita Hills receive more precipitation than the northwestern slopes due to the orographic rainfall pattern (Jaetzold and Schmidt 1983). An annual mean temperature varying from 16°C to 18° C is experienced on the hills; while an annual mean temperature of 25° C occur in the surrounding plains. The major rivers in the district are Tsavo, Voi and Lumi. Small springs and streams in the district include Njuguini, Sanite, Njokubwa Kitobo, Maji Wadeni, Humas Springs and Lemonya Springs. There are two lakes, Jipe and Challa both found in Taita Taveta Division. Lake Challa is a crater lake with minimal economic exploitation, while Lake Jipe has some economic activities covering small scale irrigation and artisenal fishery. Both lakes are served by springs emanating from Mt. Kilimanjaro.

Taita Taveta is classified as an arid and semi-arid (ASAL) district. Out of the total area of 17,128.3 Km^2 covered by the district 10,680.7 km^2 or 62 per cent is occupied by Tsavo East and West National parks, 4,100.7 km^2 or 24 per cent is range land suitable for ranching and dry land farming, while only 2,055.4 km^2or 12 per cent is available for rain-fed agriculture. Of the 2,055.4 km^2 arable land, 1,774.5 km^2 or 74 per cent is low potential agriculture land, receiving an annual mean rainfall of 650mm.The upper zone is suitable for horticultural farming.

Three types of forests occur in the Taita Hills: indigenous forests, and traditionally protected (sacred forests called *fighis*), and plantation forests. The indigenous forest has an approximated total area of 6 km^2 with forest with closed and intact canopy with two square kilometres. The remaining four square kilometres is open forest with broken and non-contiguous canopy (Newmark 2002).

3.1.2. Tanzania - Kilimanjaro Area

Field survey was conducted in Mount Kilimanjaro area, in southern slopes of the mountain (Fig. 3.1). The area lies in Kilimanjaro Region, which is bordered to the north and east by Kenya, to the South by Tanga Region, to the Southwest by the Manyara Region, and to the West by the Arusha Region. Administratively, the region is divided into seven districts: Rombo, Hai, Moshi Rural, Moshi Urban, Mwanga, Siha and Same. Moshi Rural, in which the study site is located, is divided into 31 wards. The study site traverses Kirua Vunjo Kusini (South), Kirua Vunjo Magharibi (West) and Kirua Vunjo Mashariki (East). Kilimanjaro area has three major agroecological zones: the highland zone (1200 - 1800 m asl) with coffee - banana belt occurring below a narrow forest strip half-mile; the midland zone occur between 900 and 1200m is dominated by maize and beans, and; the lowland zone which is occurs below 900m asl) (Misana et al., 2012). The narrow forest strip was established as a social and buffer to forest on the lower edge of the forest to provide fuelwood and wood products to local people (Misana et al., 2012).

The montane forest has trees of different genera including, *Camphor*, *Ocotea* and understorey ferns and *Cyathea spp*.. The study area falls below montane forest, which Munishi (2007) describe as densely populated agro-forest area that integrates multi-purpose trees such as *Gravillea*, *Albizia*, *Cordia* and *Eucalyptus* (mainly above 900 m above sea level). The area is predominated by fertile red volcanic soils while some areas in the lowlands are dotted by black cotton soil.

Annual rainfall varies with altitude. The highlands receive an annual rainfall of about 1200 to 2000 mm; midlands (1000 to 1200 mm) and; lowlands (400 to 900 mm). The montane zone, which is a forest belt above 1800 m, receives the highest rainfall in excess of 2000 mm per year.

The area supports agricultural development in the region due to the fertile soils and favourable climate. Population density is high and varies within the agro-ecological zones. For instance, in the lower slopes population density in 2002 was 200 persons/km^2, 650 persons/km^{2}on the higher slopes. The southern slopes between 1200 to 1800 m above sea level are most densely populated zone (Soini, 2005).

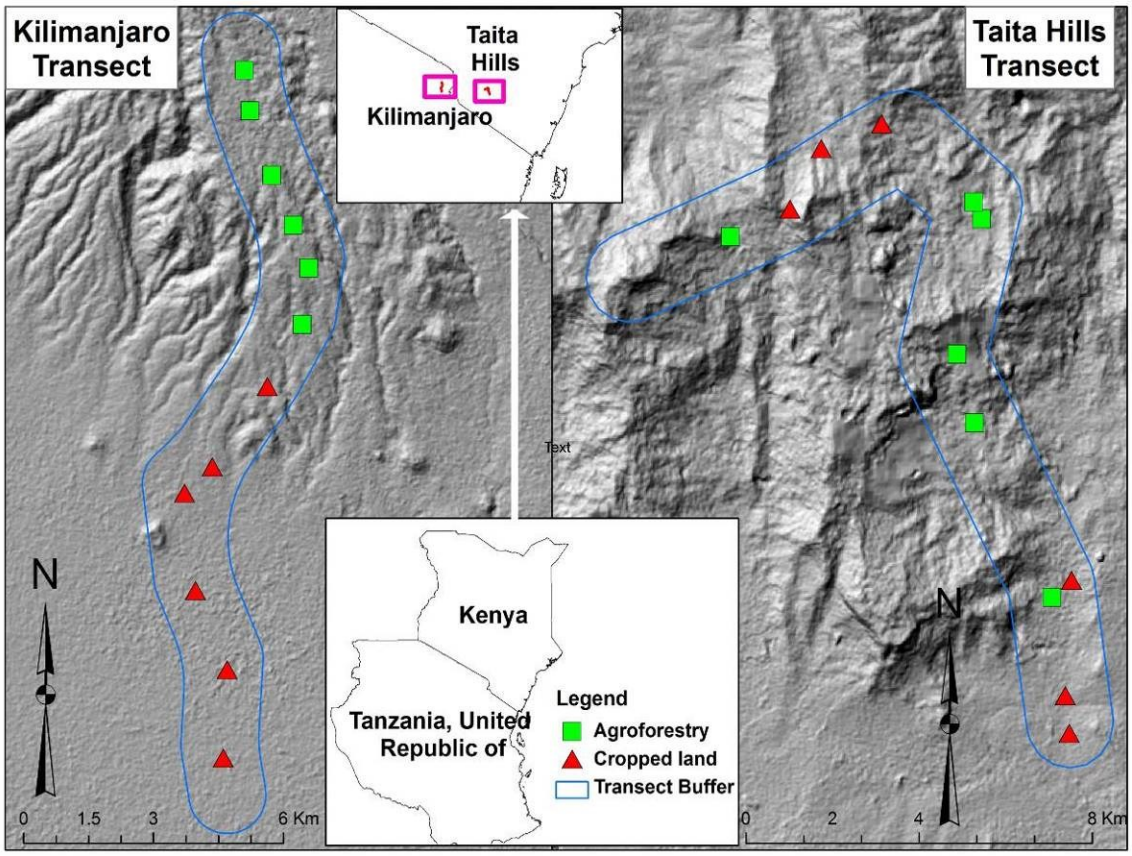

Figure 3.1 - Map of study sites showing distribution of plot locations on transect in Taita Hills (right) and Kilimanjaro (left).

3.2. Research Design

Study transects running approximately 30 km long was established on the inhabited slopes of Mount Kilimanjaro and Taita Hills. A buffer of 4 km was generated on either side of the line transect; that is 8 km wide belt transect. In Taita Hills the transect runs from Mwatate from an elevation 840 m through Wundanyi to about 2000m in Vuria. While in Mount Kilimanjaro it starts from Miwaleni area at about 730 m and running northwards to Kirua-Vunjo at an elevation of 1800 m, near the boundary of the National Park (TANAPA).

Stratified random sampling 30 georeferenced points were initially generated along the transect. The points were traced using a Global Positioning System (GPS). During the exercise, the points were

noted whether it falls in agroforestry area or cropped land, according to description of IPCC, (2006). In Kilimanjaro, 15 georeferenced points occurred in each type of cropland; while in Taita Hills, 20 occurred in agroforestry areas and 10 in cropped land. These points were further adjusted by removing some which were very close (< 1km) to each other. This was to avoid possibility of more than one point appearing in a pixel of environmental layers which some has a resolution of 930m. Finally, the number of plots used for sampling in Kilimanjaro was 12; 6 one hectare plots occurring in both agroforestry areas and cropped land. In Taita Hills, a total of 14 one hectare plots; 7 plots distributed in both agroforestry areas and cropped land. One hectare sampling plots was used for collecting primary data for species, tree biometries, and measurements of LAI. An opportunistic sampling of woody plant species was carried out for species distribution on the transect. Secondary data was acquired for species distribution data and spatial environmental layers (variables).

3.3. Data Sources and Tools

This section describes the data sources and tools used in this study.

3.3.1. Data Sources

i. Primary data

Data collected included the woody tree species, abundance, tree diameter at breast height (dbh), tree height, SunScan leaf area index, Hemispherical photographs. Field samples were acquired from one hectare plot (100 m x 100 m plot) from a transect that rran from the lowland in Kenya (Taita Hills); Mwatate area (approx. 840 m asl) to high areas in Vuria (2200 m asl). In Tanzania (Kilimanjaro), the transect ran from low lying areas of Miwaleni (716 m asl) to high areas in Kirua-Vunjo (1800 m asl). Sampling plot was established a random point across a one Kilometer buffer on either side of the line transect. Distribution along the altitudinal gradient was taken into consideration to cover rainfall and temperature gradients in the areas were considered. Identification of sites for sampling was facilitated by use of aerial photos and ground survey. Depending on the variety of land cover types across the transect, one or more plots were established.

ii. Secondary data

These are data that were acquired from various sources as input data for this study. These included species occurrence data, environmental layers such as the climate projection layers, biophysical layers and edaphic variable layers.

a) Species distribution data

Online database such as Global Biodiversity Information Facility (GBIF), PROTO were used as sources for searching species distribution data.

b) Environmental Variables:

Biophysical variable: Biophysical variable used was the Moderate Resolution Imaging Spectroradiometer (MODIS) Enhanced Vegetation Indices (EVI) (MODIS-EVI). MODIS-EVI, 16-days intervals was downloaded from the NASA archives for months corresponding to periods when field data was collected in 2012, 2013 and 2014 (Fig. 3.2, Table 3.1). These covered Taita Hills and Kilimanjaro area with the mean MODIS-EVI for the periods used as environmental variables. MODIS-EVI is considered due to the effect of EVI on minimizing variations in canopy background such as soil reflectance (Huete and Didan, 2006).

Edaphic variables: Four edaphic variables were selected for analysis; these included the soil pH, soil organic carbon (SOC), Cation Exchange Capacity (CEC), and soil bulk density (BD) (Fig.3.2, Table. 3.1). The soil variable layers were downloaded in October 2014 from isric database..

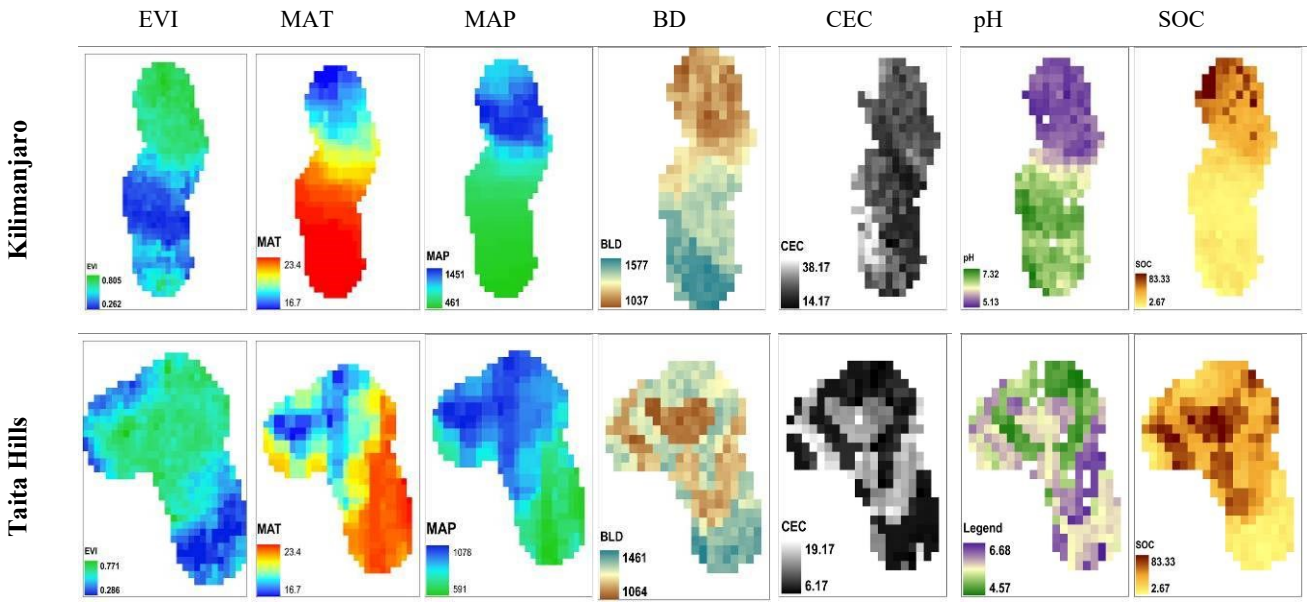

Figure 3.2 - Spatial environmental variable layers in Kilimanjaro and Taita Hills transect: EVI - Enhanced Vegetation Index, MAT - Mean Annual Temperature, BD-Soil Bulk Density, pH, and SOC-Soil Organic Carbon

Table 3. 1: The environmental factors, variables (and their units) used as predictor variables including their spatial resolution and their sources (2014).

Environmental factors	Variable	Abbr.	Unit of Measurement	Spatial Resolution	Source of data
Edaphic factors six layers mean estimate for depths; 2.5, 10, 22.5, 45, 80, and 150 cm depths	Soil Organic Carbon	SOC	C/permilles	930m	isric.org
	Cation Exchange Capacity	CEC	cmolc/kg	930m	isric.org
	pH	pH			isric.org
	Bulk Density	BD	kg/m3	930m	isric.org
Climate factors	Mean Annual Temperature (WorldClim ID – BIO1)	MAT	^{O}C	659m	WorldClim
	Mean Annual Precipitation (WorldClim ID – BIO12)	MAP	mm y^{-1}	659m	WorldClim
Biophysical factor	Enhanced Vegetation Index MODIS-EVI 16 days interval	EVI		659m	NASA
Land-use	Cropped land	These are sparsely populated areas predominated by mono-cropping system			
	Agro-forestry	These are moderate to densely populated areas with fruit trees, and other trees. Mixed crops both cash and food crops			

c) Climate baselines and projection layers

High-resolution ensemble climate projections for Africa were obtained from WorldClim while current climate layer variables were from the high-resolution ensemble climate projections for Africa from the WorldClim Baseline climate data; Temperature and Moisture variables (Table 3.2).
Climate layers used for SDM were the future projected climate layers, the ensembled Representative Concentration Pathway (RCP) of IPCC-AR5 (RCP4.5 and RCP8.5) at 30s resolution. The RCP4.5 and 8.5 projections were for the mid-century 2041-2070 (2055) and late-century 2071-2100 (2085).

Table 3. 2: Climate variables

Temperature (tbio)
Mean annual temperature [BIO1]
Mean diurnal range in temp [BIO2]
Isothermality [BIO3]
Temperature Seasonality [4] [BIO4]
Max temp warmest month [BIO5]
Min temp coolest month [BIO6]
Annual temperature range [5] [BIO7]
Mean temp warmest quarter [6] [BIO10]
Mean temp coolest quarter [6] [BIO11]
Potential evapotranspiration [7] [PET]
Moisture (mbio)
Mean annual rainfall [8] [BIO12]
Rainfall wettest month [BIO13]
Rainfall driest month [BIO14]
Rainfall seasonality [4] [BIO15]
Rainfall wettest quarter [6] [BIO16]
Rainfall driest quarter [6] [BIO17]
Annual moisture index [9] [MI]
Moisture index moist quarter [6] [MIMQ]
Moisture index arid quarter [6] [MIAQ]
Number of dry months [10] [DM]
Length of longest dry season [11] [LLDS]

3.3.2. Tools

a) Equipments

i. **SunScan (Delta-T Device)** was used for measuring LAI in low canopy vegetation including crops

ii. **Hemispherical camera**, Nikon D5000 fitted with a fish-eye lens adapter (Nikon FC -lens 5mm f/2.8, focal length of 5mm, and operating at manual focus mode) was used for taking hemispherical photographs for canopy gap fractions.

iii. Range pointer (with LED) was used for measuring tree heights

iv. Global Positioning System (GPS), Garmin 550 T was used for taking geographical references of sample measurements taken, tracing sampling locations in the field, laying plot designs (of 20m x 20m and 100m x 100m size).
v. Compass was used for taking slope directions, laying plot designs (of 20m x 20m and 100m x 100m size).
vi. Tape measure (50m) was used for laying plots (of 20m x 20m and 100m x 100m size) in dense canopy areas where GPS cannot receive signals from GPS satellites in space.

b) Software

i. ARCGIS 10.2 was used for generating spatial interpolations, species distribution models, and output maps
ii. CAN-EYE software was used for processing hemispherical photographs for the extraction of Leaf Area Index (LAI).
iii. R Statistics was used for statistical analysis and modeling

3.3. Methods

3.3.1. Spatial Data Preparation

The spatial environmental layers (variables) were acquired in raster format in different spatial resolutions. The layers were resampled to 930m resolution in ArcGIS 10.2, the smallest scale for edaphic variables. The transect buffer area was used for clipping the raster layers using extract by mask in ArcGIS. Plot data points were overlaid on the layers to ensure not more than one plot occur in a pixel of 930m resolution. Pixel values on where the plots occur were extracted by Extract to Point tool in ArcGIS where attributes of all environmental layers were created in one data point layer. The data point values was exported to spreadsheet from where attributes were linked up and used for statistic analysis and spatial modeling.

3.3.2. Distribution of environmental variables

Extracted values for environmental values were analysed against elevation values and intercorrelated against each other using Pearson correlation. The values were disaggregated by types of cropland their means compared using Student t-test and variation compared by Fischer F test within and between the sites.

3.3.3. Species abundance and distribution

Species distributions were acquired from field sampling as well as existing databases both in Kenya and Tanzania. Species distributions were extracted from the databases of the National Museums of Tanzania and the National Museums of Kenya, and other organizations. Most of the data had both species and spatial attributes, which was important for analysis. Field sampling was carried out along an established transect on 1 hectare plot. GPS was used to mark geographic locations (latitude and longitude) and elevation. 14 plots were established in Taita Hills and another 12 in Kilimanjaro area. Woody plant species were assessed in these plots making observations on the population structures within the plot. Crop types, especially low canopy plants were recorded during the field survey.

3.3.4. Woody plant Species diversity indices

Various diversity indices were analyzed to assess the species association between the types of cropland in Mt. Kilimanjaro and Taita Hills . Indices used include were: Species Richness (Chao1), Evenness ($e^{\wedge H}/S$), Equitability (*J*), Dominance (D), Shannon Wiener Index. Bias corrected estimation of total species richness was derived using Chao1 (Hammer et al.,
2001). Evenness was used to indicate how similar, in abundance, the species are along the elevation gradient in each site. Evenness of species distribution was calculated based on Buzas and Gibson Evenness index (Hammer et al., 2001)

$$E=e^{\wedge H}/S \tag{3.1}$$

where *e* is the natural logarithm, *H* is Shannon index diversity and *S* is the species richness.

Equitability (*J*) was used to measure how individual species are evenly distributed among the present taxa. This measure is given by dividing Shannon diversity by the logarithm of number of taxa. Dominance of species assessed the proportion of the most abundant species in each site. Dominance *D* is given by 1-Simpson index. This value range from 0 (where all taxa are equally present) to 1 (where one taxon completely dominates the community). Berger-Parker Dominance was used to calculate the total number of individuals in the dominant taxon relative to sample population (n). The diversity of woody plant species in the types of cropland, and between the sites was derived using Shannon Diversity Index (*H*), an index which considers the number of individuals as well as number of taxa (species richness).

$$\text{Relative} \cdot \text{Density} = \frac{\text{Number} \cdot \text{of} \cdot \text{individual} \cdot \text{of} \cdot \text{the} \cdot \text{species}}{\text{Number} \cdot \text{of} \cdot \text{individual} \cdot \text{of} \cdot \text{all} \cdot \text{the} \cdot \text{species}} \times 100 \quad (3.2).$$

$$\text{Relative} \cdot \text{frequency} = \frac{\text{Number} \cdot \text{of} \cdot \text{occurence} \cdot \text{of} \cdot \text{the} \cdot \text{species}}{\text{Number} \cdot \text{of} \cdot \text{occurence} \cdot \text{of} \cdot \text{all} \cdot \text{the} \cdot \text{species}} \times 100 \quad (3.3)$$

Upscaling of species richness on a map was performed using a background environmental variable that has high correlation with the richness.

3.3.5. Comparison of diversities

Shannon diversity *t* test was used for comparing the Shannon diversities of the woody plant community in Taita Hills and Mount Kilimanjaro, and; the woody plant community in cropped land and agro-forestry within and between sites.

3.3.6. Similarity and Distance Indices

The woody plant communities were compared across the two sites using Jaccard index. This index measures similarity of the community based on binary data. The index calculated the proportion of woody plant species shared between Taita Hills and Mount Kilimanjaro. Jaccard's index is expressed as follows:

$$J = \frac{S_{KT}}{S_K + S_T + S_{KT}} \quad (3.4)$$

Where S_K and S_T are the numbers of species that are unique to Taita Hills and Mount Kilimanjaro, respectively and, S_{KT} is the number of species common to the two sites. The index (J) was then converted into percentage.

3.3.7. Measurement of Above-Ground Carbon Storage

A total of 14 plots and 12 plots of 1 ha were sampled for DBH along the elevation gradients of Taita Hills and Kilimanjaro respectively. Out of 12 plots sampled in Kilimanjaro, 6 plots occurred in both agro-forestry areas and cropped land. While, 7 plots were distributed in both cropped land and agro-forestry areas in Taita Hills.

DBH measurements were restricted on the woody plant species with DBH >= 10 cm. In Kilimanjaro, sampling was carried out from the elevation 715m asl in Miwaleni spring area to the elevation of 1700m asl near the boundary of Kilimanjaro National Park (KINAPA) while in Taita Hills, the lowest elevation was 716m asl in Mwatate and the highest was 1952m asl. A total of 982 individual

woody trees were sampled for diameter at breast height (dbh) in Kilimanjaro while in Taita, 953 trees were sampled from the lowland of Mwatate to Vuria transect at 1952m asl. Variables that were measured include the tree DBH, Height and the stock density of the population.

3.3.8. Plot Carbon Estimation

Biomass above the ground was derived from the tree biometric parameters mainly the diameter-at-breast height (*D)* and tree height (H) measured from the plot with the wood specific density as a function in the model. Database for the Global Wood Density (Zanne et al., 2009) was used for referencing the Wood Specific Gravity (ρ) of the woody trees at species level, genus or family. An improved pantropical allometric model by Chave et al., (2014) was employed for estimation of biomass above the ground. Biomass above the ground was converted to AGC at plot level using 50 %, a ratio assumed to be AGC in AGB (Marshal et al., 2012; Chave et al., 2005).

$$AGB = 0.0673 \times \left(\rho \times D^2 H\right)^{0.976} \quad (3.5)$$

The above model (eq 3.5), performed well across different types of forest and bioclimatic conditions (Chave et al., 2014). Measuring heights of all trees in dense forests and variable landscape was not easy to use inclinometer due to invisibility of the tree crown. Efforts were made to measure approximately 100 individual trees in the four plots in the forest then estimated height of the remaining individuals in a plot by height-dbh relationship model. An exponential allometric model for estimating height-diameter relationship (Marshall et al., 2012; Fang and Bailey, 1998) was used to estimate the heights for trees whose height was not recorded on the four forest plots (eq. 3.6).

$$H_{est} = H_{\min} + \{[H_{\max} - H_{\min}] \times [1 - \exp(-c \times \{dbh - 10\})]\} \quad (3.6)$$

3.3.9. Modeling Response Variables and Model Validation

Modeled response variables were Species Richness, AGCS and LAI in Taita Hills and Mount Kilimanjaro. Regression models provided means of prioritizing predictor variable used for modeling response variable on the transects. Model of species richness were generated and the Akaike Information Criterion (AIC) was used for selecting the best model that explained the relationship of response variable with the predictor variable. Regression model that had the best fit and least AIC from each site was used for modeling response variable. Out of 12 plot data, eight were used for generating regression models in each site while four plots data points were preserved from modeling

for validation of the models. These point values were selected randomly; two from agro-forestry areas and another two from cropped lands. Once the model was generated the preserved predictor variable for the plots were ran on the model to predict response variable in plots. After this, the modeled response variable and plot response variable data were compared using One-Way ANOVA and also correlation analysis.

3.3.10. Measurement of Leaf Area Index

Indirect methods for estimating LAI on ground was employed in accordance to Pfeifer et al., (2012). Hemispherical photography and SunScan measurements were made within the series of established one hectare plots that run from low to high elevations of Taita Hills and Mount Kilimanjaro. Plot for measuring LAI was designed similar to VALERI for elementary sampling units (Pfeifer et al 2012; Garrigues et al., 2002) was adopted for sampling LAI in the field. Five subplots measuring 20 x 20 m were established within 100 m x 100 m as shown in figure 3.3.

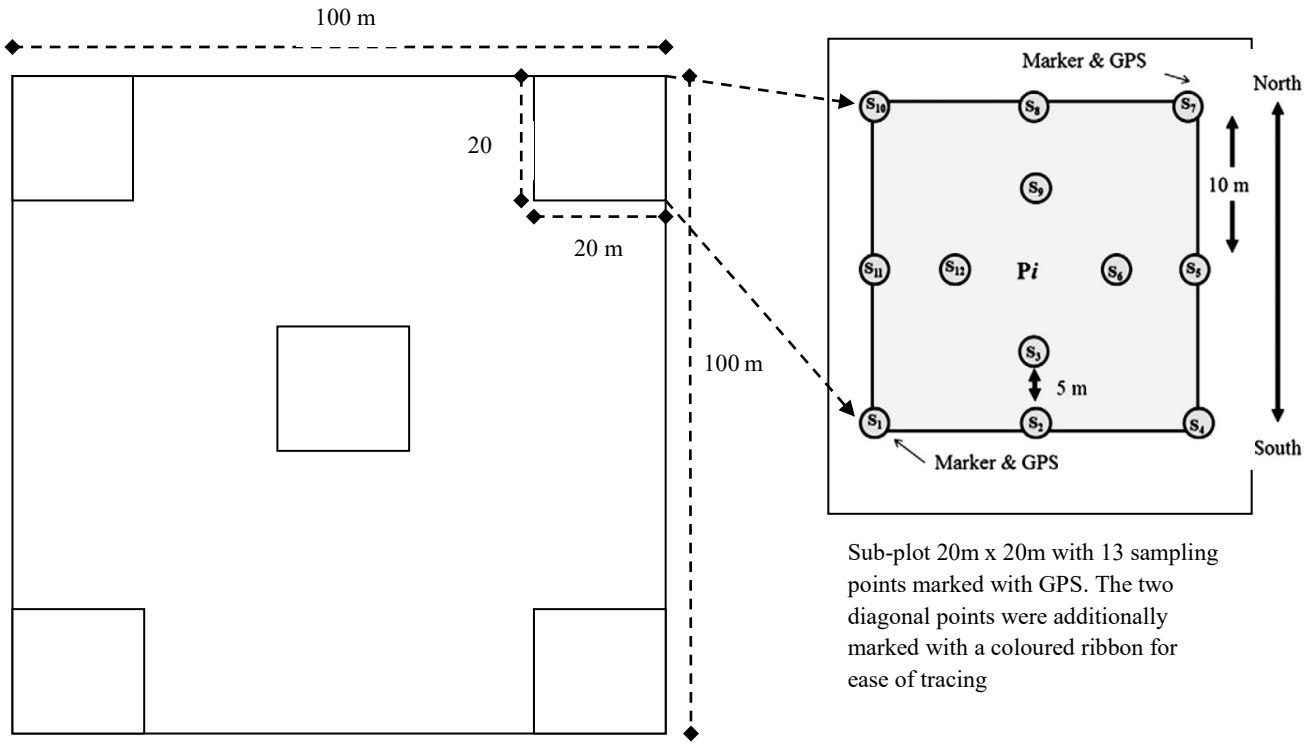

Figure 3.3 - Plot-based sampling design for measuring LAI by hemispherical photography and SunScan Instrument.

3.3.11. Measurements of LAI using SunScan Instrument

Photosynthetically Active Radiation (PAR) can be measured by SunScan Instrument below canopy using a 1 m probe with 64 light sensors (photodiode). Through this, a simplified radiative transfer approximation derives LAI using direct and diffuse attenuation through the canopy (Webb et al., 2008).

The device was used for measuring LAI within the designed VALERI sampling unit plots. Three measurements of LAI were taken at each of the 13 points of the five sub-plots within the 100m x 100m plot. Two levels of heights were used for measuring LAI using sunscan; height of 1.3m above the ground and on the ground-with the tip of the probe resting on the upper side of the slope. The probe was directed to a general direction south-north, southeast-northwest and southwest-northeast when taking three reading of LAI. This was done in order to prevent the effect of overcast of shadow that would come from the user/personnel when the sun is at an oblique angle at the East and West.

3.3.12. Operation of the sunscan device system in the field

Effective operation in the field required a remote connection that was set-up for the SunScan probe to use a radio receiver (434 MHz). However, a cable was used in case dense vegetation or uneven terrain caused obstruction of the radio wave (Fig. 3.4). Within the sunscan set-up, a sunshine sensor was mounted on a telescopic tripod at a vantage point which transmitted radio waves to the Radio receiver (434 MHz). Before reading was taken, the probe and Sunshine Sensor (BF3) was checked for matching. Personal Digital Assistance (PDA) for the device configures, observes and stores readings input from the SunScan probe. SunScan probe and Sunshine Sensor (BF3) was checked for free dirt before measurements were taken and held horizontally (maintained by a water bubble leveler) in uniform to sunlight in an open area (above canopy). SunScan probe (1 m) outputs into digital PAR readings, which was sent to the PDA via a cable link. Normally, readings from probe and the Sunshine Sensor (BF3) was accepted if they are within a range of 5 – 10 % of each other, to reduce errors contributed to canopies where transmission is below 50 %.

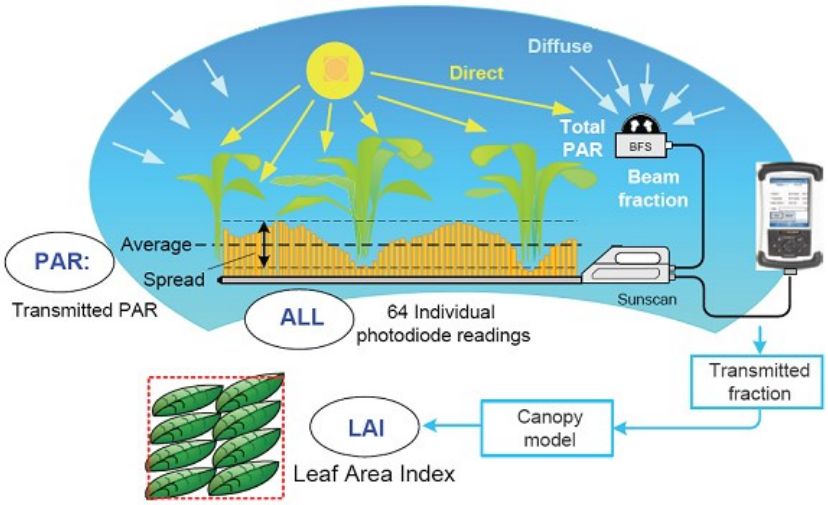

Figure 3.4 - An overview of system set-up and process for measuring LAI using SunScan (Delta T –Device)

3.3.13. Measurements of LAI using hemispherical photography

Hemispherical photographs were taken using Nikon D5000 fitted with a fish-eye lens adapter (Nikon FC -lens 5mm f/2.8, focal length of 5mm, and operating at manual focus mode). Hemispherical camera provides a wider angle of view of 180º (Jonckheere et al., 2004). Photography was undartaken at each of the 13 points established within the subplots in the 100m x 100m plots (as shown in figure 3.3), in 19 sites in Taita Hills and 13 sites in Kilimanjaro, established along the altitudinal gradients. Procedure adopted by Pfeifer et al., 2012; Gonsamo 2009 was used in the field to set up by mounting it on a tripod set with the lens facing vertically upwards, at an approximat height of 1.3 m, beneath vegetation canopy (Jonckheere et al., 2005b). Compass direction was used to orient the head of the camera to face north and the camera lens leveled to the horizontal datum using a bubble. The camera was set at an aperture of f/14. The initial shutter speed was assigned automatically (C1 = Automatic) and subsequent speed taken in arithmetic progression in adjusted manual mode. Five photographs were taken at each sampling point within the shortest time possible to avoid the changes in light regimes as recommended by Gonsamo (2009). The general slope angle and direction was measured using inclinometer and compass at each sampling point, respectively.

3.3.14. Processing of hemispherical images

This process followed a procedure that was used by Pfeifer et al., (2012). Images were downloaded for processing. Values of pixel for band blue were obtained from each RGB image for maximizing contrast between the leaf and the sky. The band is highly absorbed by the leaves and characterized by sky scattering (Jonckheere et al., 2005b; Pfeifer et al 2012). Threshold for optimal brightness was established for distinction of the vegetation from sky (Jonckheere et al., 2005b; Pfeifer et al 2012).

Pfeifer et al., (2012) used the global Ridler and Calvard method which is commonly applied for thresholding in each image (Ridler and Calvard, 1978; Pfeifer et al 2012); this was in order to rely on the results of hemispherical photography (Gonsamo and Pellika, 2008; Pfeifer et al., 2012). Extraction of band blue and threshold calculation was performed by the C-shell script (Remote Sensin Unit, University College London). These generated binary images were later analyzed using CAN-EYE V6 (Weiss and Baret, 2010; Pfeifer et al., 2012). The hemispherical lens was limited to a field of view of 60º in CAN-EYE to avoid mixed pixels that causes misclassifications towards the edge of the image (Weiss and Barret, 2010).

3.3.15. LAI-SVIs model

Enhanced Vegetation Indices of 930m resolution which corresponded to the dates of data collection in the field were downloaded from NASA archive. This was done in order to capture variation of LAI with season. Field plot data were then corresponded with the EVI pixels at the geolocation points of plots along the transect using data management tool in ArcGIS 10.2.

3.3.16. Maximum Entropy (Maxent) Model calibration and validation

i. Model Calibration: Jackknifing and analysis of variable importance

Spatial climate variability was captured by using climate spatial layer over a wider landscape of Kenya and Tanzania. In addition to this, calibration of maxent model was performed using **jackknife** in order: to achieve simplicity, local and global unbiasedness, and reduction of oversmoothing tendency. The second contribution is to set limit of confidence for a reserve estimate of a general shape using jackknife standard deviation (Adisoma, 1993).

Relative contribution of the environmental variables to the Maxent model was estimated by determining percentage contribution and permutation importance. Maxent determines the first estimate in each iteration of the training algorithm by adding the increase in regularized gain to the contribution of the corresponding variables, or subtracted from it if the change to the absolute value of lambda is negative. Permutation importance was estimated by maxent for each environmental variable in turn.

ii. Maxent Model Validation

Seven replicates were used for subsampling and cross-validation. Replicate option was used for multiple runs for the same species. In this option, the occurrence data were randomly split into a number of equal-size groups called "folds", and models were created leaving out each fold in turn. The left out turns were used for evaluation. The advantage of cross-validation is that it uses all of the data for validation, which makes better use of small data sets (Phillips et. al., 2006). Replicates were used in combination with holding 25% of the data for testing (Random Test). This enabled the ability to test the model performance while taking advantage of all available data without having an independent dataset. Replications also provided a way to measure the amount of variability in the model.

iii. Maxent Parameter tuning

Tuning the parameters of modeling poses several challenges. When the number of tune parameters is large, running the model may be prohibitive due to more time required for tuning each species separately. In maxent, several settings affect model accuracy by determining the type and complexity of dependencies on the environment that maxent tries to fit. Maxent machine was tuned to the following parameters:

- **Tuned settings:** Random test percentage (25%), Replicates (7), Replicated run type – crossvalidate, Maximum iteration – 5,000.
- **Default settings:** Regularization multiplier – 1, Max number of background points – 10,000, Convergence threshold 0.00001, Adjust sample radius – 0, Default prevalence – 0.5, Apply threshold rule – 10 percentile training presence, Threads – 1, Lq to, lqp threshold -80, Linear to lq threshold – 10, Hinge threshold 15\Beta threshold -: -1, Beta categorical -: -1, Beta lqp -: -1, and Beta hinge -: -1.

iv. Selection of suitable areas for species

After the probability distribution layers of the species were generated, selection of areas that are suitable was performed. A threshold of 0.6 and any value above was selected since these were considered to be areas very suitable for the distribution of the species selected together or separately. Selection was done at two levels: areas very suitable for a single species and; areas suitable for *Albizia gummifera*, *Mangifera indica* and *Persea americana*. Selection of the latter was performed

under multicriteria selection in ArcGIS model builder based on threshold set in the raster calculator as shown in figure 3.5.

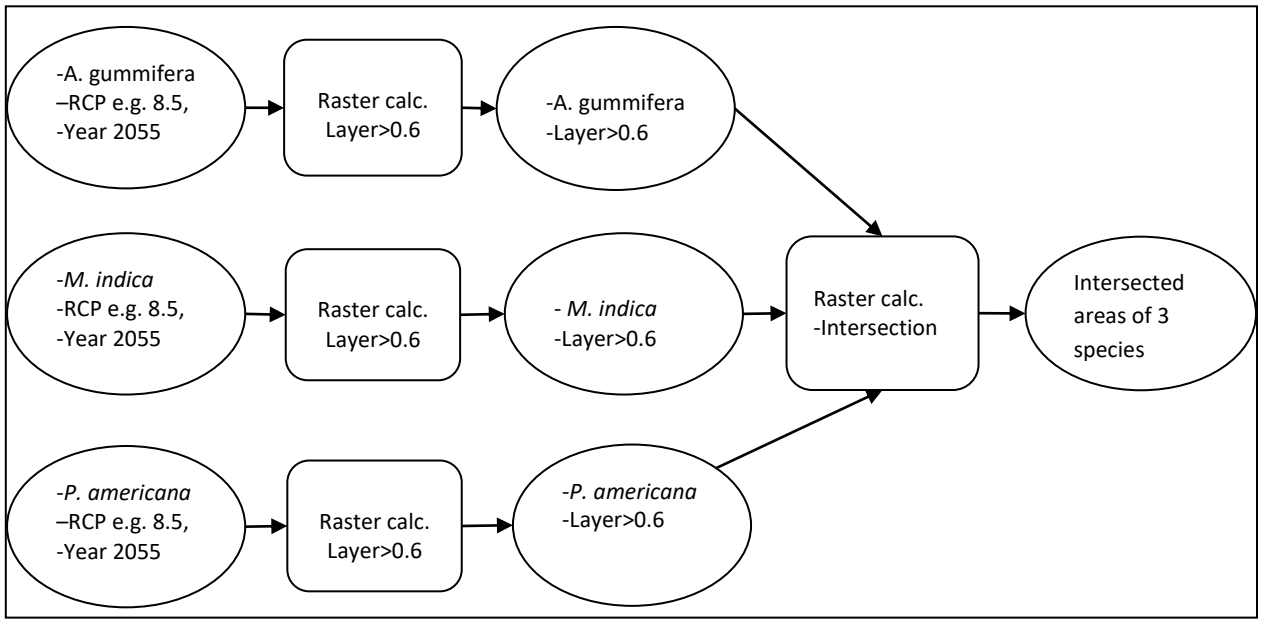

Figure 3.5 - Multicriteria selection performed in ArcGIS model builder for the intersection of suitable areas (probability > 0.6) for the projected distribution of species *A. gummifera*, *M. indica* and *P. americana*.

v. Measure of maxent model performance

Test omission rate and predicted area averaged over the replicate runs were used by maxent to generate cumulative threshold presented in a model graph. The performance of Maximum Entropy model was treated as good after observing the omission rate and the predicted omission closer to each other.in addition, the Area under Receiver Operation Curve (ROC) - Area Under Curve (AUC) was used to measure performance when it is above 0.75 (Phillips et. al., 2006; Phillips et al. 2008; Elith 2002).

3.3.17. Data Exploration

Normal distribution tests were used for diagnosis normality of datasets (variables). Visual approach was used for observing normal distributions. Both parametric and non-parametric (transformed) datasets were tested for normality. The two approaches were used for systemic, provision of a wider view of data behaviour and a more informed decision for choosing a particular transformation that optimally fits model.

Visual tests: These methods relied on the shapes of the plot graphs to diagnose the pattern of distribution of a dataset. Three approaches were considered for visual normality tests; kernel density distribution, boxplot and Q-Q plot methods. At any one time, at least two or all were used to provide a descriptive pattern of the distribution dataset based on univariate statistics.

3.3.18. Data extraction and Statistical Modeling

Environmental variable values were extracted with ArcGIS 10.2 using plot spatial references to (Fig. 3.5). The aggregation of values to major land-uses was performed in spreadsheet for Taita Hills and Kilimanjaro and later statistical analysis was used. R programme was used in the statistical analysis. Here, data was described using univariate statistics. Boxplots were used to describe the distribution of variables and visualization of the amount of variables in agro-forestry and cropped land in Taita Hills and Kilimanjaro.

Fischer's *F* test was used for testing statistical significance in data variation between types of cropland, and study sites. Difference in the mean of data was tested for significance using the Student's *t* test between agro-forestry and cropped land in study sites; agro-forestry, and cropped land between study sites.

The relationships of WPSR, AGC, and LAI with the environmental variables was assessed using Generalized Linear Model (GLM/LM). The polynomial orders (2^{nd} or 3^{rd}) order of was used for fitting relation model where non-linear patterns occur with data points The model relationship that was best explaining the distribution of AGC were qualified by an Akaike Information Criterion (AIC) that ranked models on different types of cropland and study sites. The plot data was upscaled using R program under GLM function and visualized within buffer of transect with ArcGIS 10.2.

i. Multivariate Analysis

Multivariate models were formulated based on assumptions of the multiple linear and interactions main effect mean of predictor variables on richness of the Woody Plant Species Richness (WPSR) and Above-Ground Carbon Storage (AGCS).

The initial multivariate formula treated response variables with the variation of physical factors (elevation and slope angle), and edaphic factors (SOC, CEC, BD and pH). These models were updated in R by either removing and/or adding an interactive term or additive predictor variables such as population density.

ii. Evaluation of WPSR and AGCS models

Prediction of WPSR and AGCS was performed on the surface of the physical and edaphic variables by extrapolation using GLM in R. The predicted WPSR and AGCS values were compared with the plot values by correlation to determine the model that provide better estimation of WPSR and AGCS in Taita Hills and Mount Kilimanjaro. Visual inspection of data values and spatial models generated were also used to evaluate the model. The model that provided better estimation was considered as the robust model for future application.

iii. Comparison analysis of species suitable areas

One-way ANOVA was used to compare areas that are suitable for Albizia, Mango and Avocado in each site and specific RCP and period. Pairwise comparison (Kruskal-Wallis) was used to compare suitable areas between species in sites within a specific RCP. Suitable areas for each species were compared between sites using One-Way ANOVA in a specific RCP.

Suitable areas for the projected baseline species distribution was compared with the projected future species distribution using One-Way ANOVA under same RCP, and between species suitable areas in same period of projection but different RCP. Chi^2 test was used for comparing predicted suitable and unsuitable areas for the species within sites in the same RCP and period.

Visual presentation of projected suitable areas for the species were done using bar graphs (with standard error/deviation) and time series presenting trend of change in projection of species suitable areas from baseline, projection periods 2055 and 2085 in the same RCP.

CHAPTER 4: RESULTS AND DISCUSSIONS

4.1. Introduction to Results

Results are presented in sub-sections based on the specific obectives of the study. The result based on the first objective is in sub-section 4.2 which represents the relationships of environmental variables with the elevation gradients in Mount Kilimanjaro and Taita Hills. The variables are intercorrelated on a correlation matrix which summarizes the association. The environmental variables are compared by types of cropland within site and between sites. The second objective which focuses on the distribution of the woody plant species is presented in sub-section 4.3. These are woody species with DBH > 10 cm. The results presented in this section are the species diversity indices for the two montane areas. A similarity and distance index results are presented to indicate similarity between the site and types of cropland. Relationships of woody plant species richness (WPSR) is established to the stock density of trees. The distribution of stock density is also established in the types of croplands in the two sites. Predictions for the WPSR response in the montane areas are established under univariate and multivariate models. The third objective is underscored by results in sub-section 4.4 on the above-ground carbon storage on sites and in types of cropland. Distribution of AGCS on species is presented in this section. The response of AGCS is predicted under univariate and multivariate models along the elevation gradients and within types of cropland. Results for the fourth objective, focusing on LAI, are presented in sub-section 4.5. Distribution of site LAI from hemispherical photography is presented together withits correlation with SunScan LAI. The section also has predictions of LAI under univariate models. The last sub-section is 4.6 which presents species distribution model under different RCPs and peak periods of emission. It contains results of maxent omission tests, performance, species elevation shift and changes in suitable areas.

4.2. Distribution of Environmental variables

Two types of cropland namely, cropped land and agro-forestry system were recorded in Taita Hills and Mt. Kilimanjaro. Distributions of environmental gradients were assessed within the types of croplands and along the elevation gradients. The variables include; physical variables, soil variables, and human population density.

4.1.1. Physical variable relationships

Slope angle (degree) shows significantly increasing trend with increase of elevation in both Kilimanjaro (*R=0.63, p=0.03*) and Taita Hills (*R=0.61, p=0.02*) (Fig. 4.1a). Correlation of slope

angle with elevation in both Kilimanjaro and Taita Hills are apparently similar. However, the slope angle in Kilimanjaro responds relatively better to increase of elevation than in Taita Hills.

The Mean Annual Precipitation (MAP) and Mean Annual Temperature (MAT) significantly correlate highly with the elevation. MAP increases with increase of elevation (R=0.99, p=0.00); while MAT decreases with increase of elevation (R=-0.99, p=0.00) in both Kilimanjaro and Taita Hills (Fig. 4.1b). In most cases, low elevation receives lower precipitation than areas in higher elevation. Temperatures are higher in low elevation and tend to decrease with increase in elevation. Therefore, low elevations have low MAP and high MAT, while MAP is high and MAT is low in higher elevations.

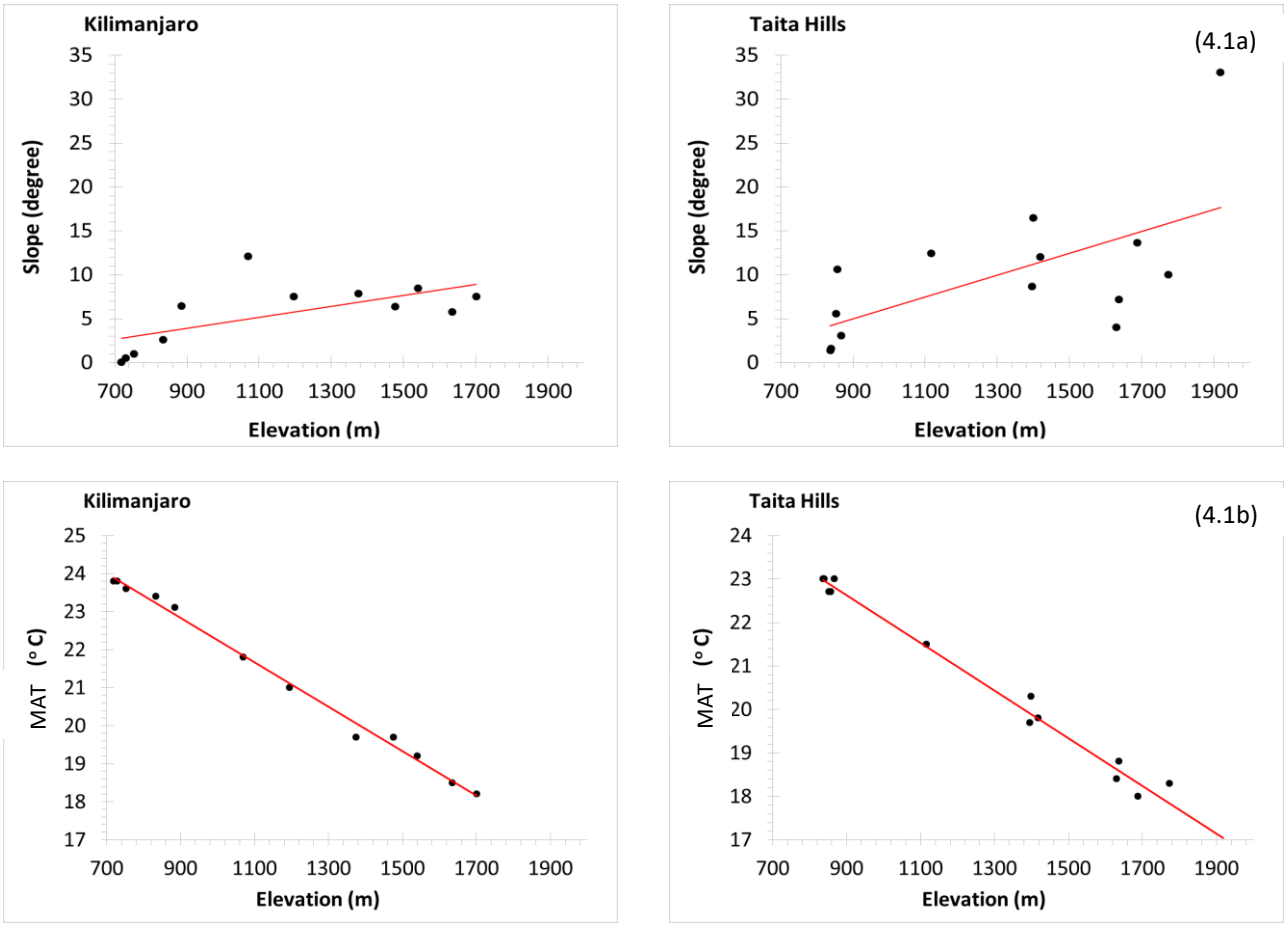

Figure 4.1 - The distribution of physical variables with increase in elevation in Mount Kilimanjaro and Taita Hills

4.1.2. Edaphic variable Versus Elevation

Soil *pH* decreases with the increase in elevation both in Taita Hills (*R=-0.55, p=0.05*) and Mount Kilimanjaro (*R=-0.95, p=0.00*) as shown in figure 4.2(a). The soil BD shows significant decreasing

trend in Mt. Kilimanjaro with increase in elevation (*R=-0.84, p=0.00*), while decrease of BD is observed in Taita Hills but not significant (*R=-0.18, p=0.54*) (Fig. 4.2b).

Increase in elevation is associated with decrease of 24% and 22% of CEC in Kilimanjaro and Taita Hills. However no significant correlation was observed observed (Fig. 4.2c).

About 96% of SOC increases with the increase of elevation in Kilimanjaro (p=0.00); while only 50% of SOC increases with increase in elevation but not significantly explained in Taita Hills (p=0.07) (Fig. 4.2d).

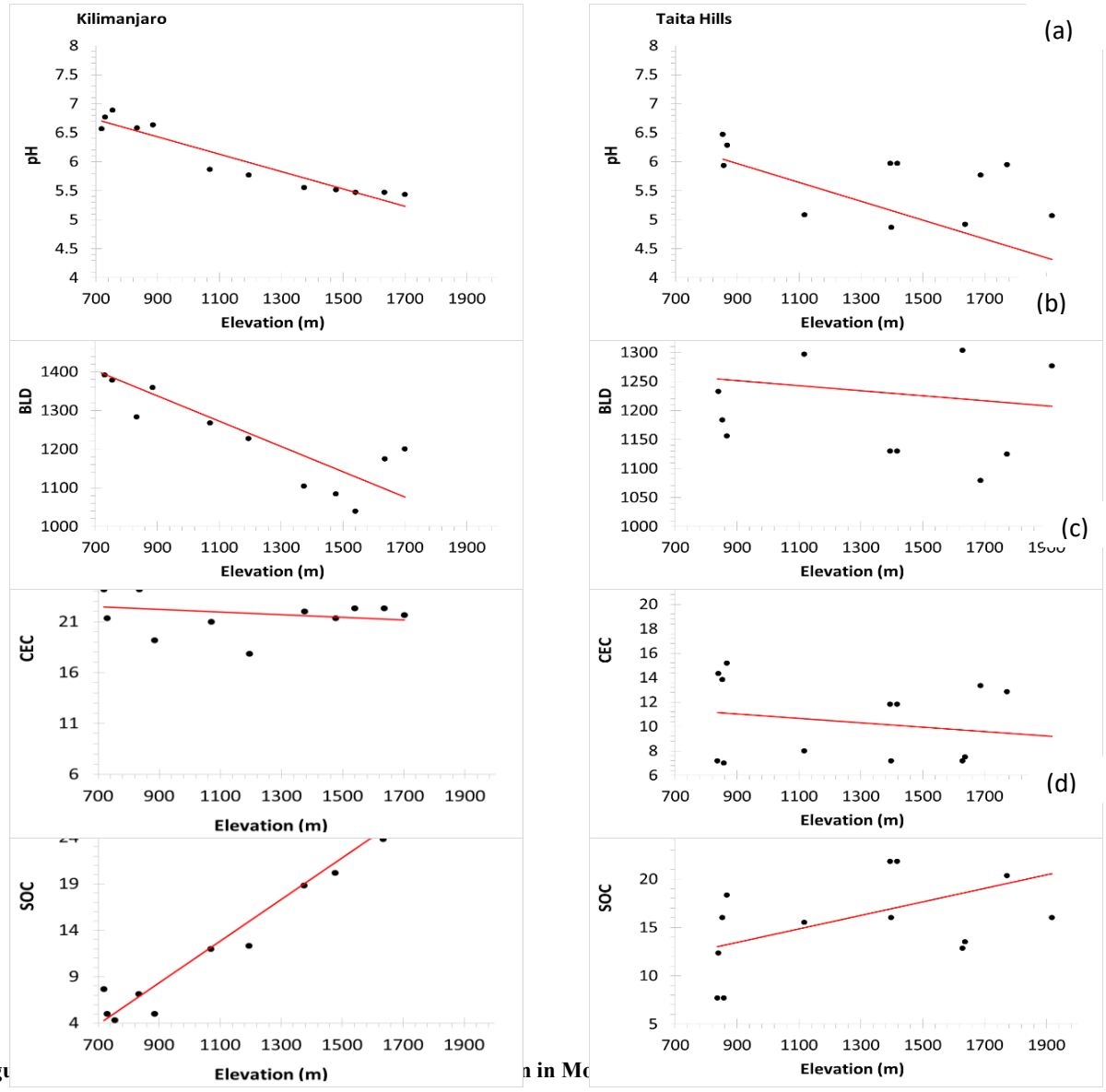

Figu **n in Mo**

4.1.3. Human Population Density

Population density distribution along the elevation gradients on Mount Kilimanjaro significantly associate (R=0.65, p= 0.02) as evident in figure 4.3. Only 10% of the population density is explained

by the increase in elevation in Taita Hills but this is not significant. No significant difference was observed on population density between the sites and between the elevation categories.

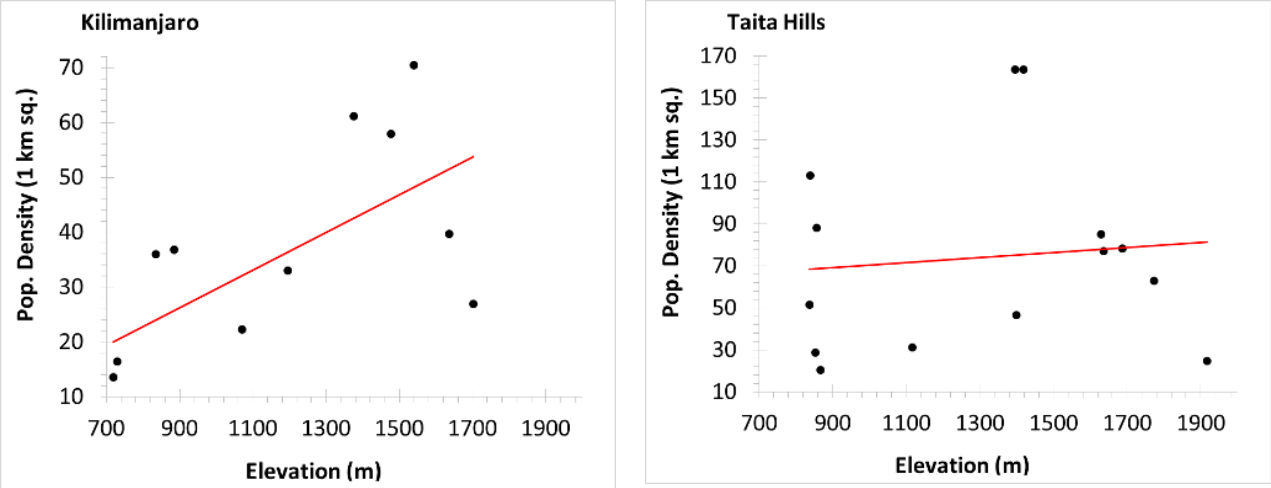

Figure 4.3 - The distribution of population density (1km2) along the elevation gradient in Kilimanjaro (R=0.65, p=0.02) and Taita Hills (R=0.1, p>0.05).

4.1.4. Comparison of environmental variables in Croplands

i. Climate Variables

The mean of the annual temperature (MAP) for cropped land in Kilimanjaro is 23.3±0.31 ºC, which is 3.75 ºC more than the mean of MAT in agro-forestry area 19.55±0.44 ºC. This does not show significant variation but the mean of MAT is significantly different (t=7.02, p=0.000) (Fig. 4.4; Table. 4.1). The difference of MAT between the cropped land and agro-forestry areas in Taita is 1.65 ºC; which is 2.3 times less than the difference in Kilimanjaro (Fig. 4.4; Table. 4.1). No significant differences were observed in the variance and mean of MAT in cropped land and agro-forestry in Taita Hills (Fig. 4.4; Table. 4.1). Significant variation occur in MAT in cropped lands in Taita Hills and Kilimanjaro (F=8.00, p=0.040).

The cropped land of Kilimanjaro has mean MAP twice the amount in agro-forestry (Fig. 4.4; Table. 4.1) and this is significantly different (t=-8.28, p=0.000). However, no significant variation occur in MAT in cropped land and agro-forestry. Despite MAP in cropped land in Taita Hills being higher than the amount in cropped land in Kilimanjaro (Fig. 4.4; Table. 4.1), no significant difference is observed in their variance and mean. The mean for MAP in agro-forestry in Kilimanjaro (1249.85±59.66 mmy^{-1}) and Taita Hills (919.45±64.85 mmy^{-1}) do not vary significantly except on their means (t=3.75, p=0.004) (Fig. 4.4; Table. 4.1).

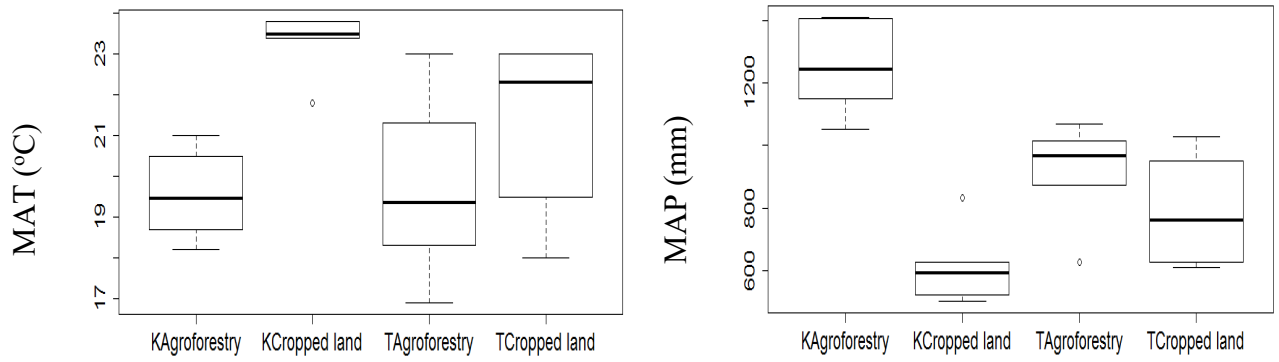

Figure 4.4 - Boxplot for the distribution of MAT and MAP in cropped land and Agro-forestry areas in Kilimanjaro and Taita Hills. KAgro-forestry means Agro-forestry in Kilimanjaro etc.

ii. Enhanced Vegetation Index

The difference in mean EVI in agro-forestry area and cropped lands in Kilimanjaro is 0.29 while in Taita Hills, it is 0.07. Significant difference occur in EVI variance and mean in agro-forestry and cropped lands on Mount Kilimanjaro (F=3.36, p=0.000; t=-6.64, p=0.000). Cropped land in Taita has significantly high EVI mean than in cropped land in Kilimanjaro (t=-3.47, p=0.000); though not significantly varied (Fig. 4.4; Table. 4.1).

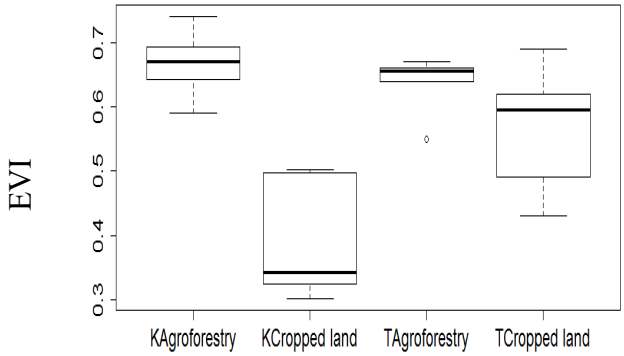

Figure 4.5 - Boxplot for the distribution of EVI in cropped land and Agro-forestry areas in Kilimanjaro and Taita Hills. KAgro-forestry means Agro-forestry in Kilimanjaro etc.

iii. Edaphic factors

The mean for pH in cropped land (0.38±0.04) and Agro-forestry (0.67±0.02) in Kilimanjaro are significantly different in their variance and means (F=43.26, p=0.001; t=7.24, p=0.000). The pH in agro-forestry in Taita Hills and Kilimanjaro varies significantly (F=45.15, p=0.001) but no significant difference on their means. The mean pH between cropped lands in Taita Hills and Kilimanjaro differ significant (t=3.27, p=0.008); however, no significant variation is observed (Fig. 4.4; Table. 4.1).

The mean of SOC in agro-forestry in Kilimanjaro is significantly different with SOC in cropped land (t=-8.20, p=0.000). SOC in cropped lands in Taita Hills and Kilimanjaro significantly varies (F=7.63, p=0.044) and differ in their means (t=-3.53, p=0.006) (Fig. 4.4; Table. 4.1). The mean of CEC in agro-forestry in Kilimanjaro (21.36±0.55) and Taita Hills (10.92±1.18) is significantly different (t=8.02, p=0.000). Similarly, the mean of CEC in cropped land in Kilimanjaro (20.25±1.38) and Taita Hills (9.03±1.37) is significantly different (t=5.75, p=0.000) (Fig. 4.4; Table. 4.1).

Agro-forestry and cropped land in Kilimanjaro differ significantly in the mean of BD (t=6.43, p=0.000). Also, BD in cropped lands in Kilimanjaro and Taita Hills significantly differ in mean (t=2.70, p=0.022) (Fig. 4.4; Table. 4.1).

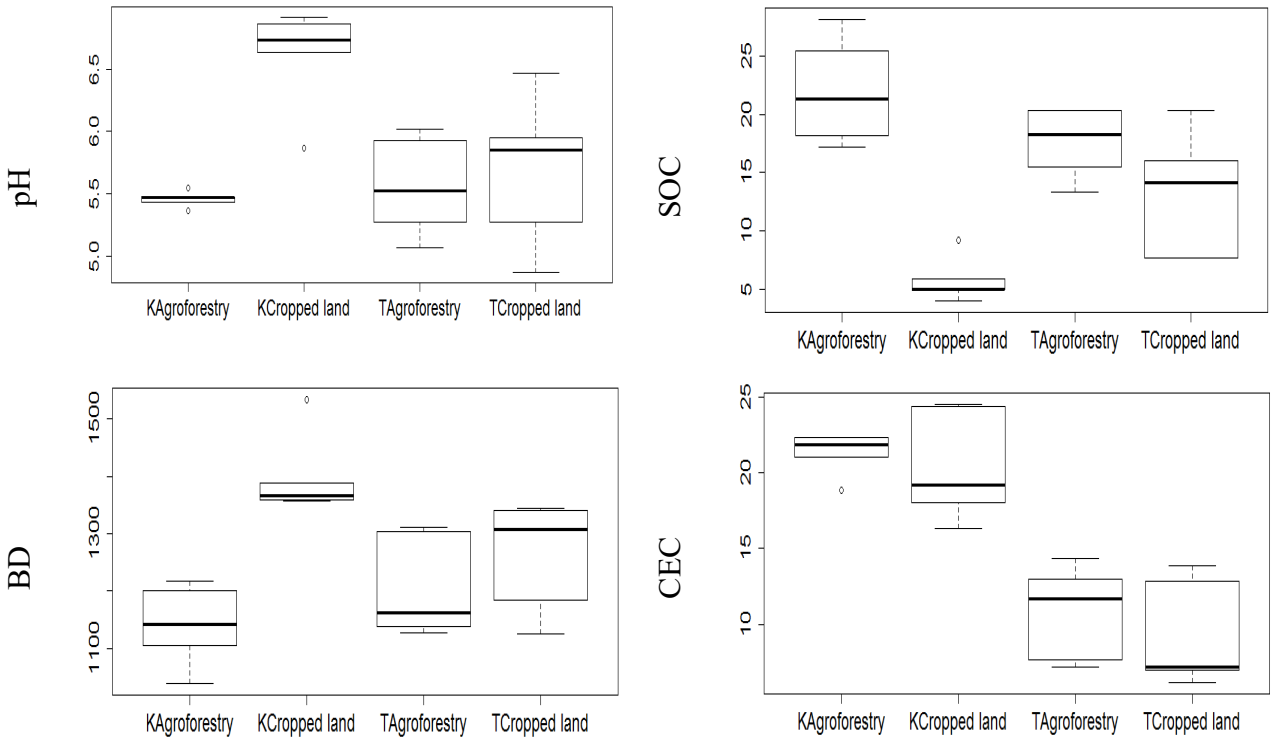

Figure 4.6 - Boxplot for the distribution of pH, SOC, CEC and BD in cropped land and Agro-forestry areas in Kilimanjaro and Taita Hills. KAgro-forestry means Agro-forestry in Kilimanjaro etc.

Table 4. 1: The distribution of MAT, MAP, EVI, pH, SOC, CEC, BD in cropped lands and Agro-forestry areas in Taita Hills and Kilimanjaro.

Variable	Comparison		Mean±SE		Fischer's F test		Student's t test	
			Kilimanjaro	Taita	F	p	t	p
MAT	Between Sites	Agro-forestry	19.55±0.44	19.7±0.92	4.44	0.13	-0.15	0.89
		Cropped Land	23.3±0.31	21.35±0.87	8.00	0.04	-2.11	0.06
	Within Site	Cropped land Vs Agro-forestry		Kilimanjaro	1.99	0.47	7.02	0.00
				Taita	1.11	0.92	1.30	0.22
MAP	Between Sites	Agro-forestry	1249.85±59.66	919.45±64.85	1.18	0.86	3.75	0.00
		Cropped Land	612.37±48.67	789.86±74.23	2.33	0.38	2.00	0.07
	Within Site	Cropped land Vs Agro-forestry		Kilimanjaro	1.50	0.67	-8.28	0.00
				Taita	1.31	0.77	-1.32	0.22
EVI	Between Sites	Agro-forestry	0.67±0.02	0.64±0.02	1.27	0.80	1.04	0.32
		Cropped Land	0.38±0.04	0.57±0.04	1.06	0.95	-3.47	0.01
		Cropped land Vs Agro-forestry		Kilimanjaro	3.36	0.00	-6.64	0.00
				Taita	4.51	0.12	-1.60	0.14
pH	Between Sites	Agro-forestry	5.46±0.02	5.56±0.16	45.15	0.00	-0.60	0.56
		Cropped Land	6.63±0.16	5.71±0.23	2.08	0.44	3.27	0.01
	Within Site	Cropped land Vs Agro-forestry		Kilimanjaro	43.26	0.00	7.24	0.00
				Taita	2.00	0.47	0.54	0.60
SOC	Between Sites	Agro-forestry	21.95±1.84	17.67±1.2	2.35	0.37	-1.95	0.08
		Cropped Land	5.67±0.74	13.33±2.04	7.63	0.04	-3.53	0.01
	Within Site	Cropped land Vs Agro-forestry		Kilimanjaro	6.20	0.07	-8.20	0.00
				Taita	2.89	0.27	-1.83	0.10
CEC	Between Sites	Agro-forestry	21.36±0.55	10.92±1.18	4.70	0.12	8.02	0.00
		Cropped Land	20.25±1.38	9.03±1.37	1.01	0.99	5.75	0.00
	Within Site	Cropped land Vs Agro-forestry		Kilimanjaro	6.44	0.06	-0.65	0.47
				Taita	1.35	0.75	-1.04	0.32
BD	Between Sites	Agro-forestry	1140.86±27.82	1200.86±34.32	1.52	0.66	-1.36	0.20
		Cropped Land	1395.00±28.09	1267.70±37.80	1.81	0.53	2.70	0.02
	Within Site	Cropped land Vs Agro-forestry		Kilimanjaro	1.02	0.98	6.43	0.00
				Taita	1.21	0.84	1.31	0.22

4.1.5. Correlation of environmental variables

MAP and MAT correlate strongly but negatively in both cropped land and agro-forestry in Taita Hills and Kilimanjaro (Table 4.2). EVI and SOC are strongly correlated in cropped lands but poorly correlated in agro-forestry area in both Taita Hills and Kilimanjaro (Table 4.2).

pH and SOC are strongly correlated in agro-forestry area in Kilimanjaro and Taita Hills but poorly correlated in cropped lands. Strong correlation occurs between SOC and BD, CEC and BD in cropped land and agro-forestry in Kilimanjaro and Taita Hills (Table 4.2).

Table 4. 2: Intercorrelation matrix of MAT, MAP, EVI, pH, SOC, CEC, BD in agro-forestry and cropped lands in Kilimanjaro and Taita Hills.

			MAT	MAP	EVI	pH	SOC	CEC	BD	
Kilimanjaro - Cropped land	MAT	Correlation		0.00	0.43	0.07	0.65	0.50	0.63	p-value
	MAP		-0.96		0.35	0.23	0.48	0.81	0.91	
	EVI		-0.40	0.47		0.73	0.01	0.37	0.12	
	pH		0.78	-0.58	-0.19		0.95	0.11	0.28	
	SOC		-0.24	0.36	0.93	0.04		0.12	0.04	
	CEC		0.35	-0.13	0.45	0.72	0.70		0.02	
	BD		-0.26	0.06	-0.70	-0.53	-0.84	-0.90		
Kilimanjaro - Agro-forestry	MAT	Correlation		0.00	0.30	0.90	0.81	0.28	0.53	p-value
	MAP		-0.95		0.53	0.79	0.61	0.32	0.48	
	EVI		-0.51	0.33		0.69	0.98	0.12	0.52	
	pH		0.07	-0.14	0.21		0.03	0.34	0.05	
	SOC		0.12	-0.27	0.01	0.87		0.14	0.01	
	CEC		0.53	-0.49	-0.71	0.47	0.68		0.02	
	BD		-0.33	0.36	0.33	-0.81	-0.92	-0.87		
Taita Hills - Cropped land	MAT	Correlation		0.00	0.43	0.07	0.65	0.50	0.63	p-value
	MAP		-0.96		0.35	0.23	0.48	0.81	0.91	
	EVI		-0.40	0.47		0.73	0.01	0.37	0.12	
	pH		0.78	-0.58	-0.19		0.95	0.11	0.28	
	SOC		-0.24	0.36	0.93	0.04		0.12	0.04	
	CEC		0.35	-0.14	0.45	0.72	0.70		0.02	
	BD		-0.26	0.06	-0.70	-0.53	-0.84	-0.90		
Taita Hills - Agro-forestry area	MAT	Correlation		0.00	0.30	0.90	0.81	0.29	0.53	p-value
	MAP		-0.95		0.53	0.79	0.61	0.32	0.48	
	EVI		-0.51	0.34		0.69	0.98	0.12	0.52	
	pH		0.07	-0.14	0.21		0.05	0.34	0.05	
	SOC		0.13	-0.27	0.01	0.87		0.14	0.01	
	CEC		0.53	-0.49	-0.71	0.47	0.68		0.02	
	BD		-0.33	0.36	0.33	-0.81	-0.92	-0.87		

Table 4. 3: Correlation\p-value table for intercorrelation analysis of Elevation, MAT, MAP, EVI, pH, SOC, CEC, BD and Population density in Kilimanjaro.

Kilimanjaro	Elev	MAT	MAP	Pop. Density	SOC	EVI	CEC	Slope	BD	pH
Elev		0.00	0.00	0.02	0.00	0.00	0.45	0.03	0.00	0.00
MAT	-1.00		0.00	0.02	0.00	0.00	0.46	0.03	0.00	0.00
MAP	0.93	-0.94		0.00	0.00	0.00	0.39	0.02	0.00	0.00
Pop. Density	0.65	-0.64	0.83		0.01	0.07	0.48	0.09	0.00	0.02
SOC	0.96	-0.96	0.91	0.68		0.00	0.77	0.05	0.00	0.00
Evi	0.84	-0.85	0.83	0.54	0.85		0.43	0.03	0.02	0.00
CEC	-0.24	0.24	-0.27	-0.23	-0.09	-0.25		0.06	0.45	0.31
Slope	0.63	-0.63	0.65	0.52	0.57	0.61	-0.55		0.02	0.01
BD	-0.85	0.84	-0.94	-0.87	-0.83	-0.65	0.24	-0.67		0.00
PH	-0.95	0.96	-0.94	-0.68	-0.93	-0.93	0.32	-0.74	0.85	

Table 4. 4: Correlation\p-value table for intercorrelation analysis of the Elevation, MAT, MAP, EVI, pH, SOC, CEC, BD and Population density in Taita Hills.

		p-values									
	Taita Hills	Elev	MAT	MAP	Pop. Density	SOC	Evi	CEC	Slope	BD	PH
Correlation Values	Elev		0.00	0.00	0.73	0.07	0.00	0.44	0.02	0.54	0.15
	MAT	-0.99		0.00	0.67	0.07	0.00	0.44	0.02	0.51	0.14
	MAP	0.97	-0.97		0.62	0.04	0.00	0.39	0.02	0.51	0.13
	Pop. Density	0.10	-0.12	0.14		0.40	0.73	0.58	0.50	0.26	0.93
	SOC	0.50	-0.50	0.55	0.25		0.00	0.03	0.37	0.00	0.51
	Evi	0.73	-0.71	0.82	-0.10	0.72		0.85	0.07	0.16	0.50
	CEC	-0.22	0.22	-0.25	0.16	0.57	0.06		0.23	0.00	0.06
	Slope	0.61	-0.62	0.62	-0.20	0.26	0.50	-0.35		0.92	0.99
	BD	-0.18	0.19	-0.19	-0.32	-0.86	-0.40	-0.84	0.03		0.18
	PH	-0.40	0.42	-0.42	0.03	0.19	-0.20	0.52	0.00	-0.38	

4.1.6. Key Findings for objective 1

Environmental variables MAT, CEC, BD and pH correlate negatively with elevation in the montane areas. While, MAP, Slope, Population Density, SOC and EVI positively correlate with elevation. Edaphic variables, except CEC, significantly correlate with elevation in Kilimanjaro. Only MAT, MAP, EVI and Slope significantly correlate with the elevation in Taita Hills. Distribution of MAT, MAP, EVI and edaphic variables in agroforestry areas and cropped lands on Mount Kilimanjaro are significantly different but not in Taita Hills. However, MAT, MAP and EVI in cropped lands in the two sites are significantly different.

4.3. Woody plant species distribution, diversity and structure along the elevation of Taita Hills and Mount Kilimanjaro

4.2.1. Woody plant Species Diversity Indices

Between sites: WPS sampled in Taita Hills and Mount Kilimanjaro show, under rarefaction curve, the species almost reached asymptote level (Fig. 4.7). That is, very few sampling would be required in the two sites in order to reach the level where no more species would be recovered on the sites.

The estimated species richness of the woody plant species on the inhabited section of the sites are relatively similar; 70 (Chao1) in Kilimanjaro and 74 (Chao1) in Taita Hills. Species diversity is relatively higher in the two sites. However, the latter has more diverse species indicated by Shannon Index (H=3.41) than in Mount Kilimanjaro (H=3.24) (Table 4.5). Species diversity is significantly different between the inhabited areas of the two sites (t=3.06, p=0.002).

The distribution of woody species in Kilimanjaro site, $e^{\wedge H}/S=0.38$, is fairly even than in Taita Hills slope ($e^{\wedge H}/S$=0.42). Thus, the distribution of woody species tends to vary more in Taita Hills. Species abundance are relatively distributed among the present taxa (ratio) in the two sites; given by *Equitability (J);* in Kilimanjaro J=*0.77*) and Taita Hills (J=0.80) (Table 4.5). Very low dominance (D) of species in the two sites indicates no species is dominant in Taita (D=0.06) and Kilimanjaro (D=0.07) but are relatively distributed along the sites. Species dominance in the two sites is very low.

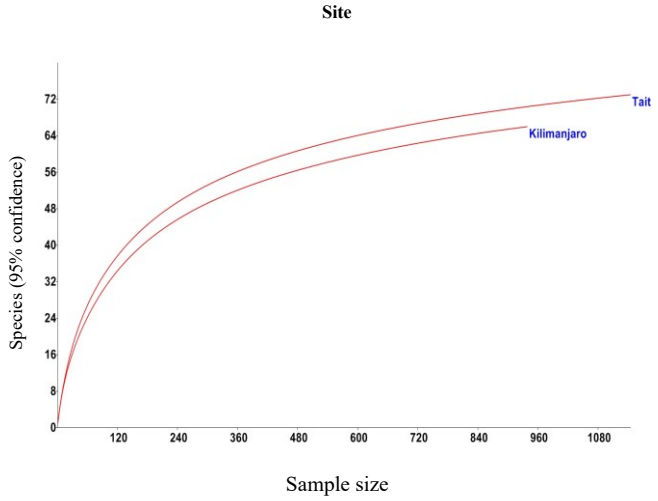

Figure 4.7 - Species rarefaction - accumulation curves of species against sample in Kilimanjaro and Taita Hills

Croplands between sites: The rarefaction curve of the sampled individual woody plant species in agro-forestry in Kilimanjaro reached asymptote level (Fig. 4.8). Very few or no species would be

recovered with increased sampling efforts in the area. While, agro-forestry areas in Taita Hills still requires more sampling in order to reach the level where no more species would be recovered (Fig. 4.8). Sampling in Cropped land in Taita Hills show species accumulation reaching near asymptote level but species sampled in Kilimanjaro Cropped land requires more sampling.

The inhabited areas of Taita Hills have more species richness in agro-forestry areas (Chao1=58) and Cropped lands (Chao1=50) than the croplands in Kilimanjaro (Table 4.5). Thus, croplands in Taita Hills are more diverse than the croplands in Kilimanjaro (Table 4.5) Hills (H=3.30) and Kilimanjaro (H=3.13) (Table 4.5). Shannon diversity t test performed shows that significant differences occur between the diversities in agro-forestry areas between sites (t=4.16, p=0.00) and in Cropped lands between sites (t=1.99, p=0.05), and agro-forestry and Cropped lands within sites, Kilimanjaro (t=2.49, p=0.01) and Taita Hills (t=2.25, p=0.02).

The individual woody plant species in agro-forestry areas in Kilimanjaro (n=6) are evenly distributed ($e^{\wedge H}/S$=0.43) among the species per ha more than the individuals in Taita Hills agro-forestry areas (n=8) ($e^{\wedge H}/S$=0.38). The distribution of individual species in Cropped lands in Kilimanjaro (n=6) and Taita Hills (n=7) are relatively similar in evenness (Table 4.5).

In agro-forestry areas and Cropped lands, the distribution of the individual species among the present taxa is relatively similar, in Kilimanjaro and Taita Hills, respectively. However, *Equitability* is higher in Cropped lands than agro-forestry areas (Table 4.5).

Agro-forestry areas and Cropped lands have very low dominance (D=1-Simpson), meaning all species in the croplands in the two sites are equally present and very few or no species is dominant (Table 4.5). *Persea americana* is the most dominant species (D=0.019) along the elevation gradients of Mount Kilimanjaro and in agro-forestry within the site. In Taita Hills, *G. robusta* dominate the (D=0.036) and in agro-forestry within the site. The Cropped lands in Kilimanjaro is dominated by *M. indica* (D=0.024), while *Eucalyptus maculata* dominate in Cropped lands in Taita Hills (D=0.017) (Table 4.6).

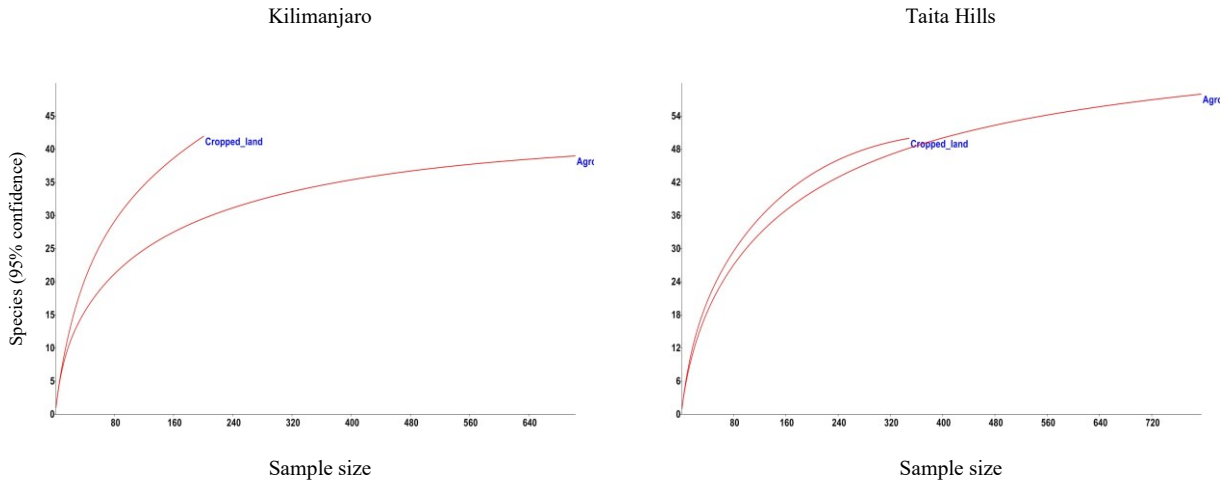

Figure 4.8 - Species rarefaction - accumulation curve of species against sample in types of cropland in Kilimanjaro and Taita Hills

Table 4. 5: Species indices. Individuals per ha.

	Site		Agro-forestry		Cropped land	
Diversity Indices	**Kilimanjaro (n=12)**	**Taita Hills (n=15)**	**Kilimanjaro (n=6)**	**Taita Hills (n=8)**	**Kilimanjaro (n=6)**	**Taita Hills (n=7)**
Taxa (S)	66	73	39	58	42	50
Individuals	75	76	117	100	33.53	49.9
Dominance (D)	0.07	0.06	0.09	0.09	0.08	0.06
Simpson (1-D)	0.93	0.94	0.91	0.91	0.92	0.94
Shannon (H)	3.24	3.41	2.82	3.10	3.13	3.30
Evenness (e^H/S)	0.38	0.41	0.43	0.38	0.54	0.54
Brillouin	2.59	2.74	2.48	2.60	2.28	2.55
Menhinick	7.38	8.35	3.60	5.81	7.25	7.08
Margalef	14.58	16.61	7.98	12.39	11.67	12.53
Equitability (J)	0.77	0.79	0.77	0.76	0.84	0.84
Fisher (α)	201.80	819.50	20.46	57.96	0	0
Berger-Parker	0.14	0.19	0.17	0.25	0.23	0.13
Chao-1	70	74	40	59	42	50

4.2.2. Similarity and Distance index: Jaccard's index

The distribution of WPS in Taita Hills and Kilimanjaro indicate sites share about 32% of the total 104 species recorded in the two sites (cluster C, Fig. 4.9). 30% of the species are unique to Mount Kilimanjaro (cluster B, Fig. 4.9) while 39% are unique to Taita Hills (cluster A, Fig. 4.9). These species are indicated on the similarity and distance cluster analysis (Fig. 4.9).

Agro-forestry areas and cropped lands in Kilimanjaro share 26% of the 66 species recorded (cluster C, Fig. 4.10). About 38% of the species only occur in cropped lands (cluster A, Fig. 4.9) while 33% are unique to agro-forestry areas in Kilimanjaro (cluster B, Fig. 4.10).

About 48% of the 73 species recorded along the elevation gradients of Taita Hills are shared by agro-forestry areas and Cropped land (cluster B, Fig. 4.11). Species that are unique to agro-forestry areas in Taita Hills comprises 32% (cluster C, Fig. 4.11) and while those for cropped land forms only 20% (cluster A, Fig. 4.11).

A total of 77 species occur in agro-forestry areas in Taita Hills and Mount Kilimanjaro. About 26% of the species are shared between agro-forestry areas in the two sites while 25% and 45% are unique to agro-forestry areas in Taita Hills and Kilimanjaro, respectively. Cropped land in Taita Hills and Kilimanjaro recorded about 76 species. Out of this, 21% is shared by cropped land in the two sites while 34% and 45% are unique to Kilimanjaro and Taita Hills respectively.

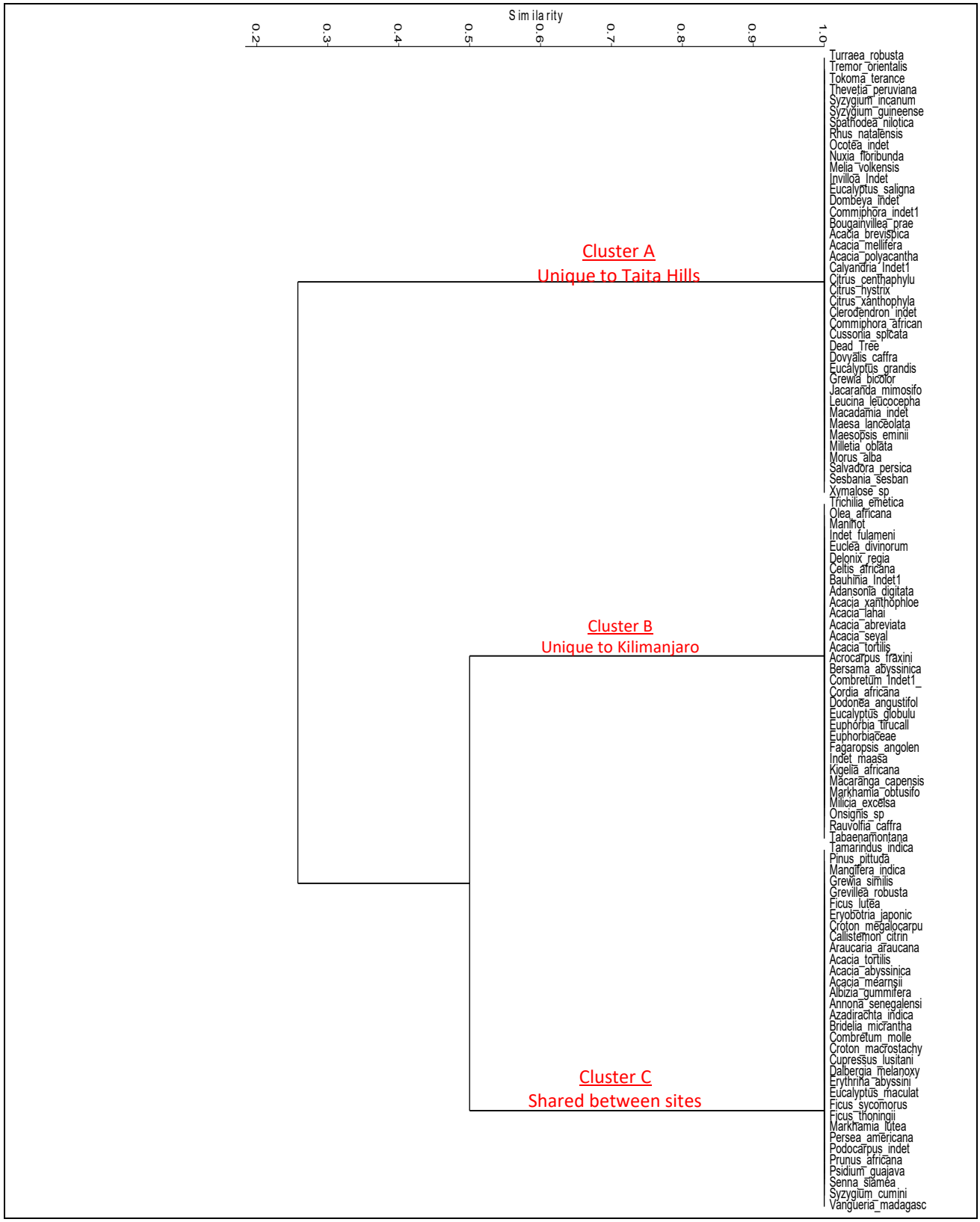

Figure 4.9 - Similarity clusters of the Woody Plant Species on inhabited section of Mount Kilimanjaro and Taita Hills.

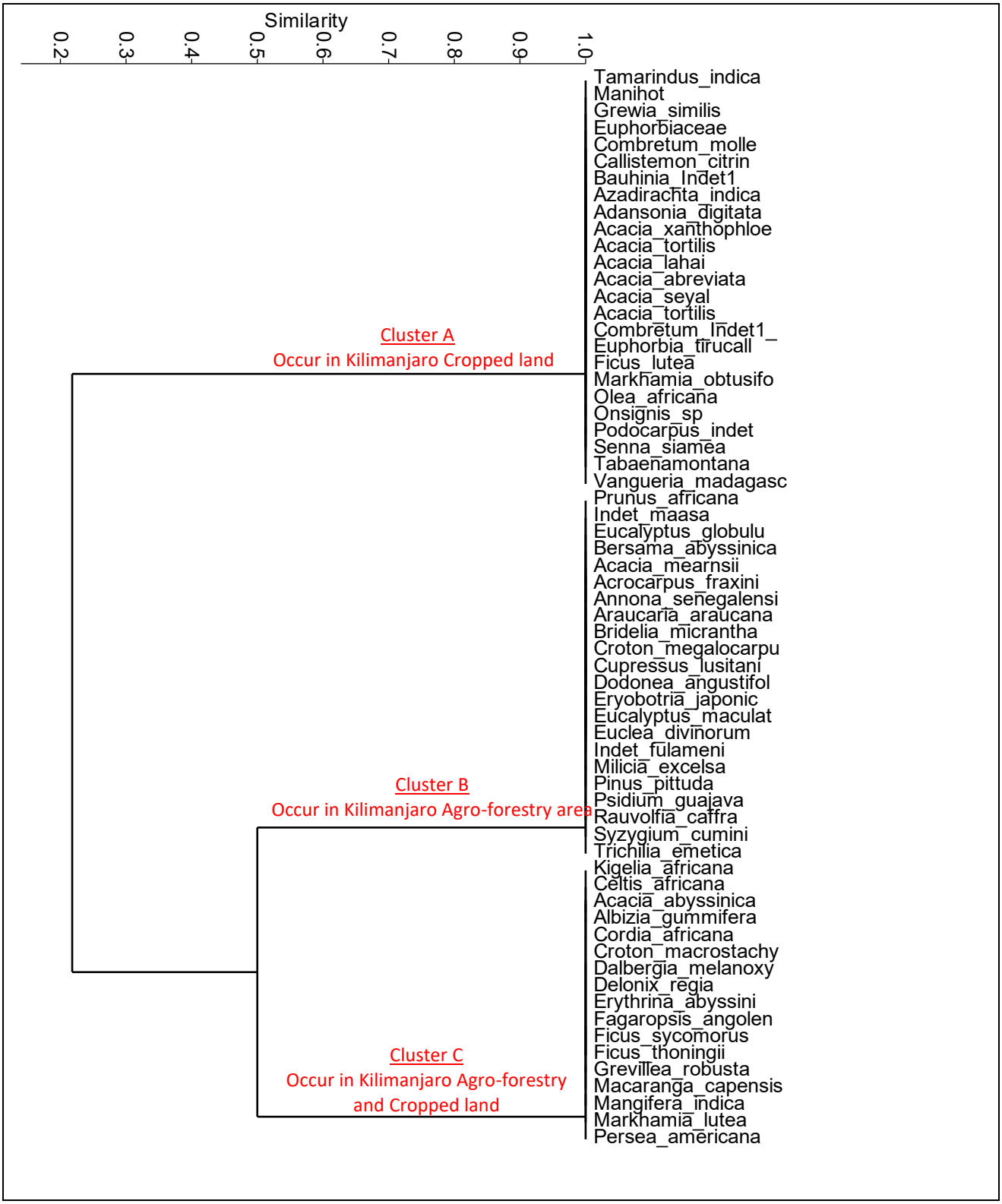

Figure 4.10 - Similarity clusters of the Woody Plant Species in types of cropland in Mount Kilimanjaro.

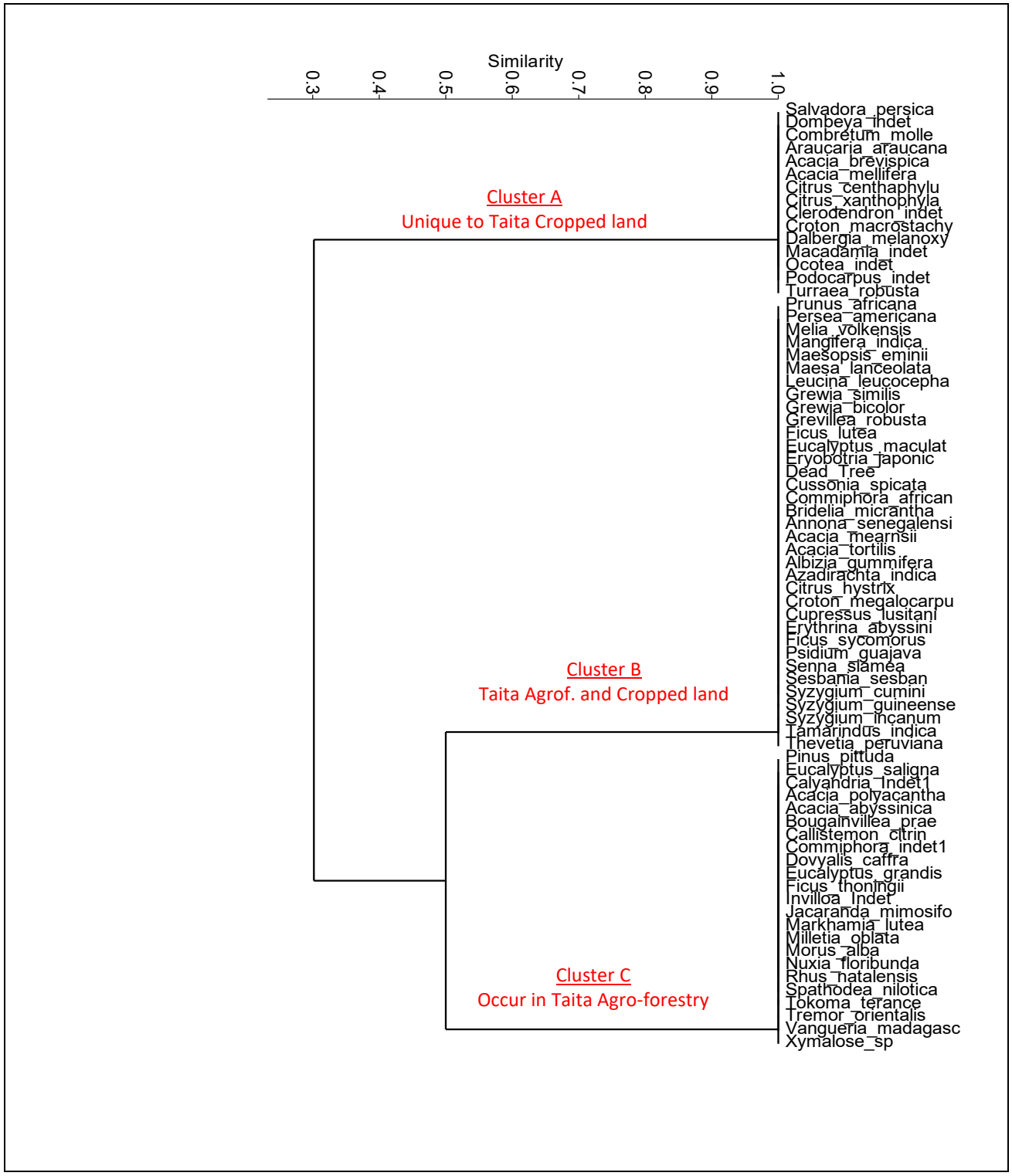

Figure 4.11 - Similarity clusters of the Woody Plant Species in types of cropland in Taita Hills.

4.2.3. Stock density distribution

Taita Hills and Mount Kilimanjaro have relatively similar stock density of 75 and 76 individuals per hectare, respectively, in each site. No significant differences occur between the stock density in Taita Hills and Mount Kilimanjaro.

Grevillea robusta, which is the dominant species in Taita Hills, has highest density distribution, approximately 19 % per hectare, compared to all species in the two sites (Appendix I). *G. robusta* also dominate in agro-forestry areas in the two sites. *Persea americana*, which has a density distribution 14% is dominant in Kilimanjaro is followed by *G. robusta* with density distribution of 11 % (Fig. 4.12 and Appendix I).

The Cropped lands in Kilimanjaro are dominated by *Mangifera indica*, 9 individual per ha (Fig. 4.12 and Appendix II); while *Eucalyptus maculata* is abundant 4 individuals per ha in Taita Hills (Fig. 4.13 and Appendix III). Stock density of WPS in agro-forestry in Kilimanjaro is 59 individuals per ha (Chao1), and 16 per ha in Cropped land (Table 4.5). The two types of croplands significant differ in Kilimanjaro ($F=6.32$, $p=0.01$).

High stock density occur in agro-forestry areas in Taita Hills with densities of 100 per ha and Cropped land with 50 individuals per ha (Table 4.5). However, the density distribution between the agro-forestry and Cropped land in Taita Hills are not significantly different ($F=3.64$, $p=0.05854$). The stock density in agro-forestry areas and cropped land between the two sites do not differ significantly (Table 4.5).

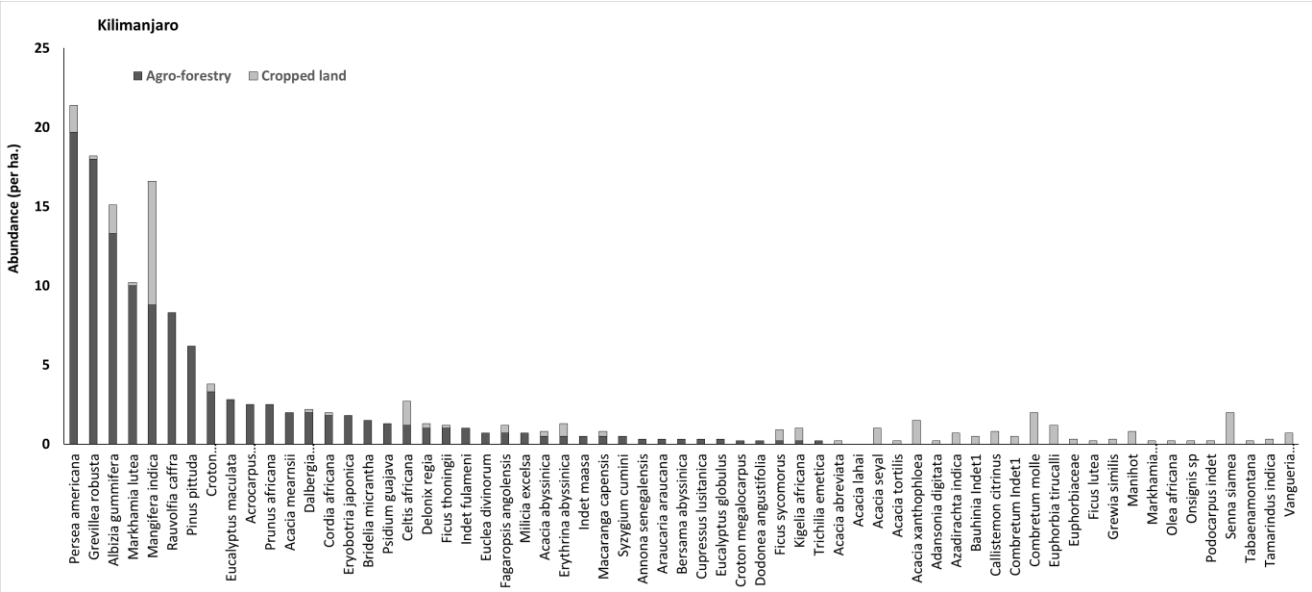

Figure 4.12 - Woody plant species and distribution of abundance in types of Cropland in Kilimanjaro

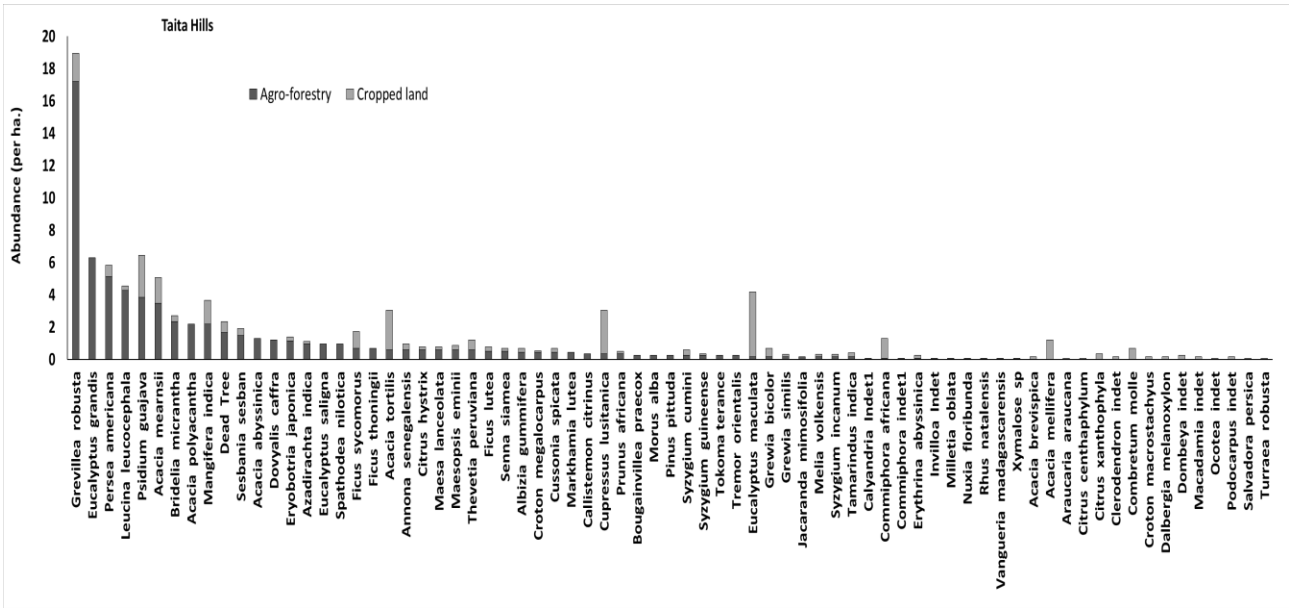

Figure 4.13 - Woody plant species and distribution of abundance in types of Cropland in Taita Hills.

4.2.4. Relative frequency and density distribution

The most frequently observed WPS in Kilimanjaro are *A. gummifera* (frequency=75%) and *M. indica* (frequency=74%) followed by *G. robusta* (frequency=67%). *Grevillea robusta* has high frequency of occurrence (80%) in Taita Hills followed by *P. americana* (73%) and *Psidium guajava* (67%).

Agro-forestry areas in Kilimanjaro have a high frequency of 100% for *A. gummifera*, *G. robusta*, *Prunus africana*. While, the woody species with the highest frequency in Taita Hills agro-forestry are *G. robusta* and *P. americana* each with a frequency of 100%.

The Cropped land of Mount Kilimanjaro has *Acacia seyal* with high frequency of distribution compared to other species (frequency=67%) followed by *M. indica*, *Croton macrostachyus*, *Ficus sycomorus*, *Combretum molle*, each with frequency of 50%. Five woody species have relatively high frequency of distribution of 57% compared to the other species in Cropped land. These include *G. robusta*, *P. guajava*, *Ficus sycomorus*, *Mangifera indica* and *P. americana*.

Relative frequency of woody plant species are more varied with the increase in relative density in Taita Hills than in Kilimanjaro (Fig 4.14a). Increase in species relative frequency in Kilimanjaro would probably reach a point where it levels out before attaining 100% distribution even with the increase in species relative density. In Taita Hills, some woody species might attain 100% relative frequency but their relative density must be high.

The stock density varies with the increase in the woody plant species richness in Mount Kilimanjaro (R^2=0.60, F=15.13, p= 0.00) under linear model (Fig. 4.14b). While, in Taita Hills the relationship is very strong and significantly increases with the increase of WPSR under quadratic model (Fig. 4.14b).

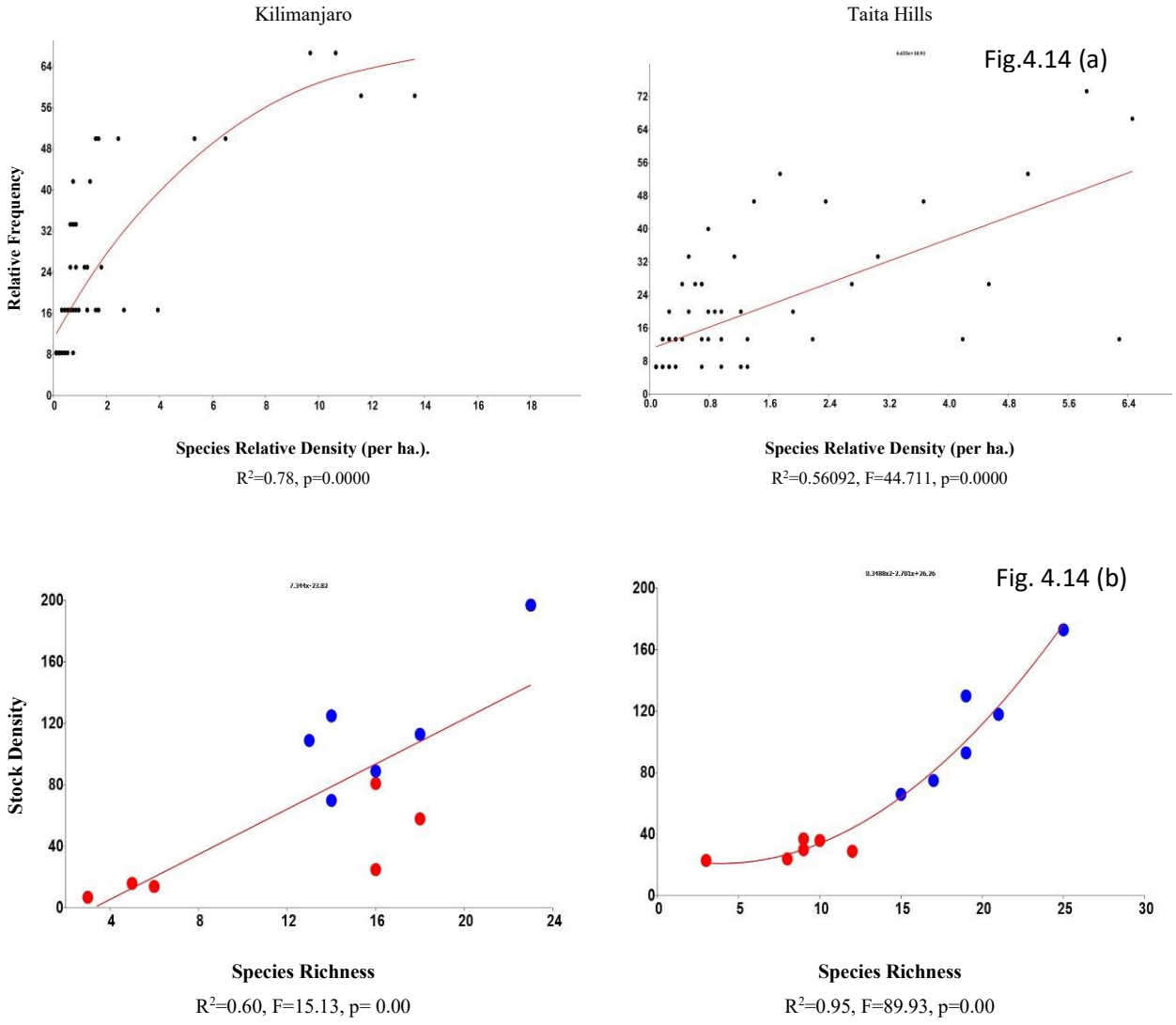

Figure 4.14 - Relationship of relative frequencies and relative density, and stock density with the woody palnt species richness in Kilimanjaro and Taita Hills.

4.2.5. Comparison of Stock Density in Types of Cropland

Relative densities of woody species in agro-forestry areas in Kilimanjaro and Taita Hills were higher than Cropped lands mean (Mean±SE) relative abundance in Kilimanjaro (117.17±17.83) and

(109.17±16.21). However, no significant difference is observed on agro-forestry between the sites (Fig. 4.15). In Taita Hills, both mean and variation of relative density in agro-forestry area is significantly higher than in Cropped land; t=4.8431, p=0.00; F=46.12, p=0.00. Only mean of the relative density of the woody plant species in Kilimanjaro differ significantly between agro-forestry and Cropped land (t=3.89, p=0.0029933) (Fig. 4.15).

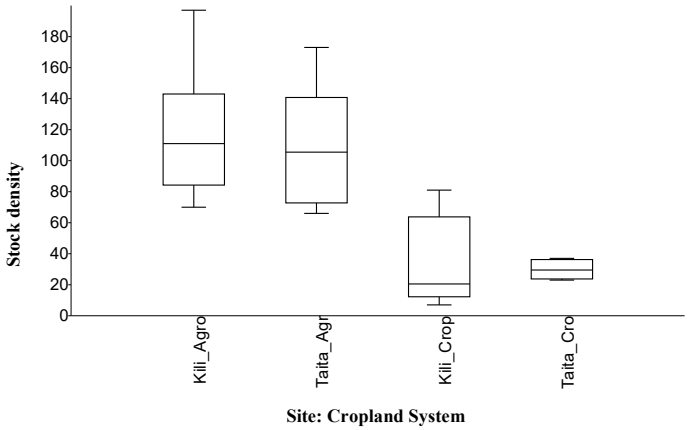

Figure 4.15 - Boxplot showing the distribution of stock density (abundance) of WPS in Taita Hills and Kilimanjaro, in different croplands (Agro-forestry and Cropped land).

4.2.6. Prediction of Woody Species Richness

i. Univariate Model Response

Relationships of the woody species richness were assessed against predictor variables: physical variables (elevation and slope); edaphic variables (soil BD, pH, SOC and CEC); biophysical variable (EVI), and human population density. The interactions of the richness with the environmental variables provided a local based model.

a. **Physical variables**

WPSR in Kilimanjaro significantly increases with the increase in elevation (R^2=0.58, p=0.02; 2nd polynomial fit) (Fig. 4.16b, Table 4.6) and slopes (R^2=0.66, p=0.01: 2nd polynomial fit) (Fig. 4.16a, Table 4.6) but tend to decrease as elevation and slopes approaches maximum levels along transect. Increase in slope angle in agro-forestry areas in Taita Hills and Mount Kilimanjaro is associated with decrease in woody species richness though not significantly. On the other hand, species richness increases with increase in slope angle in the cropped land in the two sites but the relationship is not significant.

In Taita Hills, richness increases significantly with the increase in elevation from the lower elevation areas (R^2=0.90, p=0.00: 2nd polynomial fit) but decreases drastically towards the higher elevation areas, while richness increases significantly with the increase in slope (R^2=0.62, p=0.01: Linear fit) (Fig. 4.16a, Table 4.6). Significant change in woody species richness is observed in in Taita Hills agro-forestry with change in elevation but not in Kilimanjaro. That is, species richness in Taita Hills agro-forestry decreased significantly with the increase in elevation (R^2=0.71, p=0.03: Linear fit). Richness changes significantly with increase in elevation only in Kilimanjaro (R^2=0.87, p=0.5) (Fig. 4.16b, Table 4.6).

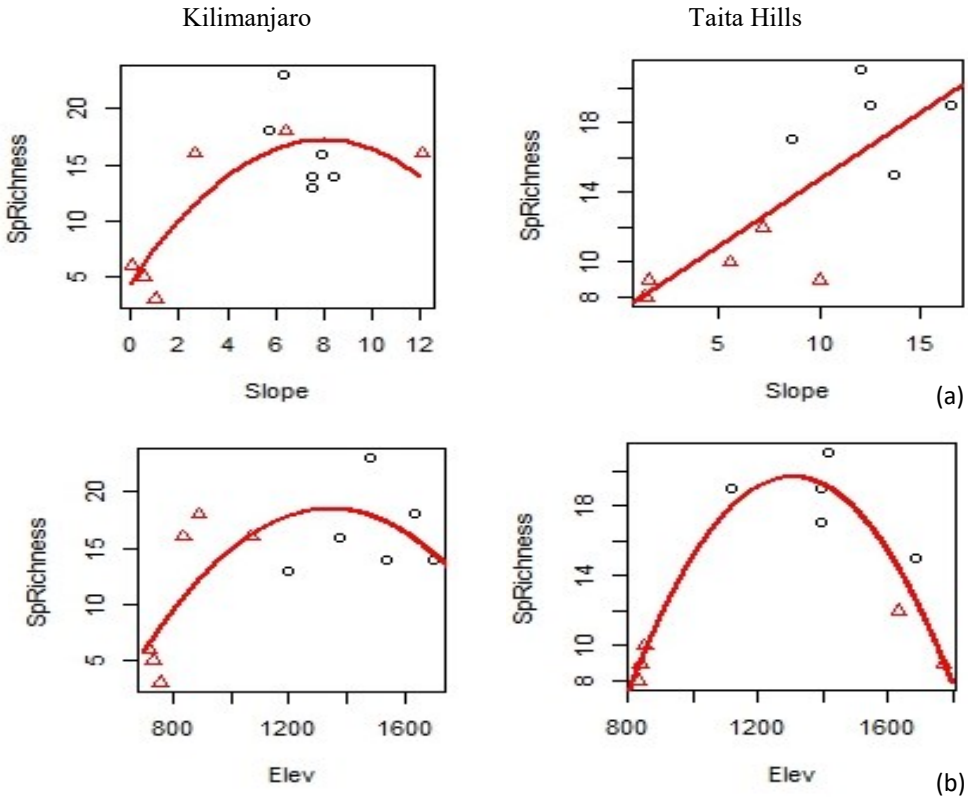

Figure 4.16 - WPSR (SpRichness) with the variation of the physical variables (slope and elevation) in Kilimanjaro and Taita Hills.

b. Edaphic Variables

The woody species richness decreases with the increase in soil BD and pH in both transects of Taita Hills and Mount Kilimanjaro. The decrease in richness is only significant in Kilimanjaro, pH (R^2=0.41, p=0.02: Linear fit) (Fig. 4.14a, Table 4.6) and BD (R^2=0.35, p=0.04: Linear fit) (Fig. 4.17b, Table 4.6). The distribution of richness increases slightly and then drastically decreases, significantly, with the increase in CEC in Kilimanjaro (R^2=0.78, p=0.00; 2nd polynomial fit). However, increase in richness observed in Taita Hills is not significantly related to the increase in CEC (Fig. 4.17c, Table 4.6). Species richness increases with the increase in SOC in Taita Hills and Kilimanjaro but no significant relationship observed (Fig. 4.17d, Table 4.6).

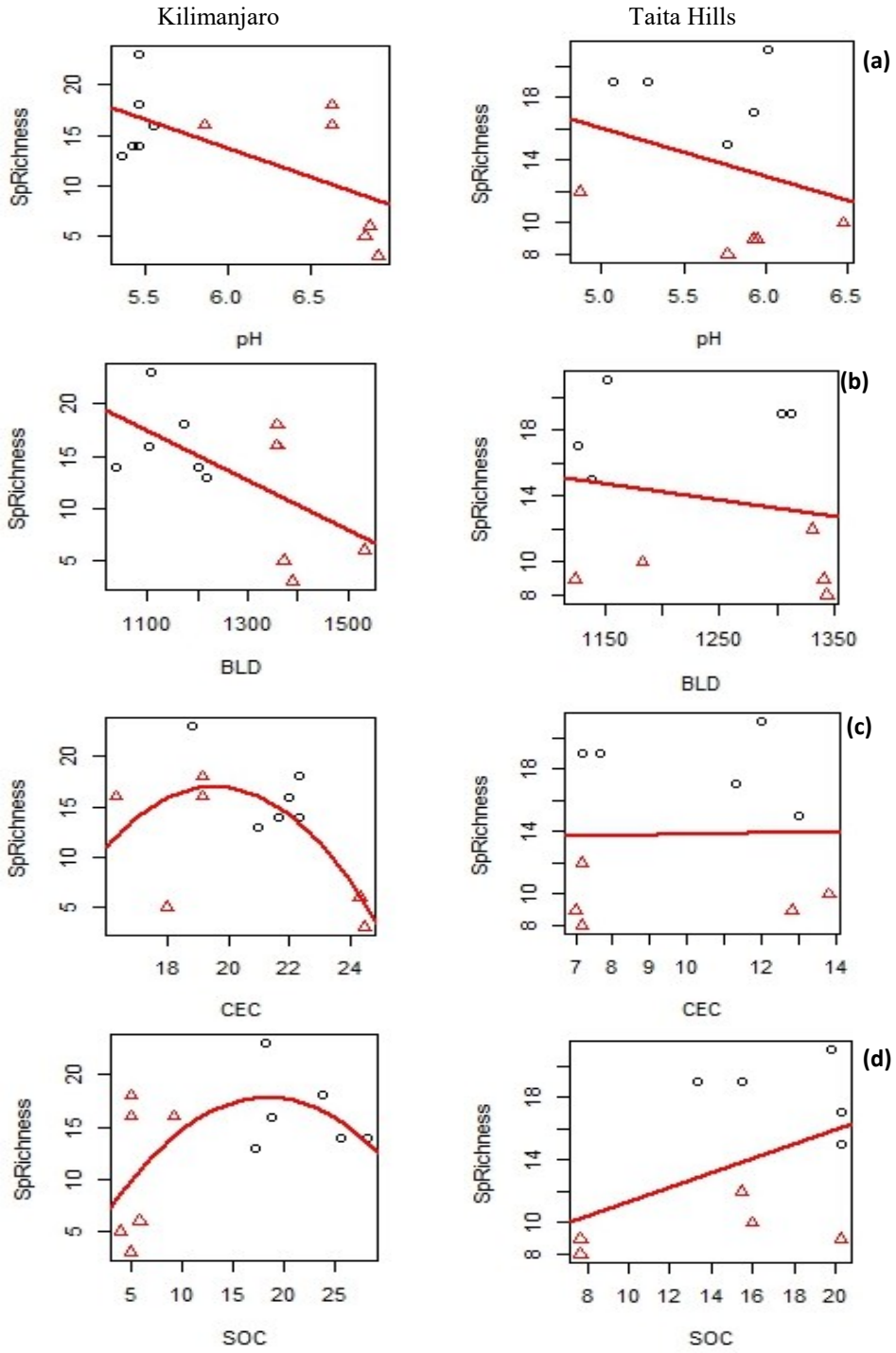

Figure 4.17 - WPSR (SpRichness) distribution with the variation of the soil variables (pH, BD, CEC and SOC) in Kilimanjaro and Taita Hills.

c. Enhanced Vegetation Index

In both slopes of Taita Hills and Mount Kilimanjaro, woody species richness increases with the increase in EVI but no significant relationship is observed in the two sites (Fig. 4.18a, Table 4.6).

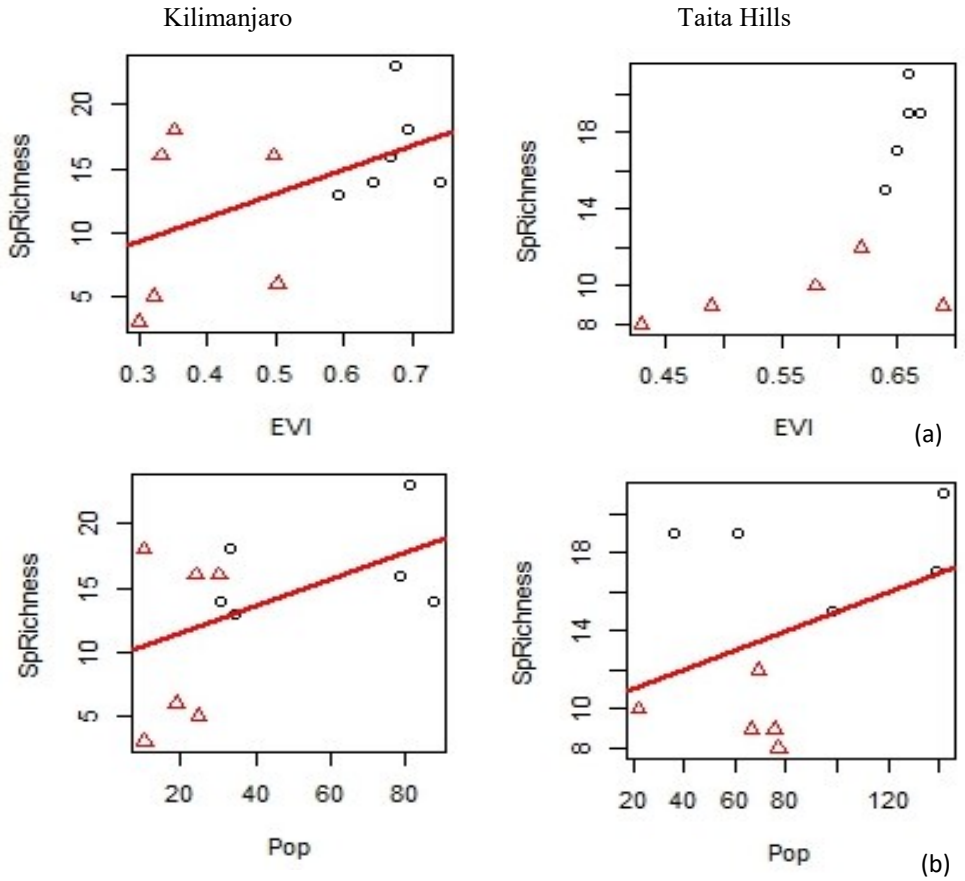

Figure 4.18 - WPSR (SpRichness) distribution with variation of the Enhanced Vegetation Index (EVI) and Population Density (Pop) in Kilimanjaro and in Taita Hills.

d. Population Density

Distribution of woody species richness increases with the increase of human population density in Kilimanjaro and Taita Hills (Fig. 4.18b, Table 4.6) but with no significant relationship is observed between the variables. The change in woody species richness with increase of population density is more varied on landscape where there is low to high population density (Fig. 4.18b, Table 4.6).

Table 4.6: Univariate model relationship of species richness (SpRichness) with variation of environmental variables in Kilimanjaro and Taita Hills.

Site	Species Richness Model	RSE	DF	R^2:	F:	*p-value*	AIC:
Kilimanjaro	KRichMod CEC<-lm(SpRichness~CEC+I(CEC^2))	4.89	9	0.45	3.628	0.07	76.70
	KRichMod Slope<-lm(SpRichness~Slope+I(Slope^2))	3.82	9	0.66	8.80	0.01	70.79
	KRichMod Elev<-lm(SpRichness~Elev+I(Elev^2))	4.26	6.21	0.58	6.21	0.02	73.39
	KRichMod pH<-lm(SpRichness~pH)	4.78	10	0.41	7.02	0.02	75.41
	KRichMod BD<-lm(SpRichness~BD)	5.02	10	0.35	5.44	0.04	76.59
	KRichMod SOC<-lm(SpRichness~SOC+I(SOC^2))	5.26	9	0.36	2.54	0.13	78.45
	KRichMod EVI<-lm(SpRichness~EVI)	5.33	10	0.27	3.69	0.08	78.03
	KRichMod Pop<-lm(SpRichness~Pop)	5.45	10	0.24	3.10	0.11	78.56
Taita Hills	TRichMod Elev<-lm(SpRichness~Elev+I(Elev^2))	1.79	7	0.90	29.92	0.00	44.49
	TRichMod Slope<-lm(SpRichness ~ Slope)	3.18	8	0.62	13.20	0.01	55.31
	TRichMod Pop<-lm(SpRichness~Pop+I(Pop^2))	4.60	7	0.31	1.58	0.27	63.32
	TRichMod SOC<-lm(SpRichness~SOC)	4.61	8	0.21	2.14	0.18	62.69
	TRichMod CEC<-lm(SpRichness ~ CEC)	5.18	8	0.00	0.01	0.94	65.05
	TRichMod BD<-lm(SpRichness~BD)	5.07	8	0.4	0.36	0.57	64.62
	TRichMod EVI<-lm(SpRichness~ EVI + I(EVI^2))	4.22	7	0.42	2.54	0.14	61.60
	TRichMod pH<-lm(SpRichness~pH)	4.94	8	0.09	0.81	0.40	64.09

ii. Multivariate Model Response

Some multiple predictors play an important role in the distribution of the woody species richness along the elevation gradients of Taita Hills and Mount Kilimanjaro. Variation of elevation and slope angle apparently contribute more to the distribution of woody species richness than edaphic factors in each site. While, elevation and slope variation contribute significantly to the variation of woody species richness in Taita, edaphic variables significantly explain WPSR distribution in Kilimanjaro. The multiple linear main effect mean of elevation and slope (TRichMod1) significantly contributes 70% of the variation of the woody species richness (p=0.02, AIC=55.30) in Taita Hills (Table 4.7). When quadratic term is introduced to TRichMod1 (i.e. TRichMod2), significant variation in woody species richness in Taita Hills is observed (R^2=0.95, p=0.0003, AIC=39.5) (Table 4.7), while the addition of the quadratic term into the KRichMod1 (i.e. KRichMod2) only contributes an insignificant 58% variation in richness in Kilimanjaro (Table 4.7).

Population density was deemed an important factor that could influence the distribution of woody species richness. Thus, it was introduced into the first and the second models in each site and an assessment made on the main effect mean on the woody species richness. Addition of this factor into

the first multivariate model significantly increased the contribution of the multiple predictors (TRichMod3) on the variation of woody species richness to 86% (p=0.005, AIC=49.11) in Taita Hills (Table 4.7). The increased contribution of the new model (KRichMod3) on the variation of woody species richness in Kilimanjaro is very significant (Table 4.7). It is only in Taita Hills where population density, apparently, has an increased contribution to variation of the WPSR. When population density is added into the second model that considered quadratic term of the elevation, negligible but significant improvement on the main effect mean was observed on WPSR in Taita Hills (R^2=0.97, p=0.0007, AIC=36.91) but very weak and insignificant contribution of the model observed on the variation of WPSR in Kilimanjaro (Table 4.7). In Taita Hills, the quadratic term of the elevation seems to have more contribution on the variation of WPSR than observed in Kilimanjaro.

Independent treatment of edaphic variables SOC, CEC, BD and pH in a multivariate analysis as additive predictor variables (SpRichness~ SOC + CEC + BD + pH) does not show significant contribution to the variation of the WPSR in both sites. However, after several formulations of multivariate models by updating the above by removing and/or adding interactive terms and population density to the model significant relationships were observed with WPSR only in Kilimanjaro. The distribution of WPSR in Taita Hills does not seem to relate with the edaphic factors as observed in Kilimanjaro. The multiple main effect mean of pH and CEC contribute to 58% of variation of WPSR in Kilimanjaro (p=0.02, AIC=73.5). Separate treatment of the interactive terms of BD and CEC, and pH, CEC and BD in multivariate model shows the significant contribution of their interaction on the variation of WPSR in Kilimanjaro (Table 4.7).

Expansion of an additive model combining the physical factors, edaphic variables, and population density improved fitting of the models, especially in Kilimanjaro (Table 4.7). Inclusion of population density into the model tend to minimize the Residual Standard Error (RSE) in Taita Hills model raising the R^2 from 0.98 to 1 (RSE=0.26, F=392, p=0.04, AIC=-1.46) (Table 4.7). Under this model, population density seems to play additional role in the distribution of WPSR in Taita Hills. Application of similar model in Kilimanjaro only shows about 76% variation affected but no significant relationship (Table 4.7). Updating the model in Kilimanjaro significantly improves on the relationship of multiple predictors with the WPSR (Table 4.7). Thus, additive model of SOC and quadratic function of the elevation (2^{nd} order) significantly explain 78% variation in WPSR (F=9.67, p=0.01, AIC=67.42) (Table 4.7). Subsequent additive models that were updated in Kilimanjaro show significant relationships, but with a slight reduction in fitting of the model (Table 4.8).

Table 4. 7: The univariate and multivariate models of WPSR (SpRichness) with environmental variables in Kilimanjaro and Taita Hills.

	Model	RSE	DF	R^2	F	p-val.	AIC
Univariate Model							
Taita Hills	TrichMod Elev<-lm(SpRichness~Elev + I(Elev^2)	1.79	7	0.90	29.92	0.00	44.49
	TrichMod Slope<-lm(SpRichness~Slope)	3.18	8	0.62	13.20	0.01	55.31
Kilimanjaro	KRichMod Slope<-lm(SpRichness~Slope + I(Slope^2))	3.82	9	0.66	8.80	0.01	70.79
	KRichMod Elev<-lm(SpRichness~Elev + I(Elev^2))	4.26	9	0.58	6.21	0.02	73.39
	KRichMod pH<-lm(SpRichness~pH)	4.78	10	0.41	7.02	0.02	75.41
	KRichMod BD<-lm(SpRichness~BD)	5.02	10	0.35	5.44	0.04	76.59
Multivariate Model							
Taita Hills	TRichMod1<-lm(SpRichness~Elev + Slope)	3.08	7	0.70	7.84	0.02	55.30
	TRichMod2<-lm(SpRichness~Elev + I(Elev^2) + Slope)	1.37	6	0.95	36.44	0.00	39.50
	TRichMod3<-lm(SpRichness~Elev + Slope + Pop)	2.21	6	0.86	12.69	0.01	49.11
	TRichMod5<-lm(SpRichness~Elev + I(Elev^2) + Slope + Pop)	1.19	5	0.97	36.76	0.00	36.91
	TRichMod11<-lm(SpRichness~SOC + pH + CEC + BD + Elev + I(Elev^2) + Slope + Pop)	0.26	1	1.00	392	0.04	-1.46
Kilimanjaro	KRichMod1<-(lm(SpRichness~Elev + Slope))	4.63	9	0.50	4.58	0.04	75.37
	KRichMod5<-lm(SpRichness~ CEC + pH)	4.28	9	0.58	6.11	0.02	73.51
	KRichMod6<-lm(SpRichness ~ SOC + Slope + Elev + Pop)	3.73	7	0.75	5.23	0.03	71.20
	KRichMod7<-lm(SpRichness ~ SOC + Elev + Pop)	3.80	8	0.70	6.34	0.02	71.20
	KRichMod8<-lm(SpRichness ~ SOC + Elev)	4.04	9	0.62	7.41	0.01	72.12
	KRichMod9<-lm(SpRichness ~ SOC + Elev + I(Elev^2))	3.24	8	0.78	9.67	0.01	67.42

iii. Woody Plant Species Richness Model Comparisons

Univariate and multivariate models that significantly fitted richness model were considered for comparison to establish differences among and between them. It is assumed that models that are significantly different relate with the WPSR in a different way.

a. Mount Kilimanjaro models comparison

Univariate model with elevation as a predictor (KRichMod Elev) in Kilimanjaro is significantly different from additive model of SOC, Elevation and quadratic term of elevation (KRichMod9) (ANOVA F=7.54, p=0.03) (Table 4.8). The difference is apparently caused by inclusion of SOC into

the former model. KRichMod Elev model has AIC value of 73.39 while KRichMod9 has lower AIC of 67.42 (Table 4.8). SOC probably contribute to the difference on how the additive predictors relate with the WPSR.

The univariate slope (KRichMod Slope) is significantly different from the univariate models with pH (KRichMod pH) (ANOVA F=6.63, p=0.03) and BD (KRichMod BD) (ANOVA F=8.24, p=0.02) (Table 4.8). Thus, slope variable and pH, and BD are not related in their relationship with the WPSR in Kilimanjaro. However, KRichMod pH and KRichMod BD are not significantly different and therefore these models are assumed to be similar in predicting WPSR in Kilimanjaro (Table 4.8). KRichMod Slope is however more preferred model than the other two due to its lower AIC value (Table 4.8).

The multivariate elevation and slope (KRichMod1) is significantly different from the multivariate SOC, Elevation, and Population (KRichMod7) in their influence on WPSR (ANOVA F=5.38, p=0.05) and multivariate SOC and quadratic term of elevation (KRichMod9) (ANOVA F=10.33, p=0.01) (Table 4.8). However, KRichMod7 and KRichMod9 are not significantly different and therefore these models are assumed to be similar in modeling WPSR in Kilimanjaro. KRichMod7 is apparently the preferred model among the three models due to its low AIC value (Table 4.8).

Comparison of multivariate CEC and pH model (KRichMod5) with the KRichMod9 model (SOC and quadratic term of elevation) with WPSR indicate significant differences between the two models (ANOVA F=7.69, p=0.02) (Table 4.8). KRichMod9 model has lower AIC (R^2=0.78, p=0.01, AIC=67.42) compared to KRichMod5 (R^2=0.58, p=0.02, AIC=73.37) (Table 4.8). KRichMod9 model is also significantly different from KRichMod8 (SOC and elevation) (ANOVA F=5.98, p=0.04) (Table 4.8), with the latter having AIC=72.12, higher than KRichMod9 (Table 4.8).

The univariate elevation with quadratic term (KRichMod Elev) and multivariate SOC and quadratic term of elevation (KRichMod9) relationship with WPSR are significantly different (ANOVA F=7.54, p=0.03) (Table 4.8). It is apparent that the inclusion of SOC in the elevation model creates difference on prediction of WPSR. Its inclusion in KRichMod Elev explains why the AIC value for KRichMod9 is lower than KRichMod Elev (Table 4.8).

The difference in WPSR response to the univariate BD (KRichMod BD) and multivariate SOC, elevation and Population density (KRichMod7) is significant (ANOVA F=4.75, p=0.04), significant with multivariate SOC and elevation (KRichMod8) (F=6.43, p=0.03) and also significant with multivariate SOC, elevation with quadratic term (KRichMod9) (ANOVA F=7.98, p=0.01) (Table 4.8). KRichMod8 and KRichMod9 models are significantly different (ANOVA F=5.98, p=0.04) KRichMod9 is the most preferred because it has low AIC than the three models (Table 4.8).

Table 4. 8: Comparison of Species Richness Models from Mount Kilimanjaro; F-statistic\p-value (ANOVA) of model comparisons.

Kilimanjaro F/*p-Value* (ANOVA)										
	KRichMod Elev	KRichMod Slope	KRichMod pH	KRichMod BD	KRichMod1	KRichMod5	KRichMod6	KRichMod7	KRichMod8	KRichMod9
KRichMod Elev		1	0.09	0.06	1	1	0.17	0.11	1	0.03
KRichMod Slope	0		0.03	0.02	1	1	0.35	0.32	1	0.07
KRichMod pH	3.59	6.63		1	0.23	0.10	0.10	0.07	0.05	0.02
KRichMod BD	4.88	8.24	0		0.13	0.06	0.07	0.04	0.03	0.01
KRichMod1	0	0	1.67	2.77		1	0.09	0.05	1	0.01
KRichMod5	0	0	3.46	4.75	0		0.16	0.10	1	0.02
KRichMod6	2.36	1.22	3.13	3.69	3.41	2.42		0.30	0.24	1
KRichMod7	3.34	1.14	3.93	4.75	5.38	3.46	1.27		0.18	1
KRichMod8	0	0	4.99	6.43	0	0	1.77	2.21		0.04
KRichMod9	7.54	4.59	6.86	7.98	10.33	7.69	0	0	5.98	

N.B: KRICHMOD = Kilimanjaro Species Richness Model

b. Taita Hills Models Comparisons

Univariate elevation (TRichMod Elev) and univariate slope (TRichMod Slope) relates significantly with WPSR on transect (ANOVA F=18.23, p=0.00) (Table 4.9). TRichMod Elev has a lower AIC (44.49) compared to TRichMod Slope (AIC=55.31), hence preferred compared to the latter (Table 4.9).

The relationship of multivariate elevation and slope (TRichMod1) with the WPSR significantly differ with how the multivariate slope and elevation with quadratic pattern (TRichMod2) (ANOVA F=29.58, p=0.00), multivariate elevation, slope and population density (TRichMod3) (ANOVA F=7.60, p=0.03) and multivariate elevation with quadratic term, slope and population density (TRichMod5) (ANOVA F=20.96, p=0.00) relate with WPSR (Table 4.9). Among these models, only TRichMod3 and TRichMod5 significantly differ on their relationship with WPSR (ANOVA F=15.70, p=0.01 (Table 4.9). TRichMod5 has the lowest AIC (36.91) than models considered in this comparisons (Table 4.9).

Table 4. 9: Comparison of Species Richness Models from Taita Hills; F-statistic\p-value (ANOVA) of model comparisons.

Taita Hills F/*p-Value* (ANOVA)								
	TRichMod Elev	TRichMod Slope	TRichMod1	TRichMod2	TRichMod3	TRichMod4	TRichMod5	TRichMod11
TRichMod Elev		0.00	1	0.05	1	1	0.06	0.10
TRichMod Slope	18.23		0.25	0.00	0.05	0.03	0.00	0.06
TRichMod1	0	1.56		0.00	0.03	1	0.00	0.06
TRichMod2	6.08	18.76	29.58		1	0.01	0.15	0.13
TRichMod3	0	5.32	7.60	0		0.19	0.01	0.08
TRichMod4	0	7.28	0	15.34	2.16		0.01	0.08
TRichMod5	5.46	17.46	20.96	2.91	15.70	11.57		1
TRichMod11	54.58	168.99	161.14	32.44	85.20	96.57	0	

N.B: TRICHMOD = Taita Species Richness Model

iv. Evaluation of Richness models

a. Mount Kilimanjaro Richness Model Evaluation

Prediction of five models correlated significantly with the plot WPSR data in both Kilimanjaro and Taita Hills.

In Kilimanjaro area, the univariate elevation (KRichMod Elev) significantly correlated with 78% of plot WPSR (p=0.00) (Table 4.10). This model however predicts negative values for the WPSR in the lower elevation but estimates the upper range of WPSR better (Fig. 4.19). It also underestimates richness at the mid elevation area.

The prediction of the WPSR by univariate pH (KRichMod pH) and univariate BD (KRichMod BD) correlates significantly each with 61% of the plot WPSR, p=0.03 and p=0.04, respectively (Table 4.10). The two models estimate very well the range values for plot WPSR along the transect, but seems to underestimate WPSR in the mid transect areas (Fig. 4.19).

An estimated 70% of predicted WPSR by KRichMod5 (univariate CEC and pH) correlates significantly with the plot WPSR (p=0.01) (Table 4.10). The model fixes very well the range of plot WPSR but underestimates in the lower-mid transect (Fig. 4.19).

Predicted WPSR by KRichMod9 (univariate SOC, and quadratic term of elevation) correlates significantly with 78% of the plot WPSR (Table 4.10). The model fixes the upper plot WPSR value very well but the lower transect is predicted to be negative (Fig. 4.19).

Model KRichMod5 (multivariate CEC and pH) is apparently preferred in Kilimanjaro among the models generated; this is followed by KRichMod pH and KRichMod BD.

Table 4. 10: Validation of prediction models with observed WPSR in Kilimanjaro using correlation (R).

MODEL	Model Validation (PredRich. Vs PlotRich)	
Univariate Model	**R**	**p-value**
KRichMod Slope<-lm(SpRichness~Slope + I(Slope^2))	-0.13	0.68
KRichMod Elev<-lm(SpRichness~Elev + I(Elev^2))	0.78	0.00
KRichMod pH<-lm(SpRichness~pH)	0.61	0.03
KRichMod BD<-lm(SpRichness~BD)	0.61	0.04
Multivariate Model		
KRichMod1<-(lm(SpRichness~Elev + Slope))	0.45	0.14
KRichMod5<-lm(SpRichness~ CEC + pH)	0.70	0.01
KRichMod6<-lm(SpRichness ~ SOC + Slope + Elev + Pop)	0.48	0.12
KRichMod7<-lm(SpRichness ~ SOC + Elev + Pop)	0.48	0.11
KRichMod8<-lm(SpRichness ~ SOC + Elev)	0.56	0.06
KRichMod9<-lm(SpRichness ~ SOC + Elev + I(Elev^2))	0.78	0.00

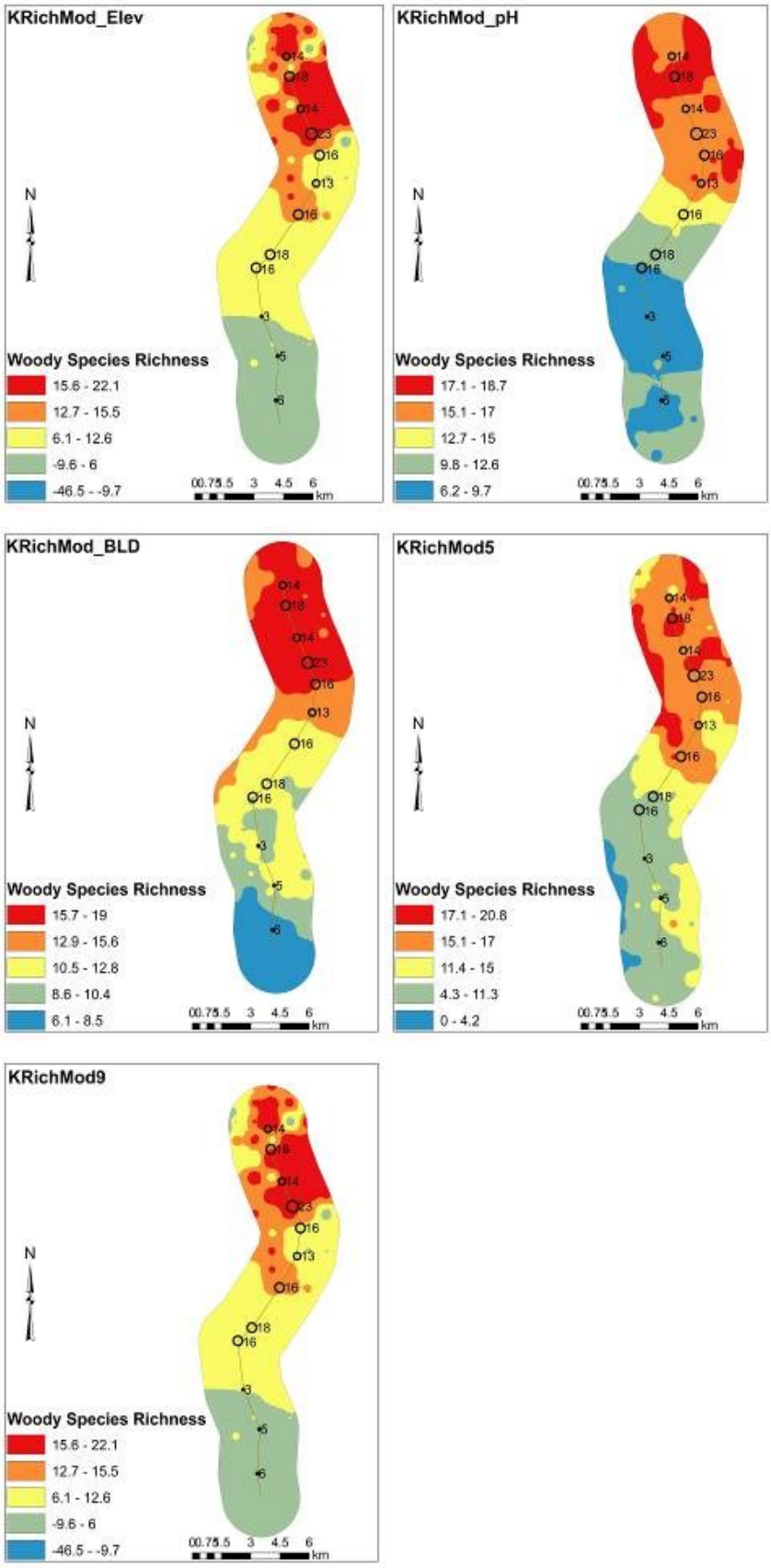

Figure 4.19 - Predicted WPSR on transect in Kilimanjaro. KRichMod is Kilimanjaro Species Richness Model.

b. Taita Hills Richness Model Evaluation

Five WPSR model predictions are significantly correlated with the plot WPSR data in Taita Hills. These models include: Univariate elevation and its quadratic terms (TRichMod Elev); multivariate elevation and slope (TRichMod1); multivariate slope and elevation and its quadratic terms (TRichMod2); multivariate elevation, slope and population density (TRichMod3), and multivariate slope, population density, elevation and its quadratic terms (TRichMod5).

Predictions of TRichMod Elev correlate significantly with 97% of the plot WPSR ($p=0.00$) (Table 4.11). The model prediction reflects the plot richness values. However, it does not extrapolate maximum richness beyond the maximum plot richness values (Fig. 4.17).

TRichMod1 predictions significantly correlate with 67% of the plot WPSR ($p=0.03$) but overestimates richness in the lower and upper transect areas (Table 4.11). The model however, extrapolates range values of WPSR that consider possible higher richness in areas observation was not made (Fig. 4.20).

WPSR predictions of TRichMod2 correlates significantly with 98% of the plot WPSR ($p=0.00$) (Table 4.11). The model prediction reflects the plot richness values. Unlike TRichMod Elev, the model extrapolates range values of WPSR that consider possible higher richness in areas observation was not made (Fig. 4.20).

TRichMod3 predictions of WPSR correlate significantly with 69% of plot WPSR values ($p=0.03$) (Table 4.11). The model appears to be under- and over-estimate some plot WPSR values. It predicts some areas would have zero richness per hectare. This is based on the estimated lower range (Fig. 4.20).

TRichMod5 predictions of WPSR correlate significantly with 97% of plot WPSR values ($p=0.00$) (Table 4.11). The model prediction reflects the plot richness values. This model is close to TRichMod Elev and 2. However, areas with high richness tend to minimize in this model (Fig. 4.20).

The most preferred model for predicting the WPSR in Taita Hills is TRichMod2 because of its extrapolation range values of richness and a reflection of predicted richness which is closer to plot WPSR. Other models tend to under or over-estimate richness and also depict unrealistic minimum range of richness in the lower transect area.

Table 4. 11: Validation of prediction models with WPSR in Taita Hills using correlation (R).

Model	Model Validation (PredRich. Vs PlotRich)	
	R	p-value
Univariate Model		
TrichMod Elev<-lm(SpRichness~Elev + I(Elev^2)	0.97	0.00
TrichMod Slope<-lm(SpRichness~Slope)	0.51	0.13
Multivariate Model		
TRichMod1<-lm(SpRichness~Elev + Slope)	0.67	0.03
TRichMod2<-lm(SpRichness~Elev + I(Elev^2) + Slope)	0.98	0.00
TRichMod3<-lm(SpRichness~Elev + Slope + Pop)	0.69	0.03
TRichMod5<-lm(SpRichness~Elev + I(Elev^2) + Slope + Pop)	0.97	0.00
TRichMod11<-lm(SpRichness~SOC + pH + CEC + BD + Elev + I(Elev^2) + Slope + Pop)	0.41	0.24

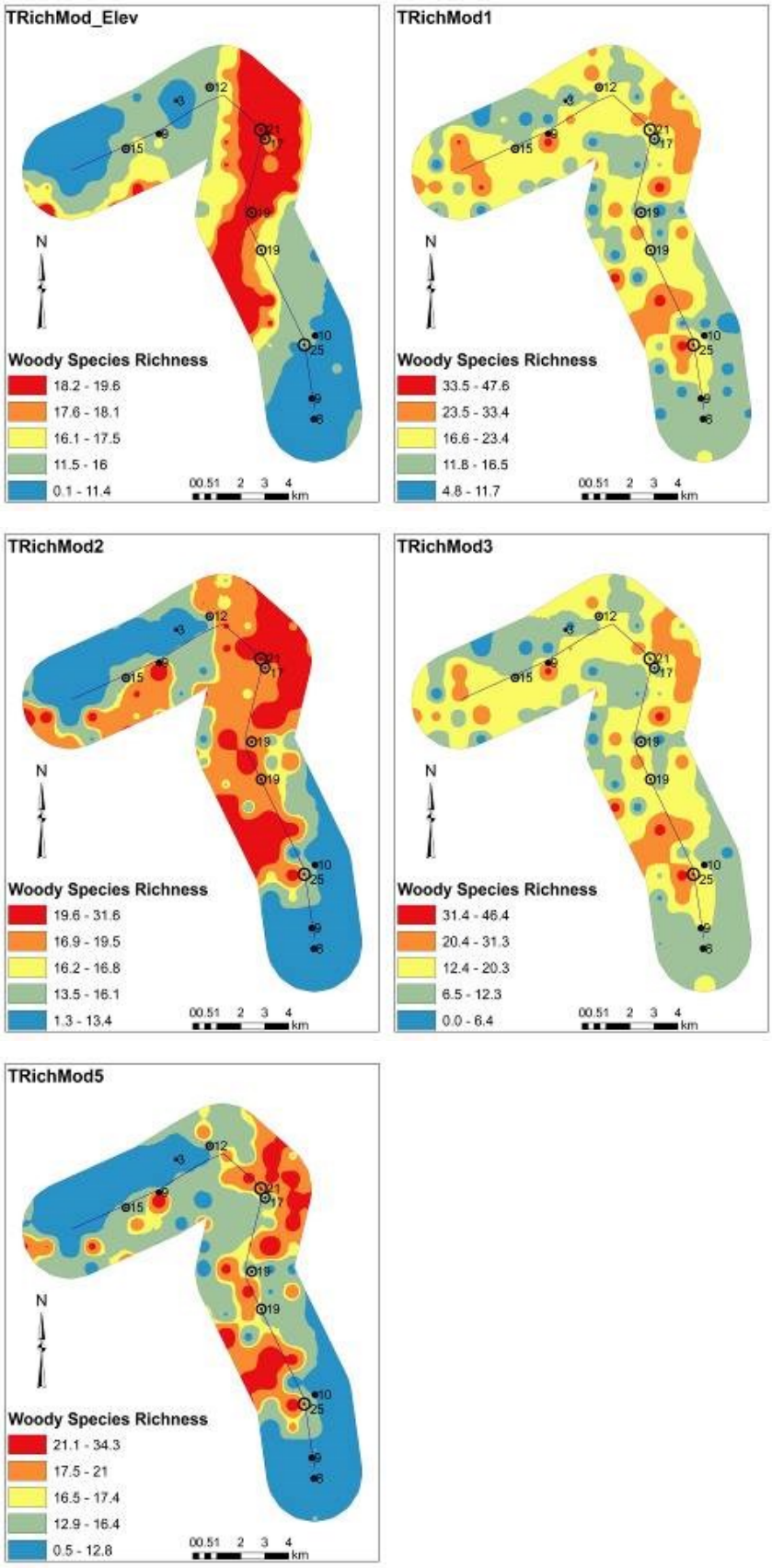

Figure 4.20 - Predicted WPSR distribution on transect in Taita Hills. TRichMod is Taita Hills Species Richness Model.

4.2.7. Key Findings for objective 2

The woody plant species richness are significantly different on the inhabited areas of Mount Kilimanjaro and Taita Hills (Shannon Diversity Test, t=3.06, p=0.002). Significant difference is also observed on WPSR in types of cropland between and within site. The two sites has about 32% of the species occurring in both sites, 30% occur only in Kilimanjaro and 39% occur only in Taita Hills. In Kilimanjaro, 26% of species in the site occur in both types of cropland. While in Taita Hills 48% of the species occur in both types of cropland. The stock density of the trees has significant relationship in Kilimanjaro (R^2=0.60, p=0.00) and Taita Hills (R^2=0.95, p=0.00). The spatial distribution of WPSR is explained better by univariate model of elevation (R^2=0.90, p=0.00, AIC=44.49) in Taita Hills and univariate model of slope (R^2=0.66, p=0.01, AIC=70.79) in Kilimanjaro. The simulteneous influence of SOC and elevation (2^{nd} order) is very useful in explaining the spatial distribution of WPSR in Kilimanjaro (R^2=0.78, p=0.00, AIC=67.42). In Taita Hills, the spatial distribution of WPSR is simultenously better explained by quadratic function of elevation, slope and population density (R^2=0.95, p=0.00, AIC=36.91).

4.4. Carbon Storage along the elevation gradient of Taita Hills and Mount Kilimanjaro

4.4.1. Site AGCS

The transect from Mount Kilimanjaro recorded a total minimum of AGCS of 1.01 Ct/ha and maximum of 68.28 Ct/ha. Areas with low and high AGCS per ha are more varied on Kilimanjaro. This is explained by the boxplot long whiskers below and above the boxplot (i.e. below 1st and 3rd quartiles) (Fig 4.21). However, areas with moderate AGCS do not vary as explained by the median (41.90) which is relatively closer to the mean (39.06±) of AGCS in Kilimanjaro (Fig 4.21).

In Taita Hills, areas with high AGCS vary more than areas with low AGCS occuring above the 3rd quartile (37.84) than below the 1st quartile (14.06) (Fig 4.21). The mean of AGC along the inhabited section of Taita Hills is 27.21±4.62 Ct/ha which is relatively closer to the median 24.2, implying that areas with moderate AGCS vary less than slope areas with low AGCS and far less than slopes with high AGCS. The amount of AGCS in Taita Hills and Kilimanjaro are however, not significantly different in the mean and variation in AGCS as tested by (t test and Fischer's test).

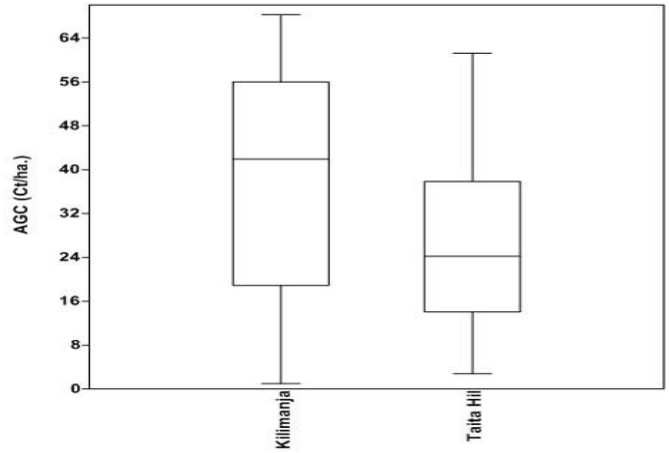

Figure 4.21 - Boxplot of AGCS distribution in Taita Hills and Mount Kilimanjaro.

4.3.2. AGCS in Types of Cropland

Cropped land in Kilimanjaro has mean AGCS estimated at 19.67±5.18 Mg C/ha. This is approximately 1/3 times the mean AGC in agro-forestry 58.45±2.75 Ct/ha in the same site. AGC varies significantly in cropped land and agro-forestry in Kilimanjaro (F=17.41, p=0.007), and their means differ significantly (t=4.62, p=0.001) (Fig. 4, 22;Table 4.12). In Taita Hills, in cropped land has mean of AGCS estimated at 13.69±1.54 Mg C/ha; approximately 1/3 times the mean AGC in agro-forestry (43.95±7.4 Mg C/ha. The AGCS in cropped lands and agro-forestry areas in Taita Hills differ significantly in means (t=4.86, p=0.001) but not in their variance (Fig. 4.21; Table 4.12). Agro-

forestry in Taita Hills has AGCS 1.3 times the amount of AGCS in Kilimanjaro with significant variation in their AFCS (F= 9.36, p=0.028) (Fig. 4.22; Table 4.12). The cropped land in Taita has AGCS is approximately 1.5 times AGCS in Kilimanjaro. The AGCS in the cropped land significantly varies (F=10.92, p=0.020) between the sites but their means are not significantly different (Fig. 4.22; Table 4.12).

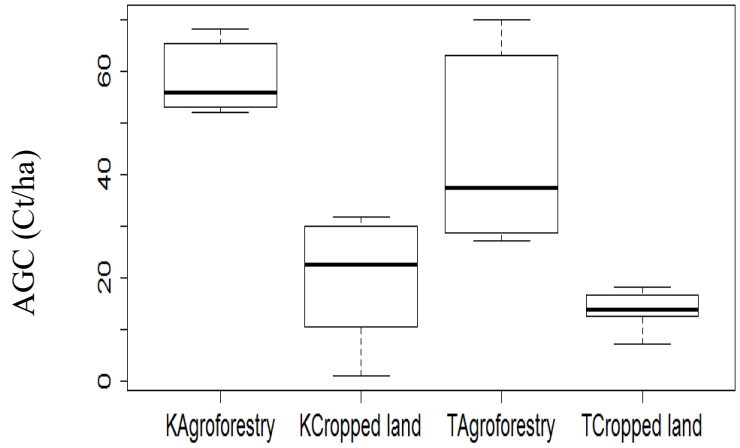

Figure 4.22 - Distribution of AGC in types of cropland in Kilimanjaro and Taita Hills. KAgro-forestry means Agro-forestry in Kilimanjaro.

Table 4. 12: AGCS distribution in cropped lands and Agro-forestry areas in Kilimanjaro and Taita Hills.

Comparison		AGCS (Mean±SE)		Fischer's F test		Student's t test	
		Kilimanjaro	Taita	F	p	t	p
Between Sites	Agro-forestry	58.45±2.75	43.95±7.4	9.36	0.03	1.95	0.08
	Cropped Land	19.67±5.18	13.69±1.54	10.92	0.02	0.58	0.57
Within Site	Cropped land Vs Agro-forestry		Kilimanjaro	17.41	0.01	4.62	0.00
			Taita	5.87	0.08	4.86	0.00

4.3.3. Species AGCS

AGCS distribution among WPS in Kilimanjaro is dominated by *A. gummifera* with storage estimated at 8.6 Mg C/ha; this is followed by *P. americana* (3.5 Mg C/ha), and *Ficus sycomorus* (3.3 Mg C/ha) (Fig. 4.23). In Taita Hills, the dominant WPS is *G. robusta* which has AGCS of about 4.6 Mg C/ha; this is followed by *M. indica* (2.6 Mg C/ha), and *Eucalyptus maculata* with 1.7 Mg C/ha (Fig. 4.24). In Kilimanjaro, the highest AGCS in agro-forestry occur on *A. gummifera* which is estimated at with 7.7 Mg C/ha, while *G. robusta* dominates Taita Hills (7.6 Mg C/ha). AGCS on Cropped land in Taita Hills and Kilimanjaro is dominated by *M. indica* which AGCS is estimated at 3.2 Ct/ha and 2.3 Mg C/ha, in respective sites.

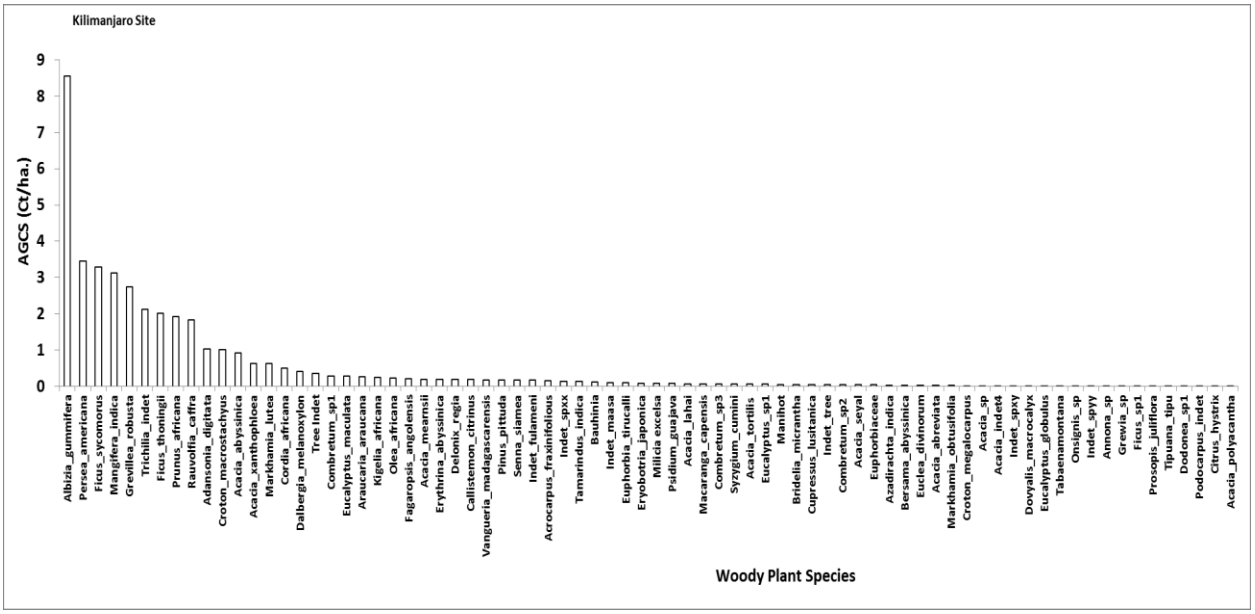

Figure 4.23 - AGCS distribution on WPS in Mount Kilimanjaro.

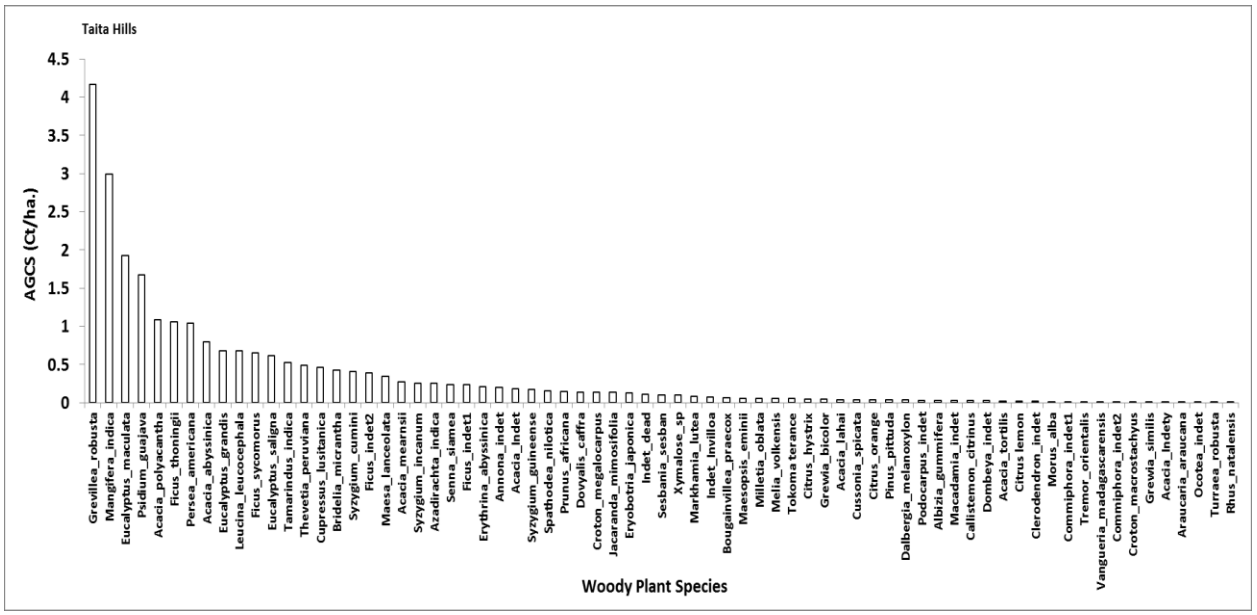

Figure 4.24 - AGCS distribution on WPS in Taita Hills.

4.3.4. Relationship of AGCS with Woody Plant Species

Distribution of AGCS increases with the increase in WPSR and stock density in Taita Hills and Kilimanjaro. Square root of AGCS increases significantly with increase in stock density of WPS in Kilimanjaro ($F=7.81$, $R^2=0.44$, $p=0.02$) (Fig. 4.25a). However, the stock density and WPSR in Kilimanjaro correlates by 77%.

AGCS significantly increases with the increase in WPSR (F=15.62, R^2=0.66, p=0.00) and stock density (F=20.19, R^2=0.72, p=0.00) in Taita Hills (Fig. 4.25b). The stock density and WPSR for Taita Hills are significantly related (R^2=0.95, F=89.93, p=0.00).

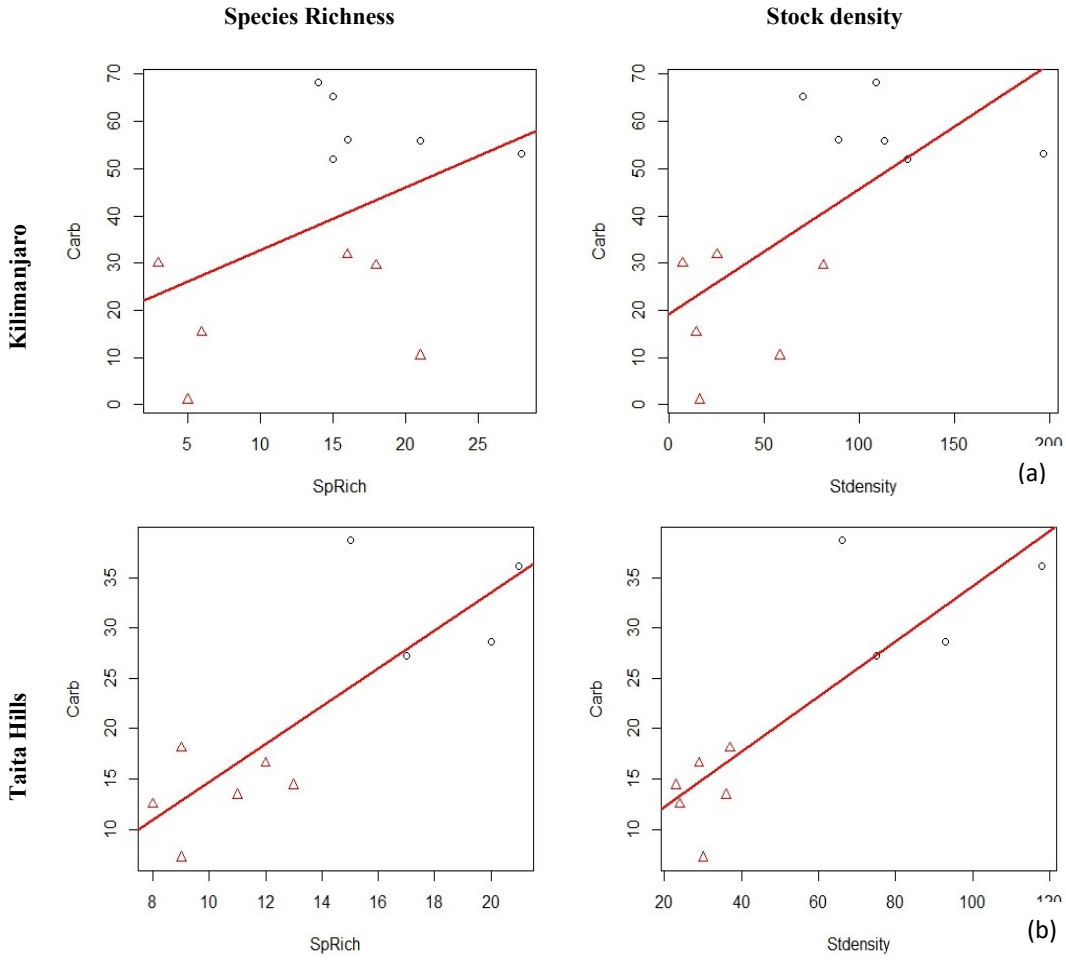

Figure 4.25 - AGCS (Carb) relationship with WPSR (SpRich), and stock density (abundance). 4.25a – in Kilimanjaro. 4.25b – in Taita Hills

4.3.5. Relationship of AGCS with environmental variables along elevation gradients

i. Univariate

Relationships of the AGCS were assessed against predictor variables: physical variables (elevation and slope); edaphic variables (soil BD, pH, SOC and CEC); biophysical variable (EVI), and human population density.

a. Physical variables

Distribution of AGCS varies highly and does not fit significantly with the increase in slope angle in Kilimanjaro slopes but certainly with the variation of elevation (F=12.54, R^2= 0.72, p=0.00) (Fig.

4.26a, Table 4.13). In Taita Hills, it is the slope angle variation that has significant influence (F=5.94, R^2=0.73, p=0.00) (Fig. 4.26a, Table 4.13) on the distribution of AGCS ompared to the elevation (Fig. 4.26b, Table 4.13). Thus, AGCS in Taita Hills increases significantly with increase of the slope. Areas in Taita Hills and Kilimanjaro with low slope gradient are preferred for crop cultivation than steep areas. However, steep areas has more preserved and planted trees or trees.

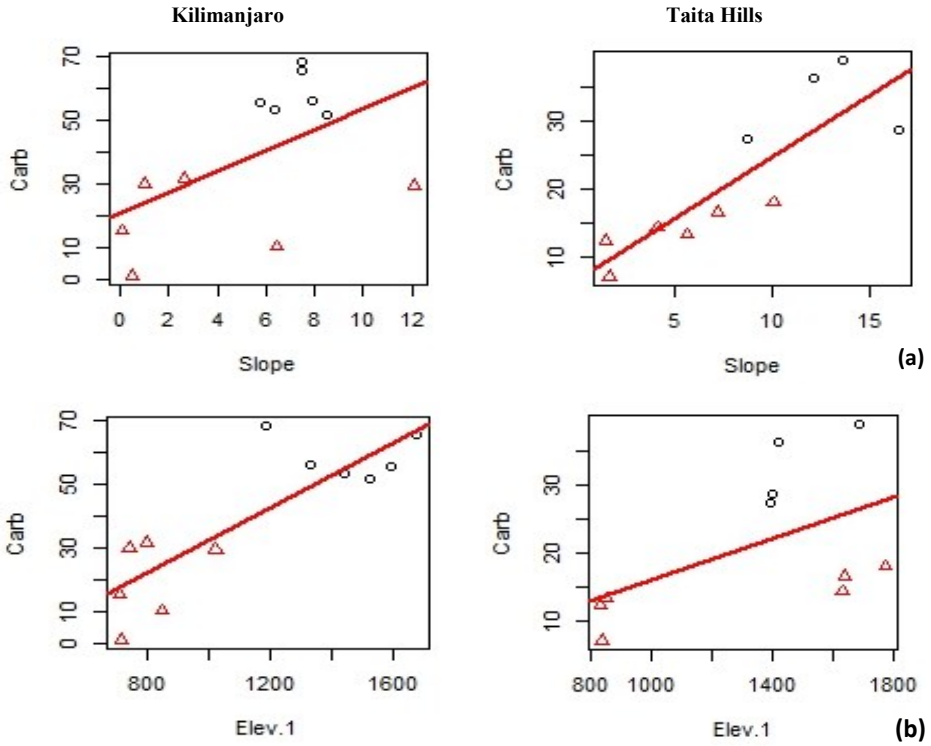

Figure 4.26 - AGCS relationship with physical variables in Taita Hills and Kilimanjaro.

b. Edaphic Variables

Relationship of AGCS with pH seems to be significant only in Kilimanjaro (F=39.14, R^2=0.80, p=0.00) but not in Taita Hills. AGCS decreases significantly with the increase in soil pH in Kilimanjaro but the trend is unclear in Taita Hills (Fig. 4.27a, Table 4.13).

AGCS shows slight increase with increase in CEC in Taita Hills and Kilimanjaro, though the relationship is not significant (Fig. 4.27b, Table 4.13). CEC is predominantly influenced by the underlying soil and geology.

The increase in AGCS relates with the increase in Soil BD levels in Kilimajaro and Taita Hills (Fig. 4.27c, Table 4.13). This increase is only significant in Kilimanjaro (F=14.97, p= 0.00.

AGCS increases significantly with increase in SOC in Kilimanjaro (R^2=0.72, p=0.00) and Taita Hills (R^2=0.56, p=0.01) (Fig. 4.27d, Table 4.13). The relationship between AGCS and SOC is stronger in Kilimanjaro than in Taita Hills. High SOC are associated with areas with more vegetation cover. Soil

pH varies with the amount of SOC, and is less in areas with more trees but high in areas will less vegetation cover.

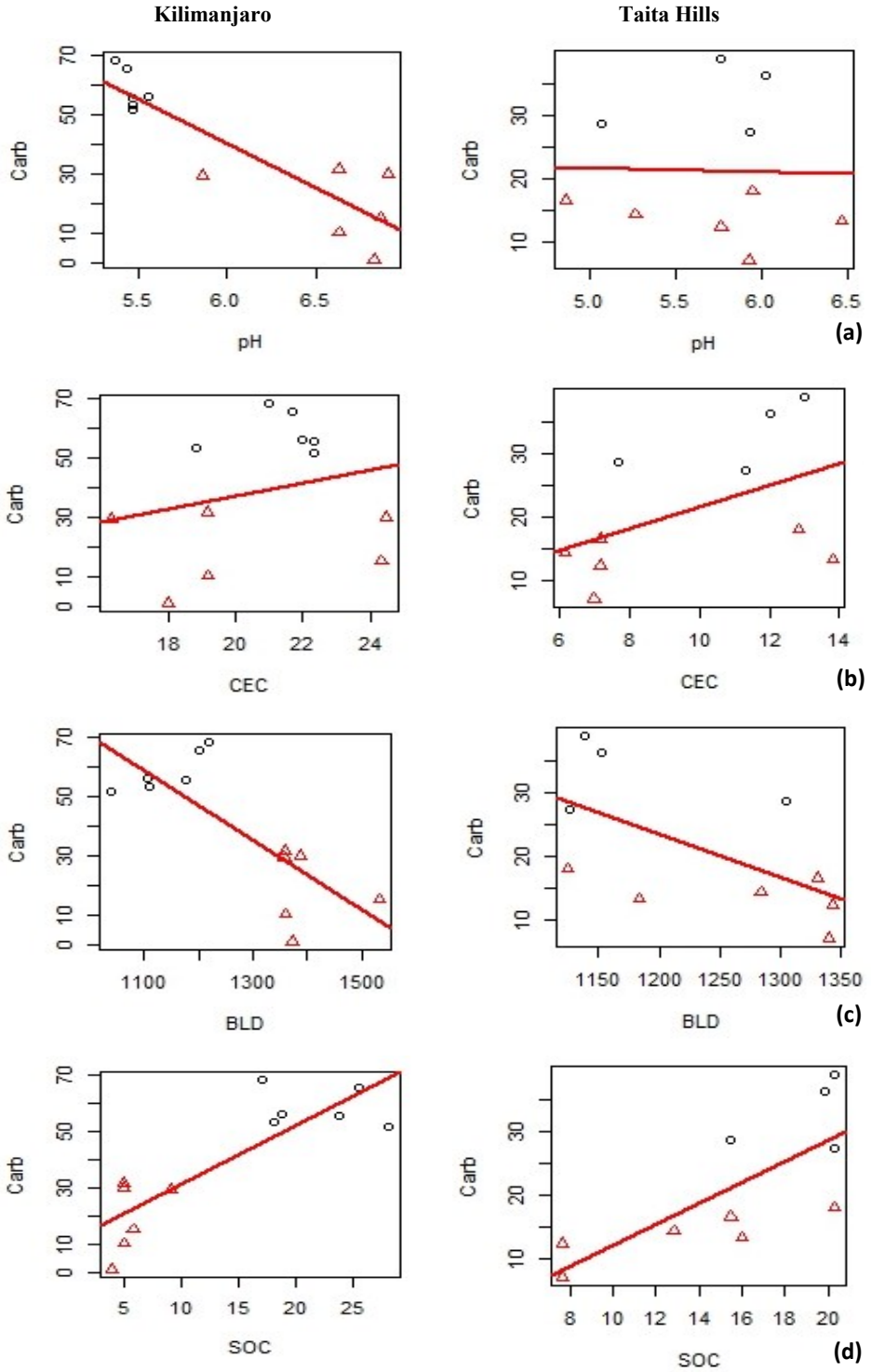

Figure 4.27 - Relationship of AGCS with the edaphic variables in Taita Hills and Kilimanjaro. 4.27a –pH. 4.27b –CEC 4.27c – BD . 4.27d –SOC.

c. Population Density

AGCS significantly increases with increase in population density in Taita Hills (Fig. 4.28, Table 4.13). Though increase in AGCS is observed with the increase in population density in Kilimanjaro, their relationship is not significant (Fig. 4.28, Table 4.13). High AGCS observed in high density areas on the slope can be explained by trees under agro-forestry.

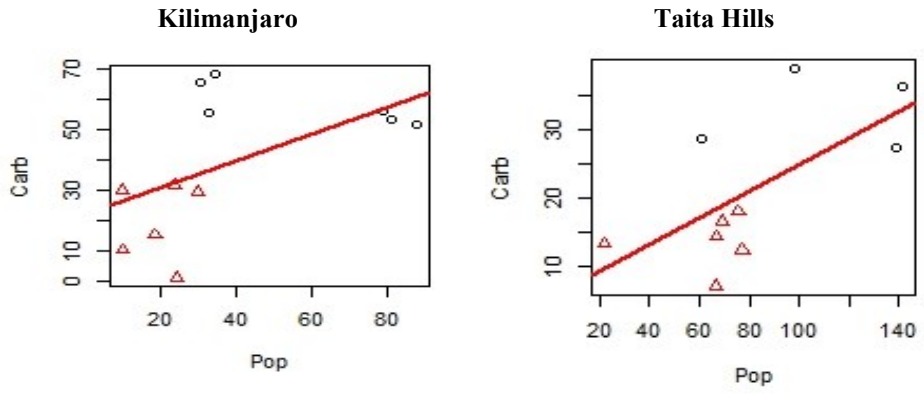

Figure 4 28 - Relationship of AGCS with population density (per 1km2) in Taita Hills and Kilimanjaro.

d. Enhanced Vegetation Index

AGCS significantly increases with increase of EVI in Kilimanjaro (R^2=0.68, p=0.00) and Taita Hills (R^2=0.41, p=0.05) (Fig. 4.29, Table 4.13). The increase of AGCS is more varied in Kilimanjaro where EVI is low. Areas with higher EVI seem to have slightly varying AGCS. Variation of AGCS seems to occur more in areas with high EVI in Taita.

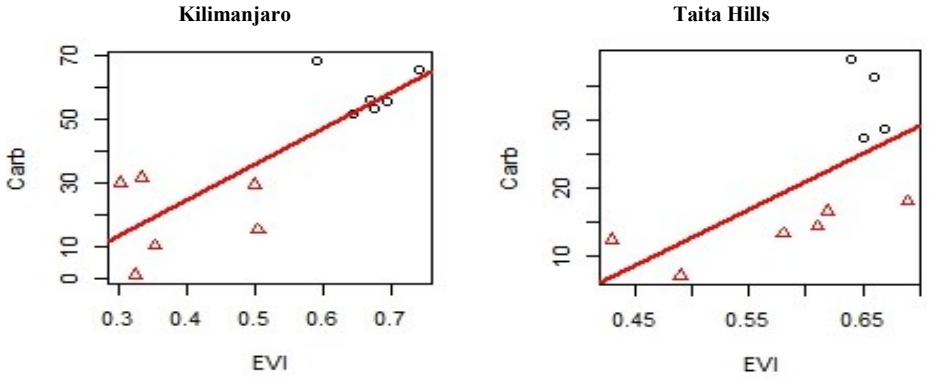

Figure 4 29 - Relationship of AGCS with Enhanced Vegetation Index (EVI) in Taita Hills and Kilimanjaro.

Table 4. 13: The univariate models for AGCS (Carb) with environmental variables in Kilimanjaro and Taita Hills.

	Univariate Model	RSE	DF	Mult. R^2	F	p-value	AIC
Taita Hills	TCarbMod Elev<-lm(Carb~Elev)	0.27	8	0.27	2.94	0.13	77.61
	TCarbMod Slope<-lm(Carb~Slope)	5.94	8	0.73	21.27	0.00	67.77
	TCarbMod pH<-lm(Carb~pH)	11.35	8	0.00	0.01	0.95	80.73
	TCarbMod SOC<-lm(Carb~SOC)	7.53	8	0.56	10.18	0.01	72.53
	TCarbMod CEC<-lm(Carb~CEC)	9.95	8	0.23	2.43	0.16	78.09
	TCarbMod BD<-lm(Carb~BD)	9.08	8	0.36	4.49	0.07	76.28
	TCarbMod Pop<-lm(Carb~Pop)	8.64	8	0.42	5.83	0.04	75.27
	TCarbMod EVI<-lm(Carb~EVI)	8.71	8	0.41	5.59	0.05	75.44
Kilimanjaro	KCarbMod Elev<-lm(Carb~Elev)	12.54	10	0.72	25.24	0.00	98.56
	KCarbMod Slope<-lm(Carb~Slope)	19.76	10	0.30	4.20	0.07	109.47
	KCarbMod EVI<-lm(Carb~EVI)	13.32	10	0.68	21.27	0.00	100.00
	KCarbMod pH<-lm(Carb~pH)	10.62	10	0.80	39.14	0.00	94.58
	KCarbMod SOC<-lm(Carb~SOC)	12.44	10	0.72	25.82	0.00	98.37
	KCarbMod CEC<-lm(Carb~CEC)	22.78	10	0.06	0.68	0.43	112.9
	KCarbMod BD<-lm(Carb~BD)	14.90	10	0.60	14.97	0.00	102.7
	KCarbMod Pop<-lm(Carb~Pop)	19.67	10	0.30	4.33	0.06	109.36

ii. Multivariate Response

Multiple predictor variables were tested for multivariate response of AGCS along the elevation gradients of Taita Hills and Mount Kilimanjaro. Combinations of some variables in multivariate model showed significant response of AGCS to the multiple predictors while, others did not. Models that significantly explained the distribution of AGCS on the mountain slopes are described below.

a. Kilimanjaro AGCS Multivariate Response

AGCS significant respond to multivariates elevation and slope in Kilimanjaro (KCarbMod1 (Table 4.14): F=11.41, R^2=0.72, p=0.00). The relationship of AGCS with elevation under multiple response analysis is significant (F=22.78, p=0.001) but not with the slope on Kilimanjaro (Table 4.14). Thus, the influence of elevation on the distribution of AGCS is more than the slope angle. Introduction of quadratic function of the elevation variable (KCarbMod2) (Table 4.14) in the above model significantly fitted and increased the multivariate relationship (F=13.77, R^2=0.84, p=0.00). Under this model, slope variable is not contributing significantly to the model response.

Response of AGCS to multiple variables of edaphic factors that constituted SOC, CEC, pH and BD (KCarbMod7) (Table 4.14) in Kilimanjaro was very strong and significantly fitted (F=16.19, R^2=0.90,

p=0.001). Predictor variables that contribute significantly under the above multivariable analysis are SOC (F=51.72, p=0.00) and pH (F=12.72, p=0.01) (Table 4.14).

When physical and edaphic factors in Kilimanjaro are combined in a model (KCarbMod12) (Table 4.14), the multivariate response of AGCS is significantly fitted (F=8.50, R^2=0.94, p=0.03). Predictor variables that contribute significantly under the above multivariable analysis are SOC (F=45.75, p=0.00) and pH (F=11.25, p=0.03).

b. Taita Hills AGCS Multivariate Response

Response of AGCS to multiple predictors (elevation and slope) variables are significant in Taita Hills (TCarbMod1 (Table 4.14): F=9.32, R2=0.73, p=0.01, AIC=69.75). The two variables plays significant contribution to the model: Elevation, F=6.89, p=0.03 and Slope angle F=11.75, p=0.01. Apparently, slope angle contributes significantly to the distribution of AGCS than the elevation in Taita Hills. When quadratic term (2nd polynomial order) of elevation is added (TCarbMod2) (Table 4.14), the relationship of AGCS to the multiple predictors slightly and significantly increases (F=6.15, R2=0.76, p=0.03, AIC=70.69).

Addition of population density into the model with the physical factors in Taita Hills (TCarbMod3) (Table 4.14) shows high and significantly fitted model (F=16.12, R2=0.89, p=0.003, AIC=62.70). All variables in the model (TCarbMod3) show significant contribution: elevation (F=14.61, p=0.01), slope (F=24.91, p=0.00), and population density (F=8.84, p=0.03). Thus, about 89% of AGCS distribution is related to the variation of simultaneous variation of elevation, slope and population density. Addition of an 2nd order polynomial to TCarbMod3 does not change the relationship.

Table 4. 14: The multivariate model for AGCS (Carb) distribution with environmental variables in Kilimanjaro and Taita Hills.

Model	Multivariate Model	RSE	DF	Mult. R^2	F	p-value	AIC
Taita Hills	TCarbMod1<-lm(Carb~Elev + Slope)	6.34	7	0.73	9.32	0.01	69.75
	TCarbMod2<-lm(Carb~Elev + I(Elev^2) + Slope)	6.49	6	0.76	6.15	0.03	70.69
	TCarbMod3<-lm(Carb~Elev + Slope + Pop)	4.36	6	0.89	16.12	0.00	62.70
	TCarbMod5<-lm(Carb~Elev + I(Elev^2) + Slope + Pop)	4.70	5	0.89	10.41	0.01	64.41
Kilima	KCarbMod1<-lm(Carb~Elev + Slope)	13.2	9	0.72	11.41	0.00	100.53
	KCarbMod2<-lm(Carb~Elev + I(Elev^2) +	10.60	8	0.84	13.77	0.00	98.05

Slope)						
KCarbMod7<-lm(Carb~SOC + CEC + pH + BD)	8.79	7	0.90	16.19	0.00	91.75
KCarbMod12<-lm(Carb~SOC + CEC + pH + BD + Elev.1 + I(Elev.1^2) + Slope)	9.35	4	0.94	8.50	0.03	92.51

iii. AGCS Model Comparisons

Model comparisons are described for the univariate and multivariate models for distribution of AGCS in the two sites. An assessment of the models was conducted in order to establish their differences and models that perform better in explaining variation of AGCS in Taita Hills and Kilimanjaro. However, Table 4.15 and 4.16 provides matrix of comparisons of all models used in the analysis. Single variables considered in modeling forms univariate models. These include the elevation, slope angle, soil pH, CEC, soil BD, SOC, EVI and population density. The single variables are combined to form multivariate model that are presented here based on the models that significantly explained AGCS distribution in Taita Hills and Mount Kilimanjaro.

a. Mount Kilimanjaro AGCS model comparison

Comparison made between the univariate models showed no significant difference on how the models influence the AGCS in Kilimanjaro (Table 4.15). Significant differences were, however, observed between some of the univariate and multivariate models. The univariate slope, CEC and population density significantly differed with the multitivariate KCarbMod1, KCarbMod2, KCarbMod7 and KCarbMod12 models (Table 4.15). Other differences were observed between multivariate KCarbMod7 model and univariate elevation model (ANOVA F=4.45, p=0.05), BD (ANOVA F=7.25, p=0.02), SOC (ANOVA F=4.35, p=0.05), EVI (ANOVA F=5.32, p=0.03), KCarbMod1 (ANOVA F=6.65, p=0.02), KCarbMod2 (ANOVA F=6.98, p=0.03) (Table 4.15).

Among these models, multivariate KCarbMod7 model (AIC=91.75) performs better than all models in the analysis. This is followed by KCarbMod12 (Table 4.13 and 4.14), which has pH, CEC, BD and SOC variables similar to KCarbMod7 model but slightly differ due to the inclusion of elevation and slope angle variables in the model. This potentially implies that soil variables simultaneously influence AGCS distribution in Kilimanjaro more than other models.

Table 4. 15: Matrix table for AGCS model comparisons for Mount Kilimanjaro.

ANOVA p-value / F	KCarbMod Elev	KCarbMod Slope	KCarbMod pH	KCarbMod CEC	KCarbMod BD	KCarbMod SOC	KCarbMod EVI	KCarbMod Pop	KCarbMod1	KCarbMod2	KCarbMod3/7	KCarbMod4/12
KCarbMod Elev		1.00	1.00	1.00	1.00	1.00	1.00	1.00	0.88	0.22	0.05	0.22
KCarbMod Slope	0.00		1.00	1.00	1.00	1.00	1.00	1.00	0.01	0.01	0.00	0.04
KCarbMod pH	0.00	0.00		1.00	1.00	1.00	1.00	1.00	1.00	0.84	0.14	0.37
KCarbMod CEC	0.00	0.00	0.00		1.00	1.00	1.00	1.00	0.00	0.00	0.00	0.03
KCarbMod BD	0.00	0.00	0.00	0.00		1.00	1.00	1.00	0.09	0.06	0.02	0.12
KCarbMod SOC	0.00	0.00	0.00	0.00	0.00		1.00	1.00	1.00	0.24	0.05	0.22
KCarbMod EVI	0.00	0.00	0.00	0.00	0.00	0.00		1.00	0.31	0.14	0.03	0.18
KCarbMod Pop	0.00	0.00	0.00	0.00	0.00	0.00	0.00		0.01	0.01	0.00	0.04
KCarbMod1	0.03	12.7	0.00	20.7	3.74	0.00	1.17	13.1		0.09	0.02	0.17
KCarbMod2	1.83	9.91	0.18	15.2	4.23	1.73	2.57	10.3	3.62		0.03	0.25
KCarbMod7	4.45	14.5	2.53	20.0	7.25	4.35	5.32	14.3	6.65	6.98		0.59
KCarbMod12	2.34	6.78	1.49	9.24	3.57	2.27	2.72	6.71	2.79	2.09	0.73	

Note: The univariate model: elevation (KCarbMod Elev) , slope (KCarbMod Slope), pH (KCarbMod pH), CEC (KCarbMod CEC), BD (KCarbMod BD), SOC (KCarbMod SOC), EVI (KCarbMod EVI) and Population density (KCarbMod Pop). The multivariate models include KCarbMod1 (elevation + slope), KCarbMod2 (Elevation + I(Elevation^2) + Slope), KCarbMod3 (SOC + CEC + pH + BD), and KCarbMod4 (SOC + CEC + pH + BD + Elevation + I(Elevation^2) + Slope).

b. Taita Hills AGCS Models Comparisons

The univariate models do not differ significantly on how they explain the distribution of AGCS in Taita Hills (Table 4.16). However, most of them differed significantly with the multivariate models in explaining the variation of AGCS along the elevation gradients. For instance univariate elevation, pH, CEC models differed significantly with multivariate models such as TCarbMod1, TCarbMod2, TCarbMod3 and TCarbMod5 (Table 4.16). The univariate BD, EVI and population density differ significantly with multivariate models TCarbMod1, TCarbMod3 and TCarbMod5 (Table 4.16). While the univariate SOC model differed significantly the multivariate model TCarbMod3 (Table 4.16) and TCarbMod5 (Table 4.16). The univariate slope model apparently has no significant difference with other models in explaining effectively the distribution of AGCS in Taita Hills (Table 4.16). Multivariate models TCarbMod1 and TCarbMod3 (ANOVA F=8.84, p=0.03), and TCarbMod2 and TCarbMod5 (ANOVA F=6.44, p=0.05) significantly differed on how they explain the distribution of AGCS. These models have physical variables except in model TCarbMod3 and TCarbMod5 where population density included in the multivariate model. They also have relatively low AIC than their comparatives hence population density apparently is critical in performance of the models.

Among these models, TCarbMod3 explain better AGCS distribution in Taita Hills. TCarbMod3 has low AIC (62.70) followed by TCarbMod5 (AIC=64.41) (Table 4.13 and 4.14). The multivariate models that siginificantly explain the distribution of AGCS in Taita Hills only has physical variables while others include population density. It is however apparent that the distribution of AGCS in Taita Hills is majorly influenced simultaneously by physical variables and population density.

Table 4. 16: Matrix table for AGCS model comparisons for Taita Hills.

p-value / F	TCarbMod Elev	TCarbMod Slope	TCarbMod pH	TCarbMod CEC	TCarbMod BD	TCarbMod SOC	TCarbMod EVI	TCarbMod Pop	TCarbMod1	TCarbMod2	TCarbMod3	TCarbMod5
TCarbMod Elev		1	1	1	1	1	1	1	0.01	0.04	0.00	0.02
TCarbMod	0		1	1	1	1	1	1	0.93	0.72	0.07	0.17
TCarbMod pH	0	0		1	1	1	1	1	0.00	0.02	0.00	0.01
TCarbMod	0	0	0		1	1	1	1	0.01	0.03	0.00	0.01
TCarbMod BD	0	0	0	0		1	1	1	0.02	0.06	0.01	0.02
TCarbMod	0	0	0	0	0		1	1	0.08	0.17	0.02	0.05
TCarbMod EVI	0	0	0	0	0	0		1	0.03	0.07	0.01	0.03
TCarbMod Pop	0	0	0	0	0	0	0		0.03	0.08	0.01	0.03
TCarbMod1	11.75	0.01	18.63	12.68	9.42	4.28	8.10	7.84		0.44	0.03	0.10
TCarbMod2	5.94	0.34	9.22	6.38	4.83	2.38	4.20	4.07	0.67		1	0.05
TCarbMod3	16.87	4.43	24.16	17.85	14.4	8.96	13.00	12.72	8.84	0		0.72
TCarbMod5	9.70	2.58	13.87	10.26	8.28	5.17	7.48	7.33	3.8648	6.44	0.15	

Note: The univariate model: elevation (TCarbMod Elev) , slope (TCarbMod Slope), pH (TCarbMod pH), CEC (TCarbMod CEC), BD (TCarbMod BD), SOC (TCarbMod SOC), EVI (TCarbMod EVI) and Population density (TCarbMod Pop). The multivariate models include TCarbMod1 (elevation + slope), TCarbMod2 (Elevation + I(Elevation^2) + Slope), TCarbMod3 (elevation + slope + Population density), and TCarbMod4 (Elevation + I(Elevation^2) + Slope + Population density).

iv. Evaluation of models

Evaluation of models was perfomed in order to ascertain the precision of the GLM predicted AGCS. Correlation analysis of AGCS predicted by GLM and observed plot carbon was undertaken. Only models that contribute significantly to the distribution of AGCS are considered in the evaluation. The Akaike Information Criterion was also generated for the evaluation. Spatial modeling of AGCS was performed on the background environmental variable and classification done using five interval classes.

a. Mount Kilimanjaro AGCS Model Evaluation

AGCS predicted by GLM significantly correlated with observed AGCS in Kilimanjaro (Table 4.17). Some of these models vary on how they predict spatial AGCS distribution in Kilimanjaro. For instance, univariate elevation model sets the upper range of spatially predicted AGCS relative to the observed AGCS in Kilimanjaro. However, spatial AGCS class limit does not compare relatively with the observed plot AGCS values in the lower and upper classes (Fig.4.30). The univariate pH model sets the lower and upper range of spatially predicted AGCS relative to the observed AGCS. Discrepancies AGCS classes were observed only in the mid classes (Fig.4.30). While, the univariate BD model sets the lower limit of AGCS negative value the upper limits of spatially predicted AGCS is very high (Fig.4.30). The predicted AGCS value classes by the univariate SOC model does not compare relatively with the observed plot AGCS values (Fig.4.30). Most of AGCS predicted by SOC model fall under two major AGCS classes that set a wide range of AGCS classes. The univariate EVI model sets the lower and the upper AGCS values comparable to the observed AGCS values, especially on the upper limit. However, it is only in the upper classes of AGCS that the predicted AGCS compares with the observed plot AGCS.

Most of multivariate models set the lower values of predicted AGCS negative. These include model KCarbMod2, KCarbMod7 and KCarbMod12 (Table 4.17). Spatial AGCS predicted by these models do not compare relatively with the observed plot AGCS values (Fig.4.30). The model KCarbMod1 does not set AGCS range values comparable to the observed plot values. Moreover, most of the predicted AGCS values donot compare relatively to the observed plot AGCS values (Fig.4.30).

The univariate pH model apparently performs better than other models in predicting AGCS in Kilimanjaro (AIC=94.29). The predicted AGCS by this model correlates highly and significantly with the observed plot AGCS. Visual assessment of the AGCS spatial model generated from the univariate pH model closely compares with the observed plot AGCS (Fig.4.30).

Table 4. 17: Evaluated AGCS prediction by correlation with observed AGCS in Kilimanjaro. PredCarb is predicted AGCS and PlotCarb is observed plot AGCS.

Model		PredCarb. Vs PlotCarb		
		R	p-value	AIC
Univariate Model	KCarbMod Elev<-lm(Carb~Elev)	0.83	0.00	99.79
	KCarbMod pH<-lm(Carb~pH)	0.90	0.00	94.29
	KCarbMod BD<-lm(Carb~BD)	0.79	0.00	102.21
	KCarbMod SOC<-lm(Carb~SOC)	0.86	0.00	97.42
	KCarbMod EVI<-lm(Carb~EVI)	0.86	0.00	97.51
Multivariate Model	KCarbMod1<-lm(Carb~Elev + Slope)	0.83	0.00	99.60
	KCarbMod2<-lm(Carb~Elev + I(Elev^2) + Slope)	0.83	0.00	99.87
	KCarbMod7<-lm(Carb~SOC + CEC + pH + BD)	0.94	0.00	87.20
	KCarbMod12<-lm(Carb~SOC + CEC + pH + BD + Elev.1 + I(Elev.1^2) + Slope)	0.92	0.00	91.33

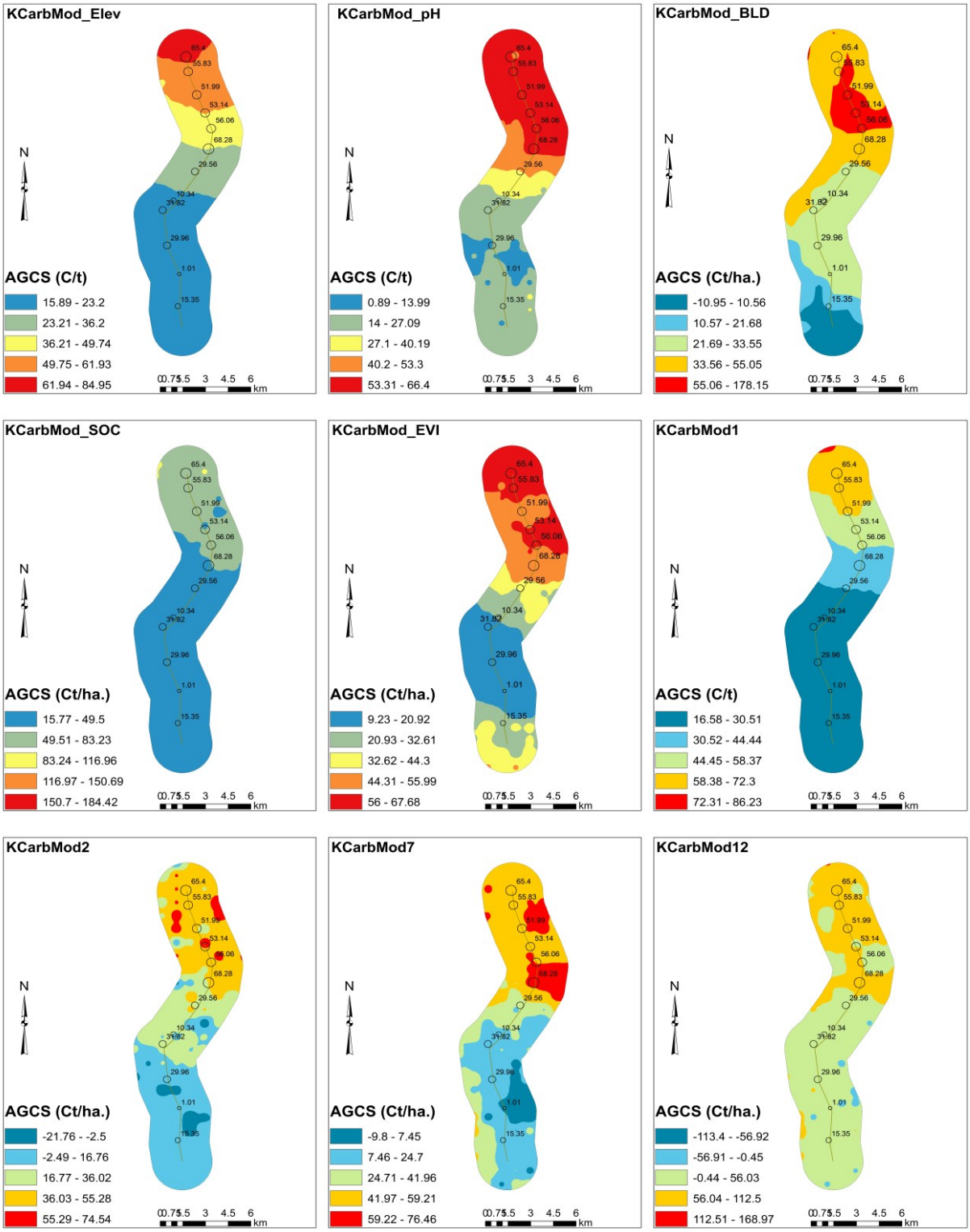

Figure 4.30 - Predicted AGCS spatial model established from univariate and multivariate models for Kilimanjaro.

Note: The univariate model: elevation (KCarbMod Elev) , slope (KCarbMod Slope), pH (KCarbMod pH), CEC (KCarbMod CEC), BD (KCarbMod BD), SOC (KCarbMod SOC), EVI (KCarbMod EVI) and Population density (KCarbMod Pop). The multivariate models include KCarbMod1 (elevation + slope), KCarbMod2 (Elevation + I(Elevation^2) + Slope), KCarbMod3 (SOC + CEC + pH + BD), and KCarbMod4 (SOC + CEC + pH + BD + Elevation + I(Elevation^2) + Slope).

b. Taita Hills AGCS Model Evaluation

Four models predicted AGCS that significantly correlated with the observed AGCS in Taita Hills (Table 4.18). These models included the univariate SOC and EVI, and multivariate TCarbMod2 (Table 4.18) and TCarbMod3 (Table 4.18).

Visual comparison of the observed plot AGCS show that most of the values do not compare with the spatially predicted AGCS by univariate slope, population density models and multivariate models TCarbMod1, TCarbMod2 and TCarbMod5 (Fig. 4.31). However, spatially predicted AGCS for univariate SOC and EVI, and multivariate model TCarbMod3 relatively compare with the observed plot AGCS values (Fig. 4.31).

The models that performs better are the multivariate model TCarbMod3 (AIC=71.11) and univariate SOC model (AIC=71.58) performs better in predicting AGCS; their prediction of AGCS significantly correlates with the observed plot AGCS. TCarbMod3 consist of physical variable (elevation and slope) and population density variables that simultaneously affect AGCS distribution in Taita Hills.

Table 4. 18: Evaluated AGCS prediction by correlation with observed AGCS in Taita Hills. PredCarb is predicted AGCS and PlotCarb is observed plot AGCS.

Model		PredCarb. Vs PlotCarb (R, p-val.)		
		R	p-value	AIC
Univariate	TCarbMod Slope<-lm(Carb~Slope)	0.567	0.10	77.04
	TCarbMod SOC<-lm(Carb~SOC)	0.77	0.01	71.58
	TCarbMod EVI<-lm(Carb~EVI)	0.67	0.03	74.79
	TCarbMod Pop<-lm(Carb~Pop)	0.05	0.89	80.71
Multivariate	TCarbMod1<-lm(Carb~Elev + Slope)	0.56	0.09	77.00
	TCarbMod2<-lm(Carb~Elev + I(Elev^2) + Slope)	0.64	0.05	75.49
	TCarbMod3<-lm(Carb~Elev + Slope + Pop)	0.79	0.01	71.11
	TCarbMod5<-lm(Carb~Elev + I(Elev^2) + Slope + Pop)	0.13	0.73	80.57

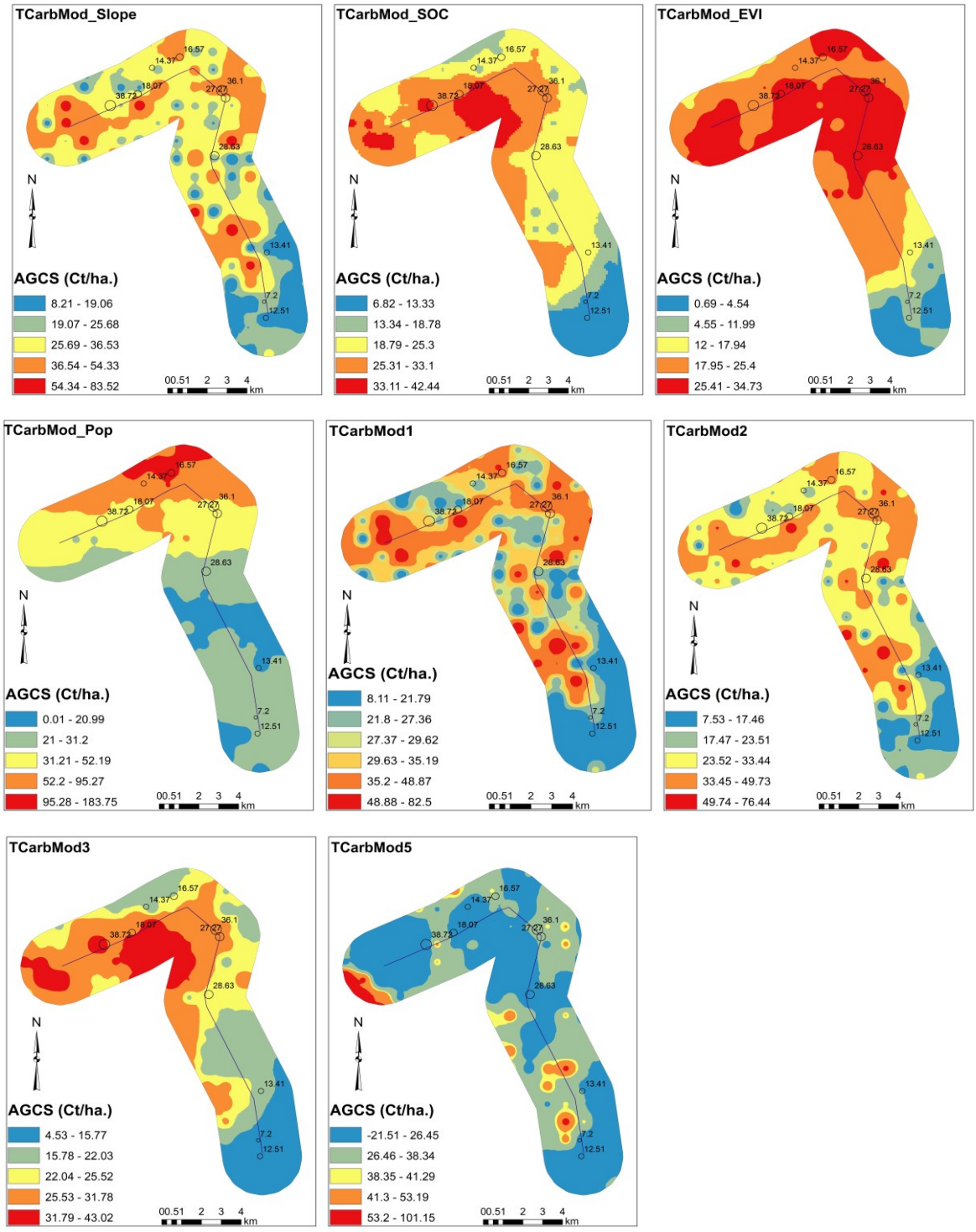

Figure 4.31 - Predicted AGCS spatial model established from univariate and multivariate models for Taita Hills.

Note: The univariate models are: slope (TCarbMod Slope), SOC (TCarbMod SOC), EVI (TCarbMod EVI) and Population density (TCarbMod Pop). The multivariate models include: TCarbMod1 (elevation + slope), TCarbMod2 (Elevation + I(Elevation^2) + Slope), TCarbMod3 (Elevation + Slope + Population density), and TCarbMod5 (Elevation + I(Elevation^2) + Slope + Population density).

4.3.6. Relationship of AGCS with environmental variables in cropland

There is significant relationship between the above-ground carbon (AGCS) with the mean annual temperature (MAT) in agro-forestry in Kilimanjaro (R^2=0.97, p=0.00) when the relationship is fitted by 2nd order of polynomial (Fig. 4.32; Table 4.19). The relationship between AGCS and MAP in agro-forestry in Kilimanjaro is significantly fitted by the 2nd order of polynomial (R^2= 0.87, p=0.045) (Fig. 4.32; Table 4.19). AGCS response to EVI in agro-forestry in Kilimanjaro is very significant (R^2=0.92, p=0.020) (Fig. 4.32; Table 4.19). AGC and CEC polynomial relationships (2nd order) in agro-forestry in Kilimanjaro is significant (R^2=0.91, p=0.027) (Fig. 4.32; Table 4.19). AGCS response to BD in agro-forestry polynomial relationship (2nd order) in Kilimanjaro is significant (R^2=0.87, p=0.045) (Fig. 4.32; Table 4.19). The relationship of AGC in agro-forestry Taita Hills on the above variables are strong but are not significant (Fig. 4.32; Table 4.19). The response of AGC to MAT, MAP, EVI, CEC and BD in cropped lands are weak and not significant in Taita Hills and Kilimanjaro (Fig. 4.32; Table 4.19).

AGC and pH polynomial relationship (3rd order) in agro-forestry in Taita Hills is very strong and significant (R^2=0.98, p=0.031) (Fig. 4.32; Table 4.19). While in cropped land in Taita Hills AGC and SOC polynomial relationship (1st order) is significant (R^2=0.70, p=0.00) (Fig. 4.32; Table 4.19).

Kilimanjaro **Taita Hills**

Agro-forestry Cropped land Agro-forestry Cropped land

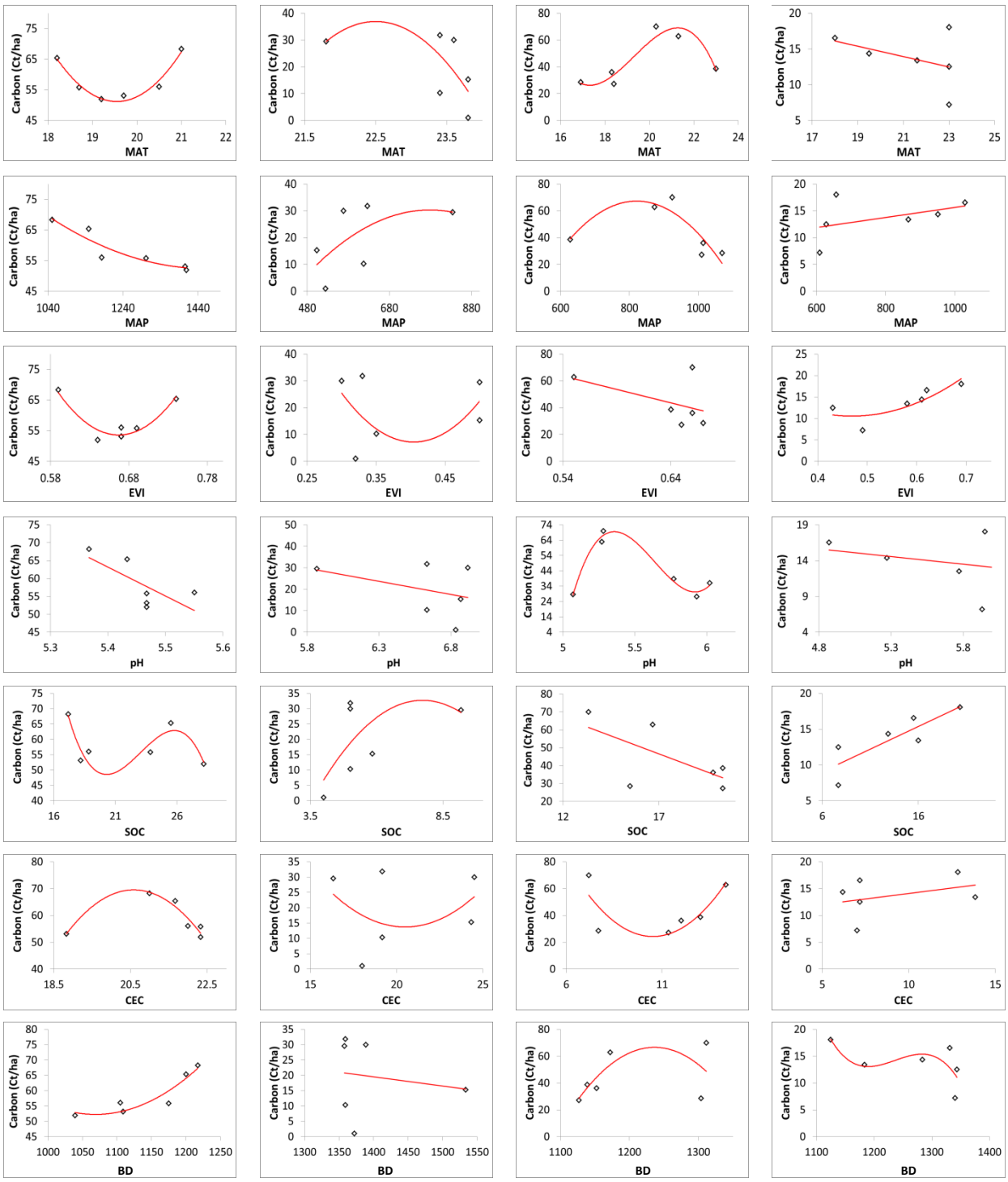

Figure 4.32 - Model relationships for AGCS with environmental variables in cropped land and Agro-forestry in Kilimanjaro and Taita Hills.

Table 4. 19: Model relationships for AGCS with environmental variables in cropped land and Agro-forestry in Kilimanjaro and Taita Hills.

		Kilimanjaro				Taita			
Variable	**Land-use**	**Fit. Order**	**R^2**	***p***	**AIC**	**Fit. Order**	**R^2**	***p***	**AIC**
MAT	Agro-forestry	x^2	0.96	0.008	36	x^3	0.91	0.135	46
	Cropped land	x^2	0.37	0.500	52	x	0.17	0.927	41
MAP	Agro-forestry	x^2	0.87	0.045	34	x^2	0.78	0.104	50
	Cropped land	x^2	0.34	0.538	52	x	0.21	0.367	37
EVI	Agro-forestry	x^2	0.92	0.020	31	x^2	0.26	0.639	57
	Cropped land	x^2	0.14	0.805	54	x^2	0.72	0.152	32
pH	Agro-forestry	x	0.50	0.115	41	x^3	0.98	0.031	38
	Cropped land	x	0.14	0.458	52	x	0.10	0.540	37
SOC	Agro-forestry	x^3	0.81	0.272	39	x	0.43	0.160	53
	Cropped land	x^2	0.36	0.507	52	x	0.70	0.038	31
CEC	Agro-forestry	x^2	0.91	0.027	32	x^2	0.64	0.213	53
	Cropped land	x^2	0.12	0.820	54	x	0.14	0.474	37
BD	Agro-forestry	x^2	0.87	0.045	35	x^2	0.29	0.599	57
	Cropped land	x	0.03	0.760	52	x^3	0.50	0.652	38

4.3.7. Key Findings for objective 3

The amounts of AGCS in the two sites are comparable. However, it is significantly varied in agroforestry areas (F=9.36, p=0.03) and cropped lands (F=10.92, p=0.02) between Kilimanjaro and Taita Hills. Within sites, AGCS significantly differs in types of cropland in Kilimanjaro (t=4.62, p=0.00) and Taita Hills (t=4.86, p=0.00). Distribution of AGCS increases significantly with increase in stock density of WPS in Kilimanjaro (R^2=0.44, p=0.02) but not with WPSR. While AGCS significantly relate with WPSR (R^2=0.66, p=0.00) and stock density (R^2=0.72, p=0.00) in Taita Hills.

The univariate models that usefully explain the spatial distribution of AGCS in Kilimanjaro are pH (R^2=0.90, p=0.00, AIC=94.29) and SOC (R^2=0.86, p=0.00, AIC=97.42). While in Taita Hills models that significantly explain better the spatial distribution of AGCS are SOC (R^2=0.77, p=0.01, AIC=71.58) and EVI (R^2=0.67, p=0.03, AIC=74.79). Under multivariate analysis, spatial distribution of AGCS in Kilimanjaro is explained better by multivariate model with SOC, CEC, pH, and BD) (R^2=0.94, p=0.00, AIC=91.33). While in Taita the multivariate model Elevation, Slope, and Population Density shows significantly explain better spatial distribution of AGCS in Taita Hills (R^2=0.94, p=0.00, AIC=71.11).

4.5. The distribution of the Leaf Area Index in Taita Hills and Mount Kilimanjaro

4.4.1. Site LAI_{Hemi}

The total average LAI in Taita Hills (1.64±0.36) is relatively higher than in Kilimanjaro (1.22±0.29). However, LAI in Taita Hills is more varied than in Kilimanjaro within the transects. Within site, LAI in the upper quartile in Kilimanjaro are more varied than the lower quartile. The value of LAI data in Taita Hills in the upper and lower quartiles are relatively varied (Fig. 4.33).

No significant differences were observed on the means and variations of LAI between the two sites. Significant differences only occured in the distribution of LAI along the elevation within the inhabited area of Kilimanjaro (t=4.24, p=0.00) and Taita Hills (t=4.58, p=0.00).

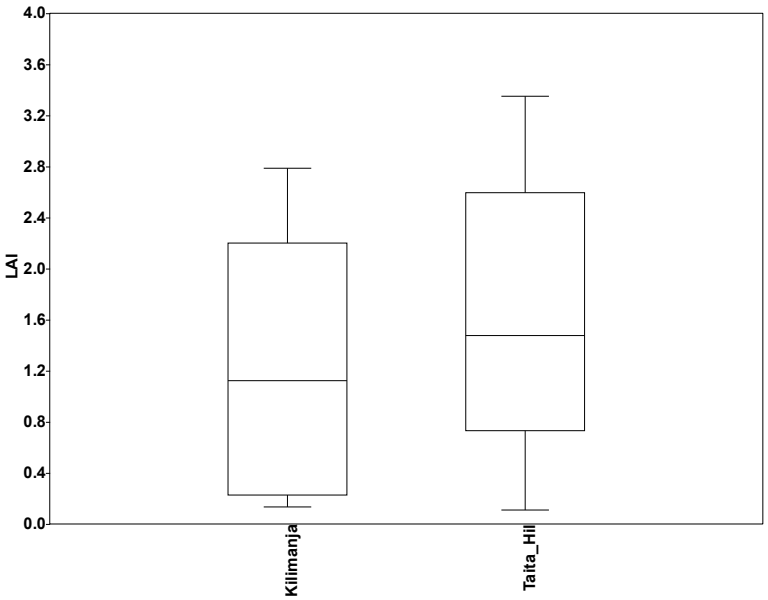

Figure 4.33 - Boxplot comparisons of Leaf Area Index in Taita Hills and Mount Kilimanjaro

Mean LAI are relatively higher in agro-forestry area than in cropped land in both sites. Agro-forestry and cropped areas in the Taita Hill transect has a higher LAI than counterparts in Kilimanjaro (Fig 4.34) (mean of LAI in agro-forestry in Kilimanjaro 2.05±0.26, Taita Hills 2.48±0.37); cropped land (Kilimanjaro 0.40±0.16, Taita Hills 0.80±0.30) (Table 4.20). The mean and variation of LAI in agro-forestry areas in both sites do not differ significantly and this also applies to the mean LAI in cropped lands.

Observation within site shows that the mean distribution of LAI between cropped land and agro-forestry in Taita Hills and Kilimanjaro are significantly different (Kilimanjaro *t=5.48, p=0.00* and

Taita Hills t=3.56, p=0.00). The variation of LAI between the two crop management system in Taita Hills and Kilimanjaro are not significant.

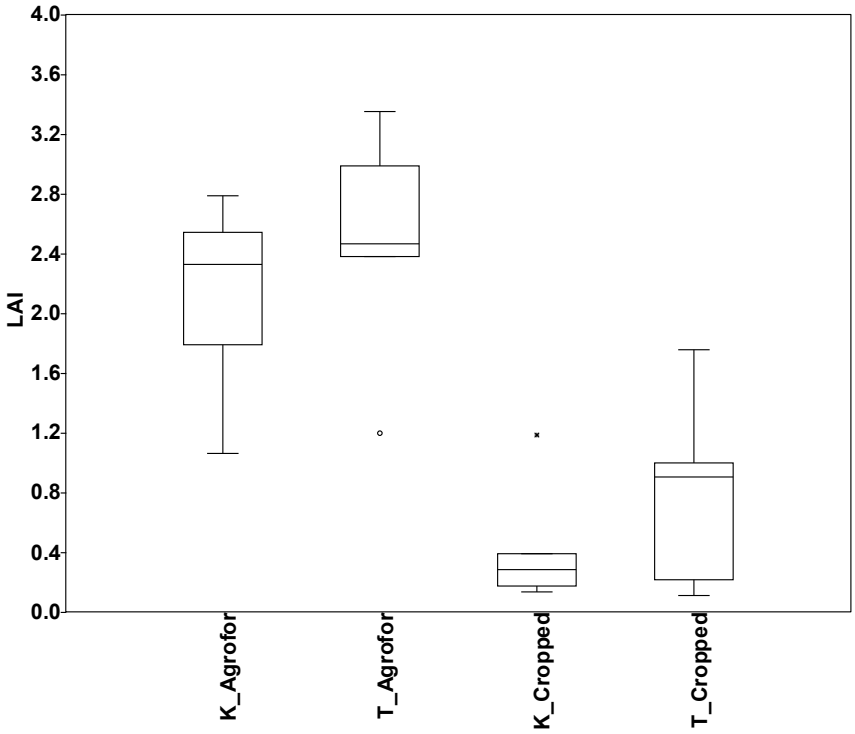

Figure 4.34 -Boxplot comparisons of Leaf Area Index (LAI) within and between types of Croplands between the inhabited area of Taita Hills and Mount Kilimanjaro. K Agrof (Agro-forestry in Mount Kilimanajro) etc.

4.4.2. Correlation of LAI_{Hemi} and $LAI_{SunScan}$

Measurements of LAI from SunScan ($LAI_{SunScan}$) and the values from hemispherical camera (LAI_{Hemi}) are strongly associated in Kilimanjaro (R=0.84, p=0.00) and Taita Hills (R=0.76, p=0.00). Kilimanjaro shows very distinct association of $LAI_{SunScan}$ with LAI_{Hemi} in the agro-forestry and cropped lands. Low levels of $LAI_{SunScan}$ are predominant in cropped lands in Kilimanjaro, while high levels of $LAI_{SunScan}$ occur in agro-forestry areas (Fig. 4.35). In Taita Hills the values of $LAI_{SunScan}$ and high LAI_{Hemi} relatively compares.

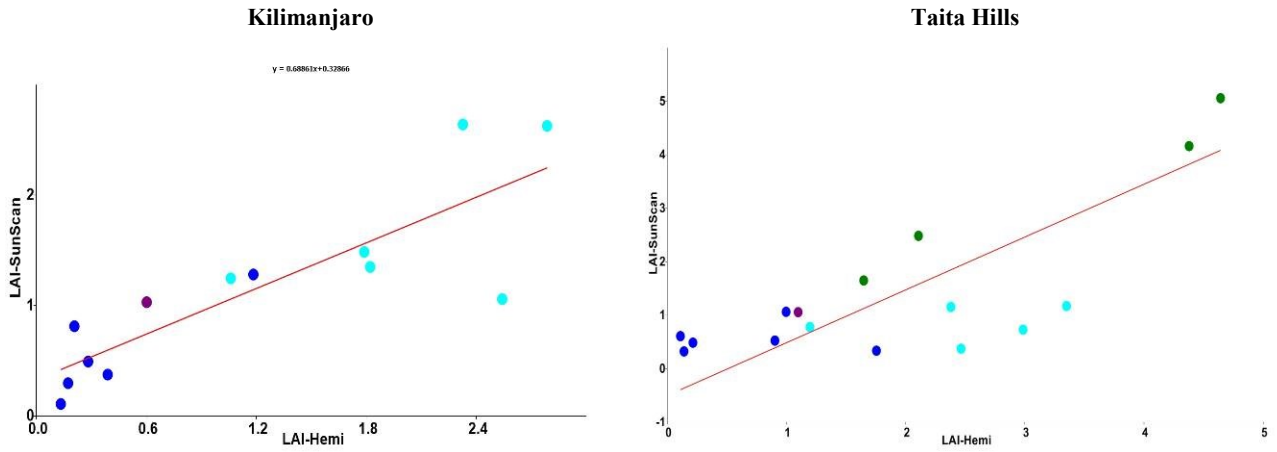

Figure 4. 1: Correlation of $LAI_{SunScan}$ with increasing LAI_{Hemi} in Kilimanjaro and Taita Hills. Blue dot (Cropped land), Cyan dot (Agro-forestry), Green dot (Forest) and purple dot (woodland).

4.4.3. Modeling LAI_{Hemi} with environmental variables

i. Modeling LAI with Elevation

Most of the distributions of LAI data points from Kilimanjaro are closer to the regression fit line. LAI on lower elevation are very close to the fit line but towards the upper elevation, few points tend slightly away from the fit line. Thus, areas with high LAI in Kilimanjaro are more varied than areas with low LAI values. LAI increases significantly with increase in elevation in Kilimanjaro transect (R^2=0.93, p=0.000) (Fig. 4.36, Table 4.20). In Taita Hills, most of LAI data points are away from the regression fit line, in the lower and upper elevation. Thus, LAI values are very varied from the lower to the upper elevation in Taita Hills, hence LAI does not show any relationship with the elevation.

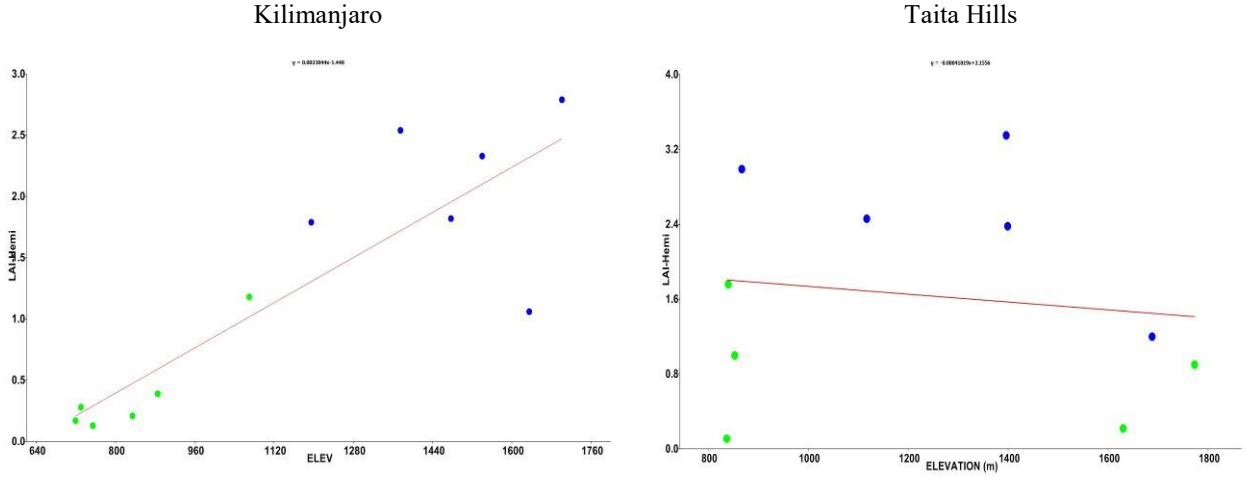

Figure 4.35 - Relationship of LAI_{Hemi} with increasing elevation in Kilimanjaro and Taita Hills. Blue dot (Agro-forestry) and Green dot (Cropped land).

Table 4. 20: Relationships of Leaf Area Index (LAI) with elevation gradients and in types of croplands in Mount Kilimanjaro and Taita Hills.

Variable Type		Model	R^2	*p-value*
Kilimanjaro	Elev. Transect	LAI_{Hemi}=0.003*Elevation – 1.89	0.93	0.00
	Agro-forestry	LAI_{Hemi} =0.002*Elevation – 0.06	0.46	0.21
	Cropped land	LAI_{Hemi} =0.003*Elevation – 1.89	0.85	0.01
Taita Hills	Elev. Transect	LAI_{Hemi} =-0.0004*Elev + 2.15	0.02	0.70
	Agro-forestry	LAI_{Hemi} =-0.002*Elev + 4.60	0.39	0.26
	Cropped land	LAI_{Hemi} =-0.0004*Elev + 1.27	0.08	0.65

Agro-forestry areas in Kilimanjaro, LAI increases with increase in elevation. However, the distribution of LAI along the elevation is varied and this is observed on the LAI data points that are scattered away from the regression fit line (Fig. 4.35). The influence of elevation on LAI in agro-forestry area is explained by about 46% of LAI (R^2=0.46, p=0.206) (Table 4.20) but this is not significantly related. In Taita Hills, distribution of LAI shows a decrease with increase in elevation. LAI data values are varied along the elevation and only 39% of LAI in Taita Hills shows decrease with increase in elevation (R^2=0.39, p=0.257), however there is no significant relationship.

The distribution of LAI in Kilimanjaro cropped land increases significantly with increase in elevation (*R^2=0.85, p=0.008*) (Table 4.20). Most of the LAI point data are closer to the regression fit line indicating that low variation occurs in the Cropped land along the elevations of Kilimanjaro. Decrease of LAI is observed with increase in elevation within Cropped land in Taita Hills. However, this relationship is not significant (R^2=0.08, p=0.65) (Table 4.20). LAI is very varied along the elevation in Cropped land in Taita Hills compared to agro-forestry areas though all show decrease in LAI with increase in elevation.

ii. Modeling LAI with Climate Variables

The LAI_{Hemi} distribution in Kilimanjaro transect shows significant decrease in values with increase in the mean annual temperature (MAT) (R^2=0.92, p=0.000) (Table 4.21). While decrease is also observed in Taita Hills, LAI_{Hemi} distribution is more varied with increase in MAT and no significant relationship is observed (Fig 4.36a). Cropped land LAI_{Hemi} in Kilimanjaro significantly relate with MAT along the elevation (R^2=0.93, p=0.002) (Table 4.21). LAI_{Hemi} values decrease with the increase of MAT. Contrary to this, in Taita Hills, the distribution LAI_{Hemi} in cropped land increases with increase of MAT. The distribution of LAI_{Hemi}, however, in agro-forestry areas of the two sites, shows decrease with increase in MAT but with no significant relationship (Table 4.21).

The mean annual precipitation (MAP) significantly influences about 70% of LAI distribution in Kilimanjaro (R^2=0.70, p=0.0006) (Table 4.21). The distribution of LAI_{Hemi} in the area is however, varied with higher amount of MAP in the area. Taita Hills transect has a highly varied LAI_{Hemi},

which increases with increase of MAP (Fig. 4.36b). This is indicated by the distribution of LAI_{Hemi} data points that tend to be away from the regression fit line. LAI_{Hemi} in Cropped land in Kilimanjaro relates with the distribution of MAP significantly (R^2=0.85, p=0.009) (Table 4.21). While LAI_{Hemi} increases with increase in MAP in Cropped land, LAI_{Hemi} in Kilimanjaro agro-forestry areas shows relative decrease with increase in MAP (Fig. 4.36b). The opposite is observed in Taita Hills where LAI_{Hemi} in cropped land relatively decreases with increase in MAP but, increases with increase in MAP (R^2 = 0.55, p = 0.150) (Fig. 4.36b, Table 4.21).

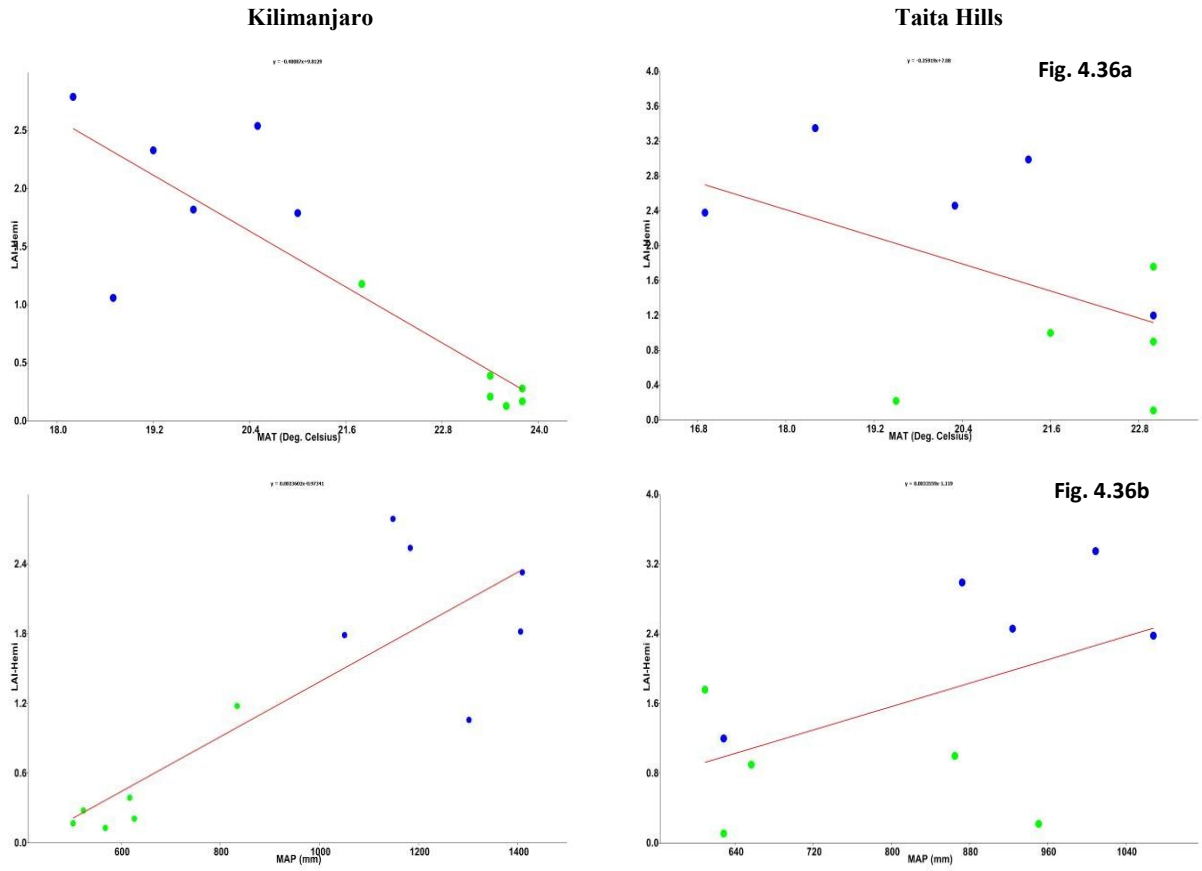

Figure 4.36 - Relationship of LAI_{Hemi} with MAT and MAP in Taita Hills and Kilimanjaro.

Table 4. 21: Relationships of Leaf Area Index (LAI) with MAP and MAT along the elevation gradients and in types of croplands in Mount Kilimanjaro and Taita Hills.

Variable Type		Model	R^2	*p-value*
Kilimanjaro	Elev. Transect	LAI_{Hemi} = -0.4877* MAT + 11.809	0.92	0.00
	Agro-forestry	LAI_{Hemi} = -0.0345* MAT + 2.73	0.00	0.91
	Cropped land	LAI_{Hemi} = -0.5064* MAT +12.19	0.93	0.00
	Elev. Transect	LAI_{Hemi} = 0.0024* MAP - 0.9697	0.71	0.00
	Agro-forestry	LAI_{Hemi} = -0.0009* MAP + 3.2048	0.05	0.68
	Cropped land	LAI_{Hemi} = 0.0031* MAP - 1.4828	0.85	0.01
Taita Hills	Elev. Transect	LAI_{Hemi} =-0.2594* MAT + 7.0832	0.25	0.14
	Agro-forestry	LAI_{Hemi}=-0.1864* MAT +6.20	0.30	0.34
	Cropped land	LAI_{Hemi} =0.1862* MAT - 3.30	0.18	0.42
	Elev. Transect	LAI_{Hemi} = 0.0034* MAP - 1.1224	0.27	0.12
	Agro-forestry	LAI_{Hemi} = 0.0036* MAP - 0.7434	0.55	0.15
	Cropped land	LAI_{Hemi} = -0.0016* MAP + 1.9876	0.14	0.54

iii. Modeling LAI with Edaphic Variables

a. Soil Organic Carbon

LAI increases with the increase in SOC in Kilimanjaro and Taita Hills transects (Fig. 4.37). An estimated 75% of LAI relate significantly with SOC jn Kilimanjaro (R^2=0.76, p=0.00) (Table 4.22). However, LAI shows variation where SOC is high in Kilimanjaro. In Taita Hills the relationship is not significant and LAI varies with SOC whwther low or high. In addition, most of LAI data points are not close to each other.

LAI within agro-forestry areas in Kilimanjaro shows increase with the increase in SOC values whereas in Taita Hills, LAI shows slight decrease with the increase in SOC. However, there is no significant relationship occur between LAI and SOC in agro-forestry areas in Kilimanjaro and Taita Hills (Table 4.22). The LAI in Cropped land in Kilimanjaro increases significantly with increase in SOC (R^2=0.80, p=0.02) (Table 4.22). While in Taita Hills, LAI in Cropped land increases slightly with the increase in SOC but the relationship is not significant.

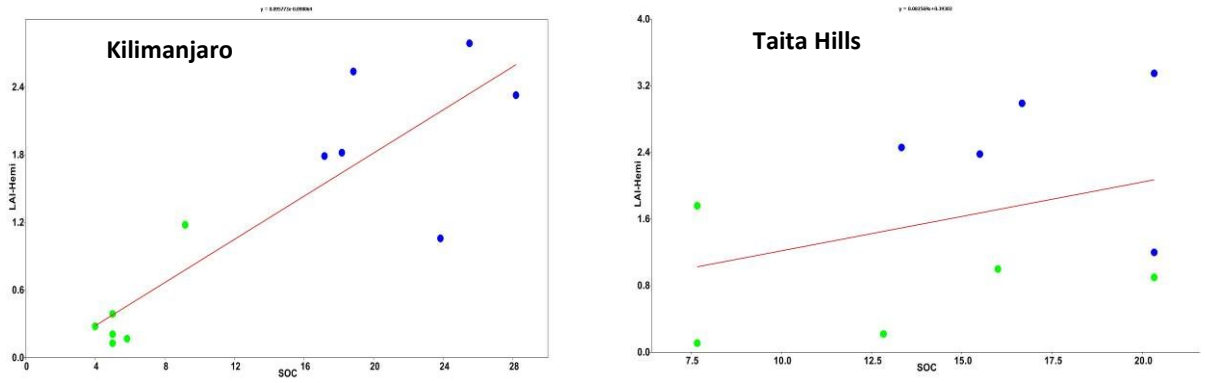

Figure 4.37 - Relationship of LAIHemi with increase in SOC in Kilimanjaro and Taita Hills. Blue dot (Agro-forestry) and Green dot (Cropped land).

b. Soil Bulk Density

LAI decreases with the increase in soil bulk density (BD) in transects in Kilimanjaro and Taita Hills (Fig. 4.38). The decrease in Kilimanjaro is however, significantly related to the increase in BD (R^2=0.70, p=0.00) (Table 4.22), while the distribution of LAI in Taita Hills is more varied with the distribution of BD along the elevation and therefore, not related with the increase in BD.

LAI in agro-forestry in Kilimanjaro are more varied than values in cropped land. On the other hand, in Taita Hills, variation of LAI occurs in both cropped land and agro-forestry. LAI does not relate with the increase in BD along the elevation gradient.

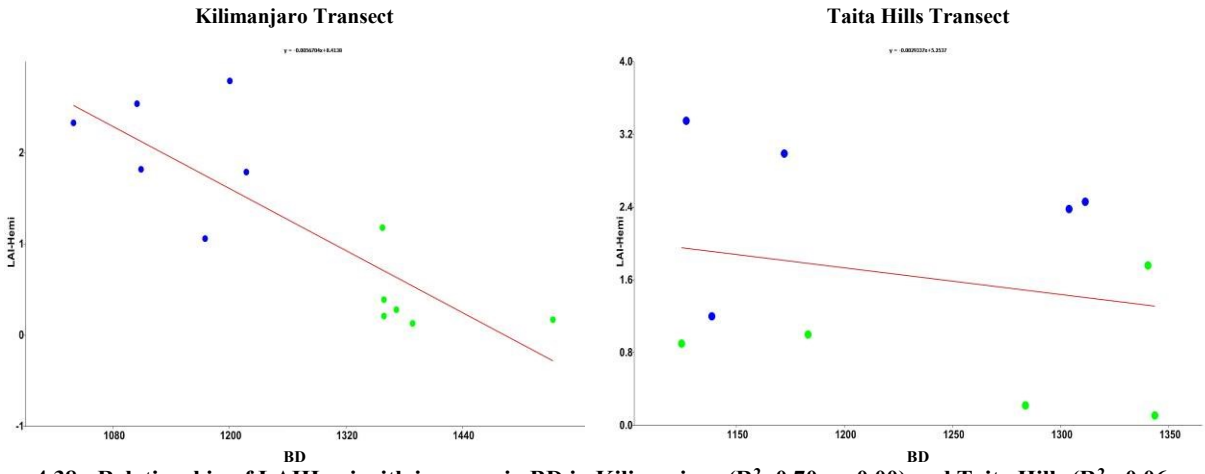

Figure 4.38 - Relationship of LAIHemi with increase in BD in Kilimanjaro (R^2=0.70, p=0.00) and Taita Hills (R^2 =0.06, p= 0.51). Blue dot (Agro-forestry) and Green dot (Cropped land).

Table 4. 22: Relationships of Leaf Area Index (LAI) with edaphic variables along the elevation gradients and in types of croplands in Mount Kilimanjaro and Taita Hills.

Variable Type		Model	R^2	*p-value*
Kilimanjaro	Elev. Transect	LAI_{Hemi} = 0.0956* SOC - 0.0951	0.76	0.00
	Agro-forestry	LAI_{Hemi} = 0.03* SOC + 1.3952	0.05	0.68
	Cropped land	LAI_{Hemi} = 0.1961* SOC - 0.7158	0.80	0.02
	Elev.Transect	LAI_{Hemi}=-1.5086* pH +10.34	0.80	0.00
	Agro-forestry	LAI_{Hemi} =10.631* pH -55.991	0.04	0.714
	Cropped land	LAI_{Hemi} =-1.0166* pH +7.1282	0.95	0.00
	Elev. Transect	LAI_{Hemi} = -0.0057* BD + 8.4027	0.70	0.00
	Agro-forestry	LAI_{Hemi} = -0.0021* BD + 4.4335	0.05	0.88
	Cropped land	LAI_{Hemi} = -0.0021* BD + 3.2824	0.13	0.48
	Elev. Transect	LAI_{Hemi} =0.020056*CEC +0.80689	0.48	0.13
	Agro-forestry	LAI_{Hemi} =0.46959*CEC -7.9754	0.02	0.81
	Cropped land	LAI_{Hemi} =-0.11684*CEC +2.7593	0.48	0.13
Taita Hills	Elev. Transect	LAI_{Hemi} = 0.0827* SOC + 0.3895	0.12	0.32
	Agro-forestry	LAI_{Hemi} = -0.0353* SOC + 3.0832	0.02	0.83
	Cropped land	LAI_{Hemi} = 0.0003* SOC + 0.7926	0.00	1.00
	Elev.Transect	LAI_{Hemi}=-2.5953* pH +16.355	0.07	0.46
	Agro-forestry	LAI_{Hemi} =-2.2269* pH +14.644	0.00	0.96
	Cropped land	LAI_{Hemi} =1.553* pH -8.3308	0.28	0.36
	Elev. Transect	LAI_{Hemi}= -0.0029* BD + 5.255	0.06	0.51
	Agro-forestry	LAI_{Hemi} = -0.0003* BD + 2.8834	0.00	0.96
	Cropped land	LAI_{Hemi} = -0.0006* BD + 1.5858	0.01	0.66
	Elev. Transect	LAI_{Hemi} =0.34365*CEC -1.8167	0.05	0.53
	Agro-forestry	LAI_{Hemi} =-0.25654*CEC +5.2209	0.00	0.98
	Cropped land	LAI_{Hemi} =0.18425*CEC -0.93391	0.06	0.70

c. Soil pH

LAI_{Hemi} decreases with the increase in soil pH both in Taita Hills and Mount Kilimanjaro. In Kilimanjaro, the decrease is significantly related to the increase of soil pH (R^2=0.80, p=0.00) (Table 4.22). Distribution of LAI_{Hemi} in areas with low pH in Kilimanjaro is varied and these occur in agro-forestry area (Fig. 4.39). LAI_{Hemi} in Cropped land in Kilimanjaro is less varied as most points are observed tending closer to the fit line. The LAI values in cropped land in Kilimanjaro are mostly distributed where soil pH tends to be higher along the elevation gradient (Fig. 4.39). Their distribution is significantly related to the soil pH (R^2=0.95, p=0.01) (Table 4.22). In Taita Hills, on the other hand, the distribution of LAI does not relate with the increase in soil pH along the elevation gradient. Variations of LAI occur in low and high pH and, in agro-forestry areas and Cropped land (Fig. 4.39). Though, LAI_{Hemi} in agro-forestry areas are relatively higher than the values in cropped land.

Kilimanjaro Taita Hills

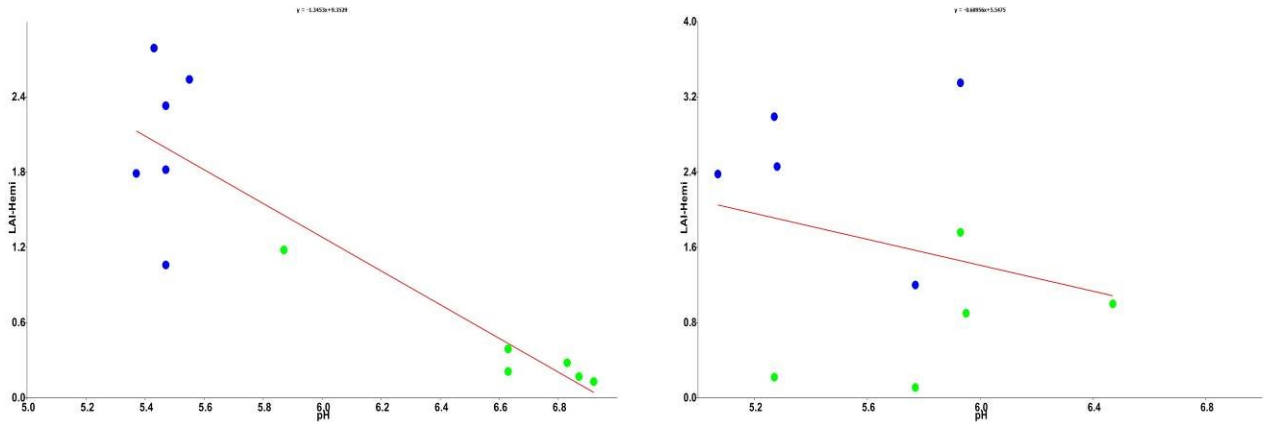

Figure 4.39 - Relationship of LAI_{Hemi} with increase in pH in Kilimanjaro (R2=0.80, p=0.00) and Taita Hills (R2=0.07, p=0.46). Blue dot (Agro-forestry) and Green dot (Cropped land).

d. Cation Exchange Capacity

The distribution of LAI_{Hemi} is highly varied with the increase of CEC along the elevation gradient in both Taita Hills and Mount Kilimanjaro. Negligible increase in LAI_{Hemi} is observed with the increase of CEC in the two sites but no significant relationships (Fig 4.40). Decreasing trend in LAI with increase in CEC occurs in agro-forestry areas in Kilimanjaro transect (R^2=0.48, p=0.12642) but relationship not significant (Table 4.22). The amounts of LAI_{Hemi}, however, are higher in the agro-forestry than in cropped land in the two sites.

Kilimanjaro Taita Hills

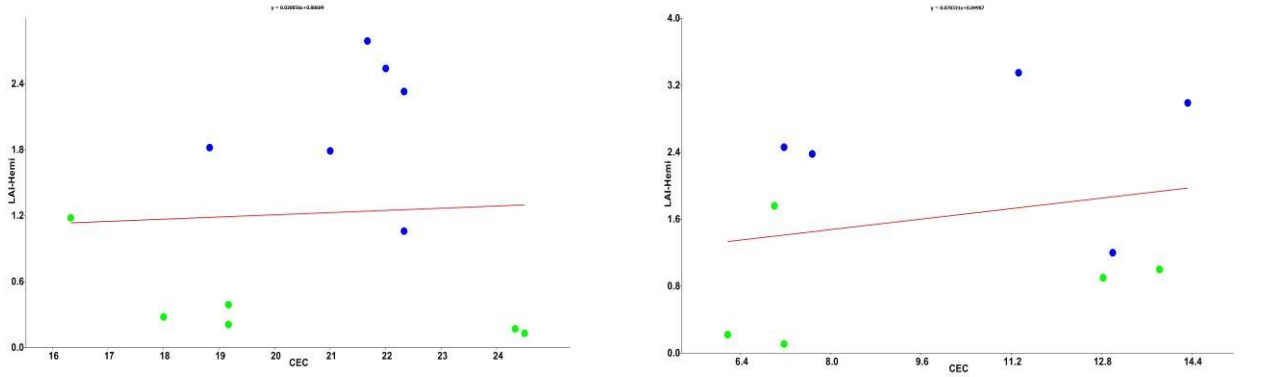

Figure 4.40 - Relationship of LAI_{Hemi}i with increase in pH in Kilimanjaro (R2=0.00, p=0.88) and Taita Hills (R2=0.05, p=0.52). Blue dot (Agro-forestry) and Green dot (Cropped land).

iv. Modeling LAI with Human Population Density

LAI_{Hemi} increases in areas with increase in population density in Kilimanjaro transectand the relationship of LAI_{Hemi} with population density along the elevation gradient is significant (R^2=0.54, p=0.01). No relationship is observed between LAI_{Hemi} and population density distribution along the elevation gradient in Taita Hills (Table 4.23). In Kilimanjaro transect, high LAI_{Hemi} occur in areas with high population density and agro-forestry areas (Fig. 4.41) while in Taita Hills, high LAI_{Hemi} occur in agro-forestry areas though than in Cropped land though no pattern of distribution observed with increasing population density along the elevation gradient.

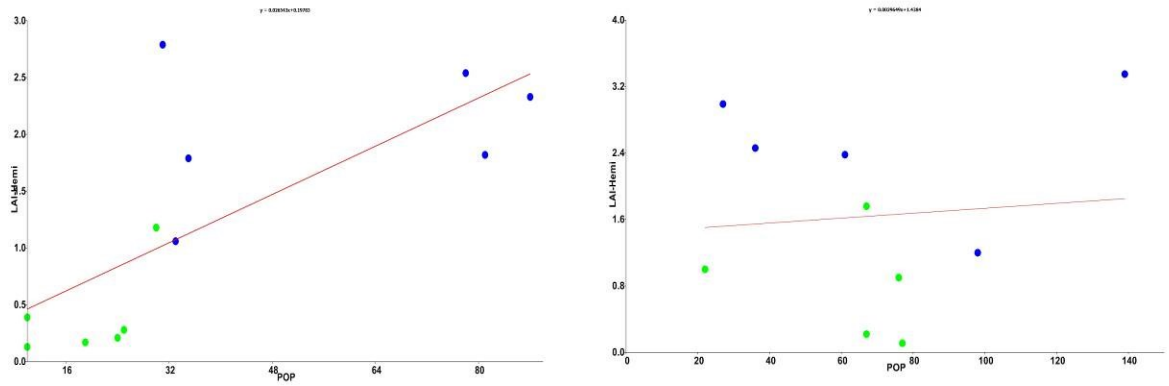

Figure 4 41 - Relationship of LAI_{Hemi} with increase in population density in Kilimanjaro (R^2 =0.54, p= 0.01) and Taita Hills (R^2 =0.01, p= 0.76). Blue dot (Agro-forestry) and Green dot (Cropped land).

Table 4. 23: Relationships of Leaf Area Index (LAI) with population density along the elevation gradients and in types of croplands in Mount Kilimanjaro and Taita Hills.

Variable Type		Model	R^2	*p-value*
Pop. density	Elev.Transect	LAI_{Hemi} = 0.036277*PopDen - 0.17855	0.54	0.01
	Agro-forestry	LAI_{Hemi} = 0.023019*PopDen +0.72757	0.08	0.60
	Cropped land	LAI_{Hemi} = 0.047942*PopDen -0.5493	0.33	0.23
Taita Hills	Elev.Transect	LAI_{Hemi} = 0.003*PopDen + 1.4363	0.01	0.76
	Agro-forestry	LAI_{Hemi} = -0.0074*PopDen + 1.2496	0.06	0.68
	Cropped land	LAI_{Hemi} = 0.0004*PopDen + 2.4443	0.00	0.95

v. Modeling LAI with Enhanced Vegetation Index

The increase of LAI_{Hemi} is significantly associated with the increase of EVI (R=0.75, p=0.00) along the elevation gradient in Kilimanjaro (Table 4.24). The amount of LAI_{Hemi} in agro-forestry in Mount Kilimanjaro area are distributed on areas with high EVI while low LAI_{Hemi} are associated with areas with low EVI. However, the distribution of high LAI_{Hemi} in Mount Kilimanjaro is more varied in areas with high EVI, with most of data points tending away from each other (Fig. 4.42). In Taita

Hills, low and high LAI_{Hemi} are observed in areas with high EVI while variation of LAI_{Hemi} occurs in areas with both low and high EVI (Fig. 4.42).

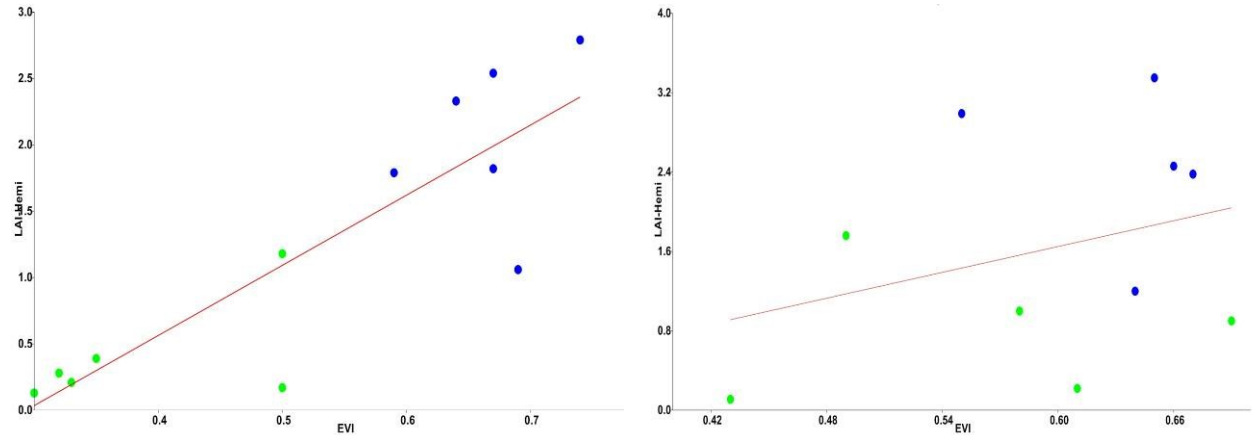

Figure 4 42 - Relationship of LAIHemi with increase in EVI in Kilimanjaro (R2=0.75, p=0.00) and Taita Hills (R2 =0.11, p= 0.36). Blue dot (Agro-forestry) and Green dot (Cropped land).

Table 4. 24: Relationships of Leaf Area Index (LAI) with EVI along the elevation gradients and in types of croplands in Mount Kilimanjaro and Taita Hills.

Variable Type		Model	R^2	*p-value*
Kilimanjaro	Elev. Transect	LAI_{Hemi} =6.1108*EVI -1.984	0.75	0.00
	Agro-forestry	LAI_{Hemi} =12.526*EVI -6.2958	0.08	0.59
	Cropped land	LAI_{Hemi} =4.3151*EVI -1.2608	0.33	0.23
Taita Hills	Elev. Transect	LAI_{Hemi} =13.335*EVI -6.324	0.11	0.36
	Agro-forestry	LAI_{Hemi} =-16.912*EVI +13.198	0.07	0.68
	Cropped land	LAI_{Hemi} =6.5488*EVI -2.8693	0.00	0.95

4.4.4. Key Findings for objective 4

Leaf Area Index in Kilimanjaro and Taita Hills are comparable. The distribution of LAI along the elevation of the two sites are significantly different Kilimanjaro (t=4.24, p=0.00) and Taita Hills (t=4.58, p=0.00). The distribution of LAI in types of cropland within the site are significantly different; Kilimanjaro t=5.48, p=0.00 and Taita Hills t=3.56, p=0.00). Spatial distribution of LAI is only explained better in Kilimanjaro by univariate models elevation (R^2=0.93, p=0.00), and pH (R^2=0.80, p=0.00) in Kilimanjaro. LAI is poorly related with the tested environmental variables in Taita Hills.

4.5. Impact of projected climate change scenarios on the selected plant species in Taita Hills and Mount Kilimanjaro

4.5.1. Baseline climate projections

i. Analysis of omission/commission of prediction

Replicate model for prediction of *A. gummifera* shows that the omission rate is closer to the predicted omission line in graph for the fractional value Vs cumulative threshold (Fig. 4.43). However, variability of the replicate model occurs mostly at the middle. The receiver operating characteristics (ROC) curve for the model replicats indicates the average test AUC for the replicate runs is 0.935 and the standard deviation is 0.011, meaning model replicates performed better in predicting the distribution of *A. gummifera.*

In the prediction of the *M. indica*, the omission rate was close to the predicted omission up to the middle but tend to move away but close up again (Fig. 4.43). The omission rate for the replicate model, however, has high variability throughout. The receiver operating characteristics (ROC) curve for the model replicate indicates the average test AUC for the replicate runs is 0.983 and the standard deviation is 0.011, meaning, model replicates performed better in predicting the distribution of *M. indica.*

The replicate model prediction for *P. americana* show the omission rate running slightly away from the predicted omission on the lower part but very close to the line from the middle to the end (Fig. 4.43). More variability occurs in the middle of the curve. The model receiver operating characteristics (ROC) curve for the model replicates for *P. americana* indicates the average test AUC for the replicate runs is 0.992 and the standard deviation is 0.002; meaning, model replicates performed better in predicting the distribution of *M. indica.*

The model predicted the species well in areas data points occur including areas away from data points as the potential distribution areas (Fig. 4.44). The predicted distribution by climate models shows the distribution of most of the species occurs in Kenya mostly around the highlands. Albizia has a wider distribution area in Kenya while in Tanzania, its distribution occur around Mount Kilimanjaro and the Arc Mountain areas. The distribution of Avocado and Mango is apparently conspicuous around Kenya highlands than in Tanzania.

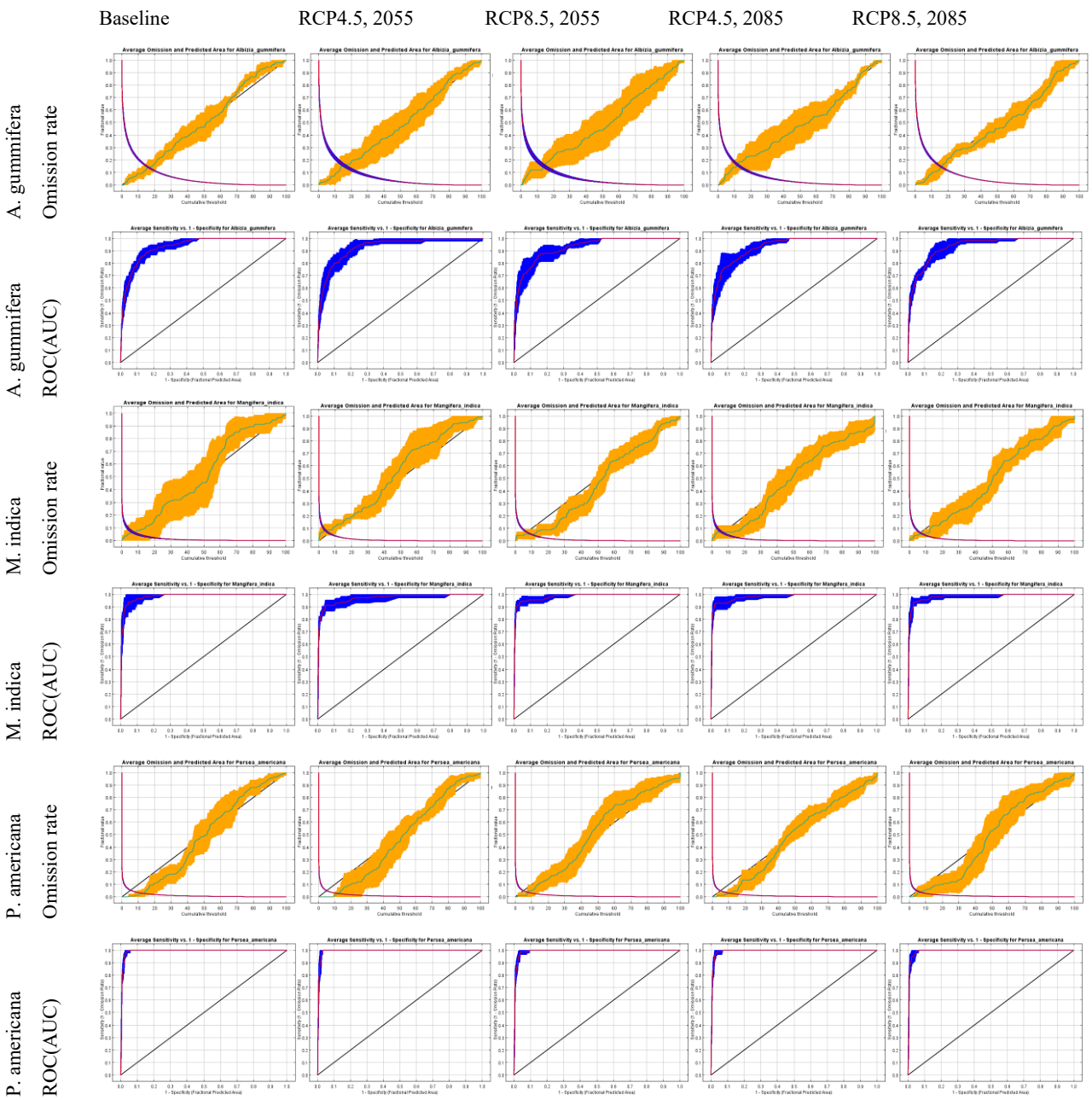

Figure 4 43 - The test omission rate and ROC (AUC) for *A. gummifera*, *M. indica* and *P. americana*.

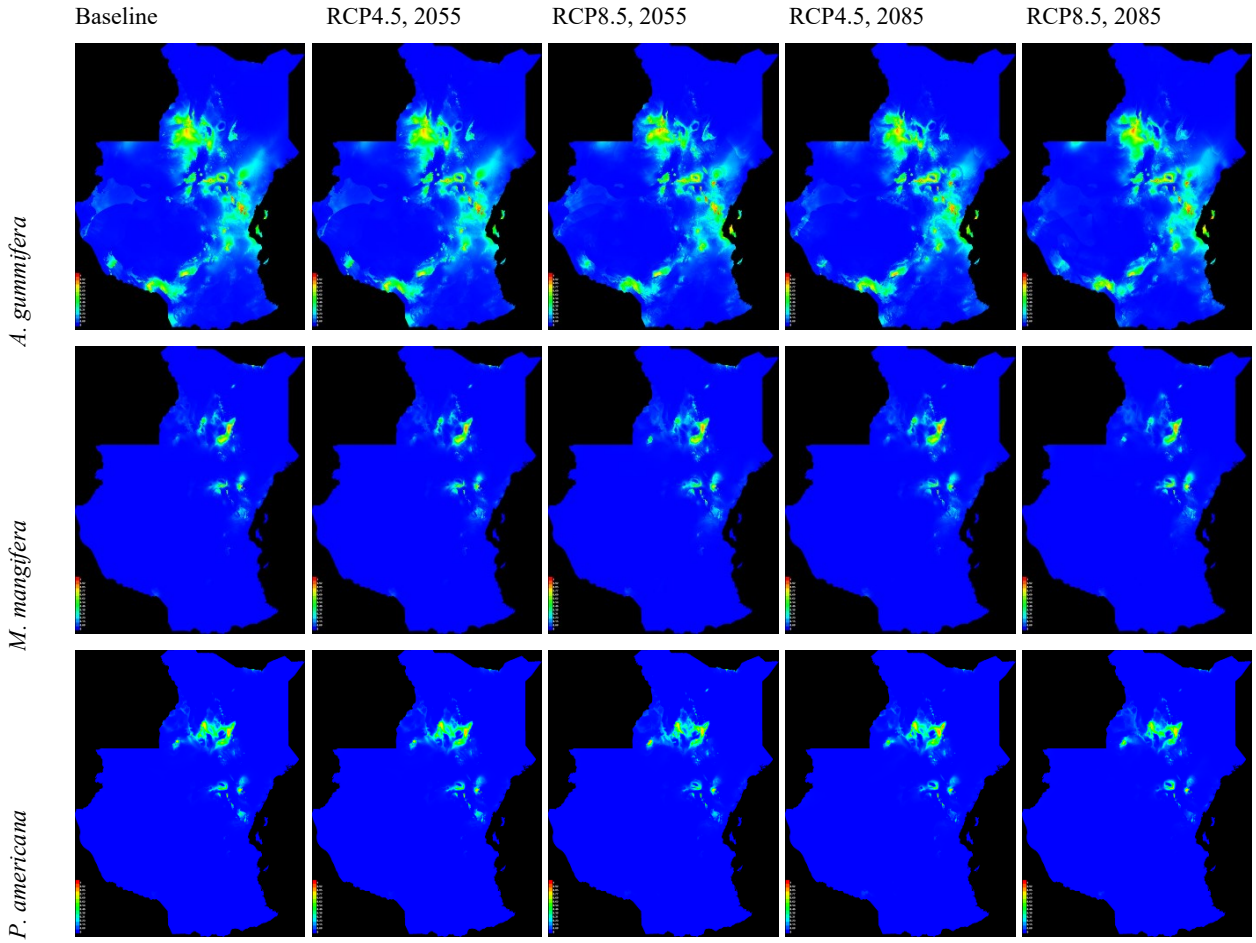

Figure 4.44 - Probability distribution of *A. gummifera*, *M. indica*, and *P. americana* from point-wise mean of 7 output grids of baseline climate projection.

ii. Variable contribution to maxent model for the species (baseline projections)

Percentage contributions of climate variables to maxent model for *A. gummifera* ranged from a min=0 to max=23.1 (meanSE 1.45±0.48); *M. indica*, min=0 and max=26.7 (meanSE 1.45±0.61), and; *P. americana*, min=0 and max=18.4% (meanSE 1.45±0.42) (Fig. 4.45).

Different climate variables contributed variedly to the model of the species; for *A. gummifera*, maximum temperature for August contributed highly to the model (23.1%). This was followed by June precipitation (21.8%) and Bio4 (9.3%) (Fig. 4.45). The November precipitation contributed highly to the maxent model for *M. indica* by 26.7% followed by Bio2 (25.8%) and precipitation for the month of May (19.9%). The maxent model for *P. americana* was contributed highly by Bio14 (18.4%) followed by the minimum monthly temperature for December (17.4%) and the mean monthly precipitation for November (12.2%) (Fig. 4.45).

The results of Two-Way ANOVA show significant differences (F=1.50, p=0.02) among the contributions of the climate variables, while no significant difference was observed among the maxent model for *A. gummifera, M. indica* and *P. americana.*

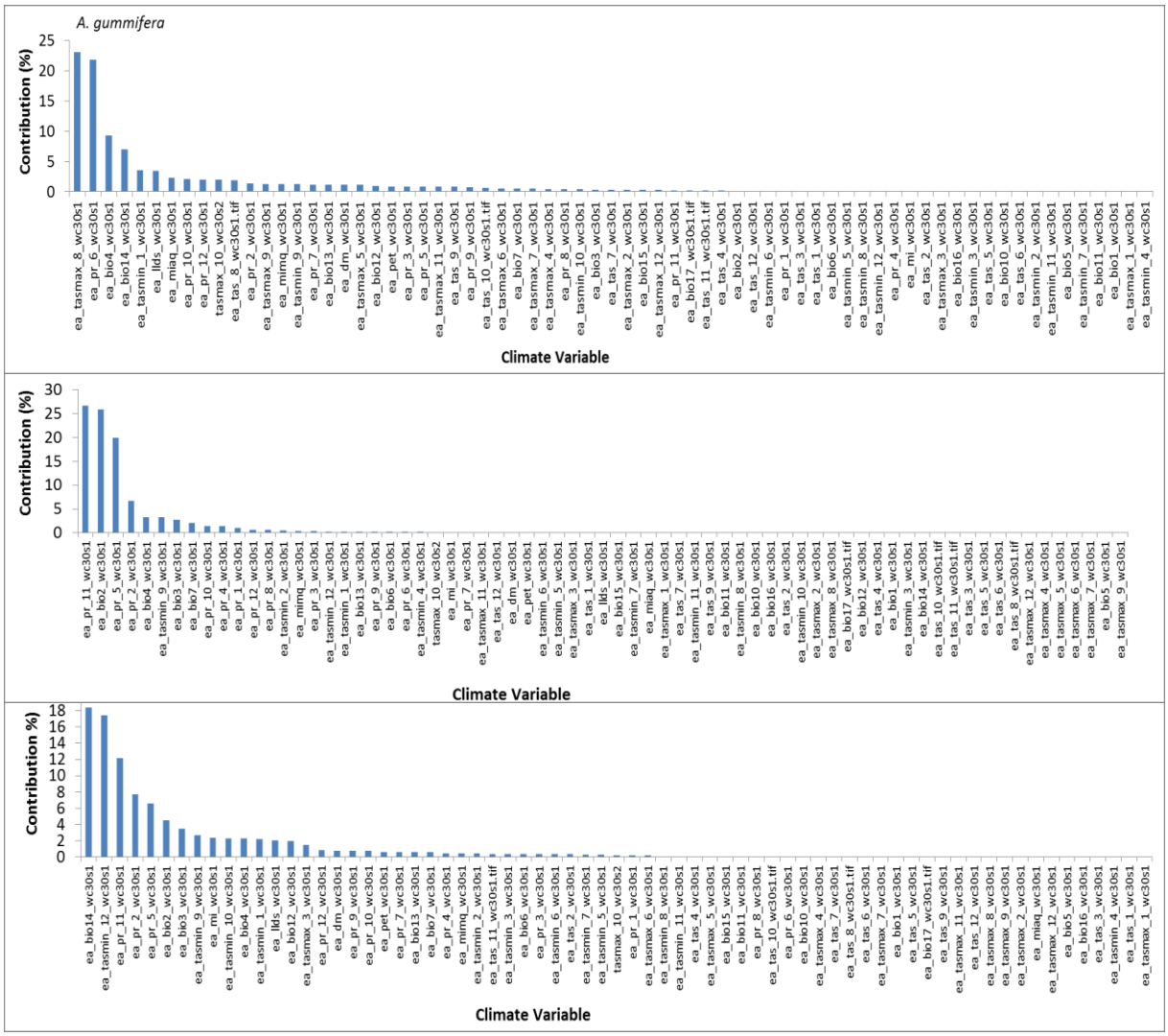

Figure 4.45 - Percentage of climate variable contribution to *A. gummifera*, *M. indica* and *P. america* maxent model average over 7 replicate runs for baseline condition.

iii. Variable Importance to maxent model for the species (current projections)

a. Jackknife Test on maxent model for A. gummifera (Baseline climate projection)

The Jackknife test of regularized training gain, test of gain and AUC for *A. gummifera* shows that the climate variable with the highest gain, when used in isolation, is the monthly maximum temperature for September (ea tasmax 9 wc30s1) (Fig. 4.46), which appears to have the most useful information

by itself. The variable that decreases the gain the most when it is omitted is the monthly precipitation for December (ea pr 12 wc30s1) (Fig. 4.46), which appears to have the most information that is not present in the other variables.

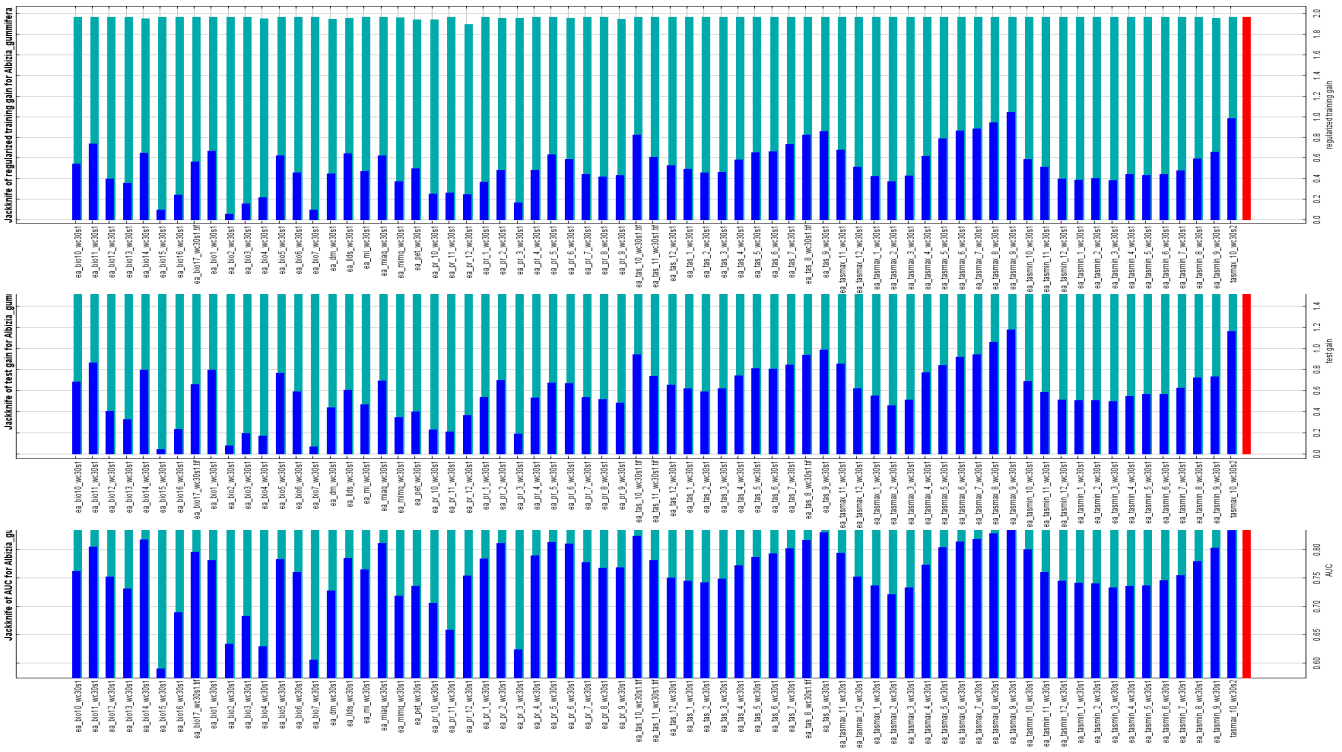

Figure 4.46 - The Jackknife of regularized training gain, test gain, and AUC for *A. gummifera* averaged values over 7 replicate runs for baseline climate condition.

b. Jackknife Test on maxent model for M. indica (Baseline climate projection)

The Jackknife test of regularized training gain, test of gain and AUC for *M. indica* shows that the climate variable, with the highest gain when used in isolation, is the monthly precipitation for November (ea pr 11 wc30s1) (Fig. 4.47), which appears to have the most useful information by itself. The variable that decreases the gain the most when omitted is the monthly precipitation for February (pr 2) (Fig. 4.47), which appears to have the most information that is not present in the other variables.

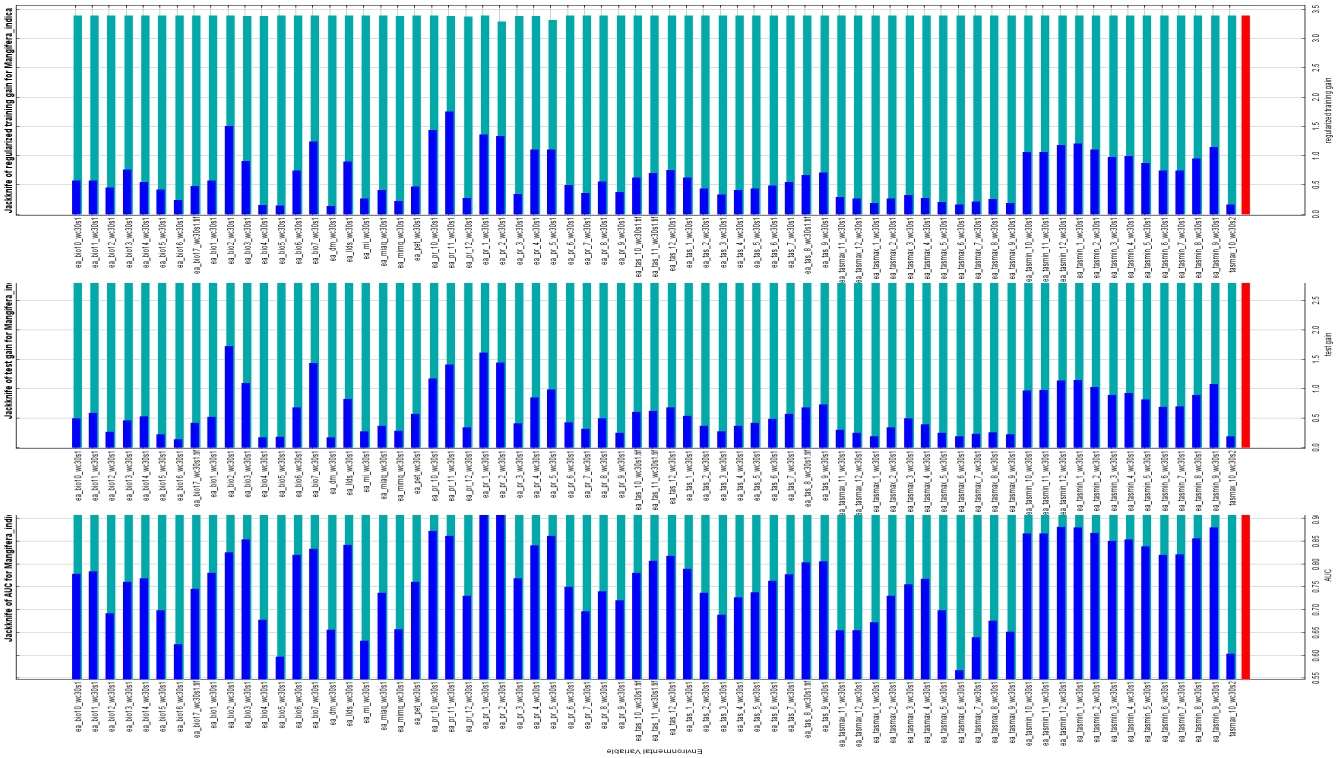

Figure 4 47 - The Jackknife of regularized training gain, test gain, and AUC for M. indica averaged values over 7 replicate runs for baseline climate condition.

c. Jackknife Test on maxent model for *P. americana* (Baseline climate projection)

The Jackknife test performed using regularized training gain, test gain and AUC for *P. americana* shows the minimum monthly temperature for January (tasmin 1) (Fig. 4.48) having the highest gain when used in isolation. The monthly precipitation for February (pr 2) and May (pr 5) (Fig. 4.48) decreases the gain when omitted when Jackknife test is performed using training gain, test gain and AUC.

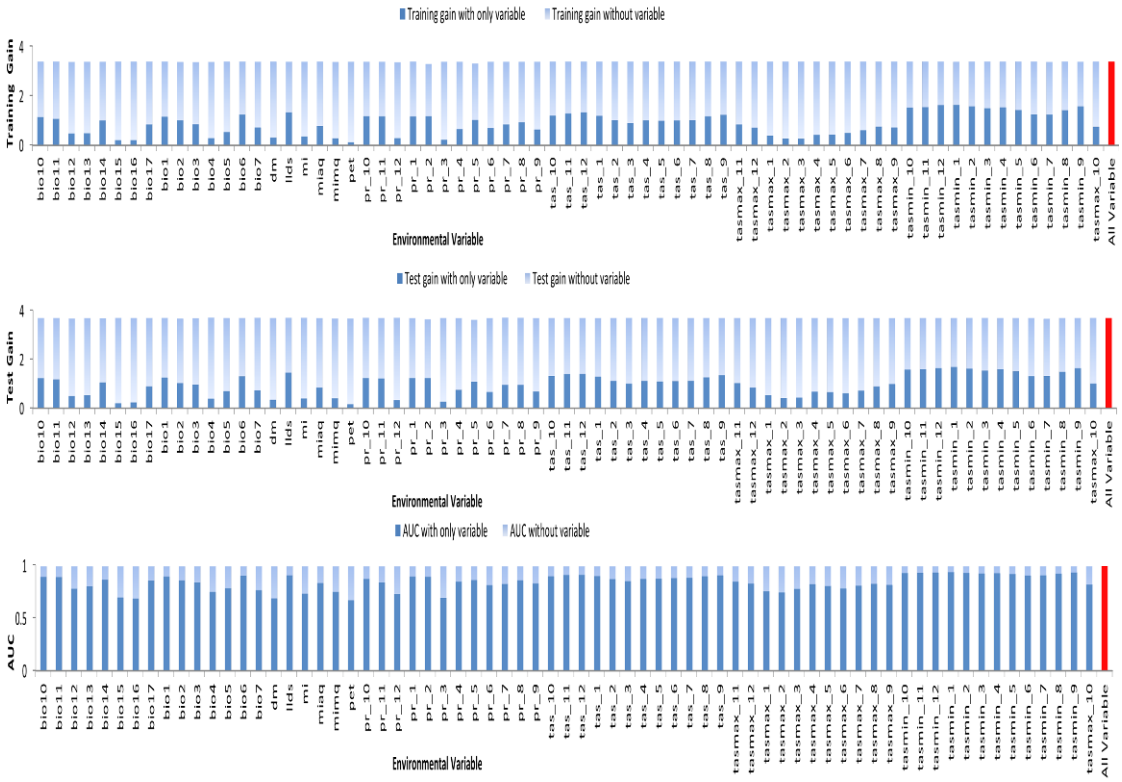

Figure 4.48 - The Jackknife of regularized training gain, test gain, and AUC for *P. americana* from averaged values from 7 replicate runs for baseline climate condition.

4.5.2. Climate projections based on RCP4.5, 2055 (mean over 2041-2070)

i. Analysis of omission/commission rate

The prediction of *A. gummifera* shows that the omission rate is very close to the predicted omission line in the graph for the fractional value Vs cumulative threshold. The replicate model varies in the middle but less at the beginning and the end of the graph. The model replicate has ROC curve AUC at 0.928 and the standard deviation is 0.019, meaning that the model replicate performed better in predicting the distribution of *A. gummifera.*

The omission rate is very close to the prediction omission for *M. indica* at the beginning but tends away at the middle. The replicate model is variable from the middle of the graph to the end. The receiver operating characteristics curve (average test AUC) for the species prediction is 0.969 with a standard deviation of 0.021. This implies that the replicate model performed better in the prediction of *M. indica*.

The rate of omission for prediction of *P. americana* is relatively close to the prediction omission. However it tends to move away at the beginning of the graph. Variabillity of the replicate model is observed at the beginning but decreases slightly towards the end. The receiver operating

characteristic (ROC) curve indicates that an averaged test AUC for the replicate runs is 0.993 and the standard deviation is 0.002.

ii. Variable contribution to maxent model for the species (RCP 4.5, 2055)

Percentage contributions of climate variables to maxent model for *A. gummifera* ranged from a min=0 to max=29.5 (meanSE 1.44±0.52); *M. indica*, min=0 and max=31.7 (meanSE 1.45±0.61), and *P. americana*, min=0 and max=22.5% (meanSE 1.45±0.43) (Fig. 4.49).

Different climate variables contributed differently to the model of the species; for *A. gummifera*, maximum temperature for August contributed highly to the model (29.5%). This was followed by June precipitation (19.7%) and Bio4 (7.1%) (Fig. 4.49). Bio2 contributed highly to the maxent model for *M. indica* (31.7 %) followed by the November precipitation (24%) and precipitation for the month of May (14.8%). The maxent model for *P. americana* was contributed highly by the monthly precipitation for January (22.5%), followed by the monthly minimum temperature of October (13%) and, the monthly minimum temperature of September (12.5%) (Fig. 4.49).

Two-Way ANOVA showed no significant difference among the environmental variables and among the species distributions. The pairwise test (Kruskal-Wallis) indicated that the distribution of *A. gummifera* and *M. indica* are significantly different (p=0.03).

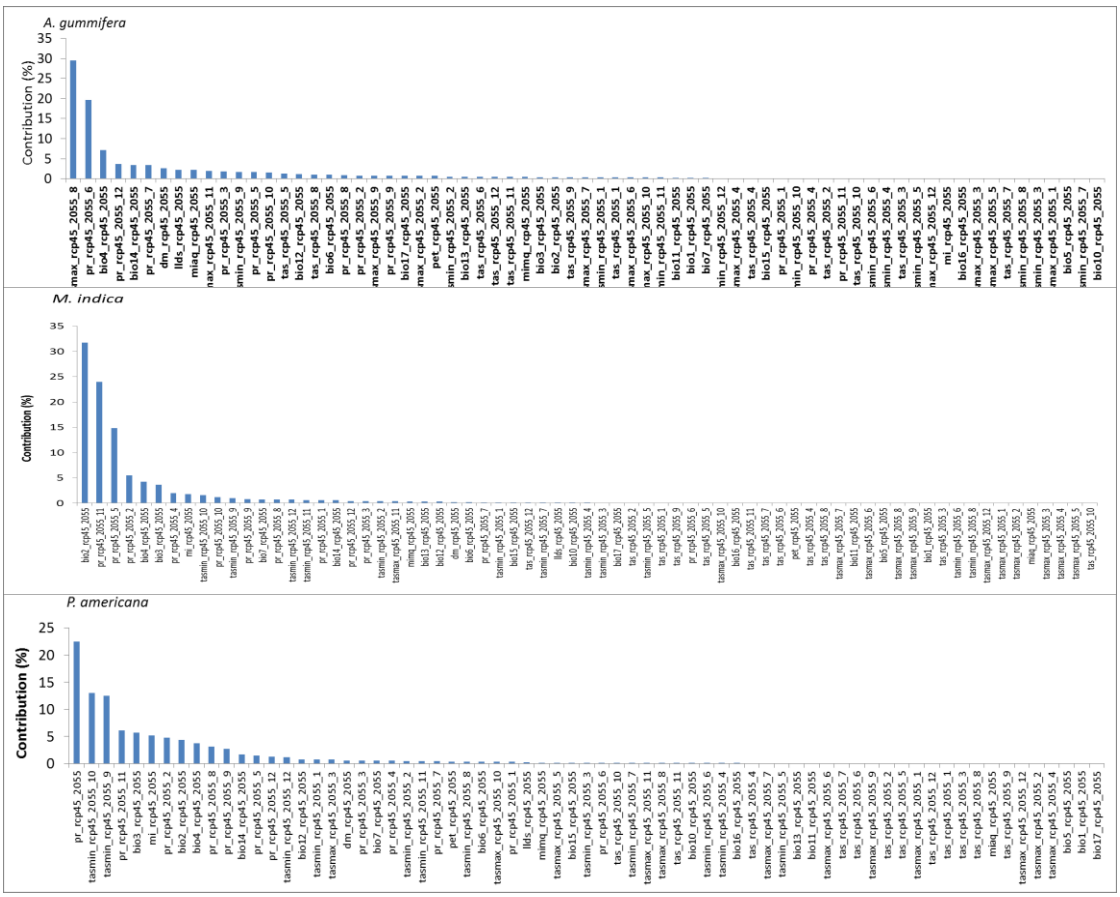

Figure 4.49 - Percentage of climate variable contribution to A. gummifera, M. indica and P. America maxent model average over 7 replicate runs for RCP4.5, 2055 (mean over 2041-2070).

iii. Variable Importance to maxent model for the species (RCP4.5, 2055)

a. Jackknife Test on maxent model for *A. gummifera* on rcp4.5 2055

The Jackknife test of regularized training gain, test of gain and AUC for maxent model for *A. gummifera* shows that the monthly maximum temperature for September gain most when used in isolation hence it has the most useful information (Fig. 4.50). The monthly precipitation for December (RCP4.5, 2055) decreases gain the most and therefore appears to have the most information that is not in other variables.

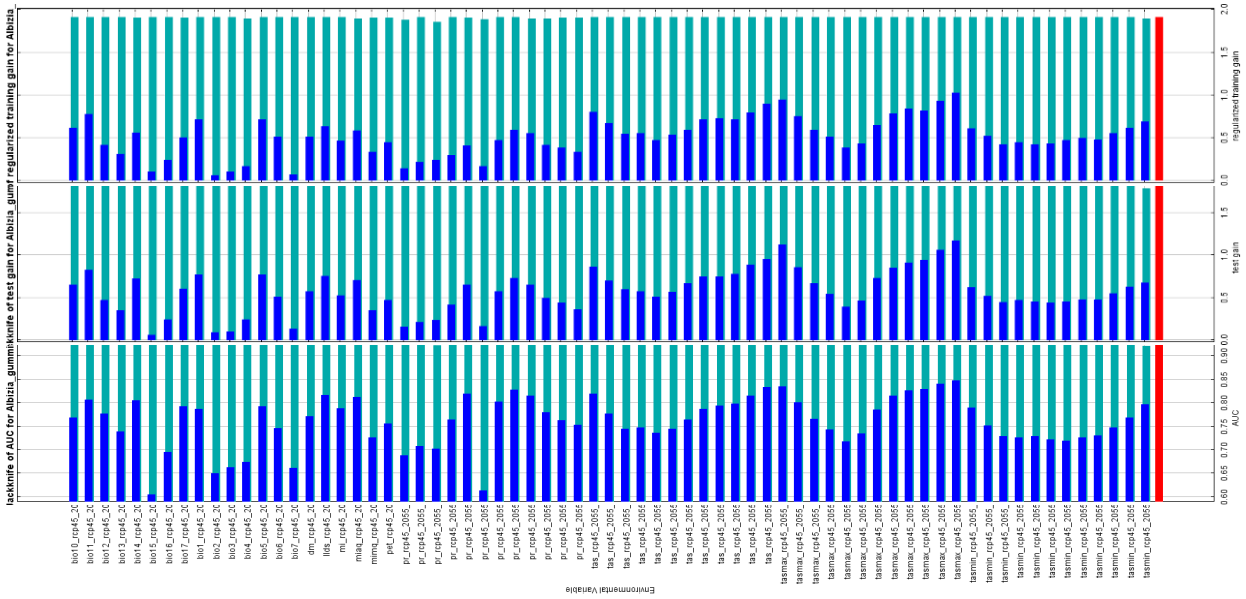

Figure 4 50 - The Jackknife of regularized training gain, test gain, and AUC for *A. gummifera* averaged values over 7 replicate runs for RCP4.5, 2055.

b. Jackknife Test on maxent model for *M. indica* RCP4.5 2055

The Jackknife test of regularized training gain and test of gain for maxent model for *M. indica* shows that the monthly precipitation of November (pr rcp45 2055 11) has the highest gain when used in isolation and therefore appears to have the most useful information by itself (Fig. 4.52). The AUC test on data showed most gain with the monthly precipitation of February (pr_rcp45_2055_2). The variable that decreases the gain in the jackknife test of regularized training gain, test of gain and AUC for maxent model for *M. indica* is the monthly precipitation of February (pr_rcp45_2055_2) (Fig. 4.52).

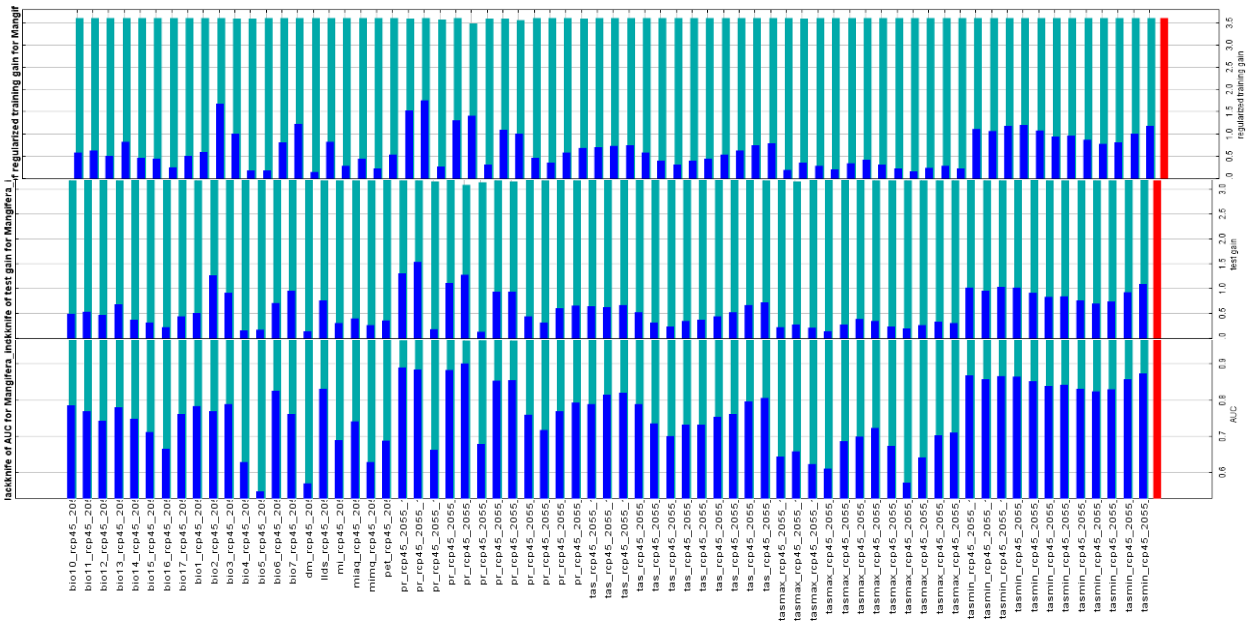

Figure 4 51 - The Jackknife of regularized training gain, test gain, and AUC for *M. indica* values averaged over 7 replicate runs for RCP4.5, 2055.

c. Jackknife Test on maxent model for *P. americana* RCP4.5 2055

The Jackknife test of regularized training gain, test of gain and AUC for maxent model for *P. americana* indicate that the monthly minimum temperature for January (tasmin rcp45_2055_1) has the highest gain when used in isolation (Fig. 4.52). This variable, therefore, appears to have the most useful information by itself. While, the monthly precipitation for February (pr_rcp45_2055_2) decreases the gain the most when it is omitted in the Jackknife test of regularized training gain, test of gain and AUC, which therefore appears to have the most information that is not present in other variables.

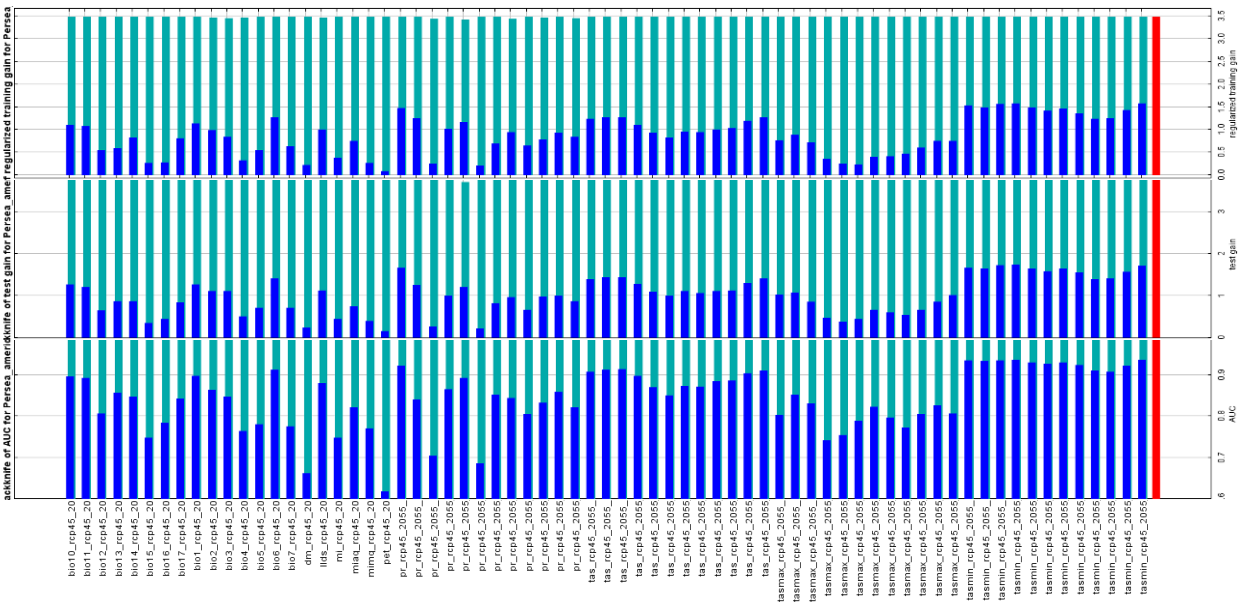

Figure 4.52 - The Jackknife of regularized training gain, test gain, and AUC for *P. americana* averaged values over 7 replicate runs for RCP4.5, 2055.

4.5.3. Climate projections based on RCP 8.5, 2055 (mean over 2041-2070)

i. Analysis of omission/commission rate

The omission rate for the replicate prediction of *A. gummifera* was very close to the prediction omission. Neverthelssr the omission rate for the replicate model is variable. The receiver operating characteristics (ROC) curve has the average test AUC for the replicate run at 0.926 and the standard deviation was 0.020.

Prediction of *M. indica* shows the omission rate tends away from the prediction omission but very close towards the end. The prediction of the replicate model is, however, variable throughout. The ROC curve shows that the average test AUC for the replicate runs is 0.983 with a standard deviation of 0.008.

P. americana prediction model has omission rate close to the prediction omission however the model is variable. The ROC curve for prediction of the species has an average test AUC for the replicate runs at 0.991 and the standard deviation is 0.002.

ii. Variable contribution to maxent model for the species (RCP 8.5, 2055)

A. gummifera: The monthly maximum temperature for August (tasmax rcp85 2055 8) contributes highly to the replicated maxent model for *A. gummifera* by 28.1%. This is followed by the monthly

precipitation for June (pr rcp85 2055 6) that contribute by 23.6% and Bio4 (bio4 rcp85 2055) by 8.7 % (Fig. 4.54). In the prediction of *M. indica*, the Mean Annual Temperature contributes highly to the maxent model by 31.9% followed by the monthly precipitation for November and August contributing by 24.3% and 8.4%, respectively (Fig. 4.54). The monthly precipitation for August and the minimum monthly temperature for October contributed to the maxent model for the prediction of *P. americana* by 18.3 and 18.1% respectively. The monthly precipitation for November comes third, contributing 10.6% (Fig. 4.54).

The maxent model for the three species, based on the climate variables, are not significantly different (Two-Way ANOVA), while the contribution of climate variables to the model for the three species is significantly different (Two-Way ANOVA; F=1.41, p=0.05). Contributions of the variables to the three species show no significant difference between the paired species (Kruskal-Wallis).

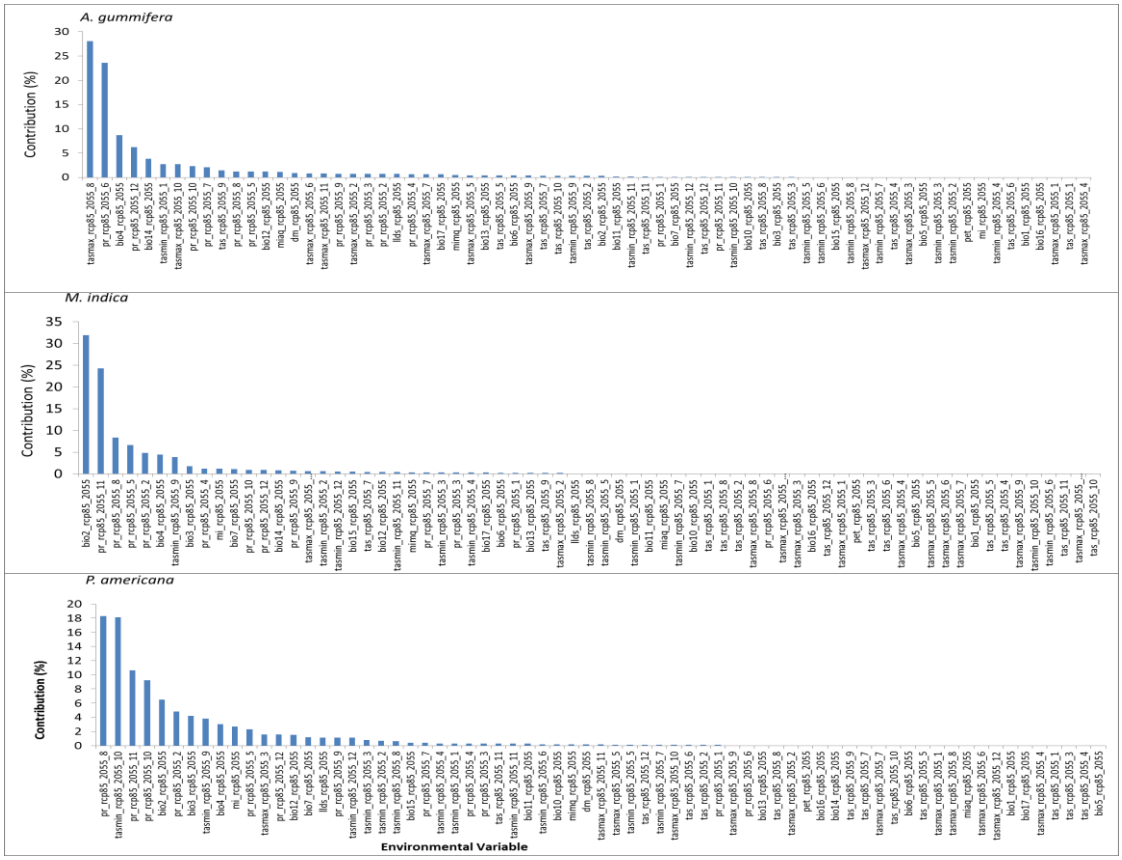

Figure 4.53 - Percentage of climate variable contribution to *A. gummifera*, *M. indica* and *P. america* maxent model average over 7 replicate runs for RCP 8.5, 2055.

iii. Variable Importance to maxent model for the species (RCP 8.5, 2055)

A. gummifera: The environmental variable with highest gain in the maxent model for the *A. gummifera, M. indica* and *P. americana* when used in isolation is bio10 rcp85 2055, which therefore appears to have the most useful information by itself. The environmental variable that decreases the gain the most when it is omitted is bio10 rcp85 2055 which therefore appears to have the most information that is not present in the other variables.

4.5.4. Climate projections based on RCP4.5, 2085 (mean over 2071-2100)

i. Analysis of omission/commission rate

The omission rate for the maxent model for the *A. gummifera* is very close to the predicted omission. Variability of the replicate model is observed mostly at the middle of the curve. The ROC curve has the averaged test AUC for the replicate runs at 0.931 with the standard deviation of 0.017.

In the prediction of *M. indica* distribution, the omission rate deviates away from the prediction rate at the beginning of the curve but immediately runs closely to the prediction rate. However, variability of the maxent model is observed throughout the curve. The AUC for the ROC curve for the replicate runs averagely at 0.981 with the standard deviation of 0.012.

The replicate maxent model for prediction of *P. americana* has omission rate that also tends away at the beginning of the curve but immediately runs very close to the predicted rate, though the replicate model is variable. The AUC for the ROC curve for the replicate model averages at 0.992 with the standard deviation of 0.002.

ii. Variable contribution to maxent model for the species (RCP 4.5, 2085) (mean over 2071-2100)

Maximum monthly temperature for August (tasmax 8) followed by the monthly precipitation for June (pr 6), and December (pr 12), highly contributed to the replicate model for *A. gummifera* to the order of 24.8 %, 21.6% and 7.6% respectively, by 24.8 % (Fig. 4.54). Contributions to the model for *M. indica* was mostly done by the Mean diurnal range in temperature (Bio2, 28.3%), followed by the monthly precipitation for November (pr 11, 26.2%) and the monthly precipitation for May (pr 5, 13.4%) (Fig. 4.54). The monthly precipitation for October (pr 10) contributed highly (21.5%) to the replicate maxent model for *P. americana* followed by the minimum monthly temperature for October and September which contributed 15 % and 10.5% respectively (Fig. 4.54).

Two-Way ANOVA showed no significant difference among the species based, on the percentage contribution by the environmental variables and, neither among the contributions of the environmental variables to the three species.

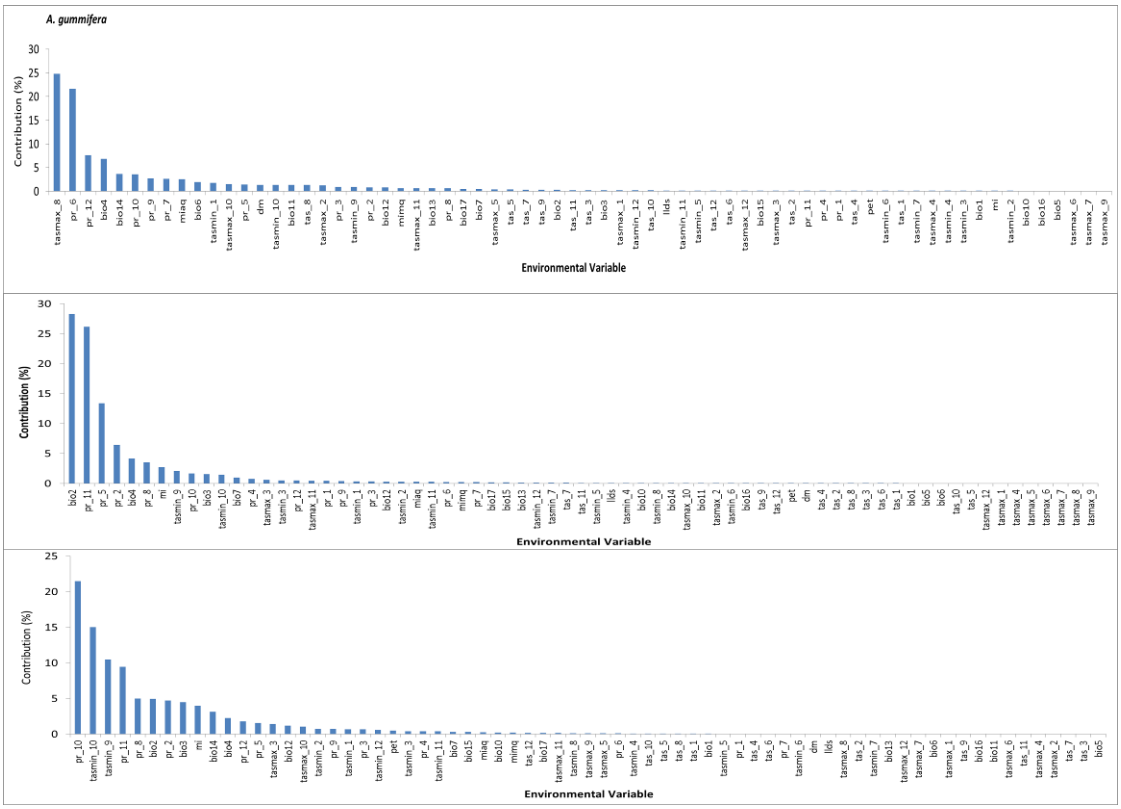

Figure 4.54 - Percentage of climate variable contribution to *A. gummifera*, *M. indica* and *P. america* maxent model average over 7 replicate runs for RCP 4.5, 2085 (mean over 2071-2100).

iii. Variable importance RCP4.5, 2085 (mean over 2071-2100)

The Jackknife test performed using regularized training and test gain, and AUC for the replicate model for *A. gummifera* shows that the maximum monthly temperature for September (tasmax 9) had the highest gain when used in isolation (Fig. 4.55). While, the monthly precipitation for December decreases the training and test gain, and AUC when omitted in the prediction model for *A. gummifera* (Fig. 4.55).

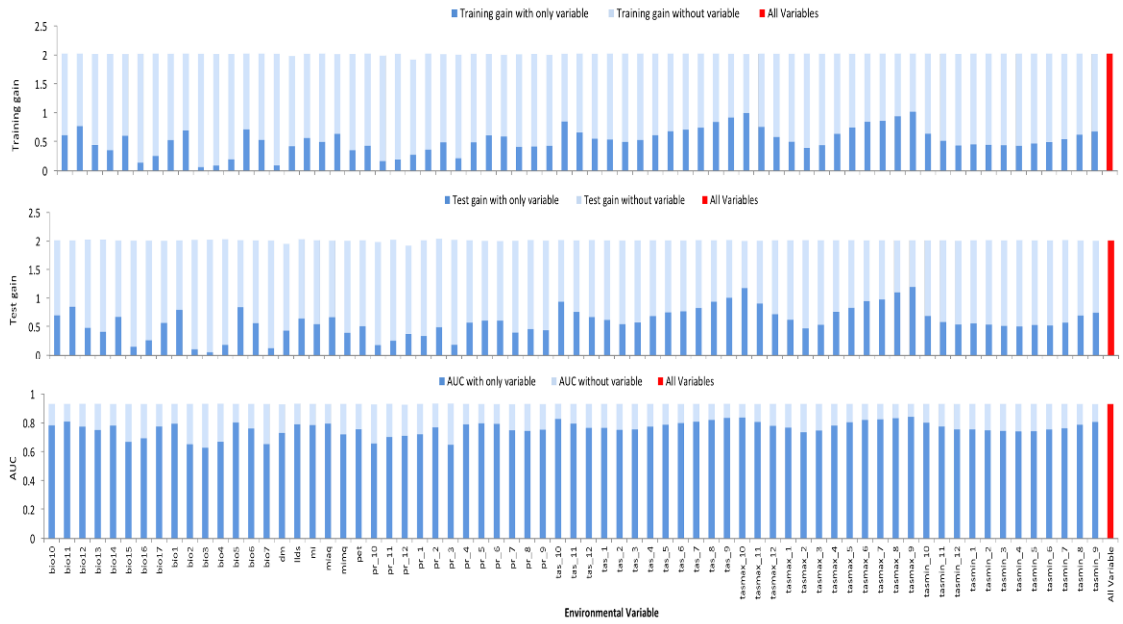

Figure 4.55 - The Jackknife of regularized training gain, test gain, and AUC for *A. gummifera* averaged values over 7 replicate runs for RCP4.5, 2085.

The Jackknife test performed using regularized training and test gain on *M. indica* shows that the monthly precipitation for November (pr 11) had the highest gain when used in isolation tests (Fig. 4.56). On the other hand AUC shows that the monthly precipitation for February (pr 2) had the highest gain when used in isolation tests.

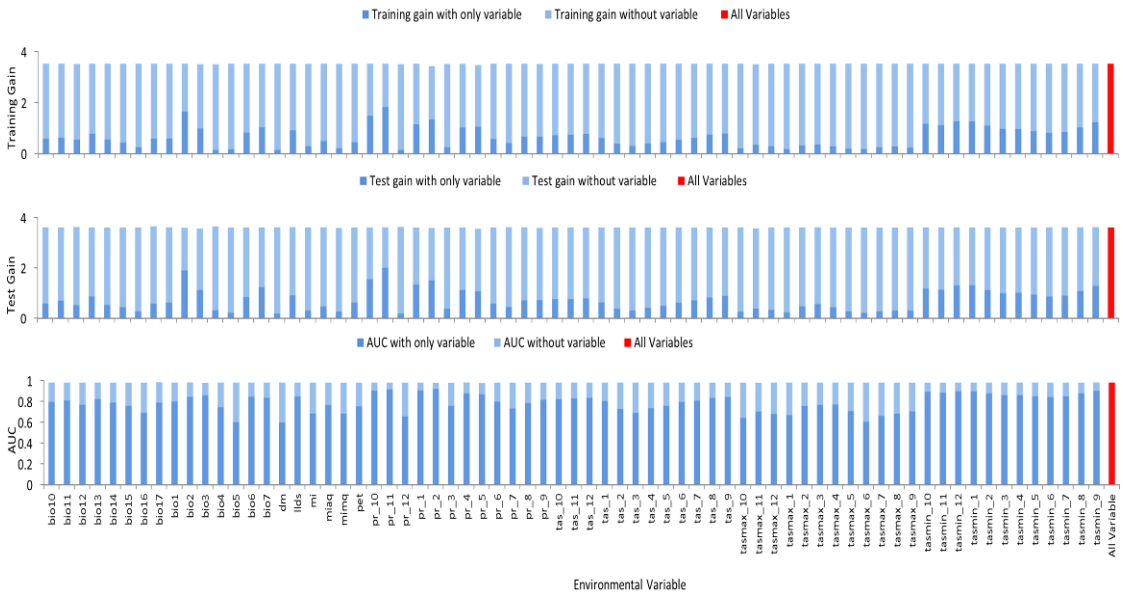

Figure 4.56 - The Jackknife of regularized training gain, test gain, and AUC for M. indica from averaged values over 7 replicate runs for RCP4.5, 2085.

The Jackknife test performed using regularized training, test gain and AUC on *P. americana* shows that the minimum monthly temperature for January (tasmin 1) had the highest gain when used in isolation (Fig. 4.57). In addition it shows that while the monthly precipitation for January decreases (pr 1) the training gain, the monthly precipitation for May (pr 5) decreases the test gain and AUC when omitted in prediction model for *P. Americana* (Fig. 4.57).

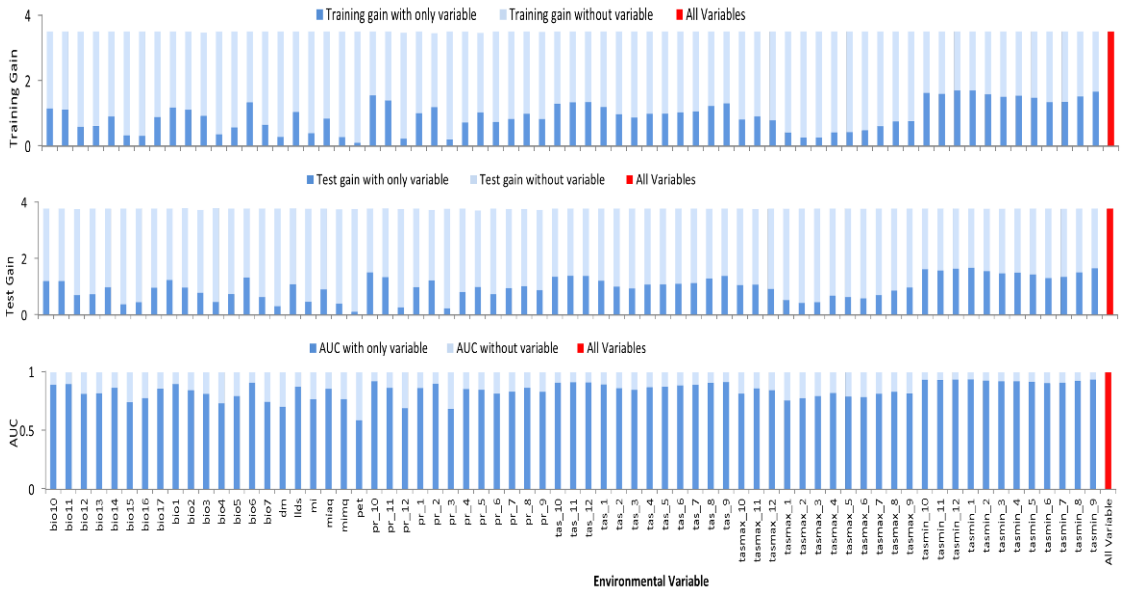

Figure 4.57 - The Jackknife of regularized training gain, test gain, and AUC for *P. americana* from averaged values over 7 replicate runs for RCP4.5, 2085.

4.5.5. Predictions by the future climate projections based on RCP 8.5, 2085 (mean over 2071-2100)

i. Analysis of omission/commission rate

The omission rate for the replicate maxent model for the *A. gummifera* and *M. indica* were very close to the predicted omission. The omission rate for the replicate maxent model for *P. americana* tends to move away from the predicted omission at the beginning but runs towards the predicted omission from the middle of the curve to the end. The ROC curve has the averaged test AUC for the replicate maxent model for: *A. gummifera* at 0.935 with the standard deviation of 0.013; *M. indica* at 0.983 with the standard deviation of 0.009; *P. americana* at 0.992 with the standard deviation of 0.002.

ii. Variable contribution to maxent model for the species (RCP 8.5, 2085) (mean over 2071-2100)

Maximum monthly temperatures for August (tasmax 8) contributed highly to the replicate model for *A. gummifera* by 21 %, followed by the monthly precipitation for June (pr 6, 19%) and October (pr 10, 8%) (Fig. 4.59). On the other hand, monthly precipitation for November (pr 11) mostly contributed to the model for *M. indica* by 26% followed by Mean diurnal range in temperature (bio 2, 24%) and the monthly precipitation for August (pr 8, 11%) (Fig. 4.59). The monthly precipitation for August (pr 8) contributed significantly to the replicate maxent model for *P. americana* (20%) followed by the monthly precipitation for November (pr 11, 15%) and the minimum monthly temperature for October (tasmin 10, 10%) (Fig. 4.59).

Two-Way ANOVA showed significant difference (F=1.78, p=0.00) among the contributions of various environmental variables to the three species. However, no significant difference was observed among the species based on the percentage contribution by the environmental variables.

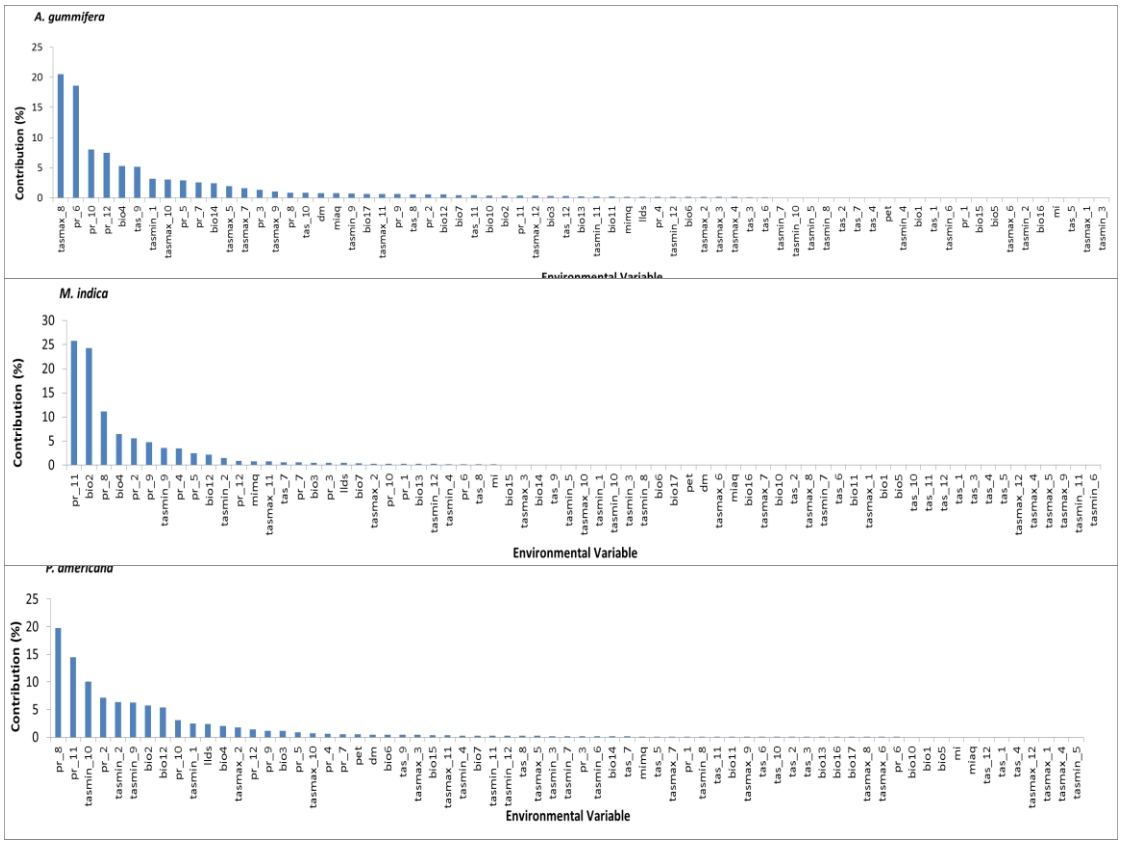

Figure 4.58 - Percentage of climate variable contribution to *A. gummifera*, *M. indica* and *P. america* maxent model average over 7 replicate runs for RCP 8.5, 2085 (mean over 2071-2100).

iii. Jackknife Test of variable importance RCP8.5 2085 (mean over 2071-2100)

The Jackknife test performed using regularized training and test gain and AUC on *A. gummifera* shows that the maximum monthly temperature for September (tasmin 9) had the highest gain when used in isolation (Fig. 4.59). While, the monthly precipitation for December (pr 12) decreases the training gain and test gain, the monthly precipitation for June (pr 6) decreases the AUC, when omitted in the prediction model for *A. gummifera* (Fig. 4.59).

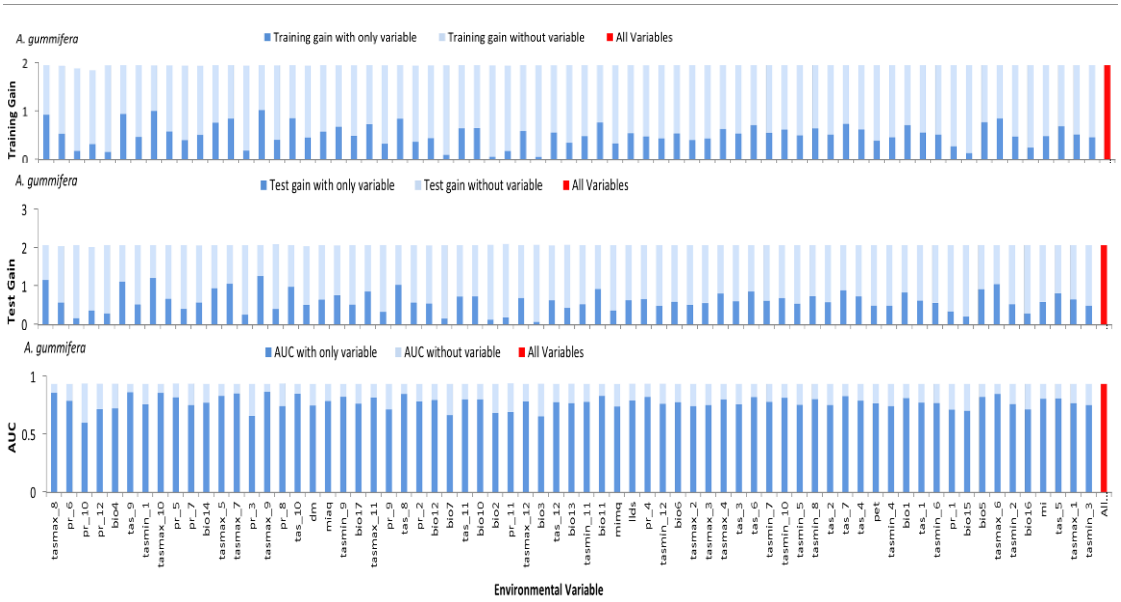

Figure 4 59 - The Jackknife of regularized training gain, test gain, and AUC for *A. gummifera* averaged values over 7 replicate runs for RCP8.5 2085.

The Jackknife test performed using regularized training and AUC on *M. indica* indicates that the monthly precipitation for November (pr 11) increases gain, and that the mean diurnal range in temperature (bio2) increases test gain, when used in isolation (Fig. 4.60). However, the monthly precipitation for February (pr 2) decreases the training gain, test gain and AUC when omitted in the prediction model for *M. indica* (Fig. 4.60).

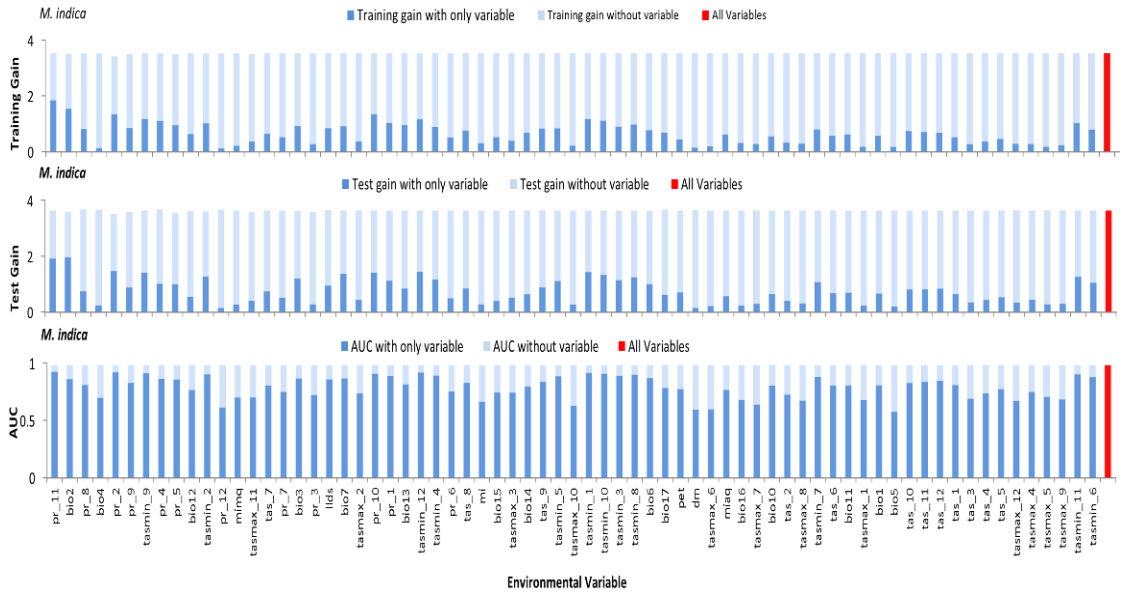

Figure 4.60 - The Jackknife of regularized training gain, test gain, and AUC for M. indica averaged values over 7 replicate runs for RCP8.5, 2085.

The Jackknife test performed using regularized training gain,test gain and AUC on *P. americana* shows that the minimum monthly temperature for January (tasmin 1) increases gain when used in isolation while the monthly precipitation for February (pr 2) decreases the training gain and test gain (Fig. 4.61). The monthly precipitation for September (pr 9) decreases AUC when omitted in the prediction model for *P. americana*.

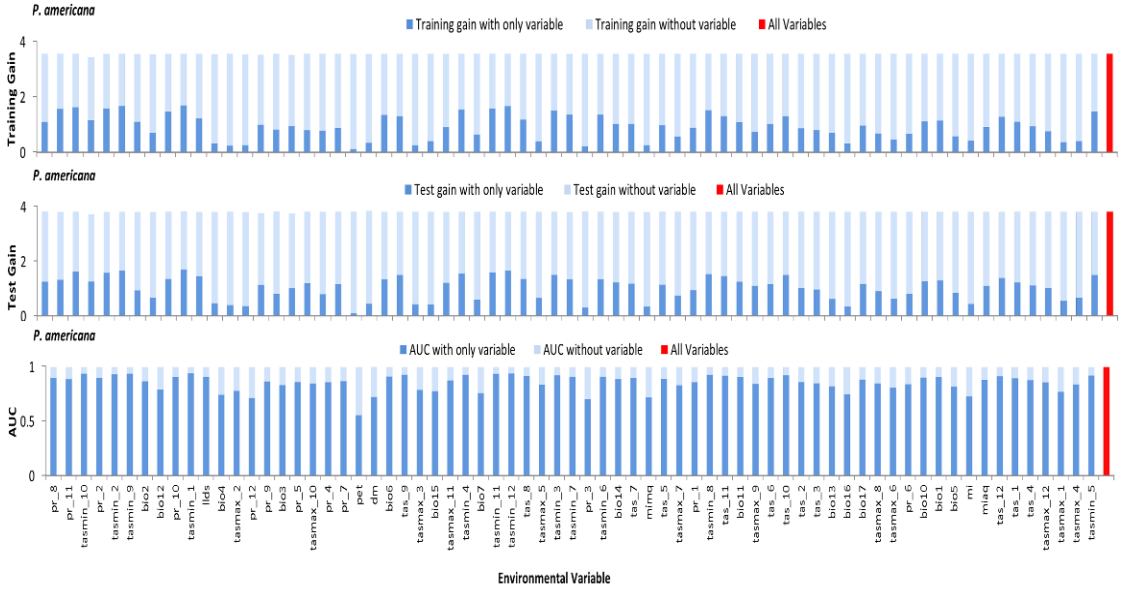

Figure 4.61 - The Jackknife of regularized training gain, test gain, and AUC for *P. americana* averaged values over 7 replicate runs for RCP8.5, 2085.

4.5.6. Predicted suitable areas

i. Species suitable areas under baseline climate condition

An estimated area of 77% of the transect area was potentially suitable for *A. gummifera* followed by *P. americana* (69%) and *M. indica* (67%) under the baseline in Taita Hills (Fig. 4.62). In Kilimanjaro, species that had highest potential suitable area along the elevation gradient was *A. gummifera*, 39% of the area, followed by *M. indica* (36%) and *P. americana* (28%) (Fig. 4.62). Comparison of suitable areas between Kilimanjaro and Taita Hills predicted under the baseline climate condition for *A. gummifera*, *M. indica* and *P. americana* shows significant difference (F=153.17, p=0.01). While, no significant difference was observed among the three species on suitable areas within site.

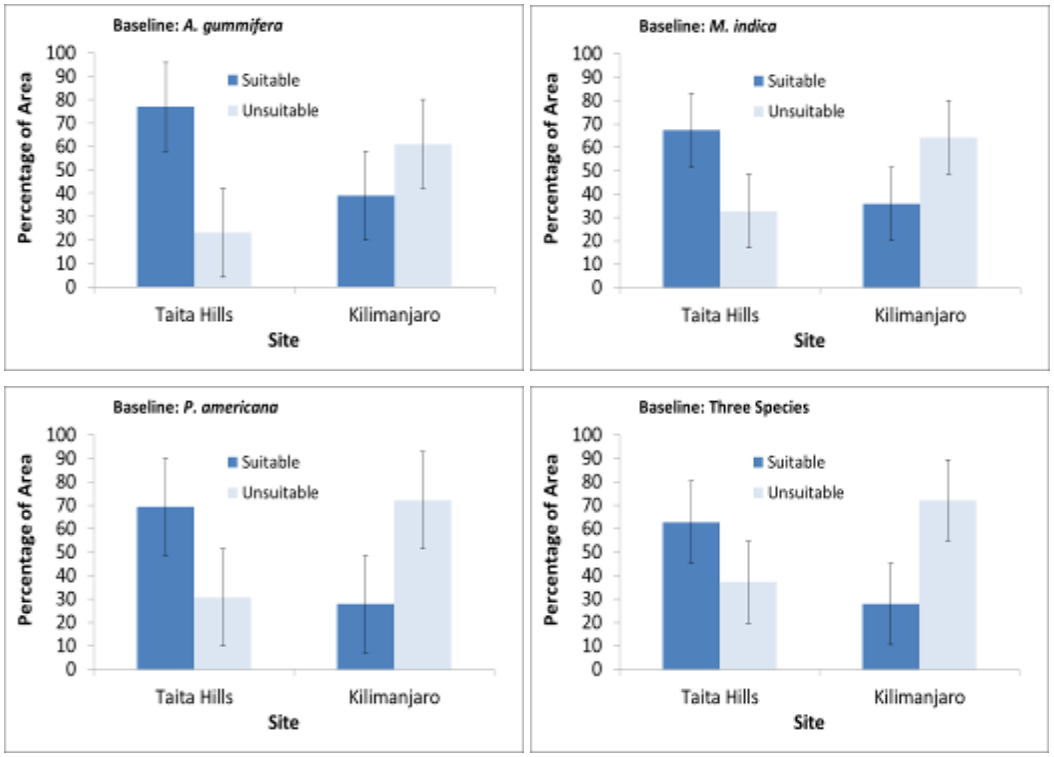

Figure 4.62 - Percentage area coverage of suitable areas and unsuitable areas for *A. gummifera*, *M. indica* and *P. americana* in Taita Hills and Mount Kilimanjaro under baseline climate conditions.

ii. Species suitable areas under RCP 4.5 (2055) climate condition

Under the climate change projection based on the RCP 4.5 (2055) in Taita Hills, *A. gummifera* has about 75% of the transect area suitable for distribution, while the one with the lowest area *P. americana* has 58% (Fig. 4.63). In Kilimanjaro area, *A. gummifera* has 32% of the transect area suitable for distribution while *P. americana* has only 15% of potentially suitable area (Fig. 4.63).

Under the RCP 4.5, 2055 Climate Projection comparison of the suitable areas for the three species between Kilimanjaro and Taita Hills were significantly different (F=303.76, p=0.00); while no significant difference was observed among the three species on suitable areas in each sites.

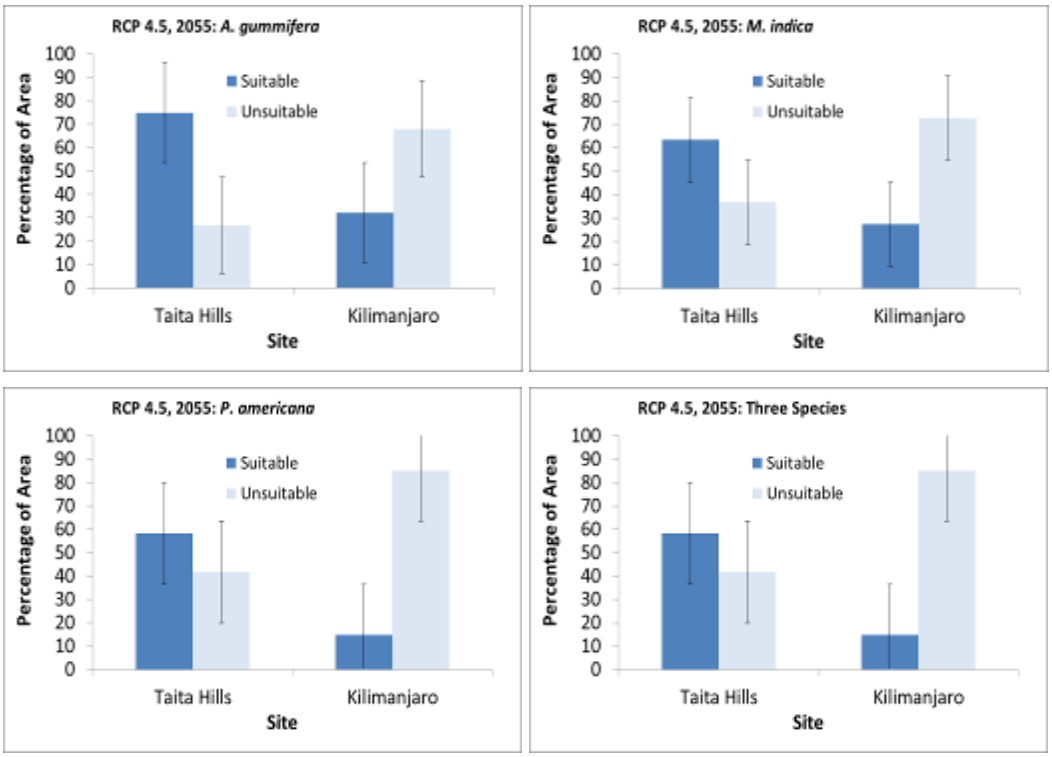

Figure 4.63 - Percentage area coverage of suitable areas and unsuitable areas for *A. gummifera*, *M. indica* and *P. americana* in Taita Hills and Mount Kilimanjaro under RCP 4.5, 2055 climate condition.

iii. Species suitable areas under RCP 8.5 (2055) climate condition

The RCP 8.5, 2055 Climate Projection estimated a large area of 80% in Taita Hills to be potentially suitable for *A. gummifera*, *M. indica* (74%) and *P. americana* (65%) (Fig. 4.64). For Kilimanjaro transect, an estimated 37% of the transect area was potentially assigned to be suitable for *A. gummifera*, 33% for *M. indica* and 14% for *P. Americana* (Fig. 4.64). The projection of climate change based on the RCP 8.5, 2055 shows that suitable areas in Kilimanjaro and Taita Hills significantly differed in area size (F=216.96, p=0.00). While no significant difference was observed among the three species on suitable areas in each sites.

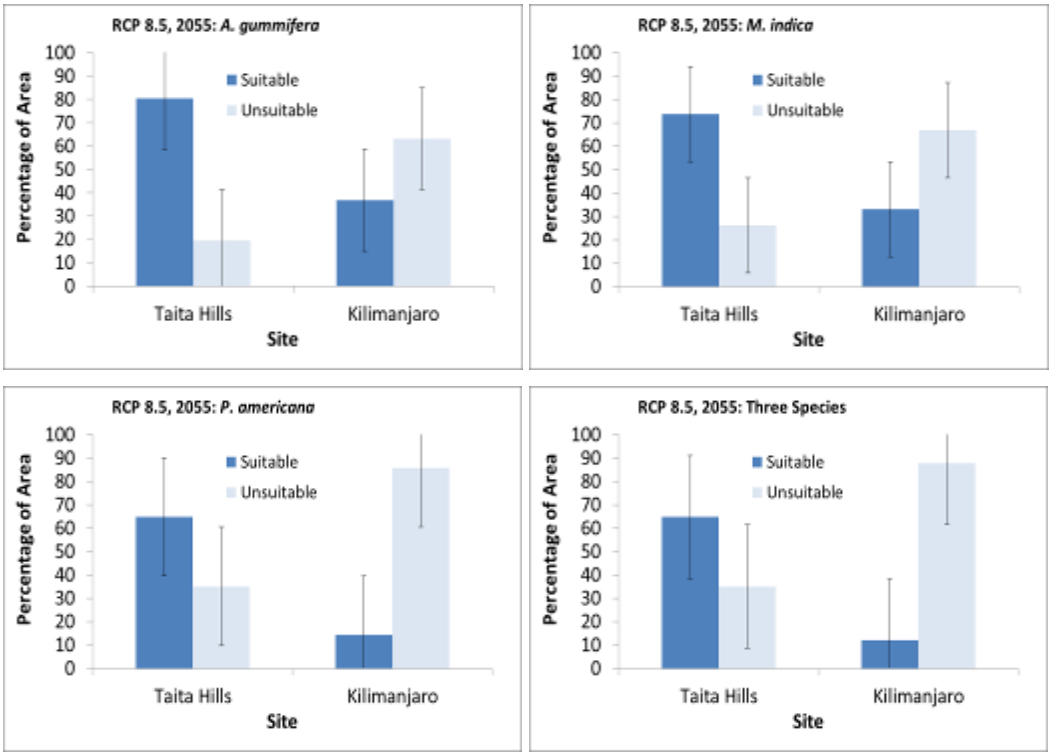

Figure 4.64 - Percentage area coverage of suitable areas and unsuitable areas for *A. gummifera*, *M. indica* and *P. americana* in Taita Hills and Mount Kilimanjaro under RCP 8.5, 2055 climate condition

iv. Species suitable areas under RCP 4.5 (2085) climate condition

An estimated 80% of the transect area in Taita Hills is predicted by the RCP 4.5, 2085 Climate Projection as potentially suitable for *A. gummifera*, *M. indica* (72%) and *P. americana* (63%) (Fig. 4.66). While in Kilimanjaro, the largest potential area of 41% is predicted to be suitable for the distribution of *A. gummifera* followed by *M. indica* (26%) and *P. americana* (18%) (Fig. 4.66). Suitable areas for *A. gummifera*, *M. indica* and *P. americana* in Kilimanjaro and Taita Hills significantly differed in area (F=393.02, p=0.00) based on the projection of climate change based on the RCP 4.5, 2085. Also, significant difference (F=28.12, p=0.03) was observed among the three species on suitable areas in each sites.

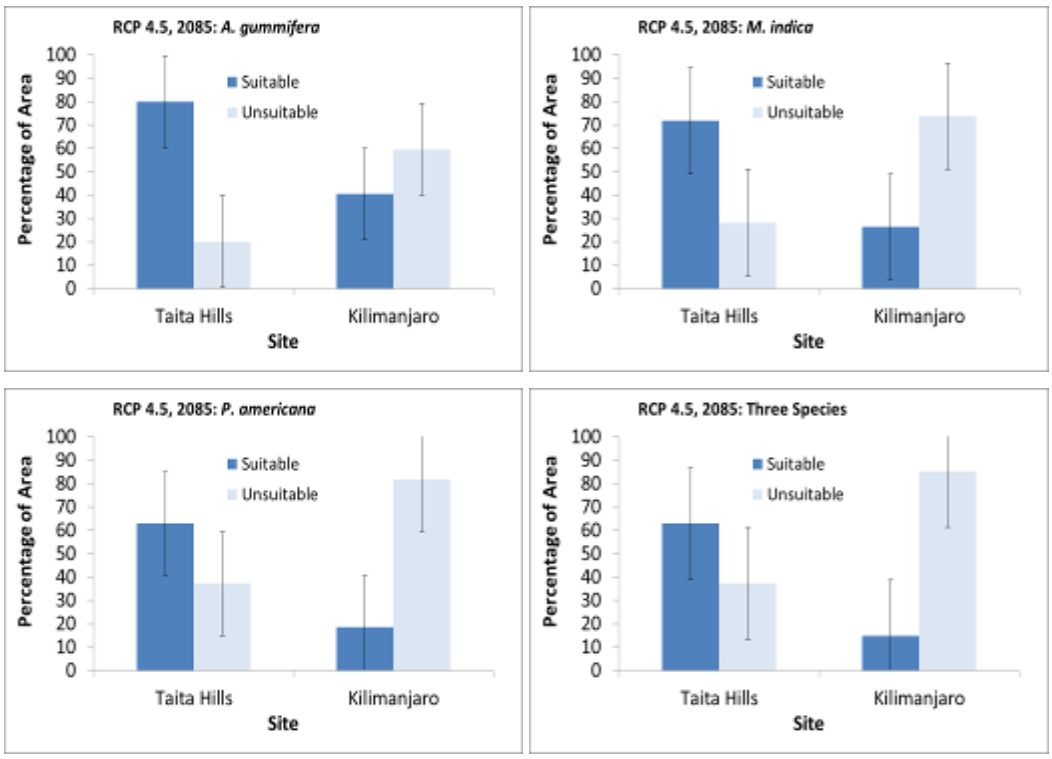

Figure 4.65 - Percentage area coverage of suitable areas and unsuitable areas for *A. gummifera*, *M. indica* and *P. americana* in Taita Hills and Mount Kilimanjaro under RCP 4.5, 2085 climate condition

v. Species suitable areas under RCP 8.5 (2085) climate condition

RCP 8.5, 2085 Climate Projection predicts 88% of the transect area in Taita Hills as potentially suitable for the distribution of *A. gummifera*, *M. indica* (80%) and *P. americana* (65%) (Fig. 4.66). In Kilimanjaro on the other hand, 37% of the transect area is predicted to be potentially suitable for *A. gummifera*. The predicted area for potential distribution of *M. indica,* apparently is the highest in the transect (59%) with *P. americana* having the lowest area of 32% (Fig. 4.66). Based on RCP 8.5, 2085, potentially suitable areas for *A. gummifera*, *M. indica* and *P. americana* in Kilimanjaro and Taita Hills do not differ significantly in size and no significant difference was observed among the species in each site either.

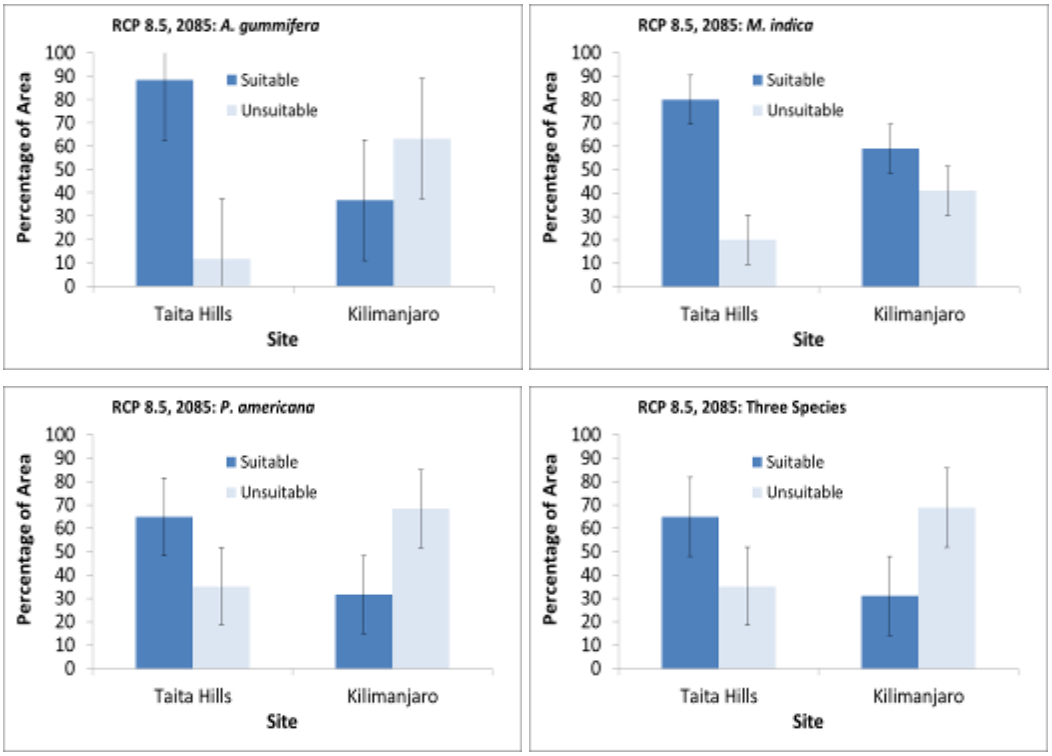

Figure 4.66 - Percentage area coverage of suitable areas and unsuitable areas for *A. gummifera*, *M. indica* and *P. americana* in Taita Hills and Mount Kilimanjaro under RCP 8.5, 2085 climate condition.

vi. Comparison of suitable areas

The Chi^2 test for comparison performed between the predicted potential suitable and unsuitable areas for *A. gummifera* in Taita Hills based on the baseline, RCP 4.5 (2085) shows significant difference (Chi^2=4.19, p=0.04). Predictions with the baseline and RCP 8.5 (2085) on the potential suitable and unsuitable areas in Taita Hills were significantly different for *A. gummifera* (Chi^2=4.19, p=0.04) and *M. indica* (Chi^2=4.34, p=0.04). Areas predicted to be potentially suitable and unsuitable for *M. indica* in Kilimanjaro by the baseline climate and RCP 8.5 (2055) are significantly different in size (Chi^2= 10.607, p=0.00). Predicted suitable and unsuitable areas for the distribution of *P. americana* in Kilimanjaro were significantly different between the baseline climate variables of the RCP 4.5 (2055) (Chi^2=5.01, p=0.04**)**, and RCP 8.5 (2055) (Chi^2= 5.91,). Comparisons of the suitable and unsuitable areas for *A. gummifera*, *M. indica* and *P. americana* in Kilimanjaro were significantly different based on the predictions by the baseline climate variables (F=22.77, p=0.04), and by RCP 4.5 (2055) (F=25.22, p=0.04). While in Taita Hills, comparisons of the suitable and unsuitable areas for *A. gummifera*, *M. indica* and *P. americana* by the predictions based on the baseline climate variables were significantly different (F=47.25, p=0.02) by RCP 8.5, 2055; (F=27.84, p=0.03) by RCP 8.5, 2085 (F=27.84, p=0.3).

4.5.7. Climate change and Species elevation shift

i. Species elevation shift Under Baseline Climate Condition

Prediction of species suitable elevation ranges in Kilimanjaro transect indicates that *Albizia gummifera* has lowest minimum elevation range of 982m while in Taita Hills transect, its lowest suitable elevation range is 923m asl (Table 4.21). The minimum suitable elevation range for *M. indica* in Kilimanjaro is predicted at 1067m while in Taita Hills it is 777m. *P. americana* has a minimum suitable elevation range of 1196m in Kilimanjaro, while in Taita Hills, it has the minimum suitable elevation range of 824m (Table 4.21). Among the three species, *A. gummifera* has the lowest minimum suitable elevation range in Kilimanjaro whereas; *M. indica* has the lowest minimum suitable elevation range in Taita Hills. While, the three species have lowest minimum elevation range in Taita Hills than in Kilimanjaro which species has relatively high minimum elevation. Thus, the species has more suitable areas than in Kilimanjaro.

ii. Species elevation shift Under RCP 4.5 Climate Change Projection

Period 2055 (mean over 2041-2070): Projection of climate change, based on RCP 4.5, for the period of 2041-2070 (2055) shows that suitable elevation for *A. gummifera* would shift upwards by 185m from 982m to lowest minimum elevation range of 1167m in Kilimanjaro (Table 4.21). While in Taita Hills, suitable elevation range for *A. gummifera* will not be affected by the projected climate change under RCP 4.5 in the year 2055. On the other hand, suitable minimum elevation range for *M. indica* is predicted to shift downwards by 275m from 1067m to 792m in Kilimanjaro (Table 4.21). However, the species will not record a shift in its current minimum elevation under the RCP 4.5 projected climate change in 2055 in Mount Kilimanjaro. *P. americana* suitable minimum elevation range is predicted to shift downwards by 104m from 1196m to 1092m in Kilimanjaro (Table 4.21), while in Taita Hills, the minimum suitable elevation range will shift downward by 47m from 824m to 777m asl (Table 4.21). Under this projection of climate change, common distribution area of the species will decrease adversely in Kilimanjaro than in Taita Hills (Fig. 4.66). The area for *M. indica* and *P. americana* will reduce under the project RCP 4.5 for period 2055 (Fig. 4.68).

Period 2085 (mean over 2071-2100): The projected climate change under RCP 4.5 for the period 2071-2100 will cause a slight upward shift of suitable minimum elevation range in Taita Hills for *A. gummifera* by 27m, from the elevation of 982 to 1009m. While, a downward shift of the minimum

suitable lower elevation for the species is observed from 923m to 777m asl in Taita Hills (Table 4.21). Under this RCP, *A. gummifera* will increase its elevation ranges in Taita Hills more in Kilimanjaro. The prediction of *M. indica* distribution under RCP4.5 for the period 2071-2100 shows that the species elevation range in Kilimanjaro will be fragmented into isolated elevation mosaicks. The lowest suitable elevation range will occur between 811-1002m asl and the upper range for the species will have suitable minimum elevation of 1316m. However in Taita Hills, suitable minimum elevation for *M. indica* will remain relatively stable during the period under observation (Table 4.21). Suitable minimum elevation range for *P. americana* predicted under RCP4.5 for the period 2085 indicate that the species will shift upwards in both Taita Hills and Mount Kilimanjaro. However, large shift in minimum elevation will be observed in Mount Kilimanjaro. The species will shift upward in Kilimanajro from the current suitable minimum elevation of 1196m to 1429m, while in Taita Hills, upward shift will be observed from the current elevation of 824m to 940m (Table 4.21). The common suitable areas for the three species under this projection of climate change, will decrease adversely in Kilimanjaro than in Taita Hills (Fig. 4.68). The area for *M. indica* will reduce and fragmented but *P. americana* will only reduce in Kilimanjaro under the project RCP 4.5 for period 2085 (Fig. 4.66). In Taita Hills, *A. gummifera* will increase in area (Fig. 4.68).

iii. Species elevation shift Under RCP 8.5 Climate Change Projection

Period 2055 (mean over 2041-2070): Climate change projection under RCP 8.5 will cause suitable elevation range for *A. gummifera* to shift upwards in the year 2055, by 65m from 982m to 1047m asl in Mount Kilimanjaro (Table 4.21). Taita Hills, on the other hand, will have suitable elevation range for *A. gummifera* shifting slightly downward by 17m from 923m to 902m asl. Due to this, Taita Hills will have more suitable elevation range for *A. gummifera* in the year 2055 than in Kilimanjaro.

The projection will cause *M. indica* to shift downwards by 264m from 1067m to 803m asl in Kilimanjaro in 2055, while no shift will be observed in Taita Hills (Table 4.21). Thus, in the year 2055 *M. indica* will gain more suitable elevation range in Kilimanjaro but Taita Hills will still have more elevation range suitable for the species under RCP 8.5.

Minimum suitable elevation range for *P. americana* will reduce in both Taita Hills and Mount Kilimanjaro in 2055 under RCP 8.5 climate change projection. *P. americana* will shift upwards by 263m in Kilimanjaro from 1196m to 1459m, while the species will shift upwards by 116m in Taita Hills (Table 4.21). A markeable decrease in minimum suitable elevation range for *P. americana* will be observed in Kilimanjaro compared to Taita Hills. Thus, the common suitable areas for the three

species under this projection of climate change, will reeduce adversely in Kilimanjaro than in Taita Hills (Fig. 4.66). The area for *M. indica P. americana* will reduce and fragmented in Kilimanjaro under the project RCP 8.5 for period 2055 (Fig. 4.68).

Period 2085 (mean over 2071-2100): Prediction of the future distribution of *A. gummifera* by RCP 8.5 for the year 2085 indicate that the suitable minimum elevation range will shift upwards by 84m from 982m to 1066m in Kilimanjaro, while in Taita Hills, the species will shift upwards by 146m thus increasing the elevation range for the species (Table 4.21). Due to the anticipated climate change, *A. gummifera* in Taita Hills will gain more elevation range than in Kilimanjaro.
Suitable minimum elevation for *M. indica* in Taita Hills will not be affected by the projected climate change under RCP 8.5 for the period 2071-2100. However, In Kilimanjaro, the suitable minimum elevation for the species will shift downwards by 310m from its present minimum suitable elevation range of 1067m to 757m asl (Table 4.21). This projection will increase the elevation range for *M. indica* in Kilimanjaro.
While the elevation ranges for *P. americana* in Kilimanjaro will increase a decrease in elevation ranges will be observed in Taita Hills under climate change projection RCP 8.5. The minimum suitable elevation range for the species would shift slightly downward from the current minimum suitable elevation of 1196m to 1146m in Kilimanjaro and in Taita Hills it will shift upwards from 824m to 924m asl (Table 4.21).
Common suitable areas for the three selected species under this projection of climate change will be comparable with the area under baseline condition in Kilimanjaro, and in Taita Hills (Fig. 4.68). The area for *M. indica* will increase in Kilimanjaro and Taita Hills under the project RCP 8.5 for period 2085 (Fig. 4.68). While, *A. gummifera* will increase in area in Taita Hills (Fig. 4.68).

Table 4. 25: Minimum suitable elevation ranges for *A. gummifera M. indica P. Americana* in Mount Kilinanjaro and Taita Hills under projected climate change by RCPs 4.5 and 8.5 for the period 2055 and 2085.

	Minimum Elevation Range (m)					
	A. gummifera		***M. indica***		***P. americana***	
Climate Projection	***Kilimanjaro***	***Taita Hills***	***Kilimanjaro***	***Taita Hills***	***Kilimanjaro***	***Taita Hills***
Current climate	982	923	1067	777	1196	824
RCP 4.5, 2055	1167 (185)	923 (0)	792 (-275)	777 (0)	1092 (-104)	777 (-47)
RCP 8.5, 2055	1047 (65)	906 (-17)	803 (-264)	777 (0)	1459 (263)	940 (116)
RCP 4.5, 2085	1009 (27)	910 (-13)	811-1002, 1316	777 (0)	1429 (233)	940 (116)
RCP 8.5, 2085	1066 (84)	777 (-146)	757 (-310)	777 (0)	1146 (-50)	924 (100)

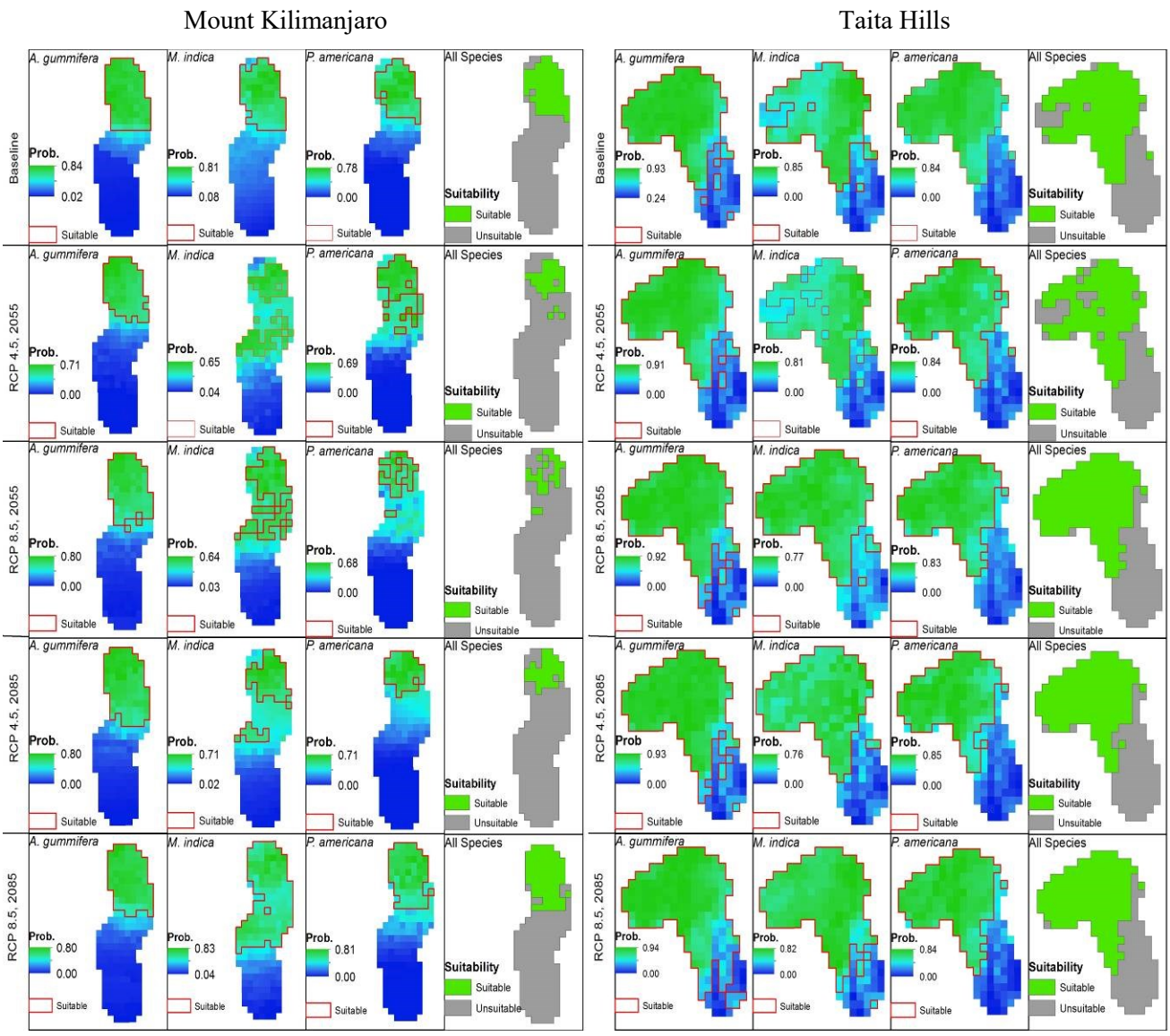

Figure 4.67 - Distribution of suitable areas of *A. gummifera*, *M. indica* and *P. americana* in of Taita Hills and Mount Kilimanjaro. Suitable areas are delineated by red boundary in the model map.

4.5.8. Key findings for objective 5

Potential upshift of Albizia gummifera (Albizia) will occur in Kilimanjaro with highest upshift of 185m to be observed under RCP 4.5, 2055. Downshift of Albizia will occur in Taita Hills with the highest downshift of 146m observed under RCP 8.5, 2085. Potential downshift of Mangifera indica (Mango) will occur in Kilimanjaro under all RCP but the highest downshift of 310m will be observed under RCP 8.5, 2085. Both upshift and downshift will be observed on Persea americana (Avocado) in the two sites. In Kilimanjaro, the highest downshift of 104m will occur under RCP 4.5, 2055. Downshift of Avocado will only occur under RCP 4.5, 2055; while,

upshift will occur under RCP 8.5, 2055 and RCP 4.5, 2085 in Kilimanjaro and Taita Hills. The highest upshift in Kilimanjaro will be 263m and Taita Hills will be 116m for Avocado.
Taita Hills has significantly higher suitable areas for Albizia, Mango and Avocado than in Kilimanjaro ($F=153.17$, $p=0.01$). Large decrease in area for Avocado is observed in Kilimanjaro under all RCPs except for RCP 8.5, 2085. Fragmentation of suitable is observed under RCP4.5 (2055) and RCP8.5 (2055). High increase in suitable area for Mango is observed with Mango in Kilimanjaro under RCP 8.5, 2085. Fragmentations of suitable are observed under RCP4.5 (2055 & 2085) and RCP8.5 (2055). Suitable area for Albizia and Mango will relatively increase in Taita Hills under RCP 8.5, 2085.

CHAPTER 5: DISCUSSION OF THE RESULTS

Taita Hills and Mount Kilimanjaro constitute part of the Eastern Afromontane that form biodiversity hotspots in the region. However, Taita Hills are part of a series of thirteen bloc mountains within the Eastern Arc Mountains. The two montane areas have a clear biogeographical difference which indicate that Mount Kilimanjaro is a more recent volcanic mountain while Taita Hills are ancient crystalline mountains (Lovett and Wasser, 2008). The lower elevation levels for the montane areas within the mountains range between 700 – 800m above sea level (Cronin et al., 2014) which starts to define biodiversity hotspots for the montane areas. Below this elevation range, dryland biodiversity is characteristically prominent around the mountain areas which makes thearea an island of unique biodiversity.

The distribution of micro-climate, vegetation and edaphic variables can be continuous in long elevation gradients while in short elevation gradients, the distributions are discontinuous (Alves et al., 2010; Ashton, 2003; Takyu et al., 2003; Daws et al., 2002). Climate conditions changes with the increase of elevation in the montane areas; for instance precipitation increases with the increase in elevation while temperatures decrease with the increase in elevation in montane areas. In the Eastern Arc, as in other tropical mountains, environmental gradients such as precipitation, temperature, and length of dry season vary with elevation (Rickart, 2001; McCain, 2005). MAP and MAT significantly varies with the elevation gradients in Taita Hills and Mount Kilimanjaro. The varying climatic conditions along the elevation gradients influence the zonation of biomes, carbon storage, soil and biophysical variables along the elevation gradients. In montane areas, vegetation zonation can be compressed within short elevation gradients influencing the appearance of cloud montane forests in lower elevations (Grubb, 1977; Alves et al., 2010).

Worth noting is the attraction that montane areas has on human settlement and agricultural activities as observed in Taita Hills and Mount Kilimanjaro due to their favourable climatic conditions and soil fertility. In addition, the areas act as water towers by continuously condensing moisture laden air that supply water to the surrounding streams in the lowland. Elevation gradients affect distribution of soil pH, Cation Exchange Capacity (CEC), Bulk Density (BD) and Soil Organic Carbon (SOC) among others. The interaction of elevation and climatic condition is very crucial in their influence on the distribution vegetation cover and in

determining the distribution of the edaphic variables along the elevation. Vegetation cover, which consists of the plant species diversity and density, increases with increase in elevation in montane areas but decreases in higher unfavaourable altitudes (Xian, 2014). Thus, levels of soil organic matter in montane areas increases with the elevation of gradients (Xian, 2014). Soil organic matter increases the soil Cation Exchange Capacity; however, areas with clay soil would have higher CEC than areas with loam or silts. During the production and decomposition processes of plant litter (organic matters), soil pH (Xian, 2014) increases and more SOC (Hontoria et al., 1999) is released into the soil. The remaining organic matter forms soil organic content that contributes to the soil bulk density (BD) in the montane areas. Thus, soil pH, BD and SOC distributions are influenced by elevation gradients in montane areas; pH and BD decreases with increase in elevation, while SOC increases with the increase in elevation (Jenny, 1941; Kononova, 1966; Burke et al., 1989; Hontoria et al., 1999). The distribution of the edaphic variables can be continuous in long elevation gradients while discontinuous in short elevation gradients (Alves et al., 2010; Ashton, 2003; Takyu et al., 2003; Daws et al., 2002).This implies that soils in the higher elevations have more SOC, low pH and BD and as the elevation decreases low SOC, high pH and BD occur. This pattern is clear in Kilimanjaro where 95% of soil pH, 96% of SOC and 84% of BD significantly relate to the change in elevation. In Taita Hills, only the distribution of pH relates significantly to change in elevation but not as strongly as observed in Kilimanjaro. Edaphic discontinuity due to steep topography and microclimate variation can be observed in short gradients compare to long elevation gradient distance.

The montane areas attract more human population density due to their favourable climate for crop growing and health among other factors (Jäger et al., 2014). Observation of human population density in Kilimanjaro, along side edaphic variables, shows an estimated 65% of human population associated with the increase in elevation; hence favourable climatic condition areas. Higher elevations are more attractive to agricultural crop production however the distribution of types of croplands would depend on climate and terrain. Agro-forestry is predominant in areas receiving high mean levels of precipitation and low mean temperatures. Most farms with agro-forestry in both Kilimanjaro and Taita Hills are distributed in the mid to upper elevation areas where climate is conducive for growth of crops while cropped lands occur mostly in the lowland areas. However, some cropped lands in Taita Hills occur in the upland where they experience equally conducive climate conditions.

Studies on the relationship of precipitation and vegetation index have always indicated very strong relationships (Nightingale and Phinn, 2003). Normally, high vegetation index occur in areas with high precipitation (Nightingale and Phinn, 2003) and this validates the Enhanced Vegetation Index observed in agro-forestry areas in Taita Hills and Mount Kilimanjaro in this study. EVI in cropped lands differ significantly between the two sites. This difference could be explained by the relatively high MAP and low MAT experienced by the areas. High EVI in an area basically implies the area has more vegetation cover, which indicates the the area receives a lot of plant litter that is converted into organic matter (Xian, 2014). Thus, as the relationship between organic matter and pH, CEC, BD and SOC is explained previously by (Xian, 2014; Hontoria et al., 1999), reason why agro-forestry areas has relatively high SOC, low pH, high CEC and low BD is probably explained. The distribution of soil pH, BD, CEC and SOC probably depend on the distribution of the soil organic matter in the types of cropland.

Elevation is a strong determinant of the distribution of tree species in montane areas (Hemp, 2006; Vazques and Givnish, 1998; Gentry, 1995; Woldu et al., 1989, Hamilton et al., 1989). There is significantly strong evidence in Taita Hills on the relationship of the woody plant species richness with the variation of elevation though this is not strong in Kilimanjaro. In Kilimanjaro banana plants and coffee plantations are dorminant in the higher elevation which could probably reduce richness of woody plant species. Few woody plants such as *Persea americana*, *Mangifera indica* and *Albizia gummifera* are notably abundant in the upper elevation in Mount Kilimanjaro.

The characteristic biological pattern of species richness in tropical mountains is a decrease in species richness with elevation, with a mid elevation hump (Rahbek, 1995, 1997; Heaney, 2001). Thus, polynomial relationship basically provides relationship between woody plant species richness and elevation in both Kilimanjaro and Taita Hills. This relationship has been accounted for by Vazguez and Givnish (1998) in Sierra de Manantlan where they found that the numbers of species, genera and families per sample declined linearly with elevation. Thus, where elevation correlates strongly with edaphic variables like in Kilimanjaro, variation of these variables strongly associate with the woody plant species richness. Contrary to this, edaphic variables correlate weakly with the change in elevation in Taita Hills. The relationship of the woody plant species with topography and edaphic variables in Mount Kilimanjaro is further validated by

findings of Zhang et al., (2016) which confirms the relationship of the physical and edaphic variables with the distribution of the woody plant species. The physical variables (elevation and slope) are identified by many studies to be the strongest predictors of woody plant species (Zhang et al., 2016) and Above-ground Carbon Storage (Marshall et al., 2012). This is well observed in the multiple predictor variables where multiple model of elevation and slope is validated statistically and spatially as combined variables with strong and high certainty influence on the distribution of the woody plant species in Taita Hills. These variables however, do not play similar influence in Kilimanjaro. Multiple model of Cation Exchange Capacity and soil pH is validated statistically and spatially as combined variables with strong and high certainty influence on woody plant species distribution.

The distribution of the woody plant species along the elevation is probably affected by the distribution of types of croplands along the elevation, due to the nature of crop management system. Unlike in Kilimanjaro, some cropped lands in Taita Hills are found in the higher elevation of inhabited areas, which potentially interrupts the distribution of woody species and continual distribution of edaphic variables. This probably explains the reason why no strong relationship is observed between the woody plant species richness and environmental variables in Taita. There are more plant species in areas with agro-forestry than cropped land due to cultivation of diversity of crops and integration of existing trees, active planting and tending or tolerance of natural regeration in fallow areas (Sodhi and Ehrlich, 2010; Schroth et al. 2004). Contrary to the above, species richness of woody plants between agro-forestry and cropped lands within Taita Hills and Mount Kilimanjaro compare relatively well/poorly. However, patterns of similarity in woody plant species composition shows cropped lands in Kilimanjaro has relatively high species; share 26% of the sites woody plant species with agro-forestry and has 38% of the species unique to the cropped land. In Taita Hills, agro-forestry has relatively high woody plant species richness; shares 48% of species with cropped lands and 32% of the sites woody plant species are unique to agro-forestry areas. Among the woody plant species recorded in Taita Hills and Mount Kilimanjaro, 32% are shared between the sites; 30% are unique to Mount Kilimanjaro while 39% are unique to Taita Hills.

Even though Taita Hills has relatively high woody plant species richness than Kilimanjaro, the latter has relatively higher above-ground carbon storage (AGCS). The mean AGCS in Taita Hills and Mount Kilimanjaro are estimated at 39.06 and 27.21 Ct/ha, respectively. These are higher

than the amount of carbon indicated for different types of agro-forestry in Unruh et al., (1993), and far much more than the amount recorded from Mwanga, Kilimanjaro area (Charles et al., 2014). The amounts of the AGCS recorded in the two sites are relatively more than the median carbon storage in sub-humid and semi-arid ecoregions (Schroeder, 1994). The relative contribution of abundant woody plant species to the AGCS is in line with the relative abundance as observed by Kirby and Potvin (2007) in Eastern Panama. For instance, in Taita Hills, *Grevillea robusta* is dominant on the slopes (D=0.036) and contributes high AGCS (4.6 Ct/ha) among other species. Unlike in Mount Kilimanjaro, *G. robusta* has the highest relative abundance of 18.2% and *Persea americana* is dominant (D=0.019) in Kilimanjaro but *Albizia gummifera* has more AGCS (8.6 Ct/ha) followed by *P. americana* (3.5 Ct/ha).

Positive relationship (59%) was reported between AGCS and morphospecies from sites in all land-use types in Ipetı´-Embera´ in eastern Panama Province, Panama (Kirby and Potvin, 2007). While in Taita Hills, 66% of AGCS is explained significantly by the distribution of the woody plant species richness along the elevation gradients, the relationship is weak in Kilimanjaro. Influence of physical variables (elevation and slope) on woody plant species richness differ in relation with AGCS. Elevation strongly and significantly affects distribution of AGCS by 72% in Kilimanjaro while in Taita Hills it seems to affect AGCS variation by 73%. The influence of slope angle and elevation has been observed to be strong, explaining 63.7% of the variation in AGCh in Udzungwa and Usambara area (Marshall et al., 2012). Apparently, edaphic variables (pH, BD and SOC) seem to correlate significantly with AGCS in Kilimanjaro while the relationship is non-existent or weak, with some variables in Taita Hills. However, population density seems to associate with about 42% of AGCS distribution in Taita Hills. Evaluation of univariate and multivariate models statistically and spatially show that soil pH is the strongest and significant predictor for AGCS by 80% in Kilimanjaro. While in Taita Hills, three variables (elevation, slope and population density) simultaneously affect the distribution of AGCS in the area.

Previously, above, the relationship of climate variables such precipitation and temperature with vegetation and elevation have been reviewed. Vegetation associates closely with the variation of climatic variables, especially precipitation and temperature and a strong association occurs between temporal and spatial patterns of NDVI with annual rainfall (Davenport and Nicholson

2007). Like other remotely sensed vegetation indices, NDVI is correlated with the Leaf Area Index (Purevdorj et al., 2010; Carlson and Ripley, 1997).

Leaf Area Index (LAI) relates with elevation and slope (Bolstad et al., 2001). A similar relationship is reported between LAI and elevation in Kilimanjaro. The relationship between the distribution of LAI along the elevation gradients of Taita is however, very poor. LAI significantly increases with increase in elevation in cropland but not in agro-forestry probably due to low variation in climatic condition and similar crop management in the latter.. Similar patterns of LAI distribution is observed with precipitation, while LAI values decrease with the increase of temperature.

Study in Amazon ecosystem reported that LAI varies with high biodiversity, topography, land use and edaphic heterogeneity (Araga˜o et al., 2005). The distribution of LAI in Kilimanjaro can be explained strongly by edaphic variables, pH, SOC, BD, while no significant relationship is observed in Taita Hills. Apparently, human population affects the distribution of LAI through land use types that cause deforestation through fire, subsistence agricultures and the keeping of land for pasture (Araga˜o et al., 2005; Nepstad et al., 2001; Alves, 2002). Under these circumstances, LAI is expected to be less, while in the more populated section of Mount Kilimanjaro LAI relates positively and significantly with population density.

Climate change is envisaged to be detrimental to montane and island biodiversity due to the restriction in range of expansion in these areas. Due to this, studies on the effect of climate change in the tropical areas focus more on the montane species, looking at their elevation shifts or disappearances (Pounds et al. 1999). Agriculture in tropical areas is mostly vulnerable to climate change, particularly subsistence agriculture. This is attributed to lack of sufficient resources for farmers to adapt to climate change. Agro-forestry as a technology can be used to sustain farming and reduce vulnerability to climate change (Verchot et al., 2006). Three agro-forestry tree species are common in Taita Hills and Mount Kilimanjaro, providing alternative food through their fruits and income to local farmers, while contributing to long-term local carbon storage in the areas. These species include *Persea americana* and *Mangifera indica* providing fruits for food and generating income, while, *Albizia gummifera* are mainly used in Kilimanjaro for shading coffee trees and providing habitat for the montane birds. Since agro-forestry also relies on climatic conditions, it will be affected equally as agriculture and natural ecosystem around the world (Luedeling et al., 2013). For instance it will be exposed to changes

in temperatures and precipitation that will perhaps affect system components. Thus, the potential benefits of carbon storage and sequestration provided by agro-forestry and support of livehood in Taita Hills and Mount Kilimanjaro will potentially be affected adversely.

Projection of climate change under Representative Concentration Pathways (RCP 4.5 and 8.5) indicate that temperature and rainfall are projected to increase in East Africa in mid and late centuries; thus the region will be hotter and wetter (Platts et al., 2014). Within this region, climate change will be highly heterogeneous in magnitude and direction of change at local scale (BirdLife International, 2012). For instance the minimum suitable elevation range for agro-forestry species will vary relatively among the three species within site; between RCPs and periods; within species between sites and between RCPs and period. These projections also point out that endemic plants in montane areas will be highly variable. Variation will occur between taxa where some ranges will expand, others will reduse while some will hardly change. Variation across the sites will also occur (BirdLife International, 2012).

Albizia gummifera in Kilimanjaro will relatively lose the minimum suitable elevation range but will be affected mostly by RCP 4.5 in the mid century by the variation of maximum temperature in August and the precipitation in June. However, in Taita Hills the species will gain more suitable areas down the slope under RCP 8.5 in the late century. The distribution of suitable areas for *Mangifera indica* will be fragmented in Kilimanjaro but its minimum suitable elevation remain stable in Taita Hills under RCP4.5 in the late century influenced mostly by variation of the mean diurnal range in temperature and the November precipitation. *Persea americana* will be affected adversely in Kilimanjaro by RCP8.5 in mid century by restricting its minimum suitable elevation range upwards. The variation of the August precipitation and the October minimum temperature will be the main factor contributing to the impact. In the late century, climate change projection under RCP4.5 will restrict the minimum suitable elevation range of *P. americana* upwards the slope of mount Kilimanjaro. This shift will be propelled by variation of the October precipitation and minimum temperature in Kilimanjaro. Similar pattern observed on *P. americana* in Kilimanjaro will be observed in Taita Hills but the range of restriction will be remarkeably less than in Kilimanjaro. This comparative analysis of potential varied responses of the three agro-forestry species in Taita Hills and Mount Kilimanjaro indicates the probable differences in the magnitude and direction of projected climate change between the sites. Apparently, agro-forestry tree species will be affected adversely in Kilimanjaro than Taita Hills.

This implies that projected climate change in Taita Hills will be relatively similar to the future conditions in the Eastern Arc, in the West Usambara where there will be stable water balance with more rain in drier months (Platts, Personal Communication).

CHAPTER 6: CONCLUSION, RECOMMENDATIONS AND AREAS FOR FURTHER RESEARCH

6.1 Conclusions

The distributions of environmental variables on inhabited montane areas differ on how they correspond to variation in elevation. Their distributions in types of croplands within a site only differ in variation but not in their means.

The distribution of the woody species, above-ground carbon and leaf area index on inhabited montane areas are affected by different environmental variables. While, their distributions in types of croplands in montane areas differ in variation of richness but less in their means.

Elevation is a strong determinant of the distribution of tree species in montane areas. Elevation and slope variables are simultaneously influencing the distribution of the woody plant species in Taita Hills, while in Kilimanjaro Cation Exchange Capacity and soil pH simultaneously influence the distribution of these species. Cropped land has more woody plant species richness in Kilimanjaro than agro-forestry. The diversity of woody plant species is however different between agro-forestry and cropped land; between sites; and between croplands within sites. However, in Taita Hills more woody plant species are in agro-forestry than cropped land.

The distribution of the Above-ground Carbon Storage is strongly influenced by elevation in Kilimanjaro but this relationship is weak in Taita Hills. This is attributed to difference in crops grown in the site.Coffee growing is Kilimanjaro area dominant than in Taita Hills. There are large trees reserved in coffee plantation in Kilimanjaro used for shading. Due to absence of coffee in most farms in Taita Hills, similar large trees are absent. Thus, carbon storage significantly increases with elevation in Kilimanjaro but not Taita Hills. Apparently, edaphic variables (pH, BD and SOC) seem to correlate significantly with AGCS in Kilimanjaro but relate weakly or not at all with some variables in Taita Hills. However, population density seems to associate with about 42% of AGCS distribution in Taita Hills. Soil pH is the strongest and significant predictor of AGCS in Kilimanjaro. In Taita Hills, on the other hand, three variables (elevation, slope and population density) simultaneously affect the distribution of AGCS in Taita Hills.

Leaf Area Index (LAI) relates with the variation of elevation and slope a similar relationship which exists between LAI and elevation in Kilimanjaro. The distribution of LAI along the

elevation gradients of Taita is however, very poor. LAI significantly increases with increase in elevation in cropland but not in agro-forestry probably due to low variation in climatic condition and similar crop management in the latter that propagates LAI distribution. Similar patterns of LAI distribution is observed with precipitation, while LAI values decrease with the increase in temperature. The distribution of LAI in Kilimanjaro can be explained strongly by edaphic variables, pH, SOC, BD, while no significant relationship is observed in Taita Hills. This difference is attributed to the way soil is managed in cropland in the two sites which determine the levels of soil variables.

Climate change is envisaged to be detrimental to montane biodiversity due to the restriction in the range of expansion in these areas. Projection of climate change under Representative Concentration Pathways (RCP 4.5 and 8.5) indicate that temperature and rainfall are projected to increase in East Africa in mid and late century, thus the region will be hotter and wetter. Climate change will affect agro-forestry. For instance, *Albizia gummifera* distribution will shift upwards in Kilimanjaro under RCP 4.5 in the mid century. The species will however gain more areas down the slope under RCP 8.5 in the late century. Suitable areas for *Mangifera indica* will be fragmented in Kilimanjaro under RCP4.5 in the late century while its distribution will be stable in Taita Hills. The range of distribution of *Persea americana* will shift upwards in both Kilimanjaro and Taita Hills by mid century under RCP8.5, while under RCP4.5 the upward shift will occur in the late century. However in Taita Hills, the extent of the shift will be considerably less than in Kilimanjaro.

5.2. Recommendations

- Elevation is a strong predictor of woody plant species richness in Taita Hills but not significant on the distribution of the above-ground carbon storage. In order to improve on AGCS in Taita Hills, sustainable cropland management system should be adopted in order to maintain and protect the current plant diversity on farms. This will ensure more carbon sequestration in Taita Hills in future.

- The envisaged climate change will potentially affect agro-forestry tree population, among others, in Taita Hills and Mount Kilimanjaro. In order to arrest this potential situation, mid and long term planning for agro-forestry development should be initiated on inhabited slopes

of both Taita Hills and Mount Kilimanjaro in order to improve on carbon storage. This effort should focus on enhancing *Persea americana* and *Albizia gummifera*, while Long-term planning should focus on enhancing the population of *Mangifera indica* in Kilimanjaro. Besides, this effort will boost the economic status of the local people who depend on agro-forestry fruit trees in Taita Hills and Mount Kilimanjaro for their livelihoods.

5.3. Areas for further studies

Based on the observations from this study, three potential studies are recommended:

- Assessment of effects of socio-economic value of woody plant species on the above-ground carbon storage in Taita Hills and Mount Kilimanjaro
- Distribution of soil factors in relation to the crop management practices in Taita Hills
- Implications of projected climate change on the income from agro-forestry fruit trees (P. americana and M. indica) in Taita Hills and Mount Kilimanjaro
- Modelling pest and diseases of Avocado along the elevation gradients of montane areas

REFERENCES

Adisoma G. S., 1993. The Application of the Jackknife in Geostatistical Resource Estimation: Robust Estimator and Its Measure of Uncertainty: PhD Dissertation, University of Arizona, Phoenix, 117p.

Alves, L.F., Vieirac, S.A., Scaranelloc, M.A., Camargoc, P.B., Santosd, F.A.M., Joly, C.A., Martinelli, L.A., 2010. Forest structure and live above-ground biomass variation along an elevational gradient of tropical Atlantic moist forest (Brazil). Forest Ecology and Management 260, 679–691.

Alves, D.S., 2002. Space–time dynamics of deforestation in Brazilian Amazonia. Int. J. Remote Sens. 14, 2903–2908

Aragoa L.E.O.C. Shimabukuro Y.E. Santo F.D.B.E. Williams M. 2005. Landscape pattern and spatial variability of leaf area index in Eastern Amazonia. Forest Ecology and Management 211 (2005) 240–256

Ashton, P. S. 2003. Floristic zonation of tree communities on wet tropical mountains revisited. Perspectives in Plant Ecology, Evolution and Systematics 6:87–104.

Baccini A., Laporte N. Goetz S.J. Sun M. Dong H., 2008. A first map of tropical Africa's above-ground biomass derived from satellite imagery. Envionmental Research Letter 3 (2008 045011 (9pp).

BirdLife International, 2012. Eastern Afromontane biodiversity hotspot. BirdLife International.

Bolstad P.V. Vose J.M. McNuIty S.G. 2001. Forest Productivity, Leaf Area, and Terrain in Southern Appalachian Deciduous Forests. Forest Science 47(3) 2001

Bréda N.J.J. 2003. Ground-based measurements of leaf area index; a review of methods, instruments and current controversies. Journal of experimental Botany, Vol. 54, No. 392, pp.2403-2417.

Brown, S. (1997) Estimating biomass and biomass change of tropical forest : A Primer.FAO Forestry paper No.134.Rome Italy,55p. Charles. L.R ., Nzunda, E.F and Munishi, P.T.K, (2013). Agro-forestry as adaptation strategy under Climate Change in Mwanga dis-trict, International Journal for Environmental Protection 3(11), pp. 29-38.

Brovkin V. 2002. Climate-vegetation interaction. Journal of Phys. France 12 (2002) , pp. 57-72.

Bytebier B. Chuah-Petiot M. 2002. A preliminary checklist of the bryoflora of the Taita Hills, Kenya

Burgess, N., D'Amico Hales, J., Underwood, E., Dinerstein, E., Olson, D., Itoua, I., Schipper, J., Ricketts, T., and Newman, K. (2004a) Terrestrial ecoregions of Africa and Madagascar: a continental assessment. Island Press, Washington DC. Pp. 1-501.

Burke, J.C., Yoker C.M., Parton W.J., Cole C.V. Flach K. and Schimel, 1989. Texture, climate, and cultivation effects on soil organic matter content in U.S. grassland soils. Soil Sci. Soc. Am. J. 53:800-805.

Carlson T.N. Riziley D.A. 1997. On the Relation between NDVI, Fractional Vegetation Cover, and Leaf Area Index. REMOTE SENS. ENVIKON. 62:241-252 (1973).

Charles R.C. Nzunda E.F. Munishi P.K.T., 2014. Agro-forestry as a resilient strategy in mitigating climate change in Mwanga District, Kilimanjaro, Tanzania. Global Journal of Bilogy, Agriculture and Health Sciences Vol. 3(2):11-17.

Chave J. Rejou-Mechchain M. Burquez A. Chidumayo E. Colgan M.S. Delitti W.B.C. Duque A. Eid T. Fearnside P.M. Goodman R.C. Henry M. Martinez-Yrizar A. Mugasha W.A. Muller-Landau H.C. Mencuccini M. Nelson B.W. Ngomanda A. Nogueira E.M. Ortiz-Malavassi E. Pelissier R. Ploton P. Ryan C.M. Saldarriaga J.G. Vieilledent G., 2014. Improved allometric models to estimate the above-ground biomass of tropical trees. Global change biology (2014) 20, 3177-3190, doi:10.1111/gcb.12629

Chave J, Coomes DA, Jansen S, Lewis SL, Swenson NG, Zanne AE (2009). Towards a worldwide wood economics spectrum. Ecology Letters 12(4): 351-366. http://dx.doi.org/10.1111/j.1461-0248.2009.01285.x

Chave J. Andalo C. Brown S., 2005. Tree allometry and improved estimation of carbon stocks and balance in tropical forests. Oecologia, 145, 87-99.

Chen, J. M., & Black, T. A. (1992). Defining leaf area index for non-flat leaves. Plant, Cell & Environment, 15, 421–429.

Clarke LE, Edmonds JA, Jacoby HD, Pitcher H, Reilly JM, Richels R (2007) Scenarios of greenhouse gas emissions and atmospheric concentrations. Sub-report 2.1a of Synthesis and Assessment Product 2.1.

Climate Change Science Program and the Subcommittee on Global Change Research, Washington DC

Cramer W.P. Solomon A.M. 1993. Climatic classification and future global redistribution of agricultural land. Climate Research 3, 97-110.

Crawley, M.J., 2007. The R Book. John Wiley & Sons Ltd, England

Davenport M.L. Nichlson S.E. 2007. On the relation between rainfall and the Normalized Difference Vegetation Index for diverse vegetation types in East Africa. International Journal of Remote Sensing Volume 14, 1993 - Issue 12

Daws, M.I., Mullins, C.E., Burslem, D.F.R.P., Paton, S.R., Dalling, J.W., 2002. Topographic position affects the water regime in a semideciduous tropical forest in Panamá. Plant Soil 238, 79–90.

Dawson T.P. Jackson S.T. House J.I. Prentice I.C. Mace G.M. (2011). Beyond Predictions: Biodiversity Conservation in a Changing Climate. Science 332, 53 (2011); DOI: 10.1126/science.1200303

Doherty R.M. Sitch S. Smith B. Lewis S.L. Thomton P.K. 2010. Implications of future climate and atmospheric CO_2 content for regional biogeochemistry, biogeography and ecosystem services across East Africa. Glob Change Biol 2010; 16:617-640

Elith, J., 2002. Quantitative methods for modeling species habitat: comparative performance and an application to Australian plants. In: Ferson, S., Burgman, M. (Eds.), Quantitative Methods for Conservation Biology. Springer-Verlag, New York, 39–58.

Elith, J., C. H. Graham, R. P. Anderson, M. Dudík, S. Ferrier, A. Guisan, R. J. Hijmans, F. Huettmann, J. R. Leathwick, A. Lehmann, J. Li, L. G. Lohmann, B. A. Loiselle, G. Manion, C. Moritz, M. Nakamura, Y. Nakazawa, J. McC. Overton, A. T. Peterson, S. J. Phillips, K. Richardson, R. Scachetti-Pereira, R. E. Schapire, J. Soberón, S. Williams, M. S. Wisz, and N. E. Zimmermann. 2006. “Novel methods improve prediction of species’ distributions from occurrence data.” Ecography. 29:129–151.

Fang, X., Bailey, R.L., 1998. Height–diameter models for tropical forests on Hainan Island in southern China. In: Marshal A.R. Willcock S. Platts P.J. Lovett J.C. Balford A. Burgess N.D. Latham J.E. Munishi P.K.T. Salter R. Shirima D.D. Lewis S.L., 2012. Measuring and modeling above-ground carbon and tree allometry along a tropical elevation gradient. Biological Conservation 154 (2012) 20-33.

Fearnside, P.M., 1997. Wood density for estimating forest biomass in Brazilian Amazonia. In: Marshal A.R. Willcock S. Platts P.J. Lovett J.C. Balford A. Burgess N.D. Latham J.E.

Munishi P.K.T. Salter R. Shirima D.D. Lewis S.L., 2012. Measuring and modeling above-ground carbon and tree allometry along a tropical elevation gradient. Biological Conservation 154 (2012) 20-33.

Fernandes, R. & S.G. Leblanc (2005). Parametric (modified least squares) and nonparametric (Theil–Sen) linear regressions for predicting biophysical parameters in the presence of measurement errors. In: Itkonen P. (2012). Estimating leaf area index and above-ground biomass by empirical modeling using SPOT HRVIR satellite in the Taita Hills, SE Kenya. Department of Geosciences and Geography University Of Helsinki

Friedl, M. A., et al. (2002), Global land cover mapping from MODIS: algorithms and early results, Remote Sens. Environ., 83, 287–302, doi:10.1016/S0034-4257(02)00078-0

Fujino J, Nair R, Kainuma M, Masui T, Matsuoka Y (2006) Multigas mitigation analysis on stabilization scenarios using aim global model. The Energy Journal Special issue #3:343–354

Garrigues S. Allard D. Weiss M. Baret F. 2002. Comparing VALERI sampling schemes to better represent high spatial resolution satellite pixel fromgroundmeasurements: How to characterize an ESU. Available for download at. http://w3.avignon.inra.fr/valeri/methodology/samplingschemes.pdf (accessed 17/08/2011).

Gasse, F. (2002) Diatom-inferred salinity and carbonated oxygen isotopes in Holocene waterbodies of the western Sahara and Sahel (Africa). Quatern. Sci. Rev. 21, 737–767.

Gemmell F M 1995 Remote Sens. Environ. 51 291–305 Gentry, 1995;

Gonsamo, A. (2009). Remote sensing of leaf area index: enhanced retrieval from close-range and remotely sensed optical observations. Academic dissertation. 66 pp. Department of Geography A147. University of Helsinki.

Good S. and Caylor K.K., 2011. Climatological determinants of woody cover in Africa. PNAS Vol. 108 No.12.

Gower, S. T., Kucharik, C. J., & Norman, J. M. (1999). Direct and indirect estimation of leaf area index, fapar, and net primary production of terrestrial ecosystems. Remote Sensing of Environment, 70, 29– 51.

Grubb P.J. 1977. Control of forest growth and distribution on wet tropical mountains: with special reference to mineral nutrition. Ann. Rev. Ecol. Syst. 8: 83 –107.

Hairiah K. Dewi S. Agus F. Velarde S. Ekadinata A. Rahayu S. van Noordwijk M., 2011. Measuring carbon stocks across land use systems: A manual. Bogor, Indonesia. World Agro-forestry Center (ICRAF), SEA Regional Office, 154 pages.

Hall, J., Burgess, N.D., Lovett, J., Mbilinyi, B. and Gereau, R.E. (2009) Conservation implications of deforestation across an elevational gradient in the Eastern Arc Mountains, Tanzania. Biol. Conserv., 142: 2510-2521.

Hamilton A.C., Ruffo C.K., Mwasha I.V., Mmari C. and Lovett J.C. 1989. A survey of forest types on the East Usambaras using the variable – area tree plot method. In: Hamilton A.C. and Bensted-Smith R. (eds), Forest Conservation in the East Usambara Mountains Tanzania. The IUCN Tropical Forest Programme, pp. 213 –225.

Heaney, L.R., 2001. Small mammal diversity along elevational gradients in the Philippines: an assessment of patterns and hypotheses. Global Ecology and Biogeography 10, 15–39. Heiskanen 2006

Hemp, A. 2009. Climate change and its impact on the forests of Kilimanjaro. African Journal of Ecology 47 (Suppl.): 3–10.

Hemp A., 2006; Continuum or zonation? Altitudinal gradients in the forest vegetation of Mt. Kilimanjaro. Plant Ecology (2006) 184:27-42.

Hijioka Y, Matsuoka Y, Nishimoto H, Masui T, Kainuma M (2008) Global GHG emission scenarios under GHG concentration stabilization targets. J Glob Environ Eng 13:97–108

Himberg N., 2011. Traditionally protected forests' role within transforming natural resource management regimes in Taita Hills, Kenya. Department of Geosciences and Geography, Faculty of Science, University of Helsinki.

Himberg N., 2006. Community-based Ecotourism as a Sustainable Development Option in the Taita Hills, Kenya. Department of Geography University of Helsinki.

Hontoria C. Rodriguez-Murillo J.C., Saa A. 1999. Relationships between soil organic carbon and site characteristics in Peninsular Spain. Soil Sci. Soc. Am. J. 63:614-621.

Huete A. Didan K, 2006. MODIS vegetation index product series collection 5 change summary. University of Arizona

IPCC, Climate Change 2007: Impacts, Adaptation and Vulnerability. Contribution of Working Group II to the Fourth Assessment Report of the Intergovernmental Panel on Climate Change (Cambridge Univ. Press, Cambridge, 2007).

Iverson LR, Prasad AM (1998) Predicting the abundance of 80 tree species following climate change in the eastern United States. Ecol Monog 66: 465–485. In: Loarie SR, Carter BE, Hayhoe K, McMahon S, Moe R, et al. (2008) Climate Change and the Future of California's Endemic Flora. PLoS ONE 3(6): e2502. doi:10.1371/journal.pone.0002502. doi:10.1371/journal.pone.0002502

Jacquemoud, S., and F. Baret, 1990, PROSPECT: A Model of Leaf Optical Properties Spectra, Remote Sens. Environ., 34:75-91.

Jaetzold R. Schmidt H., 1983. Farm management Handbook of Kenya, Volume II: Natural conditions and farm management information. Part A: West Kenya; Part B: Central Kenya; Part C; East Kenya. Nairobi: Ministry of Agriculture.

Jäger J. Moser S. Arnott J. Schaller M. 2014. Adaption to Climate Change in Mountain & Coastal Areas: Building an interface between providers and users of climate change knowledge – Insights from a Transatlantic Dialogue. Report 22, Climate Service Center, Germany

Jenny, H. 1941. Factors of soil formation. McGraw-Hill, New York.

Jonchkeere I. Fleck S. Nackaerts K. Muys B. Coppin P. Weiss M. Baret F. 2004. Review of methods for in situ leaf area index determination Part I. Theories, sensors and hemispherical photography. Agricultural and Forest meteorology 121: 19-35

Jonckheere, I., Nackaerts, K., Muys, B., Coppin, P., 2005b. Assessment of automatic gap fraction estimation from digital high-dynamic range hemispherical photography. Agr. For. Meteorol. 132 (1–2), 96–114.

Jones, C. G., Lawton, J. H., and Shachak, M. (1994). Organisms as ecosystem engineers. Oikos, 69, 373–86.

JRL (Joint Research Laboratory), 2005. GLC 2000 (Global Land Cover) data layer. Ispra, Italy: JRL.

Kirby K.R. Potvin C., 2007. Variation in carbon storage among tree species: Implications for the management of a small-scale carbon sink project. Forest Ecology and Management 246 (2007) 208–221

Kononova, M.M. 1966. Soil organic matter. 2nd ed. Pergamon Press, New York.

Krhoda, G. O. 1998. Conflicts in resource utilization resulting from highland-lowland interactions: a study of Taita Hills, Kenya. In: F. F. Ojany (ed.). *African mountains and*

highlands. Planning for sustainable use of mountain resources . The United Nations University, Tokyo, Japan. Pp. 25-39.

Laurance W.F. Fearnside P.M. Laurance S.G. Delamonica P. Lovejoy T. E. Merona J.M.R. Chambers J.Q. Gascon C., 1999. Relationship between soils and Amazon forest biomass: a landscape-scale study. Forest Ecology and Management 118 (1999) 127-138.

Landmann T. Dubovyk O., 2014. Spatial analysis of human-induced vegetation productivity decline over eastern Africa using a decade (2001-2011) of medium resolution MODIS time-series data. International Journal of Applied Earth Observation and Geoinformation 33 (2014) 76-82.

Leakey R.R.B. 1996. Definition of Agro-forestry revisited. Agro-forestry Today 8: 5–7

Lee, K.S., W.B. Cohen, R.E. Kennedy, T.K. Maiersperger and S.T. Gower. 2004. Hyperspectral versus multispectral data for estimating leaf area index in four different biomes. Remote Sensing Environment 91(3-4): 508–520.

Lovett J.C. Wasser S.K., 2008. Biogeography and ecology of the rain forest of Eastern Africa. Cambridge University Press; 0521068983

Lovett, J.C. 1990. Classification and status of the moist forests of Tanzania. Mitt. Inst. Allg. Bot. Hamb. 23a, 287–300.

Luedeling E. Kindt R. Huth N.I. Koenig K. 2013. Agro-forestry systems in a changing climate — challenges in projecting future performance. ScienceDirect
http://dx.doi.org/10.1016/j.cosust.2013.07.013

Maley, J. and Elenga, H. 1993. Le rôle des nuages **dans** l'évolution des paléoenvironnements montagnards de l'Afrique tropicale. Veille Climatique Satellitaire, Lannion 46,51-63.

Marchant R., 2007. The importance of the Indian Ocean for climate change in East Africa (in Japanese). Ship and Ocean News 13, 282-284

Marshal A.R. Willcock S. Platts P.J. Lovett J.C. Balford A. Burgess N.D. Latham J.E. Munishi P.K.T. Salter R. Shirima D.D. Lewis S.L., 2012. Measuring and modeling above-ground carbon and tree allometry along a tropical elevation gradient. Biological Conservation 154 (2012) 20-33.

McCain, C.M., 2005. Elevational gradients in diversity of small mammals. Ecology 86, 366–372.

Misana, S.B. Sokoni C. Mbonile M.J., 2012. Land-use/cover changes and their drivers in Kilimanjaro, Tanzania. Journal of Geographical and regional planning vol. 5(6), pp. 151-164.

Moser, D., S. Dullinger, T. Englisch, H. Niklfeld, C. Plutzar, N. Sauberer, H.G. Zechmeister and G. Grabherr, 2005: Environmental determinants of vascular plant species richness in theAustrianAlps. J. Biogeogr., 32, 1117-1127.

Muller-Landau, H.C., 2004. Interspecific and inter-site variation in wood specific gravity of tropical trees. Biotropica 36, 20–32.

Munishi L.K. (2007) The distribution and diversity of tree resources outside forest in southern side of Mount Kilimanjaro. Discov. Innov; Vol. 19 (Special Edition 1 & 2)

Nelson B., W., Mesquitaj R. C. G.., L. G. Pereiras,. Garciaa Quinod E Sou, G. Tewirbaa Tistaan, D L. Bovino Couto 1999. Allometric regressions for improved estimate of secondary forest biomass in the Central Amazon. For. Ecol. Manage. 117: 149-167.

Nepstad, D., Carvalho, G., Barros, A.C., Alencar, A., Capobianco, J.P., Bishop, J., Moutinho, P., Lefebvre, P., Silva Jr., U.B., Prins, E., 2001. Road paving, fire regime feedbacks, and the future of Amazon forests. For. Ecol. Manage. 154, 397–407.

Newmark W., 2002. Conserving Biodiversity in East African Forests: A Study of the Eastern Arc Mountains. Springer.

O'Brien V. 1993. Climate gradients in woody plant species richness: towards an explanation based on an analysis of southern Africa's woody flora. Journal of Biogeography (1993) 20, 181-198.

Pearson, R.G. 2007. Species' Distribution Modeling for Conservation Educators and Practitioners. Synthesis. American Museum of Natural History. Available at http://ncep.amnh.org.

Pellikka, P. B., Clark, A. Gonsamo Gosa, N. Himberg, P. Hurskainen, E. Maeda, J.Mwang´ombe, L. Omoro and M. Siljander (2013). Agricultural expansion and its consequences in the Taita Hills, Kenya. Developments in Earth Surface Processes 33, 165–179.

Pellika P.K.E. Lotjonen M. Siljander M. Lens L. 2009. Airbone remote sensing of spatiotemporal change (1995-2004) in indigenous and exotic forest cover in the taita Hills, Kenya. International Journal of Applied Earth Observation and Geoinformation.

Pfeifer M. Platts P.J. Burgess N. Swetnam R. Willcock S. Marchant R., 2013. Land use change and carbon fluxes in East Africa quantified using earth observation data and field measurements. Environmental conservation. pp. 241-252. ISSN 0376-8929.

Pfeifer M. Gonsamo A. Disney M. Pellikka P. Marchant R., 2012. Leaf area index for biomes of the Eastern Arc Mountains: Landsat and SPOT observations along precipitation and altitude gradients. Remote Sensing of Environment 118 (2012) 103-115.

Philips O. Baker T. Feldpausch T. Brienen R., 2009. RAINFOR field manual for plot establishment and remeasurement.

Phillips S.J. and Dudik M. 2008. Modeling of species distributions with Maxent: new extensions and a comprehensive evaluation. Ecography, Vol 31, pp 161-175, 2008.

Phillips S.J. Anderson R.P. and Schapire R.E., 2006. Maximum entropy modeling of species geographic distributions. Ecological Modelling, Vol 190/3-4 pp 231-259, 2006.

Phillips S.J. Dudik M. Schapire R.E., 2004. A maximum entropy approach to species distribution modeling. Proceedings of the 21st International Conference on Machine Learning, Banff, Canada, 2004

Pounds, J. A., Fogden, M. P. L., and Campbell, J. H. (1999). Biological response to climate change on a tropical mountain. Nature, 398, 611–615.

Puhr C.B. and Donoghue D.N.M. 2000. Int. J. Remote Sens. In: Baccini A., Laporte N. Goetz S.J. Sun M. Dong H., 2008. A first map of tropical Africa's above-ground biomass derived from satellite imagery. Envionmental Research Letter 3 (2008 045011 (9pp).

Pinard, M.A., Cropper, W.P., 2000. Simulated effects of logging on carbon storage in dipterocarp forest. J. Appl. Ecol. 37, 267–283.

Platts P.J. McCleanb C.J., Lovett J.C., Marchant R. 2008. Predicting tree distributions in an East African biodiversity hotspot: model selection, data bias and envelope uncertainty. Ecological modelling 218 (2008) 121–134.

Platts P.J. Omeny P.A. and Marchant R. 2014. AFRICLIM: high-resolution climate projections for ecological applications in Africa. African Journal of Ecology.

Purevdorj T.S. Tateishi R. Ishiyama T. Honda Y. 2010. Relationships between percent vegetation cover and vegetation indices. International Journal of Remote Sensing, 19:18, 3519-3535, DOI: 10.1080/014311698213795

Rahbek, C. 1995. The elevational gradient of species richness: a uniform pattern? Ecography 18, 200–205. In: Lovett J.C. Marshall1 A.R. and Carr J. Changes in tropical forest vegetation along an altitudinal gradient in the Udzungwa Mountains National Park, Tanzania. Afr. J. Ecol., 44, 478–490

Ramankutty N. Foley J.A. Olejniczak N.J. 2002. People on the land: changes in global population and croplands during the 20th century. Ambio. 2002 May; 31(3):251-7.

Ramankutty N. Foley J.A., 1999. Estimating historical changes in global land cover: croplands from 1700 to 1992. Global Biogeochemical Cycles 13(4), 997-1027.

Riahi K, Grübler A, Nakicenovic N (2007) Scenarios of long-term socio-economic and environmental development under climate stabilization. Technol Forecast Soc Chang 74:887–935

Rickart, E.A. (2001) Elevational diversity gradients, biogeography and the structure of montane mammal communities in the intermountain region of North America. Global Ecology and Biogeography, 10, 77–100. In: McCain C.M. 2007. Could temperature and water availability drive elevational species richness patterns? A global case study for bats. Global Ecology and Biogeography, (Global Ecol. Biogeogr.) (2007) 16, 1–13.

Ridler, T.W. & S. Calvard (1978). Picture thresholding using an iterative selection method. IEEE Transactions on Systems, Man, and Cybernetics SMC-8, 630–632. In: Itkonen P. 2012. Estimating leaf area index and aboground biomass by empirical modelling using SPOT HRVIR satellite imagery in the Taita Hills, SE Kenya. Department of Geosciences and Geography, University of Helsinki.

Root, T. L., Price, J. T., Hall, K. R., et al. (2003). Fingerprints of global warming on wild animals and plants. Nature, 421, 57–60. In: Sodhi N.S. Ehrlich P.R. 2010. Conservation Biology for All. Oxford University Press.

Ruohonen, K., (2011). Statistics 1. Tempere University, Finland

Saatchi SS, Harris NL, Brown S, Lefsky M, Mitchard ETA et al. (2011) Benchmark map of forest carbon stocks in tropical regions across three continents. Proceedings of the National Academy of Sciences USA, 108, 9899-9904.

Sabine, C.L., M. Heimann, P.Artaxo, D.C.E. Bakker, C.T.A. Chen, C.B. Field and N. Gruber, 2004: Current status and past trends of the global carbon cycle. Global Carbon Cycle: Integrating Humans, Climate, and the NaturalWorld, C.B. Field andM.R. Raupach, Eds.,

Island Press, Washington, Distict of Columbia, 17-44 Sanchez, P.A. 1995. Science in Agro-forestry. *Agrofor. Syst.,* 30: 5-55.

Schroeder P. 1994. Carbon storage benefits of Agro-forestry system. Agro-forestry Systems 27: 89-97, 1994.

Schroth, G., da Fonseca, G. A. B., Harvey, C. A., Gascon, C., Vasconcelos, and Izac, A.-M. N., eds (2004). Agro-forestry and biodiversity conservation in tropical landscapes. Island Press, Washington, DC.

Servant, M., Maley, J., Turcq, B., Absy, M. L., Brenac, P., Fournier, M., and Ledru, M.-P.: Tropical forest changes during the Late Quaternary in African and South American lowlands, Global Planet. Change, 7, 25–40, 1993.

Shugart H H, Chavez L B and Kasischke E S 2000 For. Sci. 46 478–86

Sjöström, M., Ardö, J., Arneth, A., Boulain, N., Cappelaere, B., Eklundh, L., de Grand-court, A., Kutsch, W.L., Merbold, L., Nouvellon, Y., Scholes, R.J., Schubert, P.,Seaquist, J., Veenendaal, E.M., 2011. Exploring the potential of MODIS EVI formodeling gross primary production across African ecosystems. Remote Sens.Environ. 115, 1081–1089.

Smith SJ, Wigley TML (2006) MultiGas forcing stabilization with minicam. The Energy Journal Special issue #3:373–392. In: van Vuuren D.P. Edmonds J. Kainuma M. Riahi K. Thomson A. Hibbard K. Hurtt G.C. Kram T. Krey V. Lamarque J.F. Masui T. Meinshausen M. Nakicenovic N. Smith S.J. Rose S.K. The representative concentration pathways: an overview. Climatic Change (2011) 109:5–31: DOI 10.1007/s10584-011-0148-z

Sodhi N.S. Ehrlich P.R. 2010. Conservation Biology for All. Oxford University Press.

Soini, E. 2005. Livelihood capital, strategies and outcomes in the Taita Hills of Kenya. ICRAF Working Paper 8. World Agro-forestry Centre, Nairobi. 48 pp. In Omoro L.M.A. 2012. Impacts of indigenous and exotic tree species on ecosystem services: Case study on the mountain cloud forests of Taita Hills, Kenya Faculty of Agriculture and Forestry of the University of Helsinki.

Spehn, E. and C. Körner, 2005: Aglobal assessment of mountain biodiversity and its function. Global Change and Mountain Regions: An Overview of Current Knowledge, U.M. Huber, H.K.M. Bugmann andM.A. Reasoner, Eds., Springer, Berlin, 393-400. In: IPCC, Climate Change 2007: Impacts, Adaptation and Vulnerability. Contribution of Working Group II to

the Fourth Assessment Report of the Intergovernmental Panel on Climate Change (Cambridge Univ. Press, Cambridge, 2007).

Takyu, M., Aiba, S., Kitayama, K., 2003. Changes in biomass, productivity and decomposition along topographical gradients under different geological conditions in tropical lower montane forests on Mount Kinabalu, Borneo. Oecologia 134, 397–404.

United Nations, 2017. Sustainable Development Goals Report. New York, USA

Unruh, J.D., Houghton, J., Lefebvre, P.A., 1993. Carbon storage in Agro-forestry: an estimate for sub-Saharan Africa. Climate Research 3, 39–52. In: Henry M., Tittonell P. Manlay R.J. Bernoux M. Albrecht A. Vanlauwe B. 2008. Biodiversity, carbon stocks and sequestration potential in above-ground biomass in smallholder farming systems of western Kenya. Agriculture, Ecosystems and Environment 129 (2009) 238–252.

Vare, H., R. Lampinen, C. Humphries and P.Williams, 2003: Taxonomic diversity of vascular plants in the European alpine areas. Alpine Biodiversity in Europe: A Europe-wide Assessment of Biological Richness and Change, L. Nagy, G. Grabherr, C. Körner and D.B.A. Thompson, Ecological Studies 167, Springer, Heidelberg,133-148.

Va´zquez G.J.A. and Givnish T.J. 1998. Altitudinal gradients in tropical forest composition, structure, and diversity in the Sierra de Manantla´ n. J. Ecol. 86: 999 –1020.

Verchot L.V. Van Noordwijk M. Kandji S. Tomich T. Ong C. Albrecht A. Mackensen J. Bantilan C. Anupama K.V. Palm C. (2007). Climate change: linking adaptation and mitigation through Agro-forestry. Mitig Adapt Strat Glob Change. DOI 10.1007/s11027-007-9105-6

Webb, N., C. Nichol, J. Wood & E. Potter (2008). User manual for the SunScan Canopy Analysis System, type SS1, Version: 2.0. 83 pp. Cambridge, U.K.: Delta-T Devices Ltd <http://www.deltat.co.uk/support-article.html?article=faq2008070800616>.

Weiss, M., & Baret, F., 2010. CAN-EYE V6.1 User Manual. EMMAH laboratory (Mediterranean environment and agro-hydro system modelisation). French National Institute of Agricultural Research (INRA).

Wise M, Calvin K, Thomson A, Clarke L, Bond-Lamberty B, Sands R, Smith SJ, Janetos A, Edmonds J (2009) Implications of limiting CO2 concentrations for land use and energy. Science 324:1183–1186

Woldu Z., Feoli E. and Nigatu L. 1989. Partitioning an elevation gradient of vegetation from southeastern Ethiopia by probabilistic methods. Vegetatio 81: 189 –198.

Xian, Y. 2014. The Study on Soil Property and Its Correlation with Species Diversity of Vegetation in Eastern Slope of Gaoligong Mountains; Southwest Forestry University: Kunming, China, 2014.

Zanne AE, Lopez-Gonzalez G, Coomes DA, Ilic J, Jansen S, Lewis SL, Miller RB, Swenson NG, Wiemann MC, Chave J (2009) Data from: Towards a worldwide wood economics spectrum. Dryad Digital Repository. http://dx.doi.org/10.5061/dryad.234

Zhang C. Li X. Chen L. Xie G. Liu C. and Pei S. 2016. Effects of Topographical and Edaphic Factors on Tree Community Structure and Diversity of Subtropical Mountain Forests in the Lower Lancang River Basin. Forests 2016, 7, 222; doi:10.3390/f7100222

Zheng G. Moskal L.M. 2009. Retrieving Leaf Area Index (LAI) Using Remote Sensing: Theories, Methods and Sensors. Sensors 2009, 9, 2719-2745; doi:10.3390/s90402719

APPENDICES

APPENDIX I: Species relative density, Frequency of distribution and dominance of woody plant species on the inhabited slopes of Taita Hills and Mount Kilimanjaro

No.	Scientific Name	Relative Abundance		Frequency %		Dominance	
		Kilimanjaro	Taita	Kilimanjaro	Taita	Kilimanjaro	Taita
1.	*Celtis africana*	1.80	0.00	58.33	73.33	1.61	0.00
2.	*Senna siamea*	1.35	0.70	50.00	6.67	0.38	0.58
3.	*Syzygium cumini*	0.34	0.61	50.00	0.00	0.13	1.08
4.	*Eucalyptus globulus*	0.22	0.00	50.00	0.00	0.04	0.00
5.	*Dodonea angustifolia*	0.11	0.00	50.00	33.33	0.01	0.00
6.	*Prunus africana*	1.69	0.52	41.67	13.33	5.42	0.48
7.	*Markhamia lutea*	6.86	0.44	33.33	13.33	2.09	0.31
8.	*Albizia gummifera*	10.24	0.70	8.33	0.00	20.79	0.20
9.	*Persea americana*	14.40	5.85	16.67	53.33	7.69	5.57
10.	*Mangifera indica*	11.25	3.67	16.67	6.67	9.15	11.53
11.	*Callistemon citrinus*	0.56	0.35	33.33	53.33	0.41	0.11
12.	*Grevillea robusta*	12.26	18.95	8.33	0.00	6.37	16.34
13.	*Grewia similis*	0.22	0.35	25.00	13.33	0.04	0.24
14.	*Acacia abyssinica*	1.80	1.31	16.67	0.00	1.71	2.10
15.	*Bridelia micrantha*	1.01	2.71	16.67	33.33	0.20	1.59
16.	*Indet maasa*	0.34	0.00	16.67	26.67	0.34	0.00
17.	*Combretum Indet1*	0.34	0.00	16.67	13.33	0.24	0.00
18.	*Cupressus lusitanica*	0.22	3.06	16.67	0.00	0.20	2.41
19.	*Euphorbiaceae*	0.22	0.00	16.67	26.67	0.13	0.00
20.	*Dovyalis macrocalyx*	0.11	0.00	16.67	66.67	0.09	0.00
21.	*Tabaenamontana*	0.11	0.00	16.67	6.67	0.04	0.00
22.	*Ficus sycomorus*	0.67	1.75	8.33	33.33	6.38	2.76
23.	*Rauvolfia caffra*	5.62	0.00	0.00	6.67	6.04	0.00
24.	*Cordia africana*	1.35	0.00	8.33	6.67	1.19	0.00
25.	*Dalbergia melanoxylon*	1.46	0.17	8.33	0.00	0.63	0.26
26.	*Combretum molle*	1.35	0.70	8.33	0.00	0.61	1.51
27.	*Acacia mearnsii*	1.35	5.07	8.33	6.67	0.48	1.30
28.	*Psidium guajava*	0.90	6.46	8.33	0.00	0.23	6.17
29.	*Acacia seyal*	0.79	0.00	8.33	0.00	0.18	0.00

30.	*Manihot*	0.56	0.00	8.33	0.00	0.17	0.00
31.	*Bauhinia Indet1*	0.34	0.00	8.33	0.00	0.28	0.00
32.	*Tamarindus indica*	0.22	0.44	8.33	0.00	0.29	1.49
33.	*Bersama abyssinica*	0.22	0.00	8.33	0.00	0.10	0.00
34.	*Ficus lutea*	0.22	0.79	8.33	0.00	0.07	2.58
35.	*Markhamia obtusifolia*	0.11	0.00	8.33	26.67	0.06	0.00
36.	*Acacia abreviata*	0.11	0.00	8.33	0.00	0.05	0.00
37.	*Croton megalocarpus*	0.11	0.52	8.33	0.00	0.04	0.40
38.	*Acacia tortilis*	0.11	3.06	8.33	6.67	0.01	1.79
39.	*Prosopis juliflora*	0.11	0.00	8.33	0.00	0.01	0.00
40.	*Podocarpus indet*	0.11	0.17	8.33	13.33	0.01	0.11
41.	*Adansonia digitata*	0.11	0.00	0.00	6.67	6.48	0.00
42.	*Croton macrostachyus*	2.59	0.17	0.00	13.33	2.17	0.03
43.	*Ficus thoningii*	0.79	0.70	0.00	6.67	3.95	3.60
44.	*Pinus pittuda*	4.16	0.26	0.00	13.33	0.56	0.24
45.	*Trichilia emetica*	0.11	0.00	0.00	6.67	4.54	0.00
46.	*Acacia xanthophloea*	2.81	0.00	0.00	20.00	1.58	0.00
47.	*Eucalyptus maculata*	1.91	4.19	0.00	6.67	0.64	6.54
48.	*Acrocarpus fraxinifolious*	1.69	0.00	0.00	6.67	0.50	0.00
49.	*Erythrina abyssinica*	0.90	0.26	0.00	40.00	0.68	0.91
50.	*Kigelia africana*	0.67	0.00	0.00	13.33	0.68	0.00
51.	*Eryobotria japonica*	1.24	1.40	0.00	26.67	0.11	0.50
52.	*Delonix regia*	0.90	0.00	0.00	0.00	0.44	0.00
53.	*Fagaropsis angolensis*	0.79	0.00	0.00	20.00	0.54	0.00
54.	*Indet fulameni*	0.67	0.00	0.00	6.67	0.55	0.00
55.	*Euphorbia tirucalli*	0.79	0.00	0.00	6.67	0.30	0.00
56.	*Acacia lahai*	0.79	0.00	0.00	13.33	0.17	0.00
57.	*Macaranga capensis*	0.56	0.00	0.00	13.33	0.26	0.00
58.	*Vangueria madagascarensis*	0.45	0.09	0.00	6.67	0.37	0.02
59.	*Azadirachta indica*	0.67	1.14	0.00	13.33	0.13	0.74
60.	*Olea africana*	0.11	0.00	0.00	6.67	0.56	0.00
61.	*Araucaria araucana*	0.22	0.09	0.00	26.67	0.42	0.02
62.	*Milicia excelsa*	0.45	0.00	0.00	20.00	0.18	0.00
63.	*Euclea divinorum*	0.45	0.00	0.00	6.67	0.13	0.00
64.	*Acacia tortilis*	0.22	0.00	0.00	6.67	0.14	0.00

65.	*Annona senegalensis*	0.22	0.96	0.00	6.67	0.04	0.81
66.	*Onsignis sp*	0.11	0.00	0.00	13.33	0.04	0.00

APPENDIX II: Species relative abundance (%) and Frequency distribution (%) of woody plant species in Agro-forestry areas and cropped lands on the inhabited slopes of Mount Kilimanjaro

Scientific Name	Relative Abundance		Frequency	
	Agro-forestry	Cropped land	Agro-forestry	Cropped land
Acacia abreviata	0.0	0.2	0.00	0.17
Acacia abyssinica	0.5	0.3	0.17	0.17
Acacia lahai	0.0	0.0	0.00	0.17
Acacia mearnsii	2.0	0.0	0.33	0.00
Acacia seyal	0.0	1.0	0.00	0.67
Acacia tortilis	0.0	0.2	0.00	0.17
Acacia xanthophloea	0.0	1.5	0.00	0.33
Acrocarpus fraxinifolious	2.5	0.0	0.33	0.00
Adansonia digitata	0.0	0.2	0.00	0.17
Albizia gummifera	13.3	1.8	1.00	0.33
Annona senegalensis	0.3	0.0	0.17	0.00
Araucaria araucana	0.3	0.0	0.17	0.00
Azadirachta indica	0.0	0.7	0.00	0.33
Bauhinia Indet1	0.0	0.5	0.00	0.17
Bersama abyssinica	0.3	0.0	0.17	0.00
Bridelia micrantha	1.5	0.0	0.33	0.00
Callistemon citrinus	0.0	0.8	0.00	0.17
Celtis africana	1.2	1.5	0.67	0.33
Combretum Indet1	0.0	0.5	0.00	0.17
Combretum molle	0.0	2.0	0.00	0.50
Cordia africana	1.8	0.2	0.33	0.17
Croton macrostachyus	3.3	0.5	0.50	0.50
Croton megalocarpus	0.2	0.0	0.17	0.00
Cupressus lusitanica	0.3	0.0	0.17	0.00
Dalbergia melanoxylon	2.0	0.2	0.67	0.17
Delonix regia	1.0	0.3	0.33	0.17
Dodonea angustifolia	0.2	0.0	0.17	0.00
Eryobotria japonica	1.8	0.0	0.50	0.00
Erythrina abyssinica	0.5	0.8	0.33	0.33
Eucalyptus globulus	0.3	0.0	0.17	0.00

Eucalyptus maculata	2.8	0.0	0.50	0.00
Euclea divinorum	0.7	0.0	0.17	0.00
Euphorbia tirucalli	0.0	1.2	0.00	0.33
Euphorbiaceae	0.0	0.3	0.00	0.17
Fagaropsis angolensis	0.7	0.5	0.50	0.33
Ficus lutea	0.0	0.2	0.00	0.17
Ficus sycomorus	0.2	0.7	0.17	0.50
Ficus thoningii	1.0	0.2	0.50	0.17
Grevillea robusta	18.0	0.2	1.00	0.17
Grewia similis	0.0	0.3	0.00	0.17
Indet fulameni	1.0	0.0	0.33	0.00
Indet maasa	0.5	0.0	0.33	0.00
Kigelia africana	0.2	0.8	0.17	0.33
Macaranga capensis	0.5	0.3	0.17	0.17
Mangifera indica	8.8	7.8	0.83	0.50
Manihot	0.0	0.8	0.00	0.17
Markhamia lutea	10.0	0.2	0.83	0.17
Markhamia obtusifolia	0.0	0.2	0.00	0.17
Milicia excelsa	0.7	0.0	0.17	0.00
Olea africana	0.0	0.2	0.00	0.17
Onsignis sp	0.0	0.2	0.00	0.17
Persea americana	19.7	1.7	0.83	0.33
Pinus pittuda	6.2	0.0	0.33	0.00
Podocarpus indet	0.0	0.2	0.00	0.17
Prunus africana	2.5	0.0	1.00	0.00
Psidium guajava	1.3	0.0	0.33	0.00
Rauvolfia caffra	8.3	0.0	1.00	0.00
Senna siamea	0.0	2.0	0.00	0.33
Syzygium cumini	0.5	0.0	0.33	0.00
Tabaenamontana	0.0	0.2	0.00	0.17
Tamarindus indica	0.0	0.3	0.00	0.17
Trichilia emetica	0.2	0.0	0.17	0.00
Vangueria madagascarensis	0.0	0.7	0.00	0.33

APPENDIX III: Species relative abundance (%) and Frequency distribution (%) of woody plant species in Agro-forestry areas and cropped lands on the inhabited slopes of Taita Hills

Scientific Name	Relative Abundance		Frequency Distribution	
	Agro-forestry	Cropped land	Agro-forestry	Cropped land
Acacia abyssinica	1.31	0.00	8.33	0.00
Acacia brevispica	0.00	0.17	0.00	8.33
Acacia mearnsii	3.49	1.57	41.67	25.00
Acacia mellifera	0.00	1.22	0.00	8.33
Acacia polyacantha	2.18	0.00	16.67	0.00
Acacia tortilis	0.61	2.45	25.00	16.67
Albizia gummifera	0.44	0.26	16.67	16.67
Annona senegalensis	0.61	0.35	16.67	8.33
Araucaria araucana	0.00	0.09	0.00	8.33
Azadirachta indica	0.96	0.17	25.00	16.67
Bougainvillea praecox	0.26	0.00	8.33	0.00
Bridelia micrantha	2.36	0.35	25.00	8.33
Callistemon citrinus	0.35	0.00	8.33	0.00
Calyandria Indet1	0.09	0.00	8.33	0.00
Citrus centhaphylum	0.00	0.09	0.00	8.33
Citrus hystrix	0.61	0.17	33.33	16.67
Citrus xanthophyla	0.00	0.35	0.00	8.33
Clerodendron indet	0.00	0.17	0.00	8.33
Combretum molle	0.00	0.70	0.00	8.33
Commiphora africana	0.09	1.22	8.33	8.33
Commiphora indet1	0.09	0.00	8.33	0.00
Croton macrostachyus	0.00	0.17	0.00	8.33
Croton megalocarpus	0.44	0.09	16.67	8.33
Cupressus lusitanica	0.35	2.71	16.67	25.00
Cussonia spicata	0.44	0.26	25.00	8.33
Dalbergia melanoxylon	0.00	0.17	0.00	16.67
Dead Tree	1.66	0.70	33.33	25.00
Dombeya indet	0.00	0.26	0.00	8.33
Dovyalis caffra	1.22	0.00	8.33	0.00
Eryobotria japonica	1.14	0.26	33.33	25.00
Erythrina abyssinica	0.09	0.17	8.33	8.33

Eucalyptus grandis	6.29	0.00	16.67	0.00
Eucalyptus maculata	0.17	4.02	8.33	8.33
Eucalyptus saligna	0.96	0.00	16.67	0.00
Ficus lutea	0.52	0.26	8.33	8.33
Ficus sycomorus	0.70	1.05	33.33	33.33
Ficus thoningii	0.70	0.00	33.33	0.00
Grevillea robusta	17.21	1.75	66.67	33.33
Grewia bicolor	0.17	0.52	8.33	8.33
Grewia similis	0.17	0.17	8.33	8.33
Invilloa Indet	0.09	0.00	8.33	0.00
Jacaranda mimosifolia	0.17	0.00	16.67	0.00
Leucina leucocephala	4.28	0.26	16.67	16.67
Macadamia indet	0.00	0.17	0.00	8.33
Maesa lanceolata	0.61	0.17	16.67	8.33
Maesopsis eminii	0.61	0.26	16.67	8.33
Mangifera indica	2.18	1.48	25.00	33.33
Markhamia lutea	0.44	0.00	16.67	0.00
Melia volkensis	0.17	0.17	8.33	8.33
Milletia oblata	0.09	0.00	8.33	0.00
Morus alba	0.26	0.00	25.00	0.00
Nuxia floribunda	0.09	0.00	8.33	0.00
Ocotea indet	0.00	0.09	0.00	8.33
Persea americana	5.15	0.70	66.67	25.00
Pinus pittuda	0.26	0.00	16.67	0.00
Podocarpus indet	0.00	0.17	0.00	8.33
Prunus africana	0.35	0.17	25.00	16.67
Psidium guajava	3.84	2.62	50.00	33.33
Rhus natalensis	0.09	0.00	8.33	0.00
Salvadora persica	0.00	0.09	0.00	8.33
Senna siamea	0.52	0.17	16.67	16.67
Sesbania sesban	1.48	0.44	16.67	8.33
Spathodea nilotica	0.96	0.00	8.33	0.00
Syzygium cumini	0.26	0.35	16.67	16.67
Syzygium guineense	0.26	0.09	8.33	8.33
Syzygium incanum	0.17	0.17	8.33	8.33

Tamarindus indica	0.17	0.26	16.67	16.67
Thevetia peruviana	0.61	0.61	8.33	16.67
Tokoma terance	0.26	0.00	8.33	0.00
Tremor orientalis	0.26	0.00	16.67	0.00
Turraea robusta	0.00	0.09	0.00	8.33
Vangueria madagascarensis	0.09	0.00	8.33	0.00
Xymalose sp	0.09	0.00	8.33	0.00